Chromosome segregation and recombination in human meiosis:

Clinical applications and insight into disjunction errors

A thesis submitted to the University of Kent for the degree of

DOCTOR OF PHILOSOPHY

in the Faculty of Science

2015

Christian Simon Ottolini

School of Biosciences

Dedicated to my family past, present and future with all my love

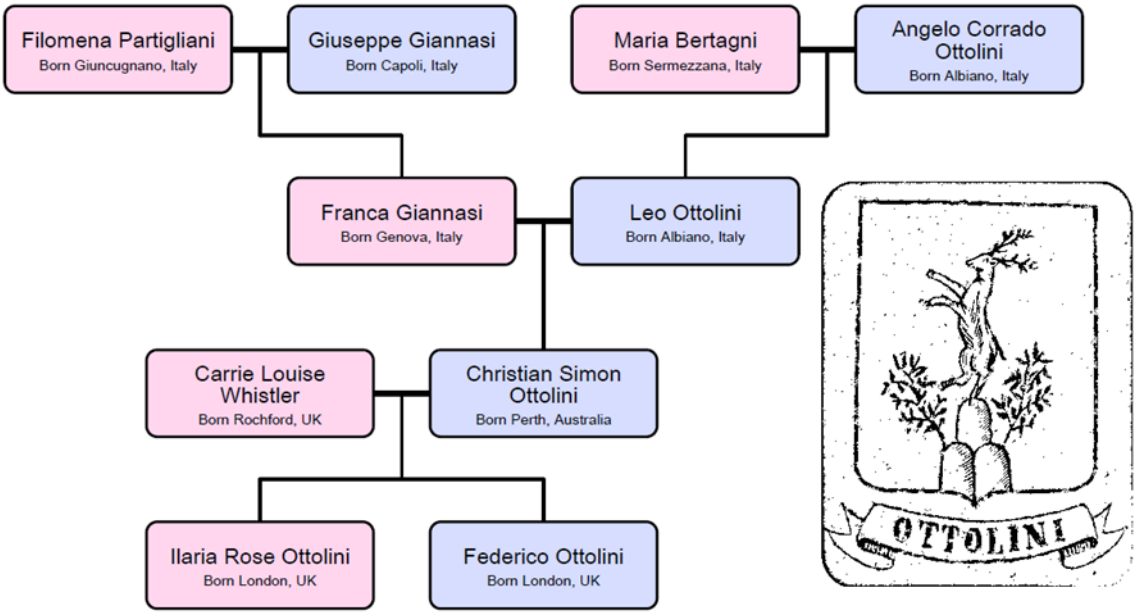

May those that have passed rest in the knowledge their sacrifices smoothed the path for those that followed, and may those that follow never forget.

Declaration

No part of this thesis has been submitted in support of an application for any degree or qualification of the University of Kent or any other University or Institute of learning.

Christian Simon Ottolini

This thesis encapsulates 10 individual pieces of published or submitted manuscripts as follows:

- *The Role of Aneuploidy Screening in Human Preimplantation Embryos by **Christian S Ottolini**, Darren K Griffin, Alan R Thornhill, Published in Aneuploidy in Health and Disease (2012).*
- *Human Embryo Biopsy Procedures by Alan R Thornhill, **Christian Ottolini** and Alan H Handyside, published in The Textbook of Assisted Reproductive Techniques, Volume 1: Laboratory perspectives Fourth Edition (2012).*
- *Aneuploidy testing by array-CGH: Applications in Preimplantation Testing by Alan R Thornhill, **Christian Ottolini**, Gary Harton and Darren Griffin published in A Practical Guide to Selecting Gametes and Embryos (2014).*
- ***Ottolini C**, Rienzi L & Capalbo A. A cautionary note against embryo aneuploidy risk assessment using time-lapse imaging. Reproductive BioMedicine Online. 2014 Mar;28(3), pp.273–275.*
- *Natesan S, Handyside AH, Thornhill AR, **Ottolini CS**, Sage K, Summers MC, Gordon A, Michaelis Konstantidis M, Wells D, Griffin DK. Live birth by PGD following confirmation by a comprehensive approach (Karyomapping) for simultaneous detection of monogenic and chromosomal disorders. Reprod Biomed Online. 2014 Nov;29(5):600-5*
- *Thornhill AR, Handyside AH, **Ottolini CS**, Taylor J, Sage K, Harton GL, Cliffe K, Affara N, Konstantinidis M, Wells D, Griffin DK. Karyomapping – a comprehensive means of simultaneous monogenic and cytogenetic PGD: Comparison with standard approaches in real time for Marfan syndrome. J Assist Reprod Genet. 2015 Mar;32(3):347-56*
- ***Ottolini CS**, Newnham LJ, Capalbo A, Natesan SA, Joshi HA, Cimadomo D, Griffin DK, Sage K, Summers MC, Thornhill AR, Housworth E, Herbert AD, Rienzi L, Ubaldi FM, Handyside AH, and Hoffmann ER, Genome-wide maps of recombination and chromosome segregation in human oocytes and embryos show selection for maternal recombination rates. Nat Genet. 2015 Jul;47(7):727-35.*
- ***Ottolini CS**, Rogers S, Sage K, Summers MC, Capalbo A, Griffin DK, Sarasa J, Wells D and Handyside AH. Karyomapping identifies second polar body DNA persisting to the blastocyst stage: implications for embryo biopsy. Reprod Biomed Online. 2015 Dec;31(6):776-82.*
- *Capalbo A*, **Ottolini CS***, Griffin DK, Ubaldi FM, Handyside AH and Rienzi L. Artificial oocyte activation with calcium ionophore does not cause a widespread increase in chromosome segregation errors in the second meiotic division of the oocyte. Fertility and Stirility (in press) ***Joint first author***
- ***Ottolini CS**, Capalbo A, Newnham L, Cimadomo C, Natesan SA, Hoffmann ER, Ubaldi FM, Rienzi L and Handyside AH. Generating maps of genome-wide recombination and chromosome segregation in human oocytes. Nature Protocols (accepted subject to reviewer's amendments).*

Where I was the primary author of the work then the text is left largely unchanged. Where I was not the primary author I have changed the text to emphasise my personal contribution. In order to allow for a coherent narrative, rather than simply annexing 10 typeset manuscripts, I have added passages to link the pieces of research together. In so doing I intend that rather than appearing 10 loosely related studies, the work appears as a coherent "whole."

Table of Contents

List of Figures

Figure **Page**

List of Tables

Table **Page**

1. Thesis Abstract

Chromosome copy number errors (or aneuploidy) of gametes and embryos occurs in humans more frequently than in any other studied species, with a spectrum of manifestations from implantation failure to affected live births. It is predominantly problem arising in maternal meiosis with at least 20% of oocytes being aneuploid, a proportion that increases dramatically with advancing maternal age. Currently the only intervention to reduce the chances of transmitting aneuploidy is by invasive embryo biopsy procedures in high-risk groups (mainly patients with advanced maternal age) undergoing *in-vitro* fertilisation. Despite the severity of this problem, aneuploidy of the human preimplantation embryo is relatively poorly understood. With this in mind the purpose of this thesis is to explore the premise underpinning the use of preimplantation genetic screening (PGS) in human embryos and investigate its clinical applications and current methodologies. A series of published works demonstrate what I believe to be a significant contribution to the development of applications for studying human preimplantation aneuploidy, also providing insight into its origins and mechanisms at the earliest stages of human development.

Specifically, I present a novel standard set of protocols as a general reference work from practitioners in the fields of embryo biopsy and array comparative genomic hybridisation (CGH - the current 'gold standard' for preimplantation aneuploidy screening). I present a summary of work encapsulated in three published clinical papers using a linkage based analysis of Single Nucleotide Polymorphism (SNP) karyotypes (Karyomapping). Karyomapping was designed as a near-universal approach for the simultaneous detection of chromosomal and monogenic disorders in a PGS setting and these results demonstrate the utility of the technique in three separate scenarios.

In order to study the underlying mechanisms of female meiosis I present my findings on the use of a calcium ionophore to activate human oocytes artificially. An algorithm based on Karyomapping (termed MeioMapping) is demonstrated for the first time specifically to investigate human female meiosis. By recovering all three products of human female meiosis (oocyte, and

both polar biopsies – herein termed “Trios”) using calcium ionophore, I present a novel protocol (commissioned by Nature Protocols) to allow exploration of the full extent of meiotic chromosome recombination and segregation that occurs in the female germline. Finally I present a published set of experiments using this protocol to provide new insight into meiotic segregation patterns and recombination in human oocytes. This work uncovers a previously undescribed pattern of meiotic segregation (termed Reverse Segregation), providing an association between recombination rates and chromosome mis-segregation (aneuploidy). This work demonstrates that there is selection for higher recombination rates in the female germline and that there is a role for meiotic drive for recombinant chromatids at meiosis II in human female meiosis.

The work presented in this thesis provides deeper understanding of meiotically derived maternal aneuploidy and recombination. More importantly it provides a vehicle within an ethical framework to continue to expand our knowledge and uncover new insights into the basis of meiotic errors that may aid future reproductive therapies.

2. General Introduction

2.1. Context of this Thesis

Aneuploidy is defined as extra or missing chromosomes in the nucleus of a cell. It occurs during cell division when chromosomes do not disjoin (separate equally) between the two new daughter cells (Hassold & Hunt 2001). Chromosome imbalance typically results in non-viability, manifesting as developmental arrest prior to implantation, miscarriage or stillbirth. Depending on the chromosomes involved, aneuploidy can also result in viable, but developmentally abnormal pregnancies, e.g. Down or Klinefelter Syndrome. Other clinical manifestations can include intrauterine growth retardation, infertility or imprinting (e.g. Prader Willi) syndromes, particularly if the original conceptus was mosaic (i.e. contained normal and aneuploid cells). As such, aneuploidy is arguably the most significant genetic hazard facing mankind.

Aneuploidy is also predominantly a human-specific problem, occurring more frequently than any other animal studies during both human gametogenesis and early embryogenesis. The most cited mechanism by which it arises is classical 'nondisjunction', however this textbook definition has been challenged repeatedly and alternative mechanisms have been proposed. It is estimated that at least 20% of human oocytes are aneuploid; a number that increases dramatically with advancing maternal age (over the age of 35 years) (Dailey *et al.* 1996b; Hassold & Hunt 2001). Conversely, the incidence of aneuploidy in sperm cells from a normal fertile male is estimated to be as low as 4-7% (Martin *et al.* 1991; Shi & Martin 2000). This can however significantly increase in some cases of severe male factor infertility (Tempest *et al.* 2004; Tempest & Griffin 2004). Given that, once aneuploidy arises in an individual, treatment is limited to mitigation of its worse effects (e.g. Down syndrome); clinical intervention mostly concentrates on reducing the chances of transmitting aneuploidy for high-risk groups, i.e. through preimplantation genetic diagnosis (PGD).

The idea of screening preimplantation embryos to eliminate the aneuploid ones is not new. A derivative of this was first achieved by Gardner and Edwards (in rabbits) in the 1960s (Gardner & Edwards 1968) but the ability to do it effectively has required rapid evolution of diagnostic

technologies to combine speed, accuracy and reliability. To date, only direct analysis of chromosomes from cells in gametes and preimplantation embryos (rather than indirect methods such as metabolic analysis) has proved successful in accurately detecting aneuploidy. Performing PGD in this way (sometimes referred to as PGS – preimplantation genetic screening – or PGD-A – PGD for aneuploidy) involves the biopsy of cellular material from the embryo or oocyte at different stages of development. Since embryo biopsy is an invasive procedure (and thus not currently considered appropriate for routine embryo selection), PGS remains a test for high-risk patient groups only, rather than for routine universal application, and is thus only offered to patients presenting with advanced maternal age, recurrent miscarriage, recurrent implantation failure and in some cases severe male factor infertility (Fritz 2008). Due to the invasive nature of embryo biopsy and the complexity of human aneuploidy in the human *in vitro* fertilisation (IVF) embryo, cost benefit analysis is crucial to achieve positive outcomes. It could be argued that, in the past, the practice of PGS has not given proper concern to these issues and thus, going forward, patient selection and understanding the mechanisms of aneuploidy should be central to an effective PGS strategy. The purpose of this thesis is to explore the premise underpinning the use of PGS in human embryos, its clinical applications and current methodologies, then make a significant contribution to the development of applications while, at the same time, providing insight into the origin of aneuploidy at the earliest stages of human development.

2.2. Origin of Aneuploidy in Humans: Current Thinking

Aneuploidy in human IVF embryos (and presumably those naturally conceived also) can primarily arise during three developmental stages: (i) pre-meiotic divisions during gametogenesis (gonadal mosaicism); (ii) meiotic divisions during gametogenesis; and (iii) early mitotic divisions of embryogenesis. Understanding the mechanism behind the mal-segregation of chromosomes at these stages gives insight into the limitations of PGS when applied clinically, and is a major aim of this thesis.

2.2.1. Gonadal Mosaicism

Errors in germ cell proliferation, or errors inherited in an otherwise somatically normal individual resulting in germ cell aneuploidy (gonadal mosaicism), can also contribute to aneuploidy of the gametes. This is perhaps the least studied of the three stages but has been proposed to account for a small yet significant proportion of aneuploid conceptions, particularly in younger women (Delhanty 2011). Generally mosaic individuals (for example mosaic Turner or Klinefelter syndrome) may be at increased risk of producing aneuploid gametes and PGD should be considered in these cases. In any event, the outcome is a hyper- or hypo-gamete and thus can be considered in a similar way to a meiotic error in the PGS context.

2.2.2. Meiosis and Chromosomal Segregation Errors

Meiosis is the production of a haploid gamete by two specialised cell divisions in which the diploid chromosome complement of normal somatic cells is reduced (a requisite for sexual reproduction). Errors in chromosome segregation during these divisions typically result in gamete aneuploidy and, it is believed, subsequent 'uniform' aneuploidy in any resulting embryo (Hassold & Hunt 2001). Although the basic principle of chromosome mal-segregation holds for both male and female meiosis in humans, the processes and resulting gametes are vastly different. Female meiosis – the process by which a single diploid germ cell develops into a single haploid ovum – involves two unequal meiotic divisions producing a mature ovum and two non-functional products containing mirror images of the chromosomes present in the ovum. These are known as polar bodies and, once extruded, apparently take no further part in development, thus making them a useful sample for inferring chromosome constitution of the oocyte itself. Failures in female meiosis make, by far, the biggest contribution to aneuploidy in human preimplantation embryos. Cytogenetic studies on oocytes and first polar bodies from assisted conception cycles have shown more than 20% of oocytes from patients with an average age under 35 to be aneuploid (Selva *et al.* 1991; Fragouli *et al.* 2006). The percentage of aneuploid oocytes increases significantly with age and has been shown to affect an average of around 70% of oocytes for

patients of advanced maternal age (Van Blerkom 1989; Angell *et al.* 1993; Kuliev *et al.* 2003; Gutierrez-Mateo *et al.* 2004; Kuliev *et al.* 2005).

There is conflicting evidence on the frequency of errors in both the first and second meiotic division with groups showing errors in both the first meiotic division (MI) (Kuliev *et al.* 2003) and more recently in the second meiotic division (MII) (Fragouli *et al.* 2011; Handyside *et al.* 2011) occurring more frequently. This discrepancy may be due in part to differences in patient maternal age of the study groups and the difference in resolution of the cytogenetic techniques used. Either way, it is clear that chromosome segregation errors occur at significant rates during both the first and second meiotic divisions of oogenesis.

Based on studies of yeast, *Drosophila* and mouse models it is generally believed that aneuploidy arises as a result of classic nondisjunction and involves the segregation of a whole chromosome to the same pole as its homologue during meiosis. Studies of human oocytes have led to an alternative model for the origin of aneuploidy (Angell 1991) suggesting that errors in meiosis can result in extra or missing chromatids (known as premature or precocious separation of sister chromatids – PSSC), as well as whole chromosomes in the daughter cells (see Figure 2.1). Early studies of human oocytes supporting the hypothesis that PSSC was the predominant mechanism leading to human aneuploidy (Angell 1991; 1993; 1994; Pellestor *et al.* 2002; Kuliev *et al.* 2003) were, however, subject to recurring criticism. It was argued that use of 'failed IVF' oocytes prolonged time in culture, sub-optimal metaphase preparation technique, and lack of rigour in the analysis may have led to interpretation errors (Dailey *et al.* 1996a; Lamb *et al.* 1996; Lamb *et al.* 1997; Mahmood *et al.* 2000). Recently, several groups performed analyses using methodology less prone to these confounding criticisms – the results of which support the hypothesis. Quantitative analysis of loss or gain of all 24 chromosomes on PB1 (Gabriel *et al.* 2011b) and sequential 24 chromosome analysis of the first (PB1) and second (PB2) polar bodies (and zygote) performed on freshly harvested oocytes used in IVF treatments have shown PSSC to be the predominant mechanism of chromosome mal-segregation in assisted reproduction derived

oocytes. One of the purposes of this thesis is to study the role of PSSC further using tools developed, in part, as a result of this thesis.

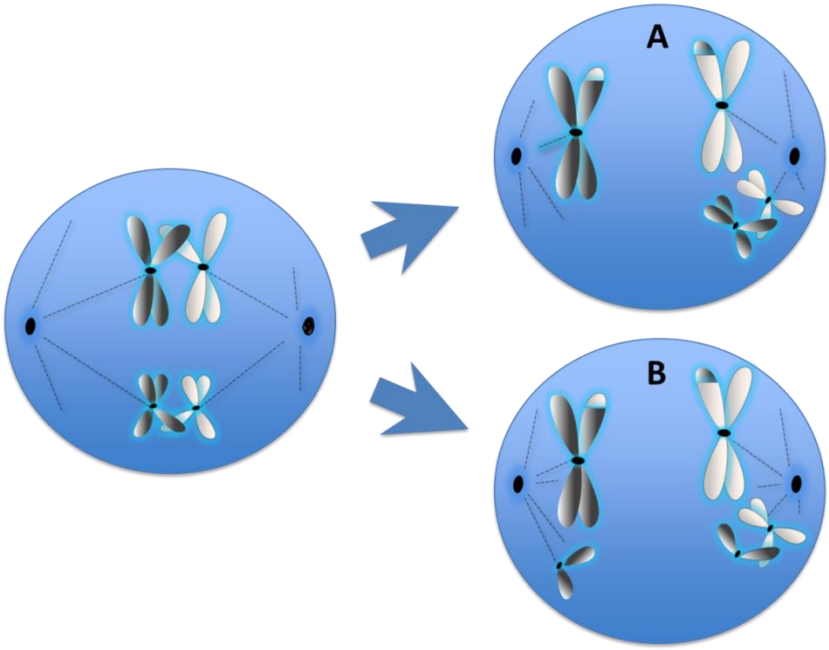

Figure 2.1. Diagrammatic representation of classic non disjunction (A) and premature separation of the sister chromatids (PSSC) (B) - the two ways aneuploidy can arise in the first meiotic division in humans (Ottolini *et al.* 2012).

In contrast to oogenesis, male meiosis results in four equivalent, functional spermatozoa from a single progenitor germ cell. The presence of typically millions of sperm per ejaculate make them easy to study *en masse*, however it is impossible, with current technology, to screen a sperm head for aneuploidy them subsequently use it for IVF/PGS. This is because aneuploidy assessment of a sperm cell inevitably results in its destruction, and unlike in the ovum, there are no by-products available from which a determination of chromosome complement can be inferred.

The overall incidence of aneuploidy in human sperm is estimated to be around 4-7% (Martin *et al.* 1991; Shi & Martin 2000) although some studies suggest it is as high as 14% in some infertile men (Johnson 1998; Shi & Martin 2001; Tempest & Griffin 2004). Spermatogenesis can

theoretically continue unchanged throughout the life of a man, however several studies have shown there to be a correlation between increased sperm aneuploidy and advanced paternal age (Griffin *et al.* 1995; Robbins *et al.* 1995; Fonseka & Griffin 2011), albeit not as dramatic as in the female. Other factors such as male factor infertility, smoking and chemotherapy can however increase sperm aneuploidy levels (Templado *et al.* 2005), making individual couples in which these risk factors are present possible candidates for PGS.

2.2.3. Mitosis and Chromosome Segregation in Early Human Development

Mitosis is the process by which a diploid cell usually divides into two chromosomally identical daughter cells. It is the primary mechanism by which a multicellular individual develops from a single fertilised oocyte (zygote). Human mitotic divisions are generally not prone to chromosome segregation errors to any great extent, except in the case of early embryo cleavage stages where cells are thought to be exquisitely prone to segregation errors (Bean *et al.* 2001). Indeed, recent studies using a variety of cytogenetic techniques on early IVF human embryos have demonstrated that more than 50% are subject to some form of mitotic error (Bielanska *et al.* 2002; Munné *et al.* 2004; Delhanty 2005; Munné 2006).

Most mitotic errors in early embryo development will lead to chromosomal mosaicism, which is defined as the presence of two or more chromosome complements within an embryo developed from a single zygote. There are three mechanisms by which mitotic aneuploidy can arise: (i) mitotic nondisjunction (resulting in one cell line with chromosome loss and one with gain); (ii) anaphase lag (resulting in chromosome loss in one cell line); or (iii) chromosome duplication (resulting in chromosome gain in one cell line) (Taylor *et al.* 2014) (see Figure 2.2). Following observations of increased incidence of chromosome loss in preimplantation embryos compared to gains and the relative paucity of reciprocal events (which would indicate nondisjunction) (Daphnis *et al.* 2005; Delhanty 2005), the predominant mechanism leading to post-zygotic errors in human embryos is likely to be anaphase lag (Coonen *et al.* 2004). Anaphase lag is described as the delayed movement during mitotic anaphase of a homologous chromosome resulting in it

not being incorporated into the nucleus of the daughter cell. The result of this is one euploid daughter cell and a daughter cell with a monosomy for the lagging chromosome (Coonen *et al.* 2004).

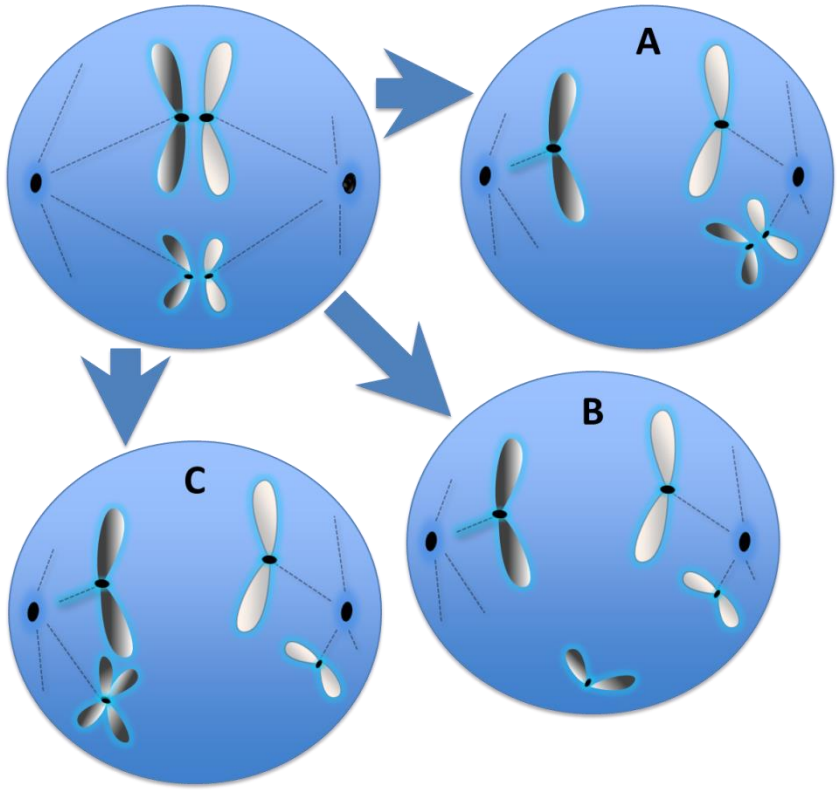

Figure 2.2. Diagrammatic representation of mitotic nondisjunction (A), anaphase lag (B) and chromosome duplication (C) - the three types of mitotic errors in humans resulting in embryo mosaicism (Ottolini *et al.* 2012).

Mosaicism is usually considered to occur largely independent of age (Delhanty 2005). However, it has been shown that mosaicism originating by the mechanism of mitotic nondisjunction could perhaps be related to advanced maternal age (Munné *et al.* 2002). Results also suggest that mosaicism involving multiple chromosomes in a high proportion of cells (chaotic embryos) appear to impair early embryo development considerably (Delhanty 2005)..

The general consensus for the viability of mosaic embryos is that, if more than half of the cells at Day 3 post fertilisation are aneuploid, the embryo is unlikely to be viable. Conversely, if a small proportion of cells are aneuploid in an otherwise healthy and euploid background, it is likely to be

viable (Delhanty 2005). Moreover, in a conceptus that is predominantly aneuploid, the primary error is usually considered to have arisen meiotically (with a second, post-zygotic event creating the euploid lineage) whereas a predominantly euploid mosaic embryo is considered to have arisen purely through a post zygotic error or errors. The occurrence of mosaicism is clearly a primary consideration for a clinical intervention that involves removal (biopsy) of cells to perform a diagnosis, based on the assumption that the diagnosis from the biopsied cells is representative of the embryo as a whole (Bielanska *et al.* 2002; Delhanty 2005).

2.2.4. Abnormal Fertilisation and its Role in Chromosome Abnormality

Abnormal fertilisation can also contribute to chromosome errors in preimplantation embryos. Approximately 1% of conceptions contain more than two paired homologous sets of chromosomes (referred to as polyploidy rather than aneuploidy) (Hassold 1986). There are two ways in which a polyploid embryo can arise: Firstly, if a diploid (2n) sperm or oocyte is involved in the fertilisation event; and secondly, if two or more haploid sperm are involved in the fertilisation of a haploid oocyte (polyspermy). The majority of all polyploid embryos are the result of polyspermy and account for around 60% of polyploid conceptions (Egozcue *et al.* 2002). Following IVF with intra-cytoplasmic sperm injection (ICSI) in which only a single sperm is inserted into each oocyte, the main mechanism leading to polyploidy in the embryo is the failure of the oocyte to extrude the second polar body (Grossmann *et al.* 1997). This results in a triploid embryo when fertilisation is achieved with a haploid sperm. Non-reduced or diploid sperm have also been shown to be involved in as many as 8.3% of polyploid conceptions (Egozcue *et al.* 2002).

2.3. Aneuploidy and the IVF Embryo

Since the first human IVF success in 1978 (Steptoe & Edwards 1978), advances in morphologic embryo grading and technologies aiding morphologic embryo selection have contributed to vastly improved IVF outcomes (Figure 2.3). Unfortunately, the morphological selection criteria for

human gametes and embryos across all developmental stages have shown only weak correlations with aneuploidy levels (Munné 2006; Gianaroli *et al.* 2007; Alfarawati *et al.* 2011a). Karyotypic analysis indicates that there is a higher rate of chromosome abnormalities in morphologically abnormal monospermic embryos than morphologically normal embryos (Pellestor 1995; Almeida & Bolton 1996). However, clear distinctions cannot be made between chromosomally normal and abnormal human embryos by morphological assessment alone (Zenzes & Casper 1992). This may be because chromosome abnormalities detected at the early stages of embryogenesis cannot induce dysmorphism, since embryonic gene expression has not yet commenced (Braude *et al.* 1988; Tesarik *et al.* 1988). There is evidence from 24 chromosome copy number analysis that morphology and aneuploidy are linked at the later stages of preimplantation embryo development (blastocyst stage). However, again the association is weak, and consequently morphologic analysis still cannot be relied upon to ensure transfer of chromosomally normal embryos. A significant proportion of aneuploid embryos are capable of achieving the highest morphologic scores even at the later stages of preimplantation development and, conversely, some euploid embryos achieve only poor morphological scores or even fail to develop (Alfarawati *et al.* 2011a).

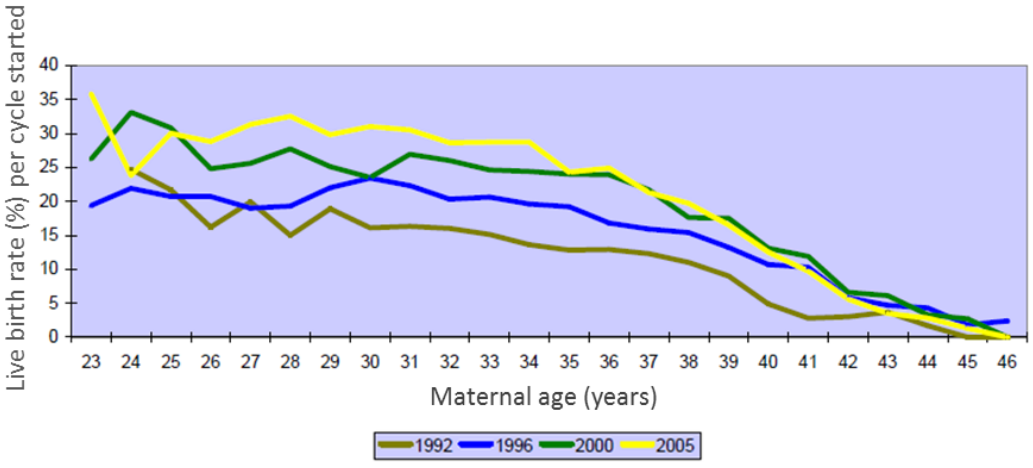

Figure 2.3. Overall IVF and IVF/ICSI success rates by maternal age in the UK from 1992-2005.

Figure adapted from Human Fertilisation and Embryology Authority website [HFEA] (2008a)

http://www.hfea.gov.uk

Other indirect aneuploidy screening methods have been trialled in the past with limited success. More recently, proteomic studies have shown to be a potentially useful tool in prenatal aneuploidy screening (Cho & Diamandis 2011; Kolialexi *et al.* 2011). By applying the same principle to preimplantation embryos, one study has identified the first protein secreted by human blastocysts that is associated with generic chromosome aneuploidy (McReynolds *et al.* 2011). Although promising, this technology is still some way from becoming a routine aneuploidy screening test, and oocyte or embryo biopsy with molecular cytogenetic analysis is still the preferred technique for PGS (Ottolini *et al.* 2014).

All molecular cytogenetic techniques involving gametes and embryos require direct access to the nuclear material of the gametes or blastomeres themselves. This process is achieved for embryos and polar bodies by cell biopsy and inevitably results in the destruction of the cells involved. With this in mind, it is important that fertilisation or embryogenesis is not compromised and the biopsy procedure impacts minimally on developmental potential.

Recent clinical trials and meta-analyses of cases have suggested no benefit, and in some cases worse IVF pregnancy outcomes following PGS; presumably the result of discard of normal embryos (diagnosed as abnormal – false positives), detrimental effects of the biopsy including reduction of cellular mass and excessive micromanipulation outside of the incubator (Mastenbroek *et al.* 2007; Twisk *et al.* 2008). These results have, however, been dismissed by many PGS practitioners due to questionable experimental design (Handyside & Thornhill 2007; Munné *et al.* 2007). Nevertheless, at the very least, these trials have reinforced the idea that embryo biopsy can only be justifiable when the benefit of the testing outweighs the cost to the embryo, since the ultimate aim of PGS is to identify chromosomally competent embryos without compromising embryo viability. The technique of biopsy is thus crucial to the overall success of PGS.

2.4. The Biopsy of Oocytes and Embryos for PGS

Biopsy for PGS is currently a two-step micromanipulation process involving the penetration of the zona pellucida followed by the removal of one or more cells for chromosome analysis. Breaching the zona is now generally performed by laser ablation (as opposed to the original techniques involving acid Tyrode's solution) as it has been shown, when used appropriately, to have no detrimental effects on embryo development in both animal and human studies (Montag *et al.* 1998; Park *et al.* 1999; Han *et al.* 2003). Specialised micromanipulation pipettes are then used to separate the required cells from the oocyte or embryo. Theoretically, PGS can be accomplished at any developmental stage from the mature (MII) oocyte to the blastocyst stage. To date, however, only three discrete stages have been proposed for clinical use: (i) polar body (oocyte and/or zygote); (ii) cleavage stage (day 3 embryo); and (iii) blastocyst (day 5, 6 or 7 embryo). Each of these stages is biologically distinct, thus having different diagnostic limitations in terms of information to be gained and impact on embryo viability. A more complete technical overview and set of guidelines for the practice of embryo biopsy was a specific aim of this thesis and is given in the subsequent chapter. For context, however, the basic principles of the approach are given below.

2.4.1. Polar Body Biopsy

The removal of the first and/or second polar body (PB1/PB2) from a human oocyte should, theoretically, have no deleterious effect on subsequent embryo, foetal and infant development as neither is required for successful fertilisation or embryogenesis (Gianaroli 2000; Strom *et al.* 2000). Biopsy and subsequent analysis of the first and second polar bodies allows the indirect interpretation of the chromosome complement of the corresponding oocyte, thereby allowing the detection of maternally derived aneuploidy in resulting embryos (Verlinsky *et al.* 1996). While biopsy of PB1 alone and a combined PB1 and PB2 strategy have been used clinically for PGS, it is becoming increasingly evident that PB1 alone has limited applicability to PGS, as only errors in MI can be detected and even MI chromatid segregation errors may not all be detected without

analysis of both polar bodies. Indeed, as much as 30% of aneuploidy of maternal origin will not be diagnosed if only PB1 is sampled (Handyside *et al.* 2011). It is therefore now becoming increasingly apparent that biopsy of both first and second polar body is essential for optimal detection of oocyte aneuploidy if used as an embryo selection tool. A further limitation is that cytogenetic analysis of either polar body does not allow the detection of aneuploidies of paternal origin nor aneuploidies arising after fertilisation in the embryo.

The process of polar body biopsy is relatively labour intensive and may involve the micromanipulation of oocytes that ultimately do not develop into therapeutic quality embryos. Sometimes up to four manipulations – ICSI, PB1, PB2 and blastomere biopsy (as a reflexive test following test failure or an ambiguous PB result) – may be required. However, in experienced hands, even 3 independent biopsy manipulations appear to have no deleterious effect on development (Magli *et al.* 2004; Cieslak-Janzen *et al.* 2006). Although simultaneous removal of PB1 and PB2 is possible on day 1 of embryo development (Magli *et al.* 2011) there may be advantages to sequential biopsy where PB1 is removed on day 0 (day of insemination) followed by the removal of PB2 on day 1. This is to avoid any degeneration of PB1 leading to possible diagnostic failure, and also to allow for the distinction between polar bodies, thereby allowing accurate identification of errors in the first and second meiotic divisions.

2.4.2. Cleavage Stage Embryo Biopsy

Historically cleavage stage biopsy was the most widely practised form of embryo biopsy for PGS worldwide. This biopsy strategy is now becoming less popular however, due to its potential detrimental effect on embryo viability and the problem of mosaicism in human cleavage stage embryos (Scott *et al.* 2013; Taylor *et al.* 2014). A typical procedure for cleavage stage biopsy involves the removal of one or two blastomeres from an embryo on day 3 post-fertilisation – usually those of suitable quality with at least five cells having entered the third cleavage division. Although cleavage stage biopsy allows the detection of maternally and paternally derived aneuploidy as well as meiosis I, II and post-zygotic errors, they are considered as a uniform group

and not distinguishable from one another. One purpose of this thesis is to make a significant step towards rectifying this issue. Indeed, the main problem of PGS associated with cleavage stage biopsy is chromosomal mosaicism, that can result in an increased rate of false positive and negative results from single cell (or two cell) analysis (Figure 2.4). As mentioned above, however, if zygotic and post-zygotic errors could be distinguished, the prognostic value of PGS could be increased.

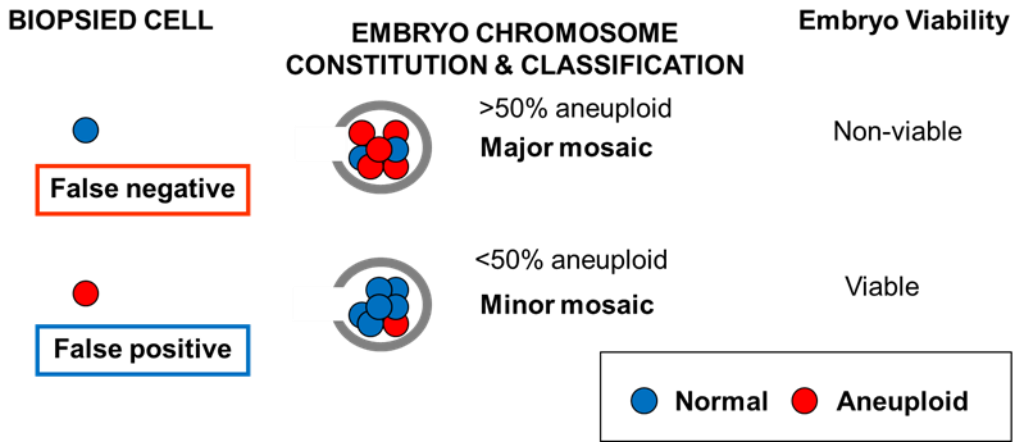

Figure 2.4. Schematic representation of possible misdiagnosis following cleavage stage biopsy of a single cell (Ottolini *et al.* 2012).

Some studies comparing undiagnosed cleavage-stage biopsied embryos and non-biopsied control embryos have shown a detrimental effect of biopsy on implantation (Cohen & Grifo 2007; Mastenbroek *et al.* 2007), most evident in embryos of suboptimal quality. Studies of animal models have also shown that the potential for the embryo to continue to develop and implant is progressively compromised the greater the proportion of the embryo is removed (Liu *et al.* 1993). While such evidence provides fuel for the argument against performing biopsy at early cleavage stages at all, evidence from frozen-thawed embryo transfers (as a proxy for biopsied embryos) in which successful implantations and live births can be achieved even following embryonic cell death demonstrates that a certain degree of cell loss is tolerated (Cohen *et al.* 2007). However, just as in the animal models, success is inversely correlated with the amount of cellular mass lost.

The successful application of cleavage stage biopsy minimising cell removal from good quality embryos shows it is compatible with normal embryo metabolism, blastocyst development and foetal growth (Hardy *et al.* 1990). Moreover, studies of pregnancies and children born after cleavage stage biopsy have identified no significant increase in abnormalities above the rate seen in routine IVF (Harper *et al.* 2006; Banerjee *et al.* 2008; Nekkebroeck *et al.* 2008).

A general consensus therefore is that cleavage stage biopsy of one cell may reduce the implantation potential of an IVF embryo of around 10%, although this figure would inevitably increase in less experienced hands (Cohen & Grifo 2007). The challenge for any future application of cleavage stage biopsy PGS, therefore, is to ensure that any benefits outweigh these costs; and it remains a question whether this will be possible even with more accurate and reliable tests, given the high levels of mosaicism.

2.4.3. Blastocyst Stage Biopsy

Blastocyst biopsy involves the sampling of trophectoderm (TE) cells, the spherical outer epithelial monolayer of the blastocyst stage embryo. Just as at cleavage stage, TE biopsy is able to detect aneuploidy arising in either gamete or post-fertilisation. It is more akin to early prenatal diagnosis when compared to the other biopsy stages as it involves the removal of around 10 cells without depleting the inner cell mass from which the foetus is derived (discussed in more detail in Aim 1a of this thesis). TE biopsy is most commonly achieved by partial zona dissection followed by a period of culture, in which time the expansion of the blastocyst will cause herniation of several cells through the artificial breach. The herniating cells (~4-10 cells) are then easily removed by excision or aspiration using micromanipulation tools with or without the aid of a laser. Sampling of several cells at this stage lessens the effect of mosaicism on producing false positive results, also overcoming the limitations of extreme sensitivity apparent with conventional single cell diagnosis (discussed in more detail in Aim 1a of this thesis).

As with cleavage stage biopsy, it has been suggested that the removal of cells may negatively impact on the embryo's developmental potential. However, skilled biopsy practitioners are able to remove trophectoderm cells and achieve comparable implantation rates to non-biopsied blastocyst stage embryos (Kokkali *et al.* 2007). It has also been proposed that sampling of the TE may not reflect the genetic composition of the inner cell mass (ICM) (Kalousek & Vekemans 1996). However, recent data comparing TE to ICM suggests 100% concordance with the exception of structural abnormalities (Johnson *et al.* 2010a).

Currently the main limitation of blastocyst biopsy is the low number of embryos that reach the blastocyst stage; a number that significantly decreases with advanced maternal age (Pantos *et al.* 1999). If very few blastocysts are available, particularly in older patients, biopsy for selection purposes may be of no benefit. Also, time constraints at the blastocyst stage dictate, in many cases, the need to cryopreserve biopsied blastocysts awaiting diagnosis. Thus, the effect of cryopreservation and subsequent thawing on embryo viability must be taken into account. Nonetheless, improved culture techniques, possible vitrification and rapid molecular analysis regimes are making blastocyst biopsy an increasingly attractive option (Schoolcraft *et al.* 2010).

2.5. Techniques Involved in PGS for Aneuploidy Screening

2.5.1. The Rise and Fall of Fluorescence In-Situ Hybridisation (FISH) as a Diagnostic Tool for PGS

Following embryo or oocyte biopsy, PGS requires cytogenetic techniques with high sensitivity and specificity to establish the chromosome composition of the embryo via the analysis of one or very few cells. Classic karyotyping techniques have proved unsuitable for preimplantation testing due to the difficulty of achieving good metaphase spreads with the limited cells available for testing (Angell *et al.* 1986; Papadopoulos *et al.* 1989). In 1993 the application of Fluorescent In-situ Hybridisation (FISH) for the single cell detection of the sex chromosomes in preimplantation embryos provided a springboard for aneuploidy detection, and clinical application of PGS soon

followed (Griffin *et al.* 1992; 1993; 1994). FISH is a highly sensitive, relatively inexpensive molecular cytogenetic tool enabling the determination of chromosome copy number at the single cell level. Its successful application rapidly led to the implementation of PGS as a clinical adjunct to IVF globally (Wilton 2002). To date, tens of thousands of PGS cases have been performed globally, attesting to its popularity (Verlinsky *et al.* 2004; De Rycke *et al.* 2015). Nonetheless, advances in technology are making FISH for PGS in oocytes and embryos a less attractive option due to a range of technical and biological considerations that are becoming increasingly apparent. These are summarised in Table 2.1.

Table 2.1: Scope and Limitations of the Three Molecular Cytogenetic Techniques on Embryo Biopsy (Ottolini *et al.* 2012).

Test	Chromosomes detected	Resolution	Parental DNA required	Polyploidy	Recombination mapping	Origin of aneuploidy	
						parent of origin	MI or MII
Fluorescence in situ hybridization (FISH)	5 to 12	low	no	yes	no	no	no
Array comparative genomic hybridisation (aCGH)	24	high	no	no	no	no	no
Single nucleotide polymorphism (SNP) array	24	highest	yes	yes	yes	yes	limited to hyperploidy

2.5.2. The FISH Technique

FISH requires the fixation of biopsied cells to a glass slide before visual analysis of hybridised fluorescent chromosome-specific DNA probes. That advantage to the observer of being able to view the presence of chromosome copy number directly is considerable. Technical problems, however, include the fact that FISH signals can overlap (making two signals appear as one, or three as two) or 'split' according to the stage of the cell cycle, making a single signal appear as two (Cohen *et al.* 2009). In the early days of clinical PGS up to five different fluorescent probes, attached to different chromosomes (typically 13, 16, 18, 21, 22 or 13, 18, 21 X and Y), were used. However, more recent studies analysing up to 12 chromosomes (X, Y, 2, 4, 13, 15, 16, 18, 19,

20, 21 and 22) at the cleavage stage described detection of 91% of chromosomally abnormal embryos reaching the blastocyst stage (Munné *et al.* 2010). In this case, if the misdiagnosis rate of each probe averaged 1%, over the two rounds of hybridisation required, an accuracy of only 88% per embryo could be achieved. The test's ability to diagnose only 91% of aneuploid embryos compounded by the 12% misdiagnosis rate per embryo would result in only 80% efficiency of the test in its ability to diagnose aneuploidy per embryo. This would inevitably result in the transfer of aneuploid embryos (false negative) or the discarding of euploid embryos (false positive). It has been widely accepted that the efficiency of each probe is reduced in subsequent hybridisation rounds (Harrison *et al.* 2000); however, a 24 chromosome FISH assay has recently been applied to preimplantation human embryos with no apparent loss of signal, even after four rounds of hybridisation (Ioannou *et al.* 2011; 2012). This technique, albeit more comprehensive, is still prone to the other issues as described above and has not been validated clinically.

The importance of low error rates on the diagnostic efficiency of PGS is strongly argued (Summers & Foland 2009; Munné *et al.* 2010), as is the need to detect all chromosomes simultaneously for aneuploidy. Notwithstanding the ability now to detect all 24 chromosomes by FISH, the issues of mosaicism, signal interpretation, clinical trial data and the development of microarray-based methods for detecting 24 chromosome copy number are now signalling the demise of FISH-based PGS approaches. Microarray-based tests are now becoming the standard and these have been made possible through the advancement of whole genome amplification (WGA) technology.

2.5.3. Whole Genome Amplification (WGA) as a Prerequisite for Chromosome Analysis for PGS

The introduction of WGA techniques has led to new, more efficient 24 chromosome molecular karyotyping tests. WGA brought with it the potential to increase the amount of cytogenetic information that can be obtained from a single nuclear genome contained in one cell. A single cell contains 6pg of DNA – far less than the 0.2-1.0µg usually required for microarray analysis – and

thus the need for amplification is paramount (Wells & Delhanty 2000). The process simply involves the transfer of the cell(s) to a microfuge tube followed by cell lysis prior to genome amplification, either by polymerase chain reaction-based methods or, more recently, multiple displacement amplification (MDA) to yield quantities of DNA in excess of 20µg from a single cell. These products can in turn be used for genome-wide analysis studies to establish chromosome copy number with impressive accuracy. One of the biggest drawbacks of single cell DNA amplification is a phenomenon known as allele dropout (ADO), where only one of the two alleles at a locus successfully amplify (Walsh *et al.* 1992; Findlay *et al.* 1995; Piyamongkol *et al.* 2003). This proved a limiting factor on the resolution and reliability of PGD for single gene disorders where individual gene sequences are analysed, but is less of an issue for array-based PGS where many probes along each chromosome are used (Ling *et al.* 2009). Further problems involving the extreme sensitivity of single cell analysis still exist in the form of failed or poor amplification. However, these failure rates can be maintained at less than 3% in experienced laboratories (Gutierrez-Mateo *et al.* 2011).

2.5.4. Comparative Genomic Hybridisation (CGH)

A detailed overview of array CGH including technical guidelines is a specific aim of this thesis and is thus given in a subsequent chapter. A general overview is given here, however, for contextual purposes.

Originally designed for molecular karyotyping of tumour cells (Kallioniemi *et al.* 1992; Kallioniemi *et al.* 1993), comparative genomic hybridisation (CGH) has been successfully adapted for the analysis of human polar bodies and preimplantation embryonic cells (Voullaire *et al.* 2000; Wells *et al.* 2002). Originally a labour-intensive and time-consuming procedure involving hybridisation to and analysis of standard cytogenetic metaphase chromosome preparations, CGH was adapted for use in microarray technology, which allowed streamlining of the process. Recent successful applications of the technology have enabled array CGH (aCGH) to become the gold standard for

PGS and is the current platform of choice for all biopsy stages in the majority of laboratories around the world (Hellani *et al.* 2008; Alfarawati *et al.* 2011b; Harton *et al.* 2013).

The process involves the separate labelling of the amplified DNA and normal reference sample using different fluorescent dyes followed by co-hybridisation to several thousand probes derived from known regions of the genome printed on a glass slide. Using quantitative image analysis, differences in the fluorescence ratio are interpreted to identify gained or lost regions along all chromosomes simultaneously, with an error rate of less than 2% (Gutierrez-Mateo *et al.* 2011). The main technical limitations of this process are: (i) that it does not supply information about chromosomal ploidy *per se*, only deviations from the most frequent level of the combined fluorescence signal; and (ii) the origin of the error is not determined. Thus haploid and polyploid embryos will appear diploid or 'normal' and meiotic errors are not distinguished from post-zygotic ones. Despite these limitations, aCGH is rapidly establishing itself as the 'gold standard' for PGS, replacing FISH-based approaches in most laboratories.

2.5.5. Single Nucleotide Polymorphism (SNP) Arrays

Single Nucleotide Polymorphisms (SNPs) are the most frequent form of DNA variation in the genome. To date over six million SNPs have been identified in the human genome (Javed & Mukesh 2010). SNPs are bi-allelic genetic markers that can be used in a variety of ways to detect chromosome copy number. SNP micro-arrays are used to detect the specific alleles present in polar bodies or embryos at up to 500,000 SNP loci. This information can, in turn, be interpreted in several ways to obtain massive amounts of genetic information. Simple quantification of the SNP alleles and analysis of heterozygosity enables diagnosis of aneuploidy including uniparental isodisomy (Northrop *et al.* 2010; Brezina *et al.* 2011; Treff *et al.* 2011). Using this method, results can be difficult to interpret above the level of background 'noise' due to the problem of amplification from a single or few cells. For this reason, methods involving comparison with parental DNA have been developed (Handyside *et al.* 2010; Johnson *et al.* 2010b; Gabriel *et al.* 2011b). Since all embryonic chromosomes are derived from parental chromosomes, predicted

genotypes based on known parental data can be used to 'clean' noisy single cell data resulting in a comprehensive and highly reliable molecular cytogenetic test for chromosome copy number (Johnson *et al.* 2010b). In addition to this, again with the aid of the known parental genotypes, a test involving Mendelian inheritance analysis of SNPs known as 'Karyomapping' has been developed. By establishing the four parental haplotypes, only informative 'key' SNPs are analysed to establish chromosome copy number, parental origin and points of meiotic recombination of the tested cells can be 'Karyomapped' (Handyside *et al.* 2010). Karyomapping has the added advantage of being able to detect not only meiotic aneuploidy, but the presence of the chromosomes carrying the mutant allele for cases involving the risk of transmission of specific known inherited disorders. Karyomapping is a technique that is central to this thesis, and part of its development as both a clinical tool and a means of understanding chromosome segregation in humans is a core element.

SNP genotyping has the potential to be the most comprehensive means for PGS. The interpretation of a SNP genotype allows diagnosis of all possible chromosome copy number aberrations. It has the capacity to perform as a high-resolution molecular cytogenetic test at higher resolution than aCGH for all types of chromosomal gains and losses, with the added ability of linkage-based analysis allowing diagnosis of inherited genetic disease (Handyside *et al.* 2010). Although largely clinically un-validated, comparative data with other platforms suggest better efficiency than both FISH and aCGH for aneuploidy screening (Johnson *et al.* 2010b; Treff *et al.* 2010a; Treff *et al.* 2010b). Recently presented clinical data of SNP array-based PGS on cleavage stage embryos suggests significant improvement of pregnancy rates following embryo transfer (Rabinowitz *et al.* 2010). One purpose of this thesis is to establish that, with further clinical validation, SNP genotyping will become part of the gold standard for PGS in the near future.

2.5.6. The Principles of Karyomapping: a technique for the simultaneous detection of single gene disorders and (the phase and parent of origin of) chromosome copy number abnormality

As mentioned previously, Karyomapping is a technique by which Mendelian principles are applied to SNP genotypes (genome-wide) to establish inheritance of chromosomes or parts of chromosomes through generations in the same family (Handyside *et al.* 2010). When applied to biopsied cells from preimplantation embryos this allows for: 1) detection of inherited diseases without patient specific test development; 2) detection of chromosomal aneuploidy or imbalance; 3) determining the parental origin of aneuploidies; 4) determining the meiotic origin of any detected trisomic chromosomes; and 5) pinpointing of meiotic genetic recombination sites.

The basic principles of Karyomapping are as follows:

1. Identifying informative SNP loci for parental haplotypes. Informative SNPs are defined as any SNP locus at which one parent is homozygous and the other parent is heterozygous. The heterozygous SNPs are informative. The minor allele (the allele that is only present in the heterozygous parent) is considered the Key SNP allele.

2. Identifying the genotype of an embryo at the predefined informative loci for both maternal and paternal SNPs. This is performed on WGA products of biopsied cells from the embryo. The embryo's genotype will identify which parental haplotype (SNP) was inherited from the heterozygous parent.

3. Using a reference genotype to establish phase. By comparing the embryo's genotype to that of a close relative (usually either genomic DNA from a sibling or grandparent for highest resolution), phase can be established. Comparing the embryo's genotype to a reference reveals which grandparental SNP (grandparental chromosome) was inherited in relation to the reference, unscrambling the haplotypes. By following the Key SNP allele, the SNP will either be the same or different to the reference and when successive loci are mapped it produces the Karyomap (Figure 2.5).

4. Identifying points of meiotic recombination (or crossover) as a shift from one grandparental haplotype to another within a chromosome. Crossovers in the reference will appear in an embryo's Karyomap as an inherent part of the process. If necessary,

these can be identified and removed; a technique that was developed as part of this thesis. This is discussed in detail in chapters 4 and 5.

Currently Karyomapping has been optimised using MDA for WGA and the Illumina platform for SNP genotyping. However, these principles can be theoretically adapted to any platform that detects SNPs. Thus, Karyomapping has an element of future-proofing as technology for SNP detection progresses.

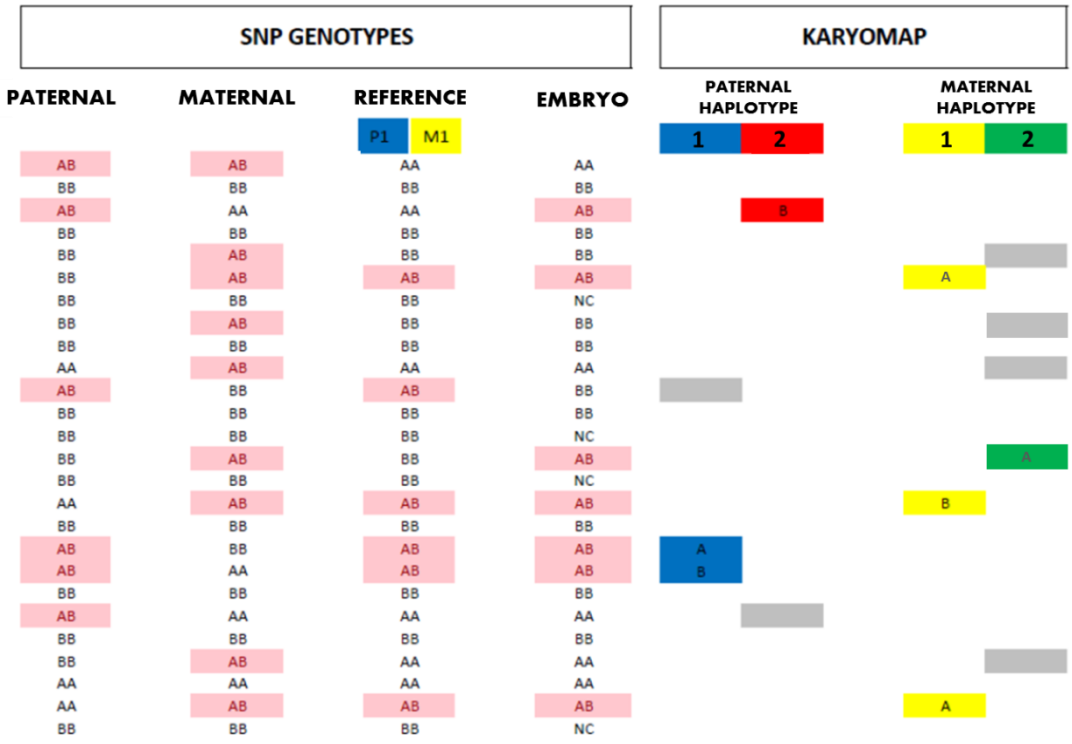

Figure 2.5. Schematic representation of the rules for Karyomapping.

Paternal, maternal, reference and a single embryo's SNP genotypes are displayed in sequence. Highlighted in pink are the heterozygous loci which enable the identification of the Key SNPs (where one parent is heterozygous) and the Key SNP allele (the allele that is present in only one of the four paternal haplotypes). By comparing the genotype of the embryo to the genotype of the reference at all informative loci the pattern of inheritance is established. The following rules apply: i) If the key SNP allele is present in both embryo and reference the parental haplotype (1) is allocated for the Karyomap (solid colour same as reference); ii) If the Key SNP allele is present in

the embryo but not the reference the parental haplotype (2) is allocated for the Karyomap (solid colour different to reference); iii) If the Key SNP allele is not present in the embryo but is present in the reference no parental haplotype is allocated for the Karyomap (grey). These loci are only considered semi-informative due to the relatively high potential of ADO of the Key SNP following WGA of single cells.

2.6. What we Have Learnt from PGS Thus Far?

It is estimated that 30% or more of even naturally conceived embryos contain the incorrect number of chromosomes (Hassold & Hunt 2001). PGS results indicate that this value may be significantly higher following assisted reproduction technology (ART) even in younger patients (Baart *et al.* 2006). Increased aneuploidy is especially evident in poor prognosis patients such as those with recurrent implantation failure (RIF) and recurrent miscarriage (RM) (Magli *et al.* 1998; Baart *et al.* 2006). Furthermore, early cytogenetic analysis also revealed evidence that reduced fecundity with advancing maternal age is, in part, due to increasing rates of aneuploidy (Munné *et al.* 1995). In these groups of patients the success rates of ART remains low despite significant advances in other patient groups (Figure 2.6). It was therefore hypothesised that if embryo ploidy could be determined and euploid embryos selected for embryo transfer, IVF pregnancy rates would increase and poor outcomes such as implantation failure and miscarriage would decrease. Few disagree with this premise, underpinning PGS as scientifically and clinically sound.

Since its inception in the mid-1990s, PGS has primarily involved the biopsy of one or two cells on the third day of embryo development followed by targeted chromosome analysis using FISH. Subsequently, diagnosed euploid embryos (for the limited number of chromosomes analysed) were transferred or cryopreserved, with the remaining embryos diagnosed as aneuploid being discarded (with or without follow-up confirmation analysis). This work was based on the theoretical premise of PGS without the support of randomised controlled trials (RCTs). All recent RCTs using cleavage stage biopsy followed by FISH analysis showed no improvement in delivery rates after PGS, with some even suggesting adverse outcomes (Staessen *et al.* 2004;

Mastenbroek *et al.* 2007; Blockeel *et al.* 2008; Hardarson *et al.* 2008; Mersereau *et al.* 2008; Debrock *et al.* 2010). The largest of these trials included over 200 patients in each of the experimental arms (control and treatment groups) and concluded that PGS resulted in a reduced delivery rate following IVF (Mastenbroek *et al.* 2007). These results, contrary to the original premise of PGS, sparked much debate with several institutions, including the practice committees of the Society of Assisted Reproductive Technology and the American Society of Reproductive Medicine (SART & ASRM) (2008b) and the British Fertility Society (Anderson & Pickering 2008), issuing statements that PGS should no longer be performed. Meanwhile, several groups criticised the trials for their poor diagnostic efficiency, practical skill levels, inappropriate patient selection and generally low pregnancy rates. They claimed that the trials were performed by inexperienced practitioners, thereby generating invalid or questionable results (Cohen & Grifo 2007; Simpson 2008).

What is not in question is that these trials have ultimately highlighted the complexity of considerations PGS requires when applied clinically. FISH of cleavage stage biopsies has clearly outlined that both technical and practical limitations exist when performing PGS to improve pregnancy outcomes. Furthermore, there is great importance and careful consideration needed in patient selection as well as an effective test selection and implementation on a case-by-case basis (Handyside & Thornhill 2007).

The success of aneuploidy screening as a selection tool for IVF to improve pregnancy rates is dependent on the efficacy of the entire testing process. It is now clear that FISH, especially for cleavage stage biopsy, is not the optimal tool for PGS. The process is subject to the following technical limitations: (i) the efficacy of the cell preparation technique; and (ii) the accuracy of the FISH test itself and its reliable interpretation. Biologically, we are constrained by the products we have to work with (embryo quality, mosaicism and nucleation) and the time in which to work with them. I believe that there is scope for PGS to improve pregnancy rates in ART, but the test used must be optimised and tailored to suit the biological and technical limitations that exist to maximise benefit at the lowest possible cost to the embryo.

2.7. Clinical Applications and Decision-Making

Aneuploidy screening by PGS using 24 chromosome micro-array analyses should improve IVF outcomes with the implementation of case-by-case cost-benefit analysis. For best results, PGS should be performed with the most comprehensive cytogenetic platform available. Currently, PGS is still considered too invasive to be employed as a routine embryo selection tool for IVF; thus, at present, it should be offered only to patients at high risk of aneuploidy. The cost of the biopsy on embryo development is only justifiable if the information gained will outweigh the cost to the cohort of embryos as a whole. For this reason, false positive results due to mosaicism and the number of testable embryos in a cohort are important in the decision-making process. Advanced maternal age (AMA) is the single largest indication for PGS as an adjunct to embryo selection to improve IVF success. Careful patient selection is still required within this group of patients to achieve the best results (see Figure 2.6). There are a number of other indications for which PGS is likely to be of most benefit, all of which are associated with a potential increased risk of aneuploidy including patients with RIF and RM. Patients with diagnosed high levels of sperm aneuploidy or severe male factor infertility may also benefit.

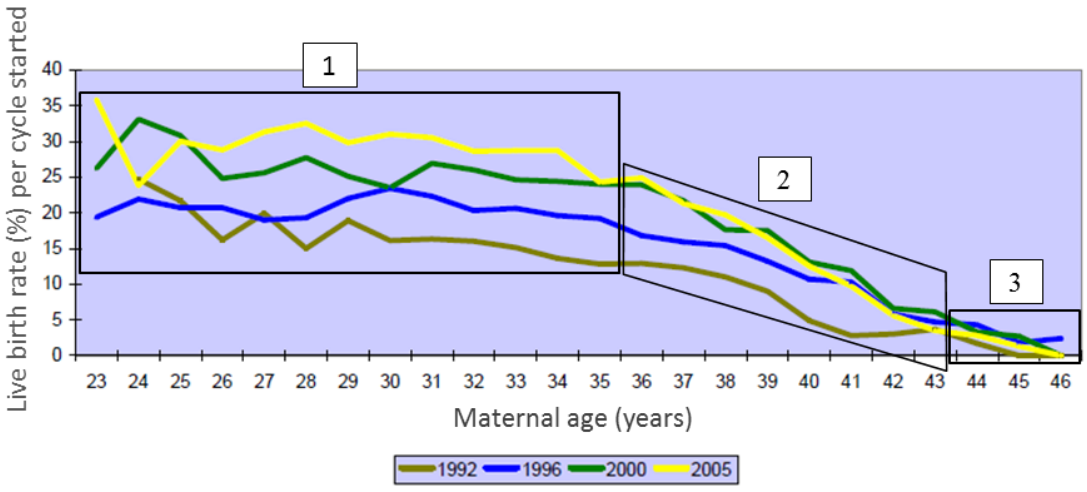

Figure 2.6. Three distinct patient groups in relation to age and IVF success rates (Ottolini *et al.* 2012).

Note the drop in success rates beyond maternal age 35 across all years (consistent with increasing rates of aneuploidy). High number of embryos and low rate of aneuploidy are expected in patient group under 35 years of age (1), thus PGS is not recommended as cost outweighs benefit of PGD. Moderate embryo numbers and increased rate of aneuploidy consistent with reduced IVF success rates of patients above 35 years (2) indicate a target group for PGS, so benefit of PGS outweighs its cost. PGS is suggested to be of no benefit for embryo selection in patients of severe AMA due to low number of embryos and high rate of aneuploidy (3), so cost outweighs benefit of PGD. Figure adapted from Human Fertilisation and Embryology Authority website (HFEA) (2008a) http://www.hfea.gov.uk

Biopsy is generally performed at three discrete developmental stages (PB, cleavage and blastocyst stage), each of which has distinct diagnostic advantages and limitations. Information gained at each developmental stage of the biopsy is critical, and specific strategies for PGS should be employed for different combinations of indication factors rather than a one-size-fits-all approach (Table 2.2).

PB biopsy theoretically has the lowest cost to embryo development but only gives information about maternally derived aneuploidy. PB biopsy is therefore of most benefit to patients of AMA with no other suspected aneuploidy input. Both PB1 and PB2 should be sampled to ensure that the majority of maternally aneuploidy is detected (Geraedts *et al.* 2011).

Theoretically, blastocyst stage biopsy is the optimal stage as it partially negates the problem of mosaicism and gives maximum aneuploidy information from maternal, paternal and post-zygotic events. In addition, the biopsy of 5-10 cells virtually eliminates the problem of ADO following WGA (Ling *et al.* 2009). However, the logistical downside is that embryos may need cryopreservation whist awaiting genetics results, a potential additional ‘cost’ to embryos. Furthermore, blastocyst development may be limited in some patients, leading to a limited cohort of blastocysts that can be biopsied simultaneously, reducing the chance of a live birth and genetic information from the cohort (Janny & Menezo 1996). Thus it should only be considered for

patients with RIF and RM, including male factor, with evidence of good blastocyst formation or proven fertility.

The inherent problem of mosaicism and false positive results is a major problem for biopsy at the cleavage stage. This, paired with the cost of removing a significant amount of the cell mass (up to 25%), suggests that use of cleavage stage biopsy should be limited to cases of male factor aneuploidy with known poor ability for blastocyst development. Removal of only a single cell is recommended to minimise cost to the embryo and prevent the dilemma of discordant results due to mosaicism (Cohen *et al.* 2007). Cleavage stage biopsy may also be considered as follow-up for equivocal results from PB biopsy (Magli *et al.* 2004; Cieslak-Janzen *et al.* 2006); see Table 2.2.

Table 2.2: Technical Limitations, Costs and Benefits of the Established Biopsy Stages for PGD-AS (Ottolini *et al.* 2012)

Biopsy stage	origin of aneuploidy					Detection of mosaicism	Day of biopsy - days post fertilisation	Associated costs and benefits	
	Maternal		Paternal						
	MI	MII	MI	MII	Post Zygotic			Benefit	Cost
PB1	yes	no	no	no	no	no	Day 0 (day of fertilisation)	Minimal manpulations. No removal of viable cells. Maximum time for analysis prior to embryo transfer.	Only information from maternal MI.
PB1 & PB2	yes	yes	no	no	no	no	Day 0 and 1	No removal of viable cells. Maximum time for analysis prior to embryo transfer.	Only information for maternal meiotic errors.
Cleavage stage (blastomere)	yes	yes	yes	yes	yes	no (Yes with limited sensitivity if >1 cell analysed)	Day 3	Information for all origin of aneuploidy. Maximise number of embryos tested. Paternal aneuploidy detected.	Mosaicism resulting in false positive and negative results. Removal of significant proportion of cell mass.
Blastocyst stage (trophectoderm)	yes	yes	yes	yes	yes	yes (only with limitation on sensitivity)	Days 5 and 6	Information for all origin of aneuploidy. Biopsy of several cells (~10 cells). No harm to ICM. Paternal aneuploidy detected.	Reduced number of embryos for testing (requires good blastocyst formation). Reduced time for diagnosis (embryo cryopreservation potentially nececary).

Biopsy, irrespective of stage, should only be performed if there are a sufficient number of oocytes or embryos to be tested. If there is limited or no embryo selection to be achieved by PGS then it (PGS) should be avoided, as there will be no benefit to IVF success rates and may even be a detrimental effect (Summers & Foland 2009). An exception to this is when PGS is used not as an embryo selection tool but as a diagnostic tool to avoid or diagnose aneuploidy. Some patients may require elimination of the possibility of aneuploidy resulting in poor outcomes such as miscarriage or birth of a child with a genetic defect. These 'must screen' patients for PGS should be considered a more likely diagnosis of inherited genetic disease and all embryos, irrespective of the number and quality, should be tested.

2.8. Specific Aims of the Thesis

Since the introduction of molecular cytogenetics into the field of human preimplantation embryos a wealth of information has been gathered on the incidence, origin and aetiology of aneuploidy. It is now well documented when and how extra or missing chromosomes arise but the big question remains 'why'. Research into the origin of human aneuploidy is clearly much needed and will

continue to provide new and exciting insights in the field. The primary purpose of this thesis is to help provide such insight. The introduction of new array technology, including SNP genotyping Karyomapping, will further improve PGS strategies and a further aim of this thesis is to bring these techniques to full clinical application.

Along with advanced maternal age, altered recombination in meiosis is the most important known aetiology related to aneuploidy and gives clues to the overall mechanism (Hassold *et al.* 2007). Algorithms applied to SNP genotyping data, including Karyomapping, can be applied for high resolution pinpointing of recombination points (Handyside *et al.* 2010; Gabriel *et al.* 2011a) and in this thesis I will explore this role further. Patterns of recombination across the genome can be correlated with chromosome mal-segregation in meiosis in an attempt to find aberrant patterns that predispose to aneuploidy. Similar strategies can be employed to different patient profiles to ascertain further aetiologies associated with aneuploidies of different origin. Further understanding of the predisposition to human aneuploidy may ultimately therefore lead to specific patient treatment, and more importantly guide the direction of studies on the molecular basis of aneuploidy. Once the mechanisms leading to aneuploidy are understood and there is an understanding of why it occurs, interventions to prevent aneuploidy could be usefully investigated.

Both scientific and clinical advance, however, require novel and robust tools and with this in mind, the specific aims of this thesis were as follows:

1. To review the literature, produce and publish a state of the art standard set of protocols as a general reference work from practitioners in the fields of:
    a. Embryo Biopsy;
    b. Array CGH.

2. To produce the first clinical cases to bring Karyomapping to full medical application, comparing it to ‘gold standard’ approaches and demonstrating how a linkage-based analysis of SNP karyotypes can be used simultaneously to detect monogenic disorders and (phase and parent of origin of) chromosome copy number:

a. For a couple at risk of transmitting Marfan syndrome;
b. For a couple at risk of transmitting Smith Lemli Opitz syndrome (in this case comparing array CGH (polar body) and Karyomapping (embryo) data.

3. To apply Karyomapping to demonstrate its clinical utility as a genome-wide 'chromosome fingerprint' in a clinical setting.

4. To investigate the use of a calcium ionophore protocol to activate human oocytes, ultimately to investigate the incidence of chromosomal aneuploidy in the activated oocytes using array CGH and Karyomapping:
    a. To induce the resumption of the second meiotic division of mature (MII arrested) human oocytes;
    b. To demonstrate patterns of pronuclear formation and polar body extrusion;
    c. To discuss the clinical implications of the observed activation patterns.

5. To develop an algorithm based on Karyomapping (termed **MeioMapping**) to investigate the mechanisms of human female meiosis (using the calcium ionophore protocol above) by recovering of all three products of human female meiosis from individual oocytes (termed Trios) to allow exploration of the full extent of meiotic chromosome recombination and segregation that occurs in the female germline.

6. To combine the techniques developed above and use both Karyomapping and MeioMapping to explore the full extent of meiotic chromosome recombination and segregation that occurs in the human oocyte:
    a. To provide new insight into meiotic segregation patterns in humans;
    b. To confirm the existence of a previously undescribed pattern of meiotic segregation (herein termed **Reverse Segregation**), a phenomenon that was observed in the pilot data and work performed in specific aim 5;
    c. To test the hypothesis that there is selection for higher recombination rates in the female germline;

d. To test the hypothesis that there is an association between recombination rates and chromosome mis-segregation (aneuploidy);
e. To test the hypothesis that there is a role for meiotic drive for recombinant chromatids at meiosis II in human female meiosis.

3. Specific Aim 1a. To review the literature, produce and publish a state of the art standard set of protocols as a general reference work from practitioners in the fields of Embryo Biopsy

This is an adaptation of the book chapter entitled 'Human Embryo Biopsy Procedures' by Alan R Thornhill, Christian Ottolini and Alan H Handyside, published in The Textbook of Assisted Reproductive Techniques, Volume 1: Laboratory perspectives Fourth Edition (2012).

3.1. My Personal Contribution to the Work

I was involved in the research, writing and editing of the published review chapter above. What follows is an adaptation of the published manuscript.

3.2. Introduction

In the mid-1980s, the development of polymerase chain reaction (PCR) strategies for amplification of specific fragments of DNA from single cells (Li *et al.* 1988; Coutelle *et al.* 1989; Holding & Monk 1989) facilitated preimplantation genetic diagnosis (PGD) of inherited disease using one or more cells biopsied from embryos at preimplantation stages after *in vitro* fertilisation (IVF) (Handyside & Delhanty 1997). As discussed in the General Introduction of this thesis, currently genetic analysis of embryos (or PGD) requires the removal of one or more cells from each embryo, making embryo biopsy comparable to amniocentesis or chorionic villus sample (CVS) at foetal stages, since the primary aim is the removal of sufficient embryonic tissue to allow diagnosis. Embryo biopsy is a two-step micromanipulation process involving the penetration or removal of part of the zona pellucida surrounding the oocyte or embryo, followed by removal of one or more cells. Theoretically, this can be accomplished at any developmental stage between the mature oocyte and blastocyst, but to date only three discrete stages have been proposed: polar body; cleavage stage; and blastocyst. Clearly, each of these stages is biologically different

and thus the strategic considerations have both advantages and disadvantages (Table 3.1). Furthermore, the different biopsy strategies both between and within developmental stages require different technical approaches (Table 3.2) each providing varying prospects of success.

Many of the biopsy techniques currently in use for human embryos (Tarin & Handyside 1993) were pioneered in animal models, notably the mouse (Monk *et al.* 1988; Wilton *et al.* 1989), rabbit (Yand & Foot 1987), cow (Ozil 1983) and marmoset (Summers *et al.* 1988). While the total number of human embryos biopsied in clinical cases is vast, relatively little work has been published to define the relative merits of different biopsy methods and their safety and efficacy in clinical application. This chapter will describe the three stages of biopsy (polar body, cleavage stage [blastomere] and blastocyst [trophectoderm]) which have been used in routine clinical practice (Harper *et al.* 2012).

Table 3.1: Strategic Considerations of Biopsy at Different Developmental Stages for Preimplantation Genetic Diagnosis (Thornhill, Ottolini & Handyside 2012)

DEVELOPMENTAL STAGE	ADVANTAGES	DISADVANTAGES
Oocyte (1st polar body)	Cell removal has no effect on embryo development Increased time to perform diagnosis prior to transfer Can transfer between PN stage and day 2 or beyond ~85% aneuploidy originates in maternal meiosis Homogeneous oocyte quality at biopsy High proportion of oocyte cohort available for biopsy Favored for some ethical, legal and societal frameworks Facilitates fresh cleavage/blastocyst stage embryo transfer	Only 1 cell available for analysis Increased risk of diagnostic error Gender determination not possible Diagnose Maternal aneuploidy (MI) and inherited disease only Misses meiosis II errors (30%) and post-zygotic aneuploidy Single cell sensitive analysis required Relatively labour-intensive/high cost to test all samples Additional follow-up confirmatory testing often needed
(1st+2nd polar bodies)	2 cells for analysis (greater accuracy/reliability) Cell removal has no effect on embryo development Increased time to perform diagnosis prior to transfer Allows embryo transfer from day 2 onwards Homogeneous oocyte quality at biopsy High proportion of oocyte cohort available for biopsy Favored for some ethical, legal and societal frameworks Facilitates fresh cleavage/blastocyst stage embryo transfer	Diagnose Maternal aneuploidy (MI/MII) & inherited disease only Gender determination not possible Simultaneous biopsy (1st polar body may degenerate) Sequential biopsy (extra manipulations required) Single cell sensitive analysis required Labour-intensive/high cost to test all samples Additional follow-up confirmatory testing often needed Misses post-zygotic aneuploidy
Cleavage stage (blastomeres)	Diagnose Maternal/Paternal aneuploidy and inherited disease Gender determination possible Large body of clinical data available 1- 3 cells available for analysis Biopsied embryos develop into normal blastocysts	Chromosomal mosaicism compromises accuracy Choice of blastomere is critical Time for analysis limited to 48-72 hrs (fresh transfer) Most cells in interphase (no karyotypic data) Reduced embryo implantation potential post-biopsy Single cell sensitive analysis required Heterogeneous embryo quality/stage at biopsy Requires extended culture for fresh embryo transfer Additional follow-up confirmatory testing often needed Requires biopsy of largest relative proportion of cell mass Relatively labour-intensive/high cost to test all samples
Blastocyst (Trophectoderm)	Sample multiple (up to 10) cells on day 5/6 Increased amplification efficiency and accuracy (reduce ADO) Increased scope for diagnostic testing (genes + chromosomes) Homogeneous embryo quality preselected (high implantation rate) Trophectoderm sampled rather than inner cell mass Fewer embryos (reduces diagnostic burden and cost) Post-zygotic aneuploidy detection Gender determination possible Embryo more robust to withstand biopsy Embryo has 'genetic stability' Lowest diagnostic failure rate Highest positive predictive value (PPV)	Time for analysis may be limited Blastocysts may need cryopreservation Requires extended culture for fresh embryo transfer High rate of cancellation prior to embryo transfer TE cells may not represent embryo proper Fewer embryos to biopsy than other stages Operator dependent biopsy success and safety Avoidance of inner cell mass critical

Table 3.2: Embryo Biopsy Methods – Benefits, Limitations and Factors Critical to Success (Thornhill, Ottolini & Handyside 2012)

Zona penetration method	Benefits	Limitations	Factors critical to success
Mechanical	Least invasive to embryo (safer) Inexpensive, portable technique Improved survival after freeze-thaw?	Steep learning curve Operator dependent Time consuming	Operator skill and speed Appropriate microtools needed Double tool holder optimal
Chemical (acidified tyrodes)	Relatively inexpensive Widespread clinical use Portable technique	Operator dependent Effect on cryopreservation Difficult to limit aperture size	Acidified tyrodes pH 2.2-2.4 Sensitive control of acid flow Rinsing acid from embryos Double tool holder optimal
Laser (1.48 µm non-contact)	Rapid and Reproducible Simple to use Integrated archiving/analysis software	Cost (30-60,000 US dollars) Not all systems portable Invisible thermal damage/stress	Laser alignment and calibration Pulse number, location & duration Distance between laser and zona Appropriate training and validation
Cell removal method **Cleavage stage blastomere biopsy**			
Aspiration	Ability to select a specific cell for analysis	Cell lysis during aspiration	Appropriate microtools needed Sensitive suction device needed
Fluid displacement	No contact between pipette and cells Rapid	Limited ability to select cell	Operator skill essential
Mechanical displacement	No contact between pipette and cells Rapid	Limited ability to select cell Damage to non-biopsied cells	Operator skill essential
Trophectoderm sampling			
Spontaneous hatching/herniation	Non-invasive (cells undisturbed within zona)	No control over timing/cell numbers Time for analysis very limited Asynchronous development/hatching	High blastocyst development rate Hatching blastocyst in vitro
Zona penetration + herniation or Stitch and pull or aspiration/laser ablation	Pre-empts spontaneous hatching Rapid/some control over cells sampled Rapid/some control over cells sampled	As above Biopsied/non-biopsied cell damage Biopsied/non-biopsied cell damage	 Operator skill essential Operator skill essential
Zona ablation and immediate aspiration with laser dissocaition of sampled cells	Blastocysts biopsied at optimal stages Control over hatching site (away from ICM)	Laser damage may reduce diagnostic reliabilit	Operator skill essential

3.3. Penetration of the Zona Pellucida

Until the advent of noncontact lasers for use in micromanipulation (see below), two basic methods were employed for penetrating the zona. Both of these were pursued initially as a means to enhance fertilisation rates with oligozoospermic men, and have now been overtaken for this purpose by the use of intracytoplasmic sperm injection (ICSI).

The first approach, partial zona dissection (PZD), involves using a fine needle to penetrate through the zona and, avoiding damage to the oocyte or embryo, penetrating out through the zona again at a distance around the circumference (Cohen *et al.* 1989). The embryo can then be detached from the holding pipette as it is effectively held on the needle, and a gentle rubbing action against the side of the holding pipette used to make a slit between the two apertures generated by the needle. Although a narrow-diameter micro-pipette can be pushed through such a slit, it is difficult to use one large enough to aspirate cleavage-stage blastomeres and, with the human embryo pressure on the zona, can lead to lysis of blastomeres and/or, where a slit has been made, force blastomeres out through the slit. The latter approach is used for embryo biopsy in some centres, but requires highly skilled micromanipulation, can be difficult to control, does not allow precise selection of blastomeres, and the risk of lysis can be high. A modification is to make two slits to create a 'flap' or 'cross' in the zona that can be flipped open, allowing more flexibility in the size of the opening created. This method is effective for both polar body and blastomere biopsy (Cieslak *et al.* 1999).

In general, mechanical methods for zona penetration are time-consuming and require skilful micromanipulation, possibly making them inaccessible to some IVF laboratories. As an alternative, zona drilling using acidified Tyrode's solution (pH 2.2-2.4) to dissolve the zona glycoproteins has been extensively used and is commercially available from most culture medium manufacturers. Again, this method was developed in the mouse embryo model, as a possible means to improve fertilisation rates with low sperm densities (Gordon & Talansky 1986). However, its use with human oocytes, while increasing the incidence of fertilisation, arrested the further development of the zygote, presumably consequent to changes in intracellular pH (Malter

& Cohen 1989). With zona drilling, the effect of the acid Tyrode's is localised to a small area of the zona using a fine micro-pipette, with an inner diameter of 5-10μm. The micro-pipette filled with acid Tyrode's is brought into direct contact with the zona at the appropriate position, and a combination of slight pulling away and 'stroking' movements, used to control the flow of acid and the area to be drilled respectively. Medium pH was originally maintained by employing phosphate buffered saline, but is now routinely maintained using modified culture medium buffered with either 4-Morpholinopropanesulphonic acid (MOPS) or 4-(2-hydroxyethyl)-1-piperazine-ethanesulfonic acid (HEPES). When the drilling is complete the micro-pipette is immediately withdrawn.

The shift across centres worldwide from zona drilling using acid Tyrode's (Geraedts et al. 1999) to laser ablation of the zona pellucida has been dramatic. Indeed, according to a survey of PGD centres, the laser has overtaken acidified Tyrode's solution as the most popular form of zona ablation accounting for more than 70% cleavage stage embryo biopsies (Harper et al. 2012). This shift may be more to do with ease of use and the elimination of the need for a double tool holder, rather than any measurable improvement in safety or efficacy.

The preferred model of laser is the near infrared (NIR) solid state compact diode 1.48μm laser. The advantage of using light as a cutting tool is that it obviates the need for disposable or reusable cutting tools, it is extremely precise and, if used appropriately, provides consistent, repeatable and rapid results. Moreover, since neither microtools nor reagents are required to dissect the zona, the opportunity for introducing contamination or pH changes in the medium surrounding the embryo is greatly reduced. The 1.48μm diode laser is small but at the appropriate pulse duration can emit light at power levels sufficient to cause selective thermal disruption of the zona pellucida glycoproteins and is not absorbed by water. This non-contact laser can be inserted into the body of the microscope on which the manipulations take place or be integrated in a special objective and the beam delivered to the target through the dish. Since the laser beam travels up through an objective that lies below the sample, localised heating causes denaturation of the zona proteins in a cylindrical spot where the laser beam is focused; the size of the aperture

created is controlled by adjusting the duration of the laser pulse. The thermal energy created produces a groove in the zona perpendicular to the microscope stage, rather than a circular aperture. However, an 'aperture' is produced in the zona at the point at which the zona is perpendicular to the microscope stage. The size of the aperture (or more accurately the width of the groove at its widest point) created in the zona ranges from 5 to 20μm and is governed by the pulse irradiation time (ranging from 3 to 100 milliseconds) or the accumulation of pulses along the length of the zona margin. The precision of the laser is illustrated by the fact that drilled mouse and human embryos show no sign of extraneous thermal damage under light or scanning microscopy (Germond *et al.* 1995).

Most clinics use this equipment for assisted hatching as well as PGD (Boada *et al.* 1998) and there appears to be no detrimental effect of the laser itself on development to the blastocyst stage or pregnancy rates in animal and human studies (Montag & Van der Ven 1999; Montag *et al.* 1998; Park *et al.* 1999; Han *et al.* 2003; Joris *et al.* 2003). However, studies of the immediate effects at the blastomere level in a mouse model have shown that the laser can cause damage if used inappropriately (Chatzimeletiou *et al.* 2001). Certainly, if the laser beam is fired in an area in direct contact with a blastomere, its viability is always compromised. However, as the pulse length and therefore localised heating is increased, the distance between the laser beam and blastomere required to avoid damage increases. Hence, care is required to drill the zona away from underlying blastomeres and from as far away as possible, and also to use minimum pulse lengths to restrict any damaging effects. Several practical guidelines have emerged to ensure safe and effective use of the laser for human embryo biopsy as follows. Wherever possible, a single aperture for cellular aspiration – double or multiple apertures may cause problems during embryo hatching as the embryo will attempt to hatch out of multiple openings which could compromise further inner cell mass development or lead to increased monozygotic twinning rate. To generate the desired aperture it is preferable to use several pulses of short duration rather than a single pulse of long duration and higher energy that could cause thermal damage. During laser use, it is imperative to maintain the oocyte or embryo as close to the bottom of the biopsy

dish as possible to allow a focussed beam to ablate the zona pellucida. As the embryo is raised above the dish surface the beam energy is diffused and can create localised heating or simply prevent effective ablation of the zona.

3.4. Polar Body Biopsy

Neither the first nor second polar body is required for successful fertilisation or normal embryonic development. Thus removal of either the first or second polar body or both for the purposes of genetic diagnosis should have no deleterious effect *per se* on the developing embryo. Originally, it was suggested that biopsy and genetic analysis of the first polar body would allow PGD of maternal defects prior to conception (Verlinsky *et al.* 1990). Apart from some arguable practical advantages (see below), this concept was also attractive as it involves manipulation of only the human egg and not the fertilised embryo, and would therefore be more acceptable to those with moral or ethical objections to screening embryos; as is the legal situation in some European countries including Switzerland (Corveleyn *et al.* 2008). For preconception diagnosis, either the first polar body alone or both the first and second polar bodies may be biopsied to provide genetic information relating to a particular embryo. Initially preconception diagnosis focussed on the former approach. However, biopsy of the first polar body has limited applicability for PGD for a number of reasons. The process of polar body biopsy is relatively labour-intensive and may involve the micromanipulation of oocytes that ultimately do not develop into therapeutic quality embryos. The procedure only allows the detection of maternal genetic defects and crossing over of homologous chromosomes during meiosis I can prevent identification of the maternal allele remaining in the oocyte, leading to a reduction in the number of embryos available for transfer (Dreesen *et al.* 1995). Also there is only the possibility of a single cell for analysis leading to a lower overall reliability (in contrast to cleavage stage biopsy in which two cells may be taken for independent analysis). As a consequence, it was suggested that more misdiagnoses would result from polar body analyses when compared with blastomere analysis (Navidi & Amheim 1991) and, to overcome these disadvantages, both the first and second polar bodies were removed for

analysis (Verlinsky *et al.* 1997) after first assessing the safety of removing the second polar body in a mouse model (Kaplan *et al.* 1995). This approach has been successfully applied to PGD for the detection of a large number and variety of different single gene disorders, chromosomal aneuploidies and maternal chromosome translocations (Verlinsky *et al.* 2004).

The first polar body can be removed from the oocyte on the day of the oocyte collection between 36 and 42 hours post-human Chorionic Gonadotrophin (hCG) injection as long as the oocyte has entered metaphase II and fully extruded the first polar body (Verlinsky *et al.* 1990). To perform polar body biopsy by mechanical means, a holding pipette and a bevelled micro-pipette (12-15μm in diameter) are needed. The oocyte is held in place with the polar body at the 12 o'clock position. The bevelled micro-pipette is passed through the zona and into the perivitelline space tangentially towards the polar body. The polar body may then be aspirated into the pipette. Alternatively, after mechanical zona dissection to form a flap or cross or laser ablation, an aspiration micro-pipette is introduced into the perivitelline space, and the polar body removed. If the polar body is still attached to the ooplasm, further incubation may be required to permit complete extrusion (Verlinsky *et al.* 1990). Most approaches to polar body biopsy have adopted mechanical or laser techniques rather than chemical methods. While live offspring resulted after treating the zona pellucida of mouse oocytes with acidified Tyrode's solution, studies using human oocytes showed that, despite fertilisation, there was an inhibitory effect on embryonic development (Malter & Cohen 1989) due to a direct effect of acid on the oocyte spindle; possibly as a result of the difference in thickness of the human and mouse zona pellucida.

The first and second polar body can be removed simultaneously (Verlinsky *et al.* 1997) from the zygote between 18 and 22hrs post-insemination but the first polar body may have degenerated by this time, leading to possible diagnostic failure and in turn leading practitioners to aim for much earlier simultaneous biopsy at eight to nine hours post-ICSI (Magli *et al.* 2011). Simultaneous biopsy of the two polar bodies is acceptable for Fluorescent In-situ Hybridisation (FISH) analysis since they can provide distinguishable results (Verlinsky *et al.* 1998). Moreover, the polar bodies are morphologically distinguishable: the first polar body tends to have a crinkled surface and may

fragment; the second polar body is generally smooth and may have a visible interphase nucleus under interference contrast. However, sequential biopsy of polar bodies, where the first polar body is removed on day zero and the second polar body on day one, is recommended for PCR analysis to determine recombination events between the first and second polar body. In addition to the obvious advantages of not damaging the embryo and allowing a maximum time for genetic analysis, at a technical level, analysis of both polar bodies allows detection of allele drop-out (ADO). ADO is the random amplification failure of one parental allele after PCR from single cells (Ray *et al.* 1996), and is therefore a significant source of potential error in PGD. Despite the removal of both polar bodies, in many cases, cleavage stage biopsy may also be required to confirm the polar body diagnosis.

Despite the large number of cycles reported using polar body biopsy and analysis, relatively few centres have used the approach. This may be due to a number of factors. First, the approach can only be applied to maternally inherited diseases. Second, diseases that are detected by assessing changes in gene product (Eldadah *et al.* 1995) would not be candidates for this approach. Third, polar body biopsy cannot be used for gender determination. Finally, biopsy of both the first and second polar bodies is required for optimal diagnostic efficiency and although this can be achieved by either sequential or simultaneous biopsy with successful results, it is labour intensive and may involve oocytes and zygotes that, ultimately, do not develop into therapeutic quality embryos. If polar bodies are sampled sequentially and cleavage stage blastomere confirmation is required, three independent manipulations are required with the possibility of ICSI in between (for PCR-based cases), making a total of four manipulations on the same oocyte and embryo. However, in experienced hands, the three independent biopsy manipulations appear to have no deleterious effect on development (Magli *et al.* 2004; Cieslak-Janzen *et al.* 2006).

3.5. Cleavage-Stage Embryo Biopsy

The first PGD cycles were carried out in late 1989 in a series of couples at risk of X-linked disease and involved cleavage stage embryo biopsy (Handyside *et al.* 1990). Cleavage-stage biopsy has remained the most widely practised form of embryo biopsy worldwide (according to ESHRE PGD Consortium accounting for around 90% of all reported PGD cycles) (Harper *et al.* 2012). However, there have been a number of modifications and improvements since 1989. In the first cases, a tapered micro-pipette with a narrow lumen (internal diameter 5-7μm) containing acidified Tyrode's solution (pH2.2-2.4) was used to drill relatively large apertures (20-30μm) in the zona. The pipette is placed close to the zona pellucida and the acidified solution gently expelled from the pipette until the zona thins and an aperture is drilled (in some cases, the zona can be seen to 'pop' as an aperture is made). The flow can be controlled via an oil-filled syringe (hydraulic), air-filled syringe (pneumatic) or by using a mouth pipette. The human zona is bilayered and the zona drilling process must be carefully monitored as the outer layer dissolves more rapidly than the inner layer. Moreover, there is great variation in zonae pellucidae both between and within cohorts of human oocytes and embryos. The final diameter of the aperture made will be determined by a combination of the above factors. An excessively large aperture may result in the unwanted loss of blastomeres but, more significantly, may indicate that the blastomeres were exposed to potentially damaging quantities of acid that could compromise further development. A second micro-pipette, filled with biopsy medium and held in a double holder alongside the acid Tyrode's pipette, can be used to aspirate single cells (Hardy *et al.* 1990; Ao & Handyside 1995; Handyside & Thornhill 1998). It is possible to use a single micro-pipette for both drilling and aspiration, but care is needed to prevent over-exposure to acid (Inzunza *et al.* 1998; Levinson *et al.* 1992). Any advantage accrued in terms of speed of the procedure may be offset by potential damage as a result of over-exposure to acid.

Cleavage stage biopsy using laser and blastomere aspiration is typically performed as follows: briefly, following laser ablation of the zona pellucida adjacent to the blastomere selected for analysis, the blastomere is aspirated by gentle suction using a polished pipette. The aperture may

be sited adjacent to either a selected blastomere or a sub-zonal space between blastomeres. A finely polished 'sampling' pipette (internal diameter of 30-40μm depending on the cell size) is used to aspirate the blastomere. The pipette is placed through the aperture, close to the blastomere to be aspirated. By gentle suction, the blastomere is drawn into the pipette whilst the pipette is withdrawn from the aperture. The aperture of the sampling pipette is critical for successful biopsy. If the internal diameter is too large for the cell being removed, the pipette will have little purchase on that cell and may result in unwanted suction on non-biopsied cells. Conversely, an undersized pipette will cause the biopsied cell to be squeezed unnecessarily, resulting in blebbing on the cell membrane and ultimately lysis, which will likely reduce the chances of a successful diagnosis in that embryo. Similarly, use of a holding pipette with an internal diameter of 30μm (i.e. larger than a regular ICSI holding pipette) ensures safe and reliable suction on the zona, particularly during difficult biopsies.

Once the blastomere is free of the embryo, it is gently expelled from the sampling pipette. Following biopsy the embryo should be rinsed in culture medium at least twice to remove residual embryo biopsy medium and acid Tyrode's (if applicable) before returning to culture. The blastomere should be washed extensively in handling medium before proceeding to the analysis. The most frequently used method of blastomere removal is aspiration, but other methods have been described and used clinically; although no studies have been conducted to compare their relative safety and efficacy.

In the extrusion method, after zona pellucida drilling the blastomere is extruded through the aperture by pushing against the zona at another site (usually at 90 degrees to the aperture) using a blunt pipette (Levinson *et al.* 1992). The slit in the zona pellucida can be introduced using mechanical means, chemical (acid Tyrode's) exposure or laser ablation.

Another variation in the method of cell removal involves fluid displacement whereby culture medium surrounding the embryo is used to displace individual cells following a zona breach. This method was pioneered in mouse embryos by introducing a slit in the zona with a sharpened needle and, through a second puncture site, injecting medium to dislodge the blastomere through

the first puncture site (Roudebush *et al.* 1990). This method requires the production of two separate apertures and considerable skill to displace the blastomere of choice, but has since been modified for clinical application (Pierce *et al.* 1997). Challenges common to both of these methods arise when ensuring the selected cell is removed and the difficulties encountered when two different cells are required for analysis.

3.5.1. Practical Considerations for Embryo Biopsy

3.5.1.1. Preparation Before Biopsy

ICSI is recommended for all PCR cases to reduce the chance of paternal contamination from extraneous sperm attached to the zona pellucida or non-decondensed sperm within blastomeres. Similarly, all cumulus cells should be removed before biopsy as these cells can contaminate both FISH and PCR diagnosis. Embryo and blastomere identity (individual drops or dishes) should be checked throughout the procedure so that diagnostic results can be reliably linked to specific embryos (Thornhill *et al.* 2005; Preimplantation Genetic Diagnosis International Society 2008). The use of standard IVF culture medium during biopsy is acceptable but its effectiveness may be highly dependent upon the developmental stage of the embryo biopsied. Commercially produced calcium- and magnesium-free (Ca^{2+}/Mg^{2+}-free) medium is widely available and is used by many centres for routine clinical cleavage-stage biopsy, with the benefit of reducing the frequency of cell lysis (Thornhill *et al.* 2005) combined with a shorter time needed to perform the biopsy procedure.

3.5.1.2. Timing of Biopsy

Since the first clinical application of PGD, culture media have been improved and optimised and the new generation of media are designed, tested and manufactured to high-quality control standards specifically for clinical use. Although embryos developed to the blastocyst stage, pregnancy rates after transfer were very low and, importantly for embryo biopsy, most embryos did not appear to compact. With the newer media, compaction on day three is much more

pronounced, which has necessitated the use of Ca^{2+}/Mg^{2+}-free medium to reverse the initial calcium-dependent adhesion (Dumoulin *et al.* 1998). The use of Ca^{2+}/Mg^{2+}-free medium also facilitates later biopsy (i.e. beyond 8-cell stage), making the timings more flexible.

Most cleavage stage biopsy takes place on the third morning following insemination, although the exact timing varies according to timings of procedures in different laboratories. One variation is to alter the timing of ICSI to allow cleavage stage biopsy at the same embryonic stage, but late on day two (biopsy at earlier cleavage stages on day two may adversely affect embryo development) (Tarin *et al.* 1992) allowing more time for genetic analysis. In cases where retarded development is observed, the possibility of delaying the biopsy procedure to allow diagnosis of a larger proportion of the embryo cohort should be considered. Furthermore, as a result of increased use of sequential media and experience with blastocyst culture and transfer, most groups routinely delay transfer until day four or five, allowing more time for analysis and with the additional aim of improving pregnancy and implantation rates, because developing embryos that have undergone further cleavage divisions following biopsy can be preferentially selected for transfer.

Most laboratories exclude very poor quality embryos or those not reaching a predefined cell stage from the embryo biopsy procedure. Of centres surveyed, most will consider only embryos at the five-cell stage and beyond only for biopsy (Geraedts *et al.* 1999). Biopsy at the four-cell stage in mouse results in a distorted allocation of cells to inner cell mass and trophectoderm and abnormal post-implantation development (Tsunoda & McLaren 1983), whereas human embryos biopsied on day two show cleavage rate retardation and smaller blastocysts (Tarin *et al.* 1992). Conversely, four-cell stage human embryos surviving freeze-thaw procedures with the loss of one or more blastomeres can develop, implant and result in live birth, albeit at a reduced rate compared with non-frozen embryos. Stringent biopsy policies have the benefits that fewer embryos need to be biopsied, fewer cells prepared and tested with only developmentally competent embryos considered. On the down side, an opportunity to identify genotypes on a full cohort of embryos may be lost.

3.5.1.3. Number of Cells to Remove During Cleavage Stage Biopsy

In deciding how many cells to biopsy from cleavage stage embryos, it is necessary to balance diagnostic accuracy with potential to implant and develop, which is progressively compromised as a greater proportion of the embryo is removed (Liu *et al.* 1993). There is no consensus on the number of blastomeres that can be safely removed during cleavage stage embryo biopsy. In many centres, a second blastomere is removed from embryos having seven or more cells regardless of the type of analysis involved, but this approach has been criticised as compromising the implantation potential of the biopsied embryo based on extrapolation from frozen-thaw embryo implantation rates (Cohen *et al.* 2007). The decision to remove one or two cells is based on many factors, including the embryo cell number and the accuracy and reliability of the diagnostic test used. If removal of two cells is considered, it is recommended to be undertaken only on embryos with six or more cells (Van de Velde *et al.* 2000). While removal of two blastomeres decreases the likelihood of blastocyst formation, compared with removal of one blastomere, day three in-vitro developmental stage is a stronger predictor for day five developmental potential than the removal of one or two cells. The biopsy of only one cell significantly lowers the efficiency of a PCR-based diagnosis, whereas the efficiency of the FISH PGD procedure remains similar whether one or two cells are removed. However, a randomised trial demonstrated that live birth rate was compromised at a level of one birth for every 33 cycles of two-cell embryo biopsy suggesting that, ideally, one cell biopsy should always be performed unless the diagnostic test is sub-optimal (Goossens *et al.* 2008).

In the case of lost or anucleate blastomeres and failed diagnosis, rebiopsy of embryos is possible but embryo cell number and timing of rebiopsy should be considered to avoid excessive harm to the embryo. Although technically challenging, the original zona breach site should be accessed to prevent later problems with embryos hatching via multiple hatching sites. No specific recommendations for time limits for embryos out of the incubator are available but, ideally, biopsy should be performed as quickly as possible to ensure pH, temperature and osmolality are

maintained. A documented record for biopsy timings is recommended for quality control/quality assurance purposes (Thornhill *et al.* 2005; Thornhill & Repping 2008).

3.5.1.4. Safety and Success Rates After Biopsy

The reliability of cleavage-stage biopsy has been established in many centres, and in the latest European Society for Human Reproduction and Embryology (ESHRE) PGD Consortium report the efficiency of successful embryo biopsy is reported as 98% in over 70,000 cleavage-stage embryos in clinical PGD cycles (Harper *et al.* 2012). Pregnancy rates after PGD are notoriously difficult to assess between different indications and centres. Nevertheless, in the largest series analysed in detail to date, mostly following cleavage-stage biopsy, pregnancy rates are only 17-22% per oocyte retrieval and 26-29% per embryo transfer depending on the indication (Harper *et al.* 2012). The reasons for the apparently low success rates are many-fold but unsurprising, considering that a proportion of embryos cannot be transferred because they are diagnosed as affected, and in many countries the number of embryos transferred is limited to a maximum of two. It is anticipated that pregnancy rates per embryo transfer will be significantly higher regardless of indication following blastocyst biopsy, primarily because of the higher implantation potential per biopsied embryo, but a rigorous assessment of pregnancies per started cycle will provide a true assessment of the value of blastocyst biopsy. The potentially detrimental effects of embryo biopsy, particularly if performed poorly, also contribute to reduced success rates. Data from a randomised trial provides some insight into the possible detrimental effects of biopsy with a reduction in implantation potential evident in undiagnosed biopsied embryos compared with non-biopsied control embryos (Mastenbroek *et al.* 2007; Cohen & Grifo 2007). A separate trial dramatically reduced implantation rates from biopsied versus non-biopsied cleavage-stage embryos (without any genetic selection), which further supports the notion that cleavage-stage embryo biopsy is costly to the embryo particularly if poorly performed (Scott *et al.* 2013). It is well established in mammalian embryos that as an increasing proportion of the embryo is removed or destroyed before transfer, implantation and foetal development rates decline suggesting a lower

limit of embryo mass compatible with implantation and development (Rossant 1976). Reduction of 50% or more of the cell mass frequently results in cell proliferation in the absence of normal differentiation, thus it is important to minimise the cellular mass removed at biopsy. However, cell reduction within this limit is compatible with normal embryo metabolism, blastocyst development, and foetal growth, while cell numbers in the trophectoderm (TE) and inner cell mass (ICM) of blastocysts were in proportion to the cellular mass removed at biopsy, making cleavage stage biopsy for PGD a viable option (Hardy *et al.* 1990). Hence, human cleavage-stage biopsy is delayed until just before the beginning of compaction, the process of intercellular adhesion and junction formation, which progressively makes removal of blastomeres more difficult and eventually impossible without causing damage to the embryo. Generally, cells identified as having completed the third cleavage division (on the basis of their size) are selected for biopsy. Theoretically, therefore, each blastomere removes only one-eighth of the cellular mass of the embryo. As zona drilling for assisted hatching may be beneficial, it is also possible that this offsets to some extent the adverse effects of reducing the cell mass of the embryo.

In frozen embryo transfer (FET) cases, viable pregnancies can be achieved and no increase in foetal abnormalities has been reported following transfer of cryopreserved embryos in which some cells have been destroyed by freezing and subsequent thawing (Sutcliffe *et al.* 1995). Indeed, estimates of the loss of implantation potential have been made based on outcomes following FET involving embryos with one or more non-viable cells after thawing (Cohen *et al.* 2007). It is now apparent that cleavage-stage biopsy should be considered a ‘cost’ to the embryo and this must always be weighed against the potential benefit to the embryo of any diagnostic testing.

3.5.1.5. Selection of Cells in the Cleavage-Stage Embryo

Biopsy at cleavage stages is based on the principle that at these stages the blastomeres remain totipotent and equivalent such that the removal of a single blastomere will: (a) provide a representative sample of the entire embryo; and (b) compromise the embryo only to the extent of one-eighth of the embryo mass rather than removal of a developmentally important blastomere. The importance of selecting a blastomere with a single visible interphase nucleus cannot be stressed enough. It is probably the most challenging aspect of cleavage-stage biopsy, and time spent in careful examination of the embryo and orienting it to selectively remove specific blastomeres is essential to attain the high diagnostic efficiencies required for clinical effectiveness. The reasons for this are that, first, an interphase nucleus is essential for FISH analysis, since the nucleus is prepared on a slide by a process of cell lysis in which individual chromosomes will not be visible and are likely to be lost (Harper *et al.* 1994). Second, post-zygotic chromosomal mosaicism arising during cleavage is known to be associated with nuclear abnormalities (Munné & Cohen 1993). The exception is binucleate blastomeres, in which there are two normal-sized nuclei. In most cases, these are generated through failure of cytokinesis, and both nuclei contain the normal diploid chromosomal complement for that embryo (Kuo *et al.* 1998). In general, multinucleate cells should not be selected at biopsy if FISH analysis for aneuploidy detection follows and the removal of mononucleate cells only is recommended (Strom *et al.* 2000). For accuracy during FISH-based diagnosis, it is advisable to only use bi- or multinucleated cells as a backup to biopsied mononucleated cells. This may be less critical for PCR based testing in which presence or absence of a specific parental chromosome is important, rather than copy number *per se*. However, even with careful blastomere selection, diagnostic efficiency is not 100%, and aneuploid results are common even in mononucleate blastomeres primarily as a result of chromosomal mosaicism (Kuo *et al.* 1998). Biopsy of two nucleated blastomeres is only possible in good-quality embryos at a sufficiently advanced stage, such that even with a two-cell biopsy policy, a mixture of embryos with one or two blastomeres for analysis is common (Van de Velde *et al.* 2000). Where possible, one of the smaller blastomeres should be selected to minimise the reduction in mass and the relative sizes of cells may provide an indication of recent mitosis. This

may also reduce the risk that a cell in metaphase will be taken, the chromosomes of which could be lost during the fixation process.

3.5.2. Concerns Surrounding Cleavage-Stage Embryo Biopsy

As with any micromanipulation procedure involving human gametes or embryos, every reasonable precaution should be taken to minimise damage and stress during the procedure. General precautions include the correct installation, calibration and maintenance of all micromanipulation equipment (particularly the laser). In advance of all clinical procedures, one should ensure that all appropriate reagents and micromanipulation tools are available, sterile and within their expiration date. Biopsy should be performed by a suitably qualified and trained person. Regular reviews of biopsy efficiency, post-biopsy morphology and cell numbers of embryos not transferred provide an indication of the possible harm as a result of biopsy as do pregnancy rates after biopsy; particularly those not developing beyond the biochemical stage (Thornhill & Repping 2008). Clearly, effects on post implantation development should also be closely monitored, as any increase in foetal malformations or congenital abnormalities would be unacceptable. To date, studies of pregnancies and children born after PGD have identified no significant increase in abnormalities above the rate seen in routine IVF (Harper *et al.* 2012; Strom *et al.* 2000; Banerjee *et al.* 2008; Nekkebroeck *et al.* 2008). The main problem in terms of diagnostic efficiency with cleavage-stage biopsy is the presence of chromosomal mosaicism that is reported to occur in up to 80% embryos (Harper *et al.* 1995; Magli *et al.* 2000; Bielanska *et al.* 2002). A full discussion of the impact of chromosomal mosaicism on the accuracy of PGD is beyond the scope of this thesis, but its impact is likely to be significant. Mosaicism is thought to be the primary reason for the high rate of false positives depleting the pool of chromosomally 'normal' embryos for transfer, and hence significantly lowering the chance of live birth following preimplantation genetic screening for chromosomal aneuploidy (PGS) compared with controls in a randomised controlled trial (Mastenbroek *et al.* 2007). Preliminary work using array comparative genomic hybridisation techniques to compare individual blastomere chromosomal constitutions

from ‘normal’ cleavage stage embryos suggests that the false positive rate in diploid/aneuploid mosaic embryos may be as low as 7%, but this requires larger scale corroboration (Wilton 2012).

3.6. Blastocyst Stage Biopsy (Trophectoderm Biopsy)

The number of cells present at the blastocyst stage make blastocyst biopsy more akin to early prenatal diagnosis and therefore, to some, more ethically acceptable (Figure 3.1). In theory, TE cells, which form the spherical outer epithelial monolayer of the blastocyst, can be removed without harming or depleting the ICM from which the foetus is derived. For blastocyst biopsy, it is therefore possible to remove up to 10 TE cells, which would overcome many of the problems encountered in single cell DNA amplification and FISH. In the case of PCR, the problems of amplification failure and allele dropout or preferential amplification would be much reduced. FISH analysis would be more successful with a virtual guarantee of a result for each sample and the problems of split signal, signal overlap or probe failure would be significantly less misleading. Indeed, when more than two cells are present in the same sample tube these problems have been shown to virtually disappear (Holding *et al.* 1993), particularly if using whole genome amplification (WGA) techniques (Nijs & Van Steirteghem 1990). With or without WGA, the availability of more cells automatically increases the diagnostic possibilities (more chromosomes analysed with FISH or more specific sequences with PCR, or both).

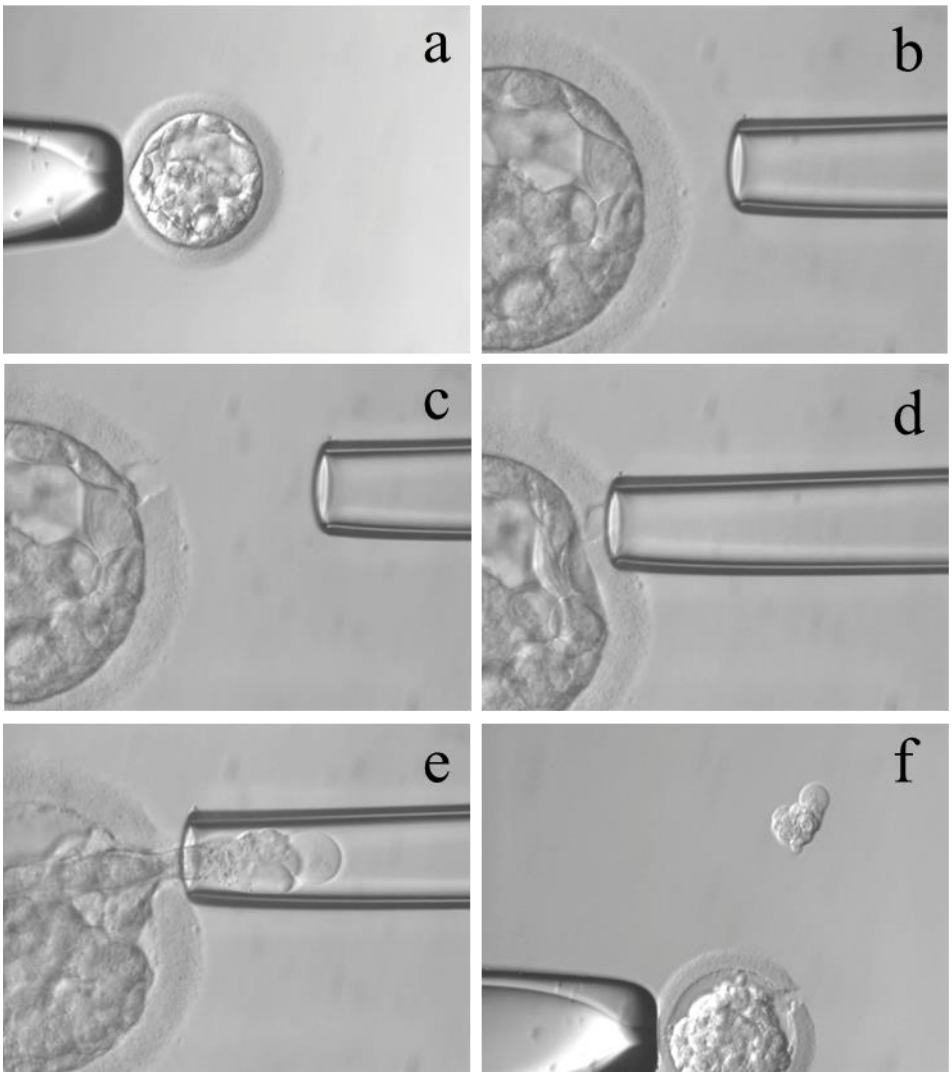

Figure 3.1. Blastocyst biopsy following laser ablation of the zona pellucida on a day five human embryo (Thornhill, Ottolini & Handyside 2012).

Aspiration of trophectodermal cells follows immediately after ablation without additional embryo culture prior to biopsy. For a more detailed account, following the steps a-f, see clinical protocol in Section 3.8.

In the mouse, TE biopsy is easily achieved by partial zona dissection using mechanical means, followed by a period in culture during which the expansion of the blastocoel cavity forces the TE to herniate out of the slit (Dokras *et al.* 1991). The herniating TE vesicle can then be excised on a bed of agarose by using a needle (which can be hand-held or attached to a micromanipulator)

and a cutting action close to the zona, which causes the embryo to roll. Both the biopsied embryo and TE vesicles often remain expanded, since they appear to be resealed possibly as a consequence of twisting at the constriction. Furthermore, to some extent, the size of the TE biopsy can be controlled by the size of the slit and the length of incubation. A similar approach was used to biopsy human blastocysts on day five or six post-insemination (Dokras *et al.* 1991) and was later used to examine effects on viability post-biopsy, with the finding that hCG production was equivalent for biopsied and non-biopsied controls (Muggleton-Harris *et al.* 1993). Another more aggressive technique to remove trophectoderm cells during blastocyst biopsy is the mechanical stitch and pull method (Veiga *et al.* 1997). The best technique seems to be to stabilise the blastocyst by gentle suction and make an incision at the pole opposite to the inner cell mass using a 2μm bevelled pipette. The pipette is pushed in and out through the zona and pulled upwards to make the incision. The blastocysts are then left for six to 24 hours until some trophectoderm herniates though the slit. When herniation involves about 10-25% of the blastocyst (10-30 cells), the trophectoderm is excised using a glass needle. As with the other stages of embryo biopsy, noncontact infrared lasers are now routinely used to not only create an opening in the zona pellucida but also to excise the herniating trophectoderm (Papanikolaou *et al.* 2008) (See Section 3.8. for a clinical protocol describing this method in more detail).

Originally, blastocyst development rates were not consistently high in laboratories and pregnancy rates following blastocyst-stage transfers were too low to consider biopsy at this stage. With improvements in culture systems, the proportion of embryos developing to the blastocyst stage has increased, and implantation rates per blastocyst transferred are significantly better than at cleavage stages (Kokkali *et al.* 2007). Another concern was the effect that removal of a proportion of the TE cells and damage of additional cells in the process would have on implantation. However, skilled practitioners are able to reliably biopsy up to 10 TE cells from blastocysts on day five using a noncontact infrared laser for zona drilling and excision of herniating TE cells, and pregnancy and implantation rates are comparable to those for non-biopsied controls (Khalaf *et al.* 1996). The high incidence of multiple pregnancies in PGD demands efforts to reduce the number

of unaffected embryos transferred, and transfer of blastocysts with high implantation potential is an effective strategy (Kalousek & Vekemans 1996).

3.6.1. Challenges Associated with Blastocyst Biopsy

The main limitation of blastocyst biopsy is the low or unpredictable number of embryos that reach the blastocyst stage *in vitro* for unselected patients, even with improved culture conditions. Since a high number of embryos are needed for successful PGD to allow for sufficient embryo selection from the desired genotype, blastocyst culture may not produce enough embryos for diagnosis and transfer to make PGD at this stage effective for all patients and may be more appropriate for younger, good-prognosis patients.

An additional problem is that TE cells may have diverged genetically from the ICM as, in approximately 2% of human conceptions, confined placental mosaicism (CPM) is observed (James & West 1994) in which the chromosome status of the embryo is different from the placenta. In a mouse model, abnormal cells were preferentially allocated to the trophectoderm (Ruangvutilert *et al.* 2000) but the situation is less clear in the human.

The level of mosaicism in the human blastocyst is lower than that in cleavage stage embryos (Evsikov & Verlinsky 1998) and, where present, often takes the form of polyploidy in the trophectodermal lineage (Derhaag *et al.* 2003) with no obvious preferential allocation of aneuploid cells to the TE lineage (Baart *et al.* 2006). Considering polyploidy cells, for PGD analyses using FISH, if enough chromosomes are analysed then any underlying abnormality (such as trisomy 21) may be recognised within the polyploidy (Kuo & Handyside, unpublished observation). Similarly, for PCR based diagnoses the presence of multiple copies of each chromosome in polyploid cells should pose few problems, so long as both parental copies of the chromosome are represented. Clearly, chromosomal differences between the ICM and TE as a consequence of high levels of mosaicism at the cleavage stage even in younger women (Geber *et al.* 1995) will reduce the accuracy of diagnosis even when multiple biopsied TE cells are available. However,

comparisons between biopsied trophectoderm and inner cell mass demonstrated high concordance in chromosomal status (Johnson 2010; Capalbo *et al.* 2011).

In summary, blastocyst biopsy is rapidly becoming a popular choice for embryo biopsy (Kokkali *et al.* 2005; de Boer *et al.* 2004) and, in contrast to previous practice focusing on poor prognosis patients, is particularly promising for younger patients aiming for single embryo transfer, with a randomised controlled trial demonstrating a 66% relative increase in ongoing pregnancy rate following 24 chromosome aneuploidy screening (Yang *et al.* 2012). Its widespread adoption in laboratories previously performing biopsy at other developmental stages is predicted allowing large-scale clinical assessment. At present, the logistics of blastocyst biopsy dictate a limited time-frame in which to perform diagnosis that might necessitate cryopreservation of biopsied blastocysts for transfer in a later unstimulated thaw cycle which, despite growing evidence of safety and efficacy, will require a cultural shift for both patients and providers.

3.7. Future Developments

A major challenge in PGD, where high value test normal embryos are available and single embryo transfer is becoming common, has been to develop an effective standardised method for cryopreservation of biopsied embryos. Attempts to use conventional slow-freezing protocols, either in the mouse model or in humans, have shown extensive damage after thawing, presumably because of the loss of protection from ice crystals in the medium provided by an intact zona pellucida (Joris *et al.* 1999; Magli *et al.* 1999; Magli *et al.* 2006). However, improved slow freezing protocols have been reported in which damage is reduced (Jericho *et al.* 2003; Stachecki *et al.* 2005; Parriago *et al.* 2007). Nevertheless, following successful application in animal models, vitrification looks set to replace slow freezing for both cleavage and blastocyst stage embryos after polar body or embryo biopsy (Agca *et al.* 1998; Baranyai *et al.* 2005; Isachenko *et al.* 2005). With the high rate of multiple pregnancies reported after PGD, it is imperative to develop effective methods of cryopreservation that will: (i) allow storage of unaffected embryos for later transfer so that the numbers transferred can be limited to two or

even single embryo transfers; and (ii) provide additional time to perform more extensive diagnostic tests. Indeed, the growing body of evidence suggesting comparable success rates (Schoolcraft *et al.* 2011) and normalised birthweights (Henningsen *et al.* 2011) from frozen-thaw transfer cycles (compared with fresh stimulated transfer cycles) may lead to a new era in which PGD cycles separate the stimulation and embryo production phase of treatment from diagnostic testing and embryo transfer phase. As a consequence, outcomes may improve overall with the added benefit to patients of having sufficient time for informed decision

With the introduction of quality management systems and accreditation in IVF laboratories (Thornhill *et al.* 2005; Preimplantation Genetic Diagnosis International Society 2008; Thornhill & Repping 2008), safer biopsy can be anticipated through agreed definitions of successful and safe biopsy, standardised training and procedures, validation of new techniques as well as calibration of new and existing instruments such as the laser. It has become clear that embryo biopsy, as with any form of invasive testing or manipulation, exacts a cost to the embryo in the form of either cellular depletion, metabolic stress or both. Thus, it is imperative to assess the potential benefit to the embryo itself in terms of improved selection or disease-free status before performing embryo biopsy. However, in the future it may be possible to diagnose inherited diseases or chromosomal imbalance in early human embryos by non-invasive analysis. The new development of time-lapse imaging in human embryology allows changes in developmental growth rates to be measured by morphokinetic analysis (Wong *et al.* 2010; Meseguer *et al.* 2011). If this approach can be developed to detect aneuploid embryos, it would shift the cost-benefit ratio away from the cost of invasive biopsy heavily towards potential benefit.

3.8. Clinical Protocol for Blastocyst Stage Embryo Biopsy

This clinical protocol describes the biopsy of human blastocysts on day five or day six of development to obtain multicellular samples for DNA amplification and genetic testing. The protocol is suitable for both hatching and non-hatching blastocysts and requires no zona breach during cleavage stages or period of culture prior to biopsy. For brevity all culture media reagents

described below are from the Quinn's Advantage Culture Media Suite (Sage, Cooper Surgical, Inc. Trumbull, CT, USA).

3.8.1. Preparation Prior to Biopsy

1. Prepare sufficient Embryo GPS culture dishes (EGPS-100, LifeGlobal) with Blastocyst medium for all embryos eligible for biopsy on the day prior to biopsy to allow for equilibration in the patient-allocated incubator section. Dish(es) should have sufficient 30µL outer wells to allow individual culture of every embryo that has undergone biopsy. Spare medium in the 60µL inner wells should also be available for washing embryos after biopsy to remove buffered medium.
2. Turn on workstation, micromanipulators and heated stage (perform routine QC checks for temperature, etc.)
3. Ensure anti-vibration table is inflated and functioning.
4. Set up one biopsy dish per embryo with QA HEPES buffered medium +10% Synthetic Serum Replacement (buffered biopsy medium – BBM) and oil for tissue culture. In Falcon 50 × 9mm Petri dish (code 351006), 3 × 10µL drops of BBM are aliquoted and covered with 4ml oil. These should be kept on a heated stage to equilibrate to 37°C for at least 15 minutes prior to use and used within 120 minutes.
5. Turn on 'SATURN' laser (Research Instruments Ltd, Falmouth, UK) and workstation computer. Open 'CRONUS' software and follow instruction booklet for alignment of laser using 'pilot' to check target is correct (refer to SATURN laser manual for additional guidance).
6. Pipette set-up is essentially the same as that done for ICSI, however in the place of the injection pipette a blastomere aspiration pipette (code K-EBPH-3035, Cook Medical Europe Ltd, Limerick Ireland) is inserted into the holder. Biopsy pipettes are available in a

range of diameters and can be bevelled if required. Current diameters used are between 25µm and 35µm and are available commercially from a number of different providers.

7. If required the angle of the biopsy pipette can be adjusted between 30° to 40° to allow optimal movement during biopsy.

3.8.2. Biopsy

1. Label the biopsy dish with the patient details, embryo number and attach a Radio Frequency Identification (RFID) tag for use with the RI Witness^{TM} system (Research Instruments, UK).
2. Allocate the biopsy dish appropriately on the witness system and transfer one embryo to the central drop in the dish. The embryos should be 'rinsed' in the extra 'wash' drops so that excess culture media does not dilute the BBM. This also reduces the chance of debris carry over and allows removal of loose cumulus cells that may otherwise present a risk of false diagnosis.
3. Place the dish on the heated stage of the micromanipulator workstation.
4. Carefully lower the holding and aspiration pipettes into the central drop (with the embryo) taking care to avoid damaging the embryo using a low powered objective (Figure 3.1a).
5. Ensure both pipettes have equilibrated and are offering sensitive control then, with gentle aspiration, secure the embryo to the holding pipette avoiding any herniating cells.

For hatching blastocysts go directly to step 9.

For non-hatching blastocysts continue with step 6.

6. Position the embryo on the holding pipette to give a clear view of the inner cell mass at 9 o'clock (i.e. away from the biopsy pipette) under high power magnification (Figure 3.1b).
7. Select appropriate laser pulse duration for the desired aperture size (Figure 3.1c) and, after selecting the laser objective, begin to make an opening in the embryo zona with a

series of laser pulses working inwards from the outer surface of the zona taking care to avoid damaging the embryo. Zona thickness variation between embryos will mean that pulse time are number of pulses will vary. Pulse duration can be altered manually if required. The exact duration and number of pulses varies with different commercially available lasers and should be validated within each centre.

8. As soon as the aperture is wide enough to accommodate the passage of several trophectoderm cells (~ 10µm), carefully press the biopsy pipette against the zona, gently expelling medium through the breach to release the cells from the internal surface of the zona (Figure 3.1d).

9. Once the trophectoderm is free from the zona, aspirate three to 10 cells into the biopsy pipette with gentle suction (Figure 3.1e). In the case of hatching blastocysts, aspirate herniating cells into the biopsy pipette.

10. Direct the laser to the thinnest part of the aspirated cells and use several laser pulses at the junctions between cells to disconnect the aspirated cells from the body of the embryo. It may be necessary to apply more suction with the biopsy pipette, taking care not to inadvertently aspirate additional cells into the biopsy pipette.

11. When the biopsied cells are free from the embryo (i.e. within the biopsy pipette), move the biopsy pipette away from the embryo and gently release the aspirated cells (Figure 3.1f). Record the approximate number of cells, their appearance and location in the drop to aid relocation at time of cell preparation.

12. Label a pre-equilibrated post-biopsy (GPS) culture dish clearly with the patient's details and attach an RFID tag. Mark the embryo number adjacent to each culture well, on the dish base with indelible marker.

13. Allocate the culture dish appropriately on the witness system and return the biopsied embryo to this culture dish – each numbered embryo in the biopsy dish should be moved to the culture well with the corresponding number. Ensure that wash drops are used to

minimise any carry-over of HEPES medium into the culture drop. Use a 275µm pipette tip to minimise any additional stress to the embryo during this movement. Manual human double witnessing must be performed and recorded for every embryo that is moved following biopsy to ensure appropriate identification.

14. Return the dish to the patient incubator section and culture until embryo transfer, vitrification or disposal.
15. The dish containing the aspirated cells for analysis should be given to the scientist performing the cell preparation (tubing or cell fixation) immediately or can be placed in the workstation for later preparation (if validated) once the biopsy is completed.
16. Perform biopsy procedure on the next eligible embryo.
17. Biopsy all embryos that are of suitable quality and have reached the appropriate stage of development. This is normally a full blastocyst of average quality or above (grade 3BB or better using Gardner's blastocyst scoring system).

3.8.3. Special Considerations

1. In many cases results of the genetic analysis can be ready within 24 hours. Embryos biopsied early on day five may be transferred fresh on day six. Any embryos biopsied later on day five or day six should be vitrified and transferred in a frozen embryo transfer cycle pending genetics results.
2. If no embryos in a cohort reach the full blastocyst stage by day six or no embryos are suitable for biopsy, the case should be reviewed by the appropriate team members. Considerations can be made to perform embryo transfer without biopsy and subsequent genetic testing subject to the patients being counselled on the risks and the chance of pregnancy. For example, patients for aneuploidy screening may elect to proceed with transfer of poor quality embryo without biopsy and genetic testing depending on the specific indication.

4. Specific Aim 1b. To review the literature, produce and publish a state of the art standard set of protocols as a general reference work from practitioners in the fields of Array CGH

This is an adaptation of the book chapter entitled 'Aneuploidy testing by array-CGH: Applications in Preimplantation Testing' by Alan R Thornhill, Christian Ottolini, Gary Harton and Darren Griffin published in A Practical Guide to Selecting Gametes and Embryos (2014).

4.1. My Personal Contribution to the Work

I was involved in the research and writing and editing of the published review chapter above. What follows is an adaptation of the published manuscript.

4.2. Introduction

As described in sections 2.1 to 2.3 of the General Introduction, aneuploidy is the term used to describe gross chromosomal imbalance in an organism or embryo, presenting as either additional (e.g. trisomy) or missing (e.g. monosomy) chromosomes. Aneuploidy arises during cell division when chromosomes fail to separate equally between the two new daughter cells (Hassold & Hunt 2001). Aneuploidy may be present in all the cells of the body and extra embryonic membranes or be represented in a conceptus having both normal and aneuploid cells (so-called mosaicism). The consequences of aneuploidy constitute a wide phenotypic spectrum from early embryonic arrest to mild infertility, with the best-known being Down syndrome (trisomy 21) and first trimester spontaneous abortion (mostly trisomies and monosomy X). The origins of aneuploidy lie in the meiotic divisions (principally in the ovary) and the early cleavage divisions of the preimplantation embryo. Arising by either nondisjunction, precocious separation of sister chromatids or anaphase lag (Hassold & Hunt 2001), the impact of aneuploidy on families can be devastating; e.g. when faced with pregnancy loss, stillbirth or a severely affected child. In all cases, aneuploidy results in

an unfavourable outcome for the family in question and is undoubtedly a major contributing factor to the relatively low fecundity of humans when compared with other species.

The concept of preimplantation genetic screening (PGS) for aneuploidy in oocytes or preimplantation embryos to both lower the risk of the above phenotypic consequences and to improve *in vitro* fertilisation (IVF) success rates is not new. Indeed it was proposed alongside the earliest developments of preimplantation genetic diagnosis (Penketh & McLaren 1987). The ability to do this effectively has required rapid evolution of diagnostic technologies to combine speed, accuracy and reliability. To date, only direct analysis of chromosome copy number has been applied clinically as indirect approaches (e.g. metabolomic analysis of embryonic products or detailed morphokinetic analysis using time-lapse imaging technology) have yet to be convincingly associated with aneuploidy incidence.

Explanations for the failure of a Fluorescence In-Situ Hybridisation (FISH) approach on blastomeres from cleavage stage embryos to demonstrate a clinical benefit in a large randomised controlled trial (Mastenbroek *et al.* 2007) and in subsequent trials (see meta-analysis) (Mastenbroek *et al.* 2011) are well documented (Cohen & Grifo 2007), focusing primarily on the safety of biopsy, the importance of low error rates on the diagnostic efficiency of PGS (Summers & Foland 2009), as is the need to detect all chromosomes simultaneously for aneuploidy. Notwithstanding the ability now to detect all 24 chromosomes by FISH using successive rounds of hybridisation, the issues of mosaicism, signal interpretation, clinical trial data and the development of microarray based methods for detecting 24 chromosome copy number are now signalling the demise of FISH-based cleavage stage embryo biopsy approaches to PGS. Microarray-based tests are now the standard and these have been made possible through the advancement of whole genome amplification (WGA) technology. Despite the undoubtedly superior technical capabilities of array comparative genomic hybridisation (CGH) compared with FISH, several prospective clinical trials showing benefit and widespread clinical use of array CGH, the policy position regarding PGS among both professional and regulatory bodies is

regrettably out of date and refers only to the historic and flawed FISH approach (Anderson & Pickering 2008; American Society of Reproductive Medicine Society Practice Committee 2008).

The classical approaches to embryo biopsy for preimplantation genetic diagnosis – polar body, cleavage stage, trophectoderm (Magli *et al.* 2004; Cieslak-Janzen *et al.* 2006; Kokkali *et al.* 2007 and reviewed in Thornhill *et al.* 2012) – are all in current clinical application for PGS, with first polar body (Wells *et al.* 2002) and combined first and second polar body (Geraedts *et al.* 2011) as well as trophectoderm biopsy (Schoolcraft *et al.* 2010), increasingly finding favour. The more well established cleavage-stage approach, while once thought to be harmless (Hardy *et al.* 1990), is now considered to reduce implantation potential especially when two cells are biopsied (Mastenbroek *et al.* 2007; Cohen *et al.* 2007), and should ideally only be used after conducting a cost-benefit analysis. The invasive nature of embryo or oocyte biopsy means that PGS has historically been targeted to specific high-risk patient groups (advanced maternal age; repeated implantation failure; recurrent pregnancy loss; and elevated sperm aneuploidy levels common in patients presenting with severe male factor infertility). More recently, PGS has been used to improve the effectiveness of elective single embryo transfer in good prognosis patients to reduce multiple birth rates while maintaining high success rates (Yang *et al.* 2012). The complex spectrum of chromosome abnormalities in the human preimplantation embryo has yet to be fully described and diagnostic procedures can be expensive to implement. Moreover, embryo biopsy is invasive, as already discussed in Specific Aim 1, and thus a robust cost-benefit analysis is essential to achieve widespread patient benefit through the use of PGS. This part of the thesis explores the current methodologies used to perform PGS using array CGH and a description of alternative and future approaches.

4.3. Biopsy Strategies

A number of different strategies have been proposed and utilised to detect aneuploidy using array CGH in oocytes and embryos. The relative merits of each have been dealt with in earlier chapters of this thesis. Briefly, first polar body (PB1) biopsy alone and combined PB1 and second polar

body (PB2) strategies have both been used clinically for PGS. However, it is increasingly evident that PB1 alone has limited applicability for PGS as up to 30% of aneuploidy of maternal origin will not be diagnosed if only PB1 is analysed (Handyside *et al.* 2012). As precocious separation of sister chromatids appears to be the predominant cause of maternal meiotic aneuploidies (Handyside *et al.* 2012; Gabriel *et al.* 2011a), PB2 must be biopsied to accurately identify all maternal aneuploidies and ensure even abnormal segregations in PB1 are not corrected in the second meiotic division. The timings of both PB1 and PB2 biopsy are critical to the efficiency of diagnosis. This was relevant when aneuploidy screening using the FISH approach was used (Verlinsky *et al.* 1996) and is equally critical when using array CGH (Magli *et al.* 2011).

Theoretically, blastocyst stage biopsy is the optimal stage for aneuploidy screening (see previous chapter) as it partially negates the problem of mosaicism and gives maximum aneuploidy information from maternal, paternal and post-zygotic events at the latest possible stage of embryo development possible in current in-vitro culture systems. In addition, the biopsy of three or more cells virtually eliminates the problem of allelic dropout (ADO) following WGA (Ling *et al.* 2009). Historically it has been viewed as a downside that embryos may need cryopreservation following trophectoderm (TE) biopsy whist awaiting genetics results. However it is becoming increasingly apparent that vitrification is a viable strategy to maintain or even potentially increase live birth rates following biopsy (Schoolcraft & Katz-Jaffe 2013). Furthermore, embryo vitrification may be considered for all PGS cases to overcome logistic issues with sample transportation and diagnostic timings. It should be noted that TE biopsy does not entirely eliminate the problem of mosaicism. Furthermore, it is possible that some embryos failing to reach blastocyst stage *in vitro* may be viable *in vivo* (Glujovsky *et al.* 2012).

4.4. Principles of Array Comparative Genomic Hybridisation (aCGH)

Originally designed for molecular karyotyping of tumour cells (Kallioniemi *et al.* 1992), CGH is a method whereby the chromosomal genotype of an unknown DNA sample can be inferred according to its relative ability to competitively hybridise with reference DNA of known genotype to

either: (i) metaphase chromosomes from a karyotypically normal reference male (metaphase CGH); or (ii) a series of specified DNA sequences at specified spots or positions on a glass slide (aCGH). A schematic representation of the principles of CGH is shown in Figure 1b.1. Like its more time-consuming predecessor, metaphase CGH, which has been used for clinical PGS (Voullaire *et al.* 2000; Wells & Delhanty 2000), array CGH is a relatively DNA hungry technique and commonly requires nanogram to microgram amounts of DNA for optimal performance. Since there is typically only approximately six picograms of DNA in a single blastomere, it is essential to perform WGA prior to the aCGH procedure itself. While array CGH can be performed using either bacterial artificial chromosome (BAC) DNA clones or specific oligonucleotides across the genome, this chapter will focus on the BAC clone approach as this has been validated and used for well over 250,000 clinical preimplantation genetic samples to date. The current 24Sure^{TM} microarray contains 2,900 unique BAC clones spaced approximately 1Mb apart, which have been extensively validated in over 2,000 post-natal clinical array experiments to exclude copy number polymorphisms and their genomic locations confirmed by reverse painting of labelled single chromosome preparations onto arrays, FISH mapping and sequencing verification. Array CGH for preimplantation testing has been pioneered by BlueGnome (Fulbourn, Cambridge, UK) and all reagents for WGA, labelling, hybridisation, washing, reference DNA, microarray slides and analytical software described below are available from BlueGnome except where noted.

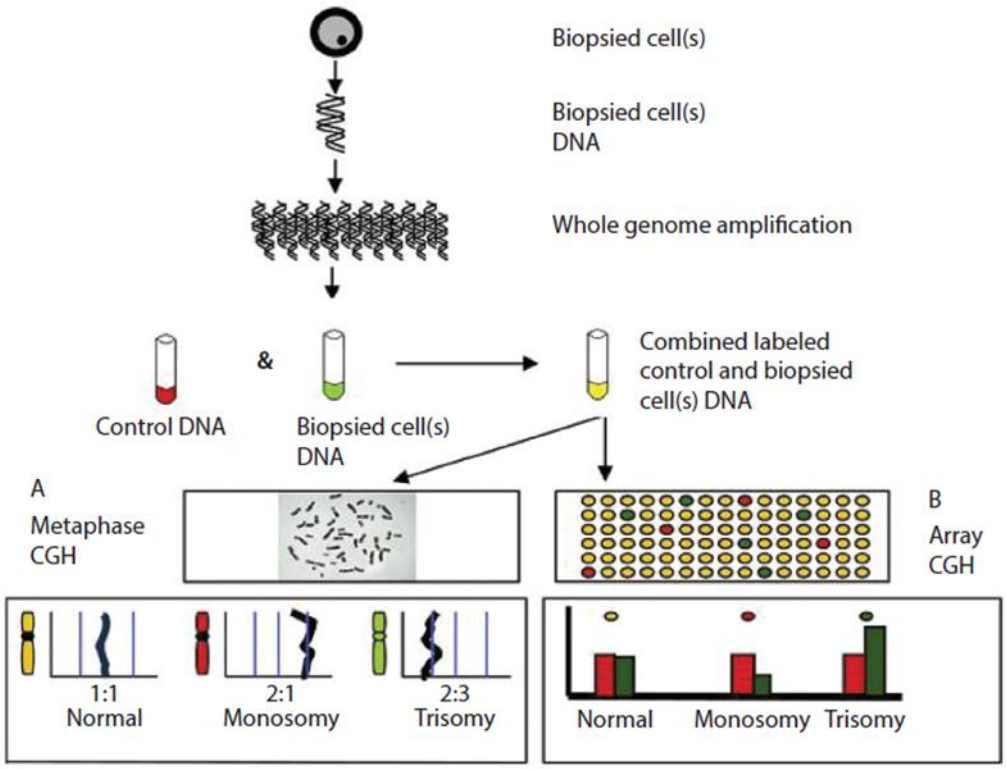

Figure 4.1. Schematic of comparative genomic hybridisation (Thornhill *et al.* 2014a).

4.4.1. Array CGH for Chromosome Enumeration

Following egg (polar body 1 and/or 2), embryo (cleavage stage) or blastocyst biopsy, the biopsied material is washed in a buffer, typically phosphate buffered saline (PBS) with an additive such as polyvinyl alcohol (PVA) to reduce cell stickiness (Harton *et al.* 2011). Following washing, the biopsy material is picked up in a very small volume (<2µl) and placed into a sterile, 0.2ml Eppendorf tube for transport to the testing laboratory. A more detailed description of this process (specifically for trophectoderm biopsy of the blastocyst) is given in section 3.8. Most laboratories perform a quick centrifugation step to ensure that the cellular material and all of the fluid are collected at the bottom of the tube. Most labs then freeze each sample prior to transport to the testing lab; however, this is not essential depending on the length of time the sample will be in transit prior to further processing. It is very important to note that mineral oil, which is typically

used as an overlay on top of biopsy material destined for polymerase chain reaction (PCR) testing, should never be used prior to WGA and aCGH as it inhibits the amplification process.

4.4.2. Whole Genome Amplification (WGA) and Labelling

A number of different WGA methods have been used historically for array CGH with the current, most often utilised method being Sureplex™ (Rubicon Genomics Inc., Ann Arbor, MI, USA and BlueGnome) that is fragment amplification-based. Self-inert degenerative primers are annealed at multiple sites along the genome. Extension then displaces downstream strands to generate multiple fragments spanning each region. The reaction produces large fragment sizes, which are reproducible between samples and are optimised for array CGH. Many of the other WGA techniques have been adapted for use in array CGH but were originally used for other purposes (for example single locus PCR and mutation detection). SurePlex™ is suitable because of its simple, short protocol, highly representative amplification and low allele dropout rates. Briefly, following sample receipt in the lab, each tube is opened in a dedicated DNA amplification clean-room, under laminar flow conditions, and the WGA reagents added (SurePlex™ kit). Amplification is performed according to the manufacturer's instructions as these kits have been validated using single cells. For SurePlex™, there is a 15 minute cell lysis (DNA extraction) step, followed by the pre-amplification steps (90 minutes) and finally amplification (30 minutes). All of these steps are performed in a single tube which reduces the likelihood of sample switches and contamination. In addition, all of these steps require the use of a PCR thermal cycler machine as they are time and temperature dependent. As the arrays are the most expensive consumable in the process, it is best to ensure amplification prior to taking the sample further through the process. Following amplification, most laboratories run an agarose gel electrophoresis step to confirm amplification. A smear of high molecular weight DNA, observed on the gel following electrophoresis, is indicative of positive amplification and all such samples may be taken forward to the fluorescent labelling steps. Low molecular weight DNA or the absence of any smear indicates poor or failed amplification. In such cases, it may be prudent to avoid running such samples on the microarrays.

Successfully amplified WGA product is labelled through nick translation with either Cy3 (green) or Cy5 (red) fluorescence and purified.

4.4.3. Hybridisation

Samples with unknown genotype (i.e. embryo biopsy) labelled in one fluorescent colour and control reference DNA (typically a karyotypically normal male) labelled in the opposite colour are separately denatured (to render them single-stranded) at 74^{o}C, prior to being mixed together in equal proportions in hybridisation buffer containing formamide and cot-1 human DNA before adding to each 24Sure^{TM} microarray. Microarrays are hybridised at 47^{o}C for at least four hours or overnight in a humidified chamber. The length of hybridisation time varies depending on the number of samples in the lab on any given day, the time samples are received during the day and the local staffing levels and shift patterns. During validation of the array in the lab, hybridisation times as short as three hours and as long as 16 hours (overnight) were tested with no differences noted (BlueGnome (now Illumina), unpublished data). On the basis of these results, hybridisation for at least four hours and no longer than 16 hours is deemed to be interchangeable (Reprogenetics Ltd, unpublished data).

4.4.4. Post-Hybridisation Washing

Following hybridisation, each microarray is washed as follows: 10 minutes in 2xSSC/0.05% Tween 20 at room temperature, 10 minutes in 1xSSC at room temperature, 5 minutes in 0.1xSSC at 60^{o}C and 2 minutes in 0.1xSSC at room temperature to remove unbound DNA.

4.4.5. Scanning

Each microarray slide is scanned using a dual channel fluorescent laser scanner is used to create TIFF images (e.g. ClearScan^{TM}, BlueGnome) for green fluorescence at 632nm and for red fluorescence at 587nm. Raw images are loaded automatically into BlueFuse^{TM} software allowing for automated evaluation of fluorescent signals (ratio analysis).

4.4.6. Scoring

Each sample is scored by a trained technologist who assesses traces for all 24 chromosomes, noting all gains and losses, as well as determining the gender of each sample. A second technologist then scores the sample blindly, with no knowledge of the initial score by the first technologist. A final score for each sample is assigned by comparing the two scores. Any discrepancies are noted and are adjudicated by a third technologist and/or the laboratory supervisor or director. Single chromatid errors can be distinguished from whole chromosome errors through examination of the mean per-chromosome hybridisation ratios (see Figure 4.2 and Gabriel *et al.* 2011a).

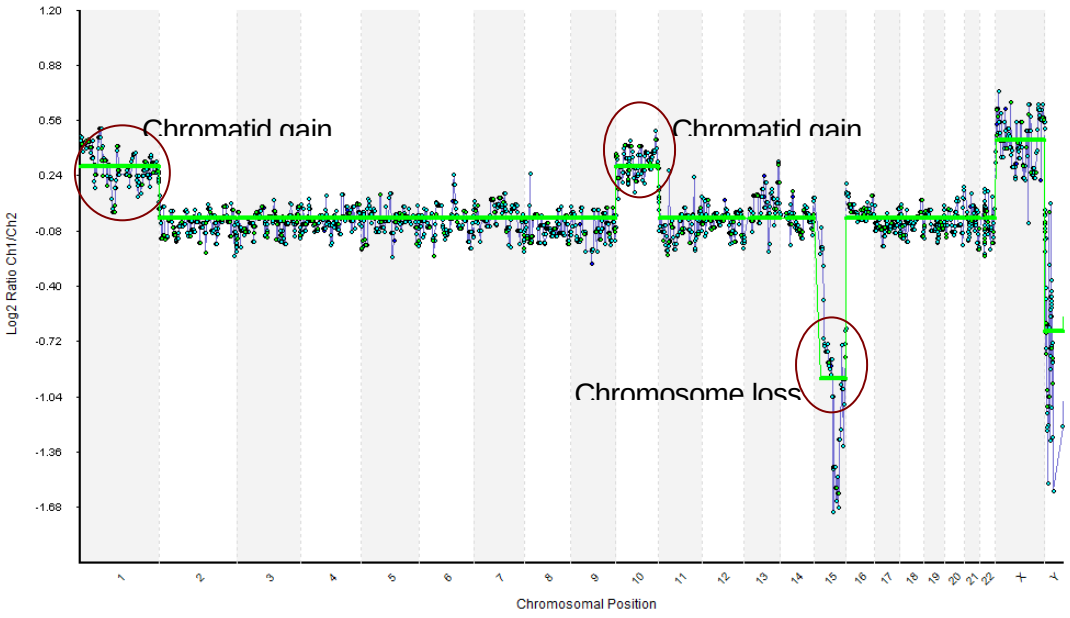

Figure 4.2. Determining chromatid versus chromosome loss in first polar body samples by array CGH (Thornhill *et al.* 2014a).

For most chromosomes (i.e. not the sex chromosomes or the aneuploid chromosomes) a clear and consistent 1:1 ratio is observed along the chromosome length. As the polar body sample was co-hybridised with male genomic DNA, a hybridisation pattern representing a 2:1 ratio for the X chromosome and a '0:2' ratio for the Y chromosome is observed. This polar body clearly shows multiple aneuploidies with chromatid gains on chromosomes 1 and 10 (single chromatid gains are consistent with a 3:2 [or 1.5:1] ratio, i.e. approximately half that of the X chromosome shift) and a loss of whole chromosome 15 (similar to the shift seen for the absent Y chromosome).

4.4.7. Reporting

Once results for all samples from each patient are finalised, a diagnostic report is prepared, signed off by an appropriately qualified person (on site or remotely) and shared with the referring laboratory and physician prior to embryo transfer (Harton *et al.* 2011).

4.4.8. Validation

In extensive validation using single cells from known cell lines against the gold standard of karyotyping, 24Sure^{TM} demonstrated 98% accuracy. In contrast to the use of cell lines, validation for embryo aneuploidy is difficult as ideally to obtain reliable and robust results one needs truth data (i.e. samples of known genotype). While the same is true of human oocytes, in that they are of unknown genotype, the ability to biopsy both the first and second polar bodies from the oocyte provides the opportunity to obtain relatively robust validation data comparing results from so-called 'trios' of both polar bodies and their corresponding oocyte, zygotes or embryos. The expectation is to see reciprocal results (i.e. chromosomal gains and losses) from aneuploid polar body and oocytes (see Figure 4.3). The presence of chromosomal mosaicism in human embryos makes it difficult to categorically identify embryos as having a single specific genotype. Thus from a mosaic embryo, individual single cell results may appear to be unrepresentative and multicellular results (e.g. from trophectoderm biopsy) potentially difficult to interpret (see Figure 4.4) and therefore help to make decisions regarding embryo selection.

To date, 24sure^{TM} and 24Sure-plus^{TM} arrays have been validated using a number of different cell types to evaluate both technical and biological performance, some examples of which are listed in Table 1b.1. Following clinical implementation it is essential to maintain accuracy and overall quality assurance of the test offered by means of test quality control measures and external quality assessment (EQA). The sex chromosomes provide a good internal control by observing the X and Y chromosome deviation from the autosomes within a euploid DNA complement. This level of deviation can be used as a guide to assess aneuploid and euploid positions on the array CGH plot. For EQA, a scheme for single cell array CGH is currently in development based on earlier single cell PGD schemes (Deans *et al.* 2013) and in many countries such schemes are required for laboratory accreditation and to meet regulatory requirements.

(a) Second polar body

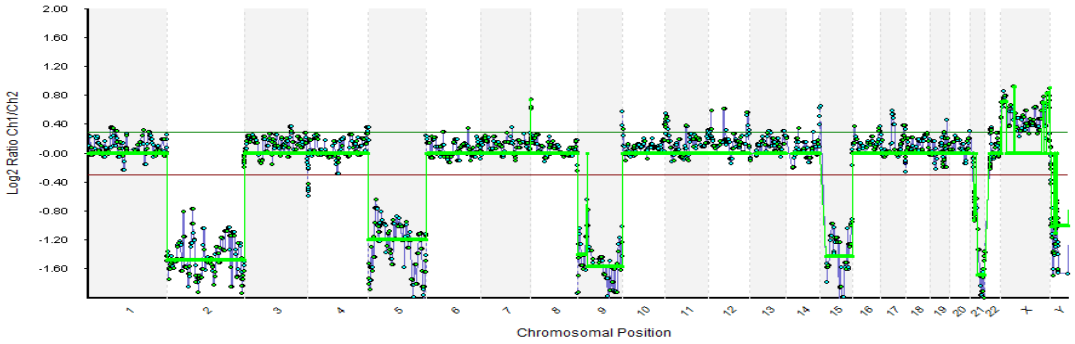

(b) Corresponding zygote

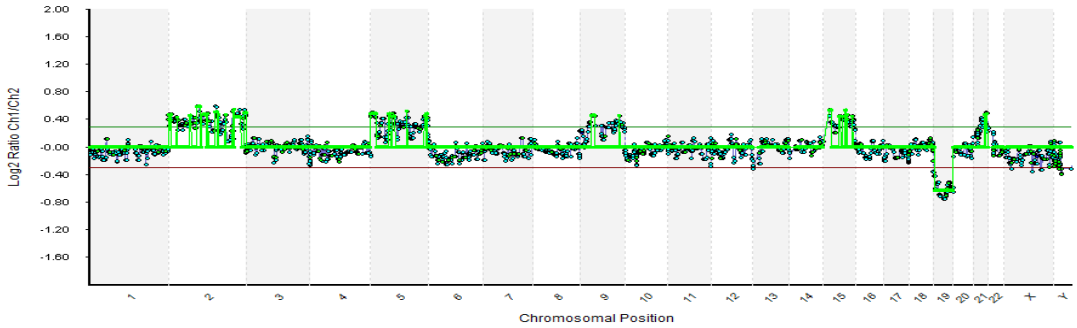

Figure 4.3. Array CGH trace from second polar body and corresponding oocyte sample (Thornhill *et al.* 2014a).

Multiple aneuploidies (gains or losses) detected in (a) the second polar body (-2, -5, -9, -15, -21) are seen in the reciprocal form in (b) the corresponding zygote (+2, +5, +9, +15, +21 and additionally -19). Note the increased amplitude of the signal:noise ratio for the polar body sample versus the zygote. In part this is due to the quantity and quality of DNA available within the respective cells.

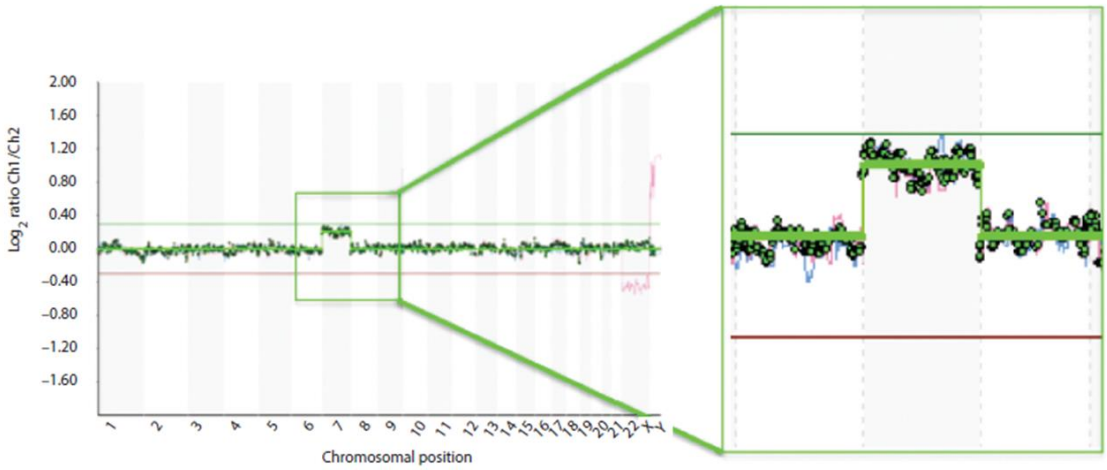

Figure 4.4. Detection of mosaicism in trophectoderm samples using array CGH (Thornhill *et al.* 2014a).

A sample of the trophectoderm from a human blastocyst show likely chromosomal mosaicism. This male embryo is euploid for all autosomes except for a mosaic trisomy of chromosome 7. Mosaicism is suspected because the signals for the chromosomes are relatively uniform and the log2 ratio shift for chromosome 7 is uniform along the length of the chromosome but does not exceed the threshold (bottom red and top green line respectively) required to call it uniformly aneuploid. It is unclear whether the presence of mosacism identifies this embryo as chromosomally abnormal and potentially nonviable. Note the generally high signal-to-noise ratio for this multicellular sample compared with that seen for polar body samples in Figure 1b.3 (aCGH traces courtesy of Dr. Francesco Fiorentino, Genoma Laboratories, Rome, Italy.)

Table 4.1: Formal Pre-Clinical Validation of 24Sure^{TM} BAC Microarray (Thornhill *et al.* 2014a)

Cell/sample type	Known genotype	Accuracy of aCGH diagnosis (%)
Blinded euploid/aneuploid ovarian carcinoma cell lines (single cells) (Dr Joyce Harper, UCL Centre for PGD, Personal Communication)	Yes	51/51 (100%)
Blinded aneuploidic cell lines (single cells) (BlueGnome, unpublished data)	45, X; 47, XY +13; 47, XY +21; 47, XYY; 47, XXY	118/121 (98%)
Human embryonic blastomeres (reanalyzed embryos) (Gutierrez-Mateo *et al.* 2011)	Various genotypes established by 12 colour FISH	53/54 (98%)
Human oocytes and polar bodies (Geraedts *et al.* 2011)	Various genotypes deduced by reciprocity between PB1/2 and corresponding oocyte	90% concordance in 226 trios (PB1/2 and oocyte)

4.5. High Resolution Array CGH for Detection of Chromosome Imbalance

Where array CGH is used to detect chromosomal imbalance in embryos derived from couples in whom at least one partner carries a balanced translocation, an assessment of: (i) the likely outcomes should be made by a qualified genetics professional; and (ii) the likely size of unbalanced products using a prediction tool (available from BlueGnome) to ensure the microarray has sufficient resolution to detect smaller products. For example, the current version of 24Sure-plus^{TM} contains 4,800 BAC clones and claims to be able to accurately detect products as small as 10Mb (with possible detection to the 2.5Mb resolution level in regions with good clone coverage). The protocol for use of 24Sure-plus^{TM} is essentially the same as for 24Sure^{TM}, the primary difference being the higher resolution microarray slide using in the 24Sure-plus^{TM} test. Aside from improved accuracy and effectively eliminating the need to provide couple specific test development, an additional benefit of using array CGH for translocation carriers is the simultaneous detection of aneuploidy for all the other chromosomes not involved in the

translocation (Alfarawati *et al.* 2011a). An example of the array trace showing reciprocal gains and losses in the predicted chromosomes (involved in the translocation) is shown in Figure 4.5.

(a) Chromosome 2 **(b) Chromosome 5**

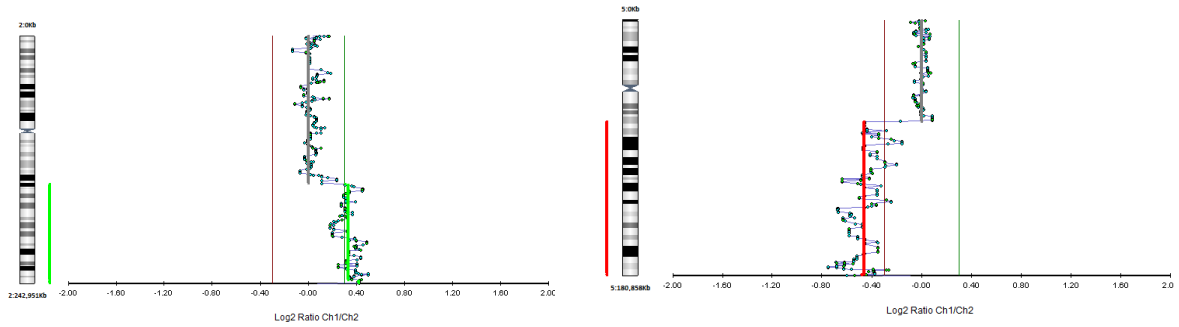

Figure 4.5. Detection of partial aneuploidies in embryonic samples from a reciprocal translocation carrier – t(2;5)(q21;q31) – using array CGH (Thornhill *et al.* 2014a).

Embryos from reciprocal translocation carriers can be used to validate 24Sure^{TM} detection of segmental aneuploidies since each affected embryo will have segmental aneuploidies based at two specific breakpoints. Detecting gains and losses at these two specific breakpoints internally validates the accuracy of the test. In this case, one parent carried the translocation t(2;5)(q21;q31) resulting in gains and losses of chromosomal material in the single blastomeres of affected embryos. Even though the deletion/duplications can be relatively small, the combination of a higher resolution microarray, known breakpoints and their predicted meiotic products and a multicellular sample makes it relatively straightforward to detect reliably.

4.6. Limitations of Array CGH

Array CGH is highly accurate (98%) and in competent hands delivers a 98% result rate. Despite its proven accuracy, array CGH has clinically relevant limitations in the field of preimplantation genetics. For example, it cannot discriminate between maternal and paternal errors. Nor can it distinguish between meiotic and mitotic errors of chromosome segregation. For the purposes of the cycle in which the testing is being done, this is not so relevant. However such additional information may provide clues as to how to treat the patient in the future. Finally, as array CGH is a method predicated on high quality DNA and successful hybridisation the possibility exists that borderline results could be mis-called (as with FISH).

4.7. Future Opportunities

While array CGH has become the gold standard for direct chromosome enumeration in embryos and oocytes, there are a number of alternatives available which could, in time, challenge its dominance. As with all competing technologies there are advantages and disadvantages (Bisignano *et al.* 2011; Handyside 2013). Comprehensive chromosomal screening using multiplex quantitative fluorescent PCR (Treff *et al.* 2012) may provide a cheaper alternative but it is not currently commercially available, thereby restricting its use. Aneuploidy can also be detected using single nucleotide polymorphism arrays using a combination of loss of heterozygosity (monosomy), quantitation of specific SNP loci and incongruous SNP calls compared with predicted Mendelian results using parental information that are incompatible with normal disomy (Handyside *et al.* 2010; Johnson *et al.* 2010; Treff *et al.* 2010; Gabriel *et al.* 2011b; Brezina *et al.* 2011). Next Generation sequencing promises to supersede all other methodologies (Handyside 2013) but currently is only cheaper than array based methods if large numbers of samples are processed simultaneously.

4.7.1. Non-Invasive Indirect Methods of Determining Aneuploidy

Weak correlations exist between the presence of embryonic aneuploidy and morphological aspects of embryo development following retrospective analysis (Munné 2006; Alfarawati *et al.* 2011b). Such findings have stimulated the field of non-invasive analysis of embryos in an attempt to identify aneuploidy in a real-time clinical setting. Time-lapse imaging and analysis appears to demonstrate that morphologic features and developmental timings of the embryo have some relationship to aneuploidy with an algorithm based on the onset and duration of blastulation correlating well with implantation rates (Campbell *et al.* 2013a; Campbell *et al.* 2013b). However this finding is only on a small sample size and is likely to be confounded by a maternal age effect (Ottolini *et al.* 2014). If the finding is confirmed in larger data sets and with appropriate sub-group analysis stratified by maternal age it may provide some useful prioritisation criteria but cannot, at present, replace the specificity and accuracy of aneuploidy testing using array CGH on biopsy samples.

Another promising morphokinetic approach is to assess dynamic fragmentation patterns within early embryos but again, it currently does not identify specific aneuploidies and cannot be regarded as a challenge to direct genetic analysis (Chavez *et al.* 2012). Indeed, it is important to note that, no morphokinetic parameter has yet been observed to discriminate between euploid and simple aneuploid (e.g. trisomy 21) embryos. Moreover, while there have been some useful predictors of viability related to specific metabolites, none so far has been linked specifically to aneuploidy rather than viability, or been able to differentiate between general chromosomal aneuploidy and specific aneuploidy (Picton *et al.* 2010; McReynolds *et al.* 2011).

4.8. Summary and Essentials

At present, array CGH may be considered the gold standard for detecting aneuploidy in single cells or multicellular samples from oocytes and embryos as a result of its reliability, reproducibility, accuracy and the large worldwide experience with it. It is possible to obtain results within 12 hours

following biopsy making it accessible to most laboratories regardless of the biopsy stage selected. While there remains some controversy over the benefit of PGS for specific patient indications, there appears to be a recent shift towards trophectoderm (multicellular) biopsy of the highest quality embryos from good prognosis patients in contrast to the historic focus on cleavage-stage biopsy of few, poor quality embryos in poor prognosis patients. Irrespective of the approach taken, the following tips below should be considered critical for effective use of this technology.

4.8.1. Quality of the IVF Laboratory

Overall quality of the *in vitro* fertilisation (IVF) programme is critical. Whenever an oocyte or embryo is subjected to a procedure outside of the incubator there is a risk involved. Thus a fundamental principle underpinning the use of aneuploidy screening is that the benefit gained should outweigh the harm, if any, caused. Thus if the success rates of the programme are already sub-optimal it is difficult to see any procedure providing sufficient benefit to rescue the cycle.

4.8.2. Embryo Biopsy

Embryo biopsy has become simpler with the availability of the non-contact infra-red laser which is common in many IVF laboratories (see section 3.3). With this laser, it is relatively simple to perform oocyte or embryo biopsy, in many cases without apparent damage to the subject. However, following indiscriminate use, invisible thermal damage might be caused which, while not immediately lethal, could have later consequences compromising development and subsequent implantation. For this reason, it is vital to perform the embryo biopsy as quickly as possible with minimal exposures to laser energy to complete the task safely and effectively. The issue of embryo selection for biopsy is not straightforward as there is inevitably a balance between the cost and efficacy of performing a biopsy on all embryos in the cohort against the

need for all information and the small chance that apparently delayed embryos (either at cleavage or blastocyst stages) still may have some implantation potential.

4.8.3. Sample Preparation and Transportation

Proper preparation of the biopsied sample, while mundane, is of critical importance. A focus on the sterility of the working area and solutions, precise volume of buffer in the microcentrifuge tube with minimal carryover of embryo culture medium (which can reduce amplification efficiency) and subsequent storage of the sample pre-analysis is paramount to ensure high diagnostic success rates. Particular care must be taken not to contaminate the sample with foreign DNA by means of good laboratory practice, appropriate apparel and dedicated cleanroom, equipment and consumables for amplification steps. A negative control of the embryo media and collection buffer should always be taken at this point to check for the absence of contamination as array CGH is not able to identify the origin of any contamination. While published protocols exist and diagnostic service laboratories generally provide their own standard operating procedures, a series of laboratory-specific validation experiments is extremely useful prior to offering the service clinically.

4.8.4. Whole Genome Amplification

A number of different methods are available and have been reported for use in preimplantation genetic testing. However, the specifications of the amplified DNA optimal for array CGH are DNA fragments of a specific size corresponding to the specific array type. For 24Sure^{TM} BAC arrays, Sureplex^{TM} (a PCR-based method) is used in preference to multiple displacement amplification (MDA).

4.8.5. Array CGH Procedure

Hybridisation is fairly robust but care should be taken to ensure microarray slides do not dry out prior to washing. The high temperature high stringency wash post-hybridisation must be temperature controlled. Lower temperatures prevent the removal of non-specific labelled DNA from the array potentially resulting in ratio data compression and generally generating noisy or ambiguous results. If the temperature is too high too much of the labelled DNA will be stripped from the array and could result in too few probes per chromosome to accurately call the result particularly for smaller chromosomes. Drying of the microarray slides is also critical; the most effective way is to mechanically remove wash buffer by centrifugation. If wash buffer is left to dry on the slides this fluoresces and will reduce data quality. After drying, slides should be scanned immediately as in some circumstances the fluorescent dyes can be degraded by atmospheric ozone. While the software is highly accurate, a combination of both automated and manual calling of results is recommended.

4.8.6. Target Population for Testing

Regardless of the testing method used, it is important to properly identify the appropriate patients who would benefit from the test. Indications for testing vary widely and it is crucial for both providers and patients to understand the difference between using the test to provide diagnostic information (for example in the case where there are very few embryos present but they are highly likely to be grossly aneuploidy) or information to enable selection of euploid embryos (to improve the likelihood of success in that embryo transfer cycle). Essentially, in the absence of comprehensive prospective randomised controlled clinical trials for each putative indication for PGS, clinics must conduct a cost-benefit exercise weighing up the potential prognostic (selection) and diagnostic (closure or alternative therapy) benefits against the financial cost to the patient and biological cost to the biopsied embryo (see General Introduction section 2.3.)

5. Specific Aim 2: To produce the first clinical cases to bring Karyomapping to full medical application, comparing it to 'gold standard' approaches and demonstrating how a linkage-based analysis of SNP karyotypes can be used simultaneously to detect monogenic disorders and (phase and parent of origin of) chromosome copy number.

The principles of Karyomapping are outlined in section 2.5.6 of the general introduction and thus the next logical step was to apply the work in a clinical setting. What follows is an account of the first two clinical cases of Karyomapping, the first for a family at risk of transmitting Marfan Syndrome, the second at risk of transmitting Smith Lemli Opitz Syndrome with a history of aneuploid embryos from previous PGD cycles. This work has been recently published as follows:

Case 1

Thornhill AR, Handyside AH, **Ottolini CS**, Taylor J, Sage K, Harton GL, Cliffe K, Affara N, Konstantinidis M, Wells D, Griffin DK. *Karyomapping – a comprehensive means of simultaneous monogenic and cytogenetic PGD: Comparison with standard approaches in real time for Marfan syndrome*. J Assist Reprod Genet. 2015 Mar;32(3):347-56

Case 2

Natesan S, Handyside AH, Thornhill AR, **Ottolini CS**, Sage K, Summers MC, Gordon A, Michaelis Konstantidis M, Wells D, Griffin DK. *Live birth by PGD following confirmation by a comprehensive approach (Karyomapping) for simultaneous detection of monogenic and chromosomal disorders*. Reprod Biomed Online. 2014 Nov;29(5):600-5

5.1. My Personal Contribution to the Work

Case 1:

I was involved in the clinical decision-making process of how the case was run. I performed the majority of the embryology, blastomere biopsy and tubing work of both clinical and follow-up samples. I performed the Karyomapping analysis using the Karyomapping Microsoft Excel macro developed by Professor Alan H. Handyside (Handyside *et al.* 2010) to compare with the standard short tandem repeat (STR) analysis. I also analysed all samples for chromosome copy number using the same Macro.

Case 2:

I recruited these patients into the Bridge Centre's Karyomapping program during a prospective patient seminar after the couple discussed their clinical history with me. I was involved in the clinical decision-making process of how the case was run. I performed all of the embryology work including sequential polar body biopsy of the first and second polar bodies, blastomere biopsy and tubing work of both clinical and follow-up samples. I performed the Karyomapping analysis using the Karyomapping Microsoft Excel macro developed by Professor Alan H. Handyside (Handyside *et al.* 2010) to compare with the standard STR analysis. I also analysed all samples for chromosome copy number using the same Excel macro for comparison to the array comparative genomic hybridisation (CGH) results of the corresponding polar bodies.

The following text is adapted from that in the original manuscripts:

5.2. Introduction

As outlined in Specific Aim 2 of this thesis, preimplantation genetic diagnosis (PGD) of single gene defects by genetic analysis of biopsied material from oocytes and embryos is clinically well established. However, there are significant drawbacks associated with current technologies in that there is an inherent need to tailor the diagnostic approach to the disorder and individual family under investigation. Diagnostic strategies also need to be optimised for single or small

numbers of cells. In practice, this can take days or weeks, with the corresponding delay, stress and reduction in fertility potential to couples as they wait for test validation. An approach that does not require individual-specific validation therefore is a priority for all families seeking PGD. Moreover, the ability to combine monogenic disorder detection with high-resolution chromosome analysis in a single test would potentially find widespread clinical application (Handyside & Xu 2012).

Targeted haplotyping by multiplex fluorescent polymerase chain reaction (PCR) of closely linked or intragenic STR markers combined with direct mutation detection improves the accuracy of embryo biopsy analysis significantly and minimises potential errors caused by undetected allele dropout (ADO) or contamination (Harton *et al.* 2011). ADO refers to the failure of one of the two alleles of a heterozygous locus to amplify. This makes a heterozygous cell appear homozygous at the affected locus, potentially leading to misdiagnosis. Furthermore, using high order multiplex protocols, this approach has been extended to multiple loci, including analysis of the human leukocyte antigen (HLA) region for selection of embryos tissue matched to existing sick children and diagnosis of translocation chromosome imbalance. However, the development of patient, disease or locus-specific protocols, and testing with single cells, is time-consuming and labour intensive. Also, this targeted approach only provides limited information on chromosome aneuploidy, which is recognised to be a major cause of *in vitro* fertilisation (IVF) failure and pregnancy loss.

As outlined in section 2.5.6, Karyomapping (Handyside *et al.* 2010) uses the principles of linkage analysis to detect monogenic disorder plus the spectrum of molecular cytogenetic abnormalities in a single assay. Thus, meiotic trisomies, including their parental origin, can be identified by the presence of both haplotypes from one parent in segments of the chromosome, resulting from the inheritance of two chromosomes with different patterns of recombination. Moreover, monosomies or deletions can be identified by the absence of either chromosome haplotype from the parent of origin. Mitotic chromosome duplication, which can arise through malsegregation of chromosomes in the cleavage divisions following fertilisation, cannot be detected by Karyomapping *per se*, since

the sequence of both chromosomes is identical. However, chromosome duplications may be clinically less significant, since they are often associated with poor morphology and developmental arrest. Karyomapping can also diagnose triploidy, parthenogenetic activation and uniparental disomy (both hetero- and iso-disomy in the presence of meiotic recombination only) (Handyside *et al.* 2010).

The purpose of this chapter was to extend Karyomapping into a clinical setting by reporting its successful use for PGD in confirming (in real time) current standards of mini-sequencing, linked markers and array CGH (aCGH). The main challenge of this work was to apply Karyomapping, firstly by adapting the protocol for clinical use in a regular PGD timeframe (24 hours), and secondly by detection of the autosomal dominant condition Marfan syndrome (Case 1) and the autosomal recessive disorder Smith-Lemli-Opitz (SLO) syndrome (Case 2). The aim was that both would ultimately lead to unaffected live births.

5.3. Materials and Methods

5.3.1. Case 1

5.3.1.1. Patient History

Marfan syndrome is an autosomal dominant disorder of the connective tissue predisposing to aortic aneurism and caused by mutations in the fibrillin-1 (FBN1) gene on ch romosome 15q21.1. A couple, in which the father is affected by Marfan syndrome and has had an aorta replacement and treatment for a detached retina, requested PGD. The father was previously referred to the Bridge Centre genetics department by an accredited National Health Service (NHS) laboratory as heterozygous for two mutations in FBN1, c.235C>T and c.3089A>G. The first, c.235C>T (p.Gln79X) is a nonsense change that has been reported in the FBN1 online mutation database http://www.umd.be/FBN1/4DACTION/WV/2699. The second variant is a missense change c.3089A>G (p.Asn1030Ser), this was not reported in the database at the time of writing. While the database does not assign specific pathologies to each mutation, the reasonable assumption was

made that one or both of these mutations in FBN1 were the cause of Marfan syndrome in this patient. While there was no molecular work up of older family members there was also no prior family history of the syndrome. Both were found to be present in his affected daughter (5 years old at the time of treatment) establishing that they are present in cis on the same paternal chromosome. The mother (36 years old at the time of treatment) had only one other natural pregnancy that resulted in a hydatidiform mole.

The patients gave informed consent for treatment by PGD/Karyomapping. Ethical approval was granted by the treatment licences awarded to the Bridge Centre, London, the Clinical Pathology Accreditation, Certificate of Accreditation awarded to the Institute of Reproductive Sciences, Oxford and the University of Kent Local Research and Ethics Committee. The patients received counselling for intra-cytoplasmic sperm injection (ICSI)/PGD at the Bridge Centre prior to treatment.

5.3.1.2. IVF Cycle

An antagonist protocol was used for ovarian stimulation. When the average follicular diameter was >16mm, 5000IU β-human Chorionic Gonadotrophin (β-hCG) was administered and the oocytes retrieved 36 hours later by ultrasound-guided transvaginal aspiration under local anaesthesia. ICSI was used for insemination of mature oocytes, six to eight hours after the oocyte retrieval, to avoid contamination by extraneous sperm. The following morning (Day 1), each injected oocyte was checked for pronuclei to confirm fertilisation.

5.3.1.3. Embryo Biopsy

Normally fertilised embryos (with two pronuclei on Day 1), which developed to the 6- to 10-cell stages on Day 3 following ICSI were transferred to calcium- and magnesium-free medium (Quinn's Advantage, Cooper Surgical, CT, USA) and one or two single blastomeres were biopsied for genetic analysis by micromanipulation after making an opening in the zona pellucida

using a non-contact infrared laser (Saturn 3, Research Instruments Ltd, Penryn, UK). The embryos were then returned to culture while the biopsied cells were thoroughly washed in non-stick wash buffer (phosphate buffered saline [PBS] with 0.1% polyvinyl pyrrolidone). The washed cells were transferred to 0.2ml PCR tubes in approximately 1-2µl of the wash buffer and frozen before transportation to Reprogenetics UK (Oxford, UK) for further processing.

5.3.1.4. Whole Genome Amplification

The whole genome of the single blastomeres was amplified by multiple displacement amplification (MDA) according to the manufacturer's instructions with modifications (Repli-g Midi kit, Qiagen, Germany). In brief, 1.5µL of PCR-grade water was added to each sample and alkaline lysis carried out by adding 2.5µl of lysis buffer (0.75µL of PCR-grade water, 1.25µL of 0.1M DTT and 0.5µL of 1M NaOH) and incubation at 60°C for 10 min. Neutralisation buffer (2.5µl 0.4M Tricine), 12.5µl PCR grade water, 29µl reaction buffer and, finally, 1µl of DNA polymerase (Repli-g Midi kit, Qiagen, Germany) was added to each sample individually for a final reaction volume of 50µl. The samples were then incubated in a thermocycler at 30°C for two hours, followed by enzyme inactivation at 65°C for 5 min.

5.3.1.5. Short Tandem Repeat and Mutation Analysis

For dominant conditions, PGD protocols that focus on the analysis of the mutation site alone are associated with an unacceptably high risk of misdiagnosis caused by ADO. Allele dropout is common at the single cell level and, as explained in section 2.5.3., results in a heterozygous cell appearing to be homozygous. In the case of PGD for Marfan syndrome, ADO affecting the mutation site on the copy of chromosome 15 carrying the mutation, could cause an affected embryo to appear normal (as only the normal allele is successfully amplified). To reduce the risk of misdiagnosis, a strategy employing a combination of mutation detection and analysis of closely linked STRs was used, revealing the paternal 15q21.1 haplotype associated with the mutation.

Only one STR marker (D15S659) was found that had different repeat alleles on each of the four parental chromosomes and was fully informative (Table 5.1; Figure 5.1). To increase accuracy, a further two STRs, one intragenic (D15S196) and a second proximal STR (D15S143), were selected which had two paternal alleles, one of which was shared with the single maternal allele.

Table 5.1: STR Sizes for Family Members (see also Figure 2.1) (Thornhill *et al.* 2014)

Patients tested	**Short tandem repeats**		
	D15S143* (Proximal flanking)	D15S196* (Intragenic)	D15S659* (Proximal)
Father (affected carrier)	**185** / 193	**271** / 275	**176** / 180
Mother (unaffected)	193	275	192 / 200
Daughter (affected carrier)	**185** / 193	**271** / 275	**176** / 200

* Linked marker alleles in **bold** are the ones associated with the **mutant** *FBN1* allele.

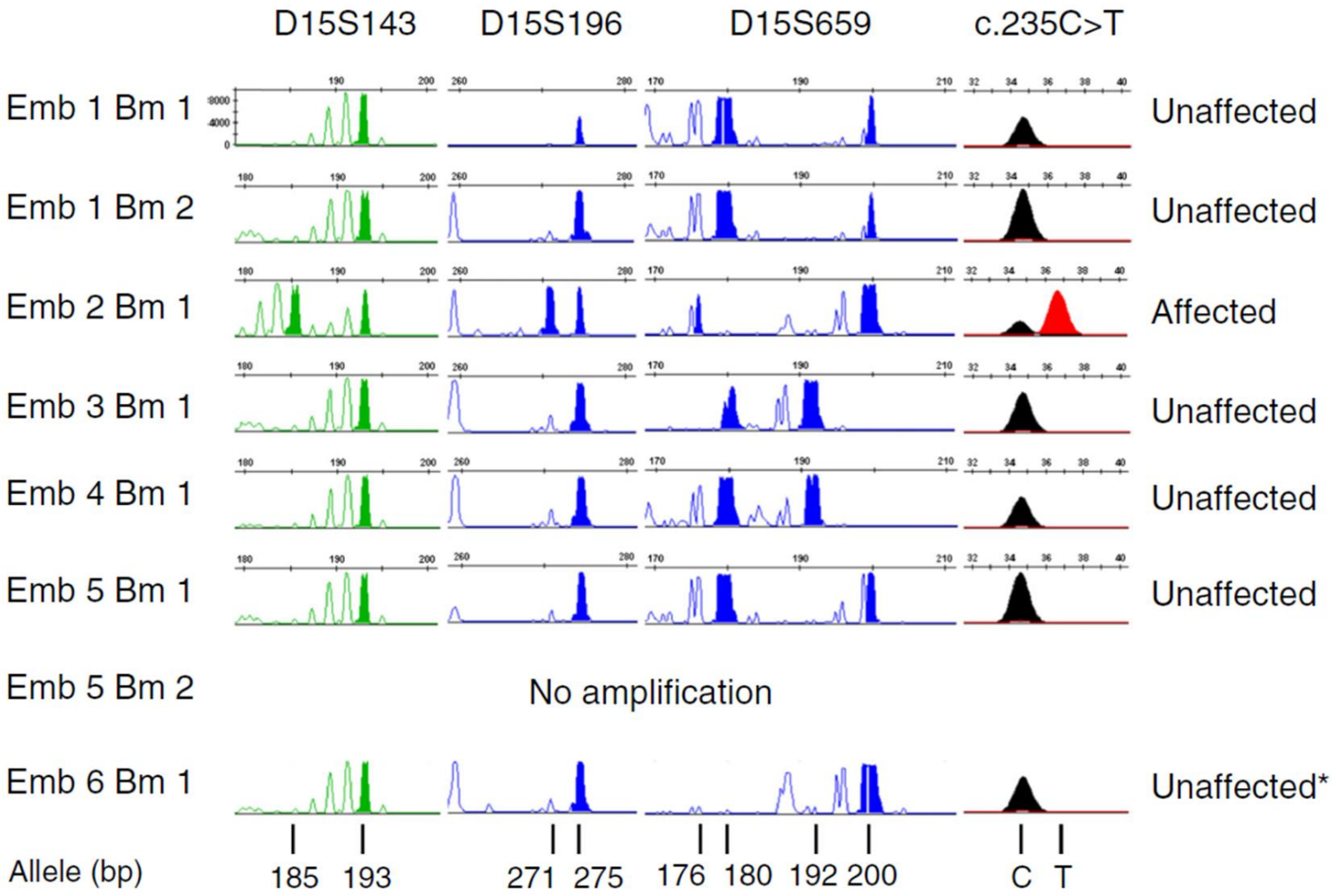

Figure 5.1. Analysis of three short tandem repeat (STR) markers and the c.235C>T mutation in FBN1 by capillary electrophoresis (Thornhill *et al.* 2014).

Following isothermal MDA, the products were amplified in a series of singleplex PCR reactions. Reaction mixtures contained PCR grade water (Roche, Germany), 1x HotMaster Taq Buffer (with 25 mM Mg2+) (5 Prime, Germany), dNTPs (200µM each) (Thermo Scientific, USA), 0.8µM each primer, 0.6 units HotMaster Taq DNA polymerase and 1µl MDA WGA DNA for a final volume of 15µl. Thermal cycling consisted of an initial denaturation step of 96ºC for 1 min, followed by 50 cycles of 94ºC for 15s, 60ºC for 15s, and 65ºC for 45s, then a final extension step of 65ºC for 2 min. Primer sequences for the linked STRs were obtained from the NCBI 'UniSTS' database(http://www.ncbi.nlm.nih.gov/unists):

D15S1435'-CCTAAGGAGGCAACAGCAAAG-3' and 5'-GTAAAGACTGGTATCTGTAGCAC-3'); D15S196 (5'-GACCTGTAGCTGAAGGGAAG-3' and 5'- ATAAAAGTGGTGGGGAAGGATG-3');D15S659(5'- GTGGATAGACACATGACAGATAGG-3' and 5'-TATTTGGCAAGGATAGATACAGG-3').

The primers utilised for amplification of the mutation site were:

5'- TGGATGGAAAACCTTACCTG-3' and 5'- CAGTTACAAAAGGCCACATTC-3'. Only the c.235C>T mutation was targeted since the two mutations identified in father and daughter were determined to be in cis (i.e. located within the same gene on the same chromosome and therefore inherited together).

5.3.1.6. Mutation Detection

The procedure for carrying out minisequencing involved two separate reactions. Initially, products derived from PCR amplification of the mutation site were treated with ExoSAP-IT (USB, Affymetrix, USA) according to manufacturer's instructions. Treated products were then subjected to minisequencing through the usage of the SNaPshot Multiplex Kit (Applied Biosystems, USA). Specifically, the reaction mixture contained 2.5µl of SNaPshot Multiplex Ready Reaction Mix, 0.5µl of 2µM minisequencing primer (F–5'-AAACCTTACCTGGCGGAAAT-3'), 0.5µl PCR grade water and

1.5µl of treated amplified product for a final volume of 5µl. Thermal cycling consisted of 25 cycles of 96°C for 10s, 50°C for 5s, 60°C for 30s.

Confirmation of the above was performed by Karyomapping on the same whole genome amplified material. Single Nucleotide Polymorphism (SNP) genotyping proceeded using the Illumina Bead chip system (Illumina inc, Cambridge UK). Genomic DNA from father, mother, affected daughter and MDA product from the embryo samples were used to interrogate the arrays. Following scanning, image data were transferred to the GenomeStudio Software framework V2010.1 (Illumina inc, Cambridge UK) and converted from fluorescence data to genotypic data based on design algorithms consistent with bead chip content (BeadStudio Software Suite, v3.1, Illumina, Inc). The genotype data was exported as an Excel compatible file for Karyomapping analysis.

A Visual Basic for Applications (VBA) macro has been described previously (Handyside *et al.* 2010) to process and analyse the SNP genotype data and construct Karyomaps in Microsoft Excel. Karyomapping was performed for diagnostic and confirmatory purposes and results were compared with the original diagnosis of PCR analysis of markers linked to the DHCR7 gene and mini-sequencing of the mutation directly. Cytogenetic data was compared with the array CGH data derived from polar bodies.

5.3.2. Case 2

5.3.2.1. Patient History

This couple was at risk of transmitting SLO syndrome; an autosomal recessive condition leading to multiple congenital abnormalities and mental retardation. Both parents are unaffected carriers with mutations in the 7-dehydrocholesterol reductase gene (DHCR7) on chromosome 11q12-q13. The female patient is of advanced maternal age with evidence of decreased ovarian reserve. The couple noted six natural pregnancies: a full term healthy daughter; two terminations for foetal SLO syndrome; two first trimester spontaneous abortions of unknown aetiology and one second trimester

pregnancy loss diagnosed with SLO syndrome. They previously completed, without success, two treatment cycles of IVF/ICSI/PGD using standard approaches.

The patients gave informed consent for treatment by PGD/Karyomapping. Ethical approval was granted by the treatment licences awarded to the Bridge Centre, London, the Clinical Pathology Accreditation, Certificate of Accreditation awarded to the Institute of Reproductive Sciences, Oxford and the University of Kent Local Research and Ethics Committee. The patients received counselling for ICSI/PGD at the Bridge Centre prior to treatment.

5.3.2.2. IVF Cycle

A short cycle flare protocol was used for ovarian stimulation. An hCG trigger (Ovitrelle) was administered after 11 days of stimulation and transvaginal ultrasound-guided oocyte retrieval performed 35 hours later.

For PGD, the primary diagnosis of chromosome constitution was performed on first and second polar bodies using array CGH. The diagnosis of SLO status was performed on cleavage stage biopsied single cells (as is common practice in the Oxford laboratory) using mini-sequencing and linked markers on whole genome amplified material from the cleavage-stage biopsied blastomeres. Karyomapping was performed to confirm the above on the same whole genome amplified material and at exactly the same time. From the outset, the decision was made to disclose all results with the exception of the Karyomapping results on the transferred embryos.

5.3.2.3. Biopsy and WGA

Biopsy of the first polar body in each oocyte was performed on the day of egg collection followed by ICSI. Biopsy of the second polar body was performed post-fertilisation. Polar bodies were subjected to whole genome amplification (WGA) using Sureplex^{TM} then aCGH using a commercial service (BlueGnome, now Illumina, Cambridge, UK) to determine aneuploidy status. Cleavage stage biopsy

proceeded at Day 3 post-fertilisation and, to perform WGA, cells were amplified using multiple displacement amplification (Repli-g Midi kit, Qiagen, Germany, with modifications). All blastomeres were tested directly for mutations in the *DHCR7* gene. STR primers for three loci-linked to the *DHCR7* gene (D11S4139, D11S4143. D11S4207 – Molecular Genetics Laboratory, Rome, Italy) were amplified in separate singleplex PCR reactions using Hot Master Taq DNA polymerase (5PRIME, Hilden, Germany), which were detected by capillary electrophoresis (3130 Genetic Analyzer [Applied Biosystems, USA]) and analysed using GeneMapper software v4.0 (Applied Biosystems, USA). Minisequencing involved the SNaPshot Multiplex Kit (Applied Biosystems, USA).

5.3.2.4. PGS and PGD

For PGD, the primary diagnosis of chromosome constitution was performed on first and second polar bodies using array CGH. The diagnosis of SLO status was performed on cleavage stage biopsied single cells (as is common practice in the Oxford laboratory) using mini-sequencing and linked markers on whole genome amplified material from the cleavage stage biopsied blastomeres. Karyomapping was performed to confirm the above on the same whole genome amplified material and at exactly the same time. From the outset, the decision was made to disclose all results with the exception of the Karyomapping results on the transferred embryos.

Modification of the original Karyomapping protocol was performed to allow diagnosis within 24 hours. SNP genotyping proceeded using the Illumina Bead chip system (Illumina inc, Cambridge UK). Genomic DNA from father, mother, previously affected foetus and MDA product from the embryo samples were used to interrogate the arrays. Following scanning, image data were transferred to the GenomeStudio Software framework V2010.1 (Illumina inc, Cambridge UK) and converted from fluorescence data to genotypic data based on design algorithms consistent with bead chip content (BeadStudio Software Suite, v3.1, Illumina, Inc). The genotype data was exported as an Excel compatible file for Karyomapping analysis.

A VBA macro has been described previously (Handyside *et al.* 2010) to process and analyse the SNP genotype data and construct Karyomaps in Microsoft Excel. Karyomapping was performed for diagnostic and confirmatory purposes and results were compared with the original diagnosis of PCR analysis of markers linked to the *DHCR7* gene and mini-sequencing of the mutation directly. Cytogenetic data was compared with the array CGH data derived from polar bodies.

5.4. Results

5.4.1. Case 1

5.4.1.1. IVF and Embryo Biopsy

10 cumulus oocyte complexes were collected and eight mature oocytes, arrested at metaphase II, inseminated by ICSI. The following morning the injected oocytes were checked and six had two pronuclei indicating normal fertilisation. All six embryos reached appropriate cleavage stages between the 6- and 10-cell stages on Day 3 post ICSI and one or two cells were biopsied for genetic analysis.

5.4.1.2. Targeted Haplotyping and Direct Mutation Analysis

Following WGA targeted haplotyping, with all three STR markers, and direct mutation analysis was successful in 7/8 (87.5%) of the single cells biopsied from six cleavage stage embryos (Table 5.2; Fig. 1). Two single cells were biopsied from two embryos but one of these from Embryo 5 failed to amplify. Analysis of the STR alleles present at the *FBN 1* locus were consistent with the mutation status in five embryos and identified four as unaffected (Embryos 1, 3-5) and one as affected (Embryo 2). In the remaining single cell biopsied from Embryo 6 with a normal allele for the mutation, only one of the maternal alleles (200bp) and neither of the paternal specific alleles (176 and 180bp) were detected with D15S659.Furthermore, the other two STR markers had only a single allele shared by both parents (193bp and 275bp respectively).The interpretation was therefore that either

the paternal chromosome with the normal *FBN1* allele was present but that ADO had occurred with D15S659, or the paternal chromosome 15 was absent from that cell and was reported as unaffected with reduced accuracy.

Table 5.2: Comparison of Targeted Haplotyping, Direct Mutation Analysis with Karyomapping for Linkage Based Diagnosis of Marfan Syndrome and Cytogenetic Analysis with Karyomapping in Single Cells Biopsied from Cleavage-Stage Embryos (Thornhill *et al.* 2014)

Embryo (blasto-mere)	Short tandem repeats (bp) Paternal/Maternal			Mutation (c.235C>T)	Interpretation	Karyomap analysis Paternal /Maternal	? Concordant	Paternal Chromosome		Maternal Chromosome		Comment
								Gain	Loss	Gain	Loss	
1 (1)	193	275	180/200	Normal allele only	Unaffected***	P2/M1	Yes				21	Mosaic loss of chr21
1 (2)	193	275	180/200	Normal allele only	Unaffected***	P2/M1	Yes					
2	**185**/193*	**271**/275*	**176**/200 *	Normal & mutant allele	Affected	P1/M1	Yes			1 (MeII)		
3	193	275	-/192**	Normal allele only	Unaffected***	-/M2 (Mat genome only)	Yes**		All chrs	10 (MeI)	19	No paternal genome
4	193	275	180/192	Normal allele only	Unaffected	P2/M2	Yes		6qter****			Embryo Transferred
5 (1)	193	275	180/200	Normal allele only	Unaffected	P2/M1	Yes					Embryo Transferred
5 (2)	NR	NR	NR	Normal allele only	Amplification failure	NR	N/A					No amp
6	193	275	200	Normal allele only	Unaffected*** (reduced accuracy)	-/M1	Yes, (given cytogenetic result)		15, 20 qter	6p dup, 8 (MeII)		Paternal monosomy 15

* Linked marker alleles in **bold** are the ones associated with the **mutant** *FBN1* allele.

**Note an allele was originally determined to be present at 180bp but, after subsequent analysis, determined to be an artefact

*** Although determined as not carrying the mutant Marfan allele, embryo not transferred for other (e.g. cytogenetic) reasons

**** This apparent deletion was identified after retrospective closer analysis of Karyomapping traces. As call rates were low in this region, it is possible that the apparent deletion was a technical artefact.

For chromosomal analysis:

MeI/MeII=meiosis I/II; qter=terminal portion of long arm of the chromosome; dup=duplication; all chrs=all chromosomes

For Karyomap analysis: P1=Paternal haplotype 1; P2=Paternal haplotype 2; M1=Maternal haplotype 1; M2=Maternal haplotype

5.4.1.3. Karyomapping Analysis

SNP genotyping and Karyomapping analysis was successful with all seven single cells from which MDA products were available. Genomic DNA samples from the parents and affected child gave call rates of about 97% and heterozygous call rates of 28-29%. Overall SNP call rates were lower in single cells, ranging from 78-82% with a significant rate of ADO (approximately 15%) and heterozygous call rates ranging from 14-20% (excluding the cell from the parthenogenetic haploid embryo). Karyomapping identified the parental chromosomes present at the *FBN1* locus on chromosome 15q21.1 in 11/12 (92%) of the chromosomes present in the seven cells analysed (Figure 5.2; Table 5.2). The only chromosome which could not be haplotyped confidently at the *FBN1* locus was the maternal chromosome 15 in Embryo 3. In that case, there was a crossover immediately distal to *FBN1* and without any intragenic informative SNP loci, the exact location of the recombination event could not be identified unequivocally. Otherwise, the paternal and maternal haplotypes identified (where present) were concordant with the targeted haplotyping and direct mutation analysis, including the proximal region of the maternal chromosome 15 in Embryo 3 (Figure 5.2).

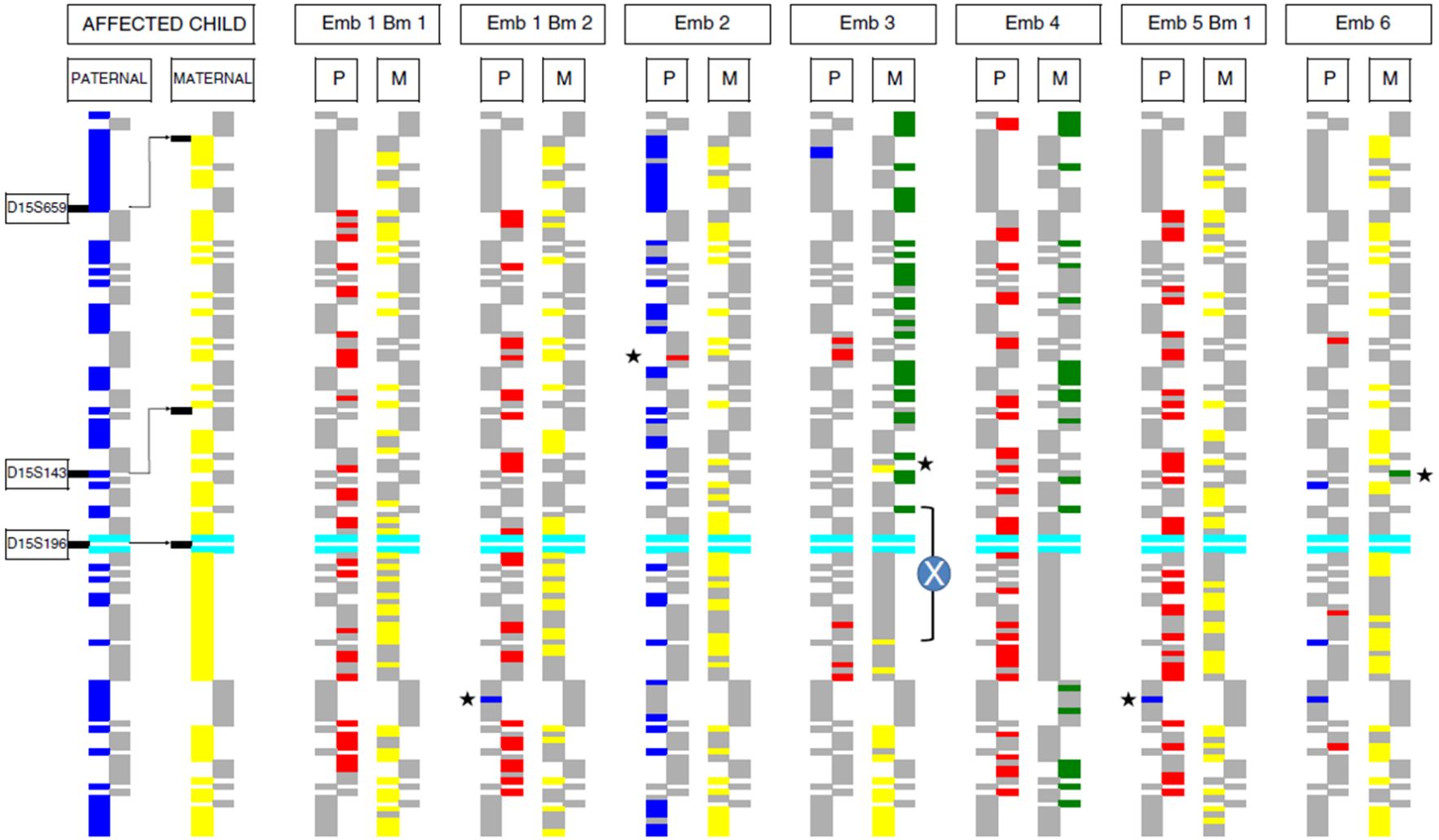

Figure 5.2. Detailed Karyomaps for chromosome 15q21.1 in single blastomeres biopsied from each cleavage-stage embryo (Thornhill *et al.* 2014).

Consecutive informative SNP loci for the four parental chromosomes are represented by two pairs of columns in each case (paternal, left and maternal, right) in which each segment is an informative SNP. Single cell genotypes identifying the presence of one of the four parental chromosomes at informative SNP loci are coloured (paternal chromosomes P1 and P2 are indicated in blue and red respectively; maternal chromosomes M1 and M2 in yellow and green respectively). The Karyomaps of a 5-6Mb region of chromosome 15q21.1 of the affected child, known to be a carrier of both paternal mutations (P1-blue) and used as a reference for phase, and seven single blastomeres biopsied from six cleavage-stage embryos are presented (M1-yellow chromosome also assigned). Otherwise, informative SNP genotypes, which indicate the absence of that chromosome or are not called, are coloured grey. The position of FBN1 relative to the SNP loci is indicated by the light blue bars. The positions of the three STR markers, D15S143, D15S196 and D15S659 used for conventional analysis are indicated on the left. Three embryos are identified as having the unaffected (red) paternal chromosome (Embryos 1, 4 and 5); one embryo has the affected paternal chromosome (blue) also present in the affected child (Embryo 2), and two embryos are missing the paternal chromosomes either because of the complete absence of the paternal genome in a parthenogenetically activated embryo (Embryo 3) or paternal monosomy 15 (Embryo 6). Crossover marked with X. * miscall.

In two embryos, Karyomapping revealed that the paternal chromosome 15 was absent with only a low proportion of random positive informative SNPs for both haplotypes (Embryos 3 and 6; Fig. 7). For Embryo 3, examination of the Karyomaps for all the other chromosomes revealed that no paternal chromosomes were present, which may have resulted from fertilisation failure and parthenogenetic activation of development, whereas in Embryo 6, the missing chromosome was an isolated paternal monosomy (Table 2.2).

Karyomapping analysis of the other chromosomes present in the single cells revealed several aneuploidies and structural abnormalities (Table 2.2). These included three maternal meiotic trisomies in three separate embryos: trisomy 1 in Embryo 2 in which both maternal chromosome haplotypes were detected on segments of both arms of the chromosome (meiosis II type), trisomy 10 in Embryo 3 with both maternal haplotypes additionally present across the centromere (meiosis I type) and trisomy 8 (meiosis II type) in Embryo 6. In addition, there was a mosaic loss of maternal chromosome 21 in Embryo 1, and possible deletions affecting paternal 6q and 20q in Embryos 4 and 6 respectively. The deletion for chromosome 6q in embryo 4 was discovered after a more detailed retrospective analysis and a low call rate in that region for this blastomere meant that this diagnosis was not 100% confident. Finally, both maternal chromosome haplotypes were present for a segment of the short arm only for chromosome 6 in Embryo 6 (partial trisomy 6p). As this abnormality was not confirmed in the whole embryo (see below), this may be an acentric fragment from the other maternal chromosome which arose by chromosome breakage during meiosis, and remained in the oocyte at fertilisation.

5.4.1.4. Follow-up Analysis of Embryos

Analysis of the three embryos that were not selected for transfer and were processed whole, confirmed the presence of the two meiotic trisomies and the maternal loss of chromosome 19 in Embryos 3 and 6 (Table 5.2). However, as expected the mosaic loss of maternal chromosome 21 in Embryo 1 was not detected. Furthermore, the presence of both maternal chromosomes for 6p

in Embryo 6 was also not detected. This is consistent with the presence of an acentric fragment arising in meiosis and segregating to the biopsied blastomere since an extra whole chromosome would normally be present in most, if not all, cells as was observed for the other meiotic trisomies.

A fourth embryo (Embryo 2) was disaggregated on Day 4 into eight single blastomeres and one two-cell sample (10 cells in total). All of these cells had identical Karyomaps and the presence of trisomy 1 was confirmed in each case (Table 5.2). There were no other mosaic chromosome abnormalities except for partial loss of maternal chromosome 13 (approximately 40.5Mb) in one cell.

5.4.1.5. Clinical Outcome

Based on the results of the targeted haplotype and direct mutation analysis (see above), two embryos diagnosed as unaffected were transferred resulting in a twin pregnancy. Delivery was premature at 28 weeks and subsequently one of the twins died following a perinatal infection. The remaining twin boy was healthy at 2 years. Another of the unaffected embryos (Embryo 1; Table 5.2), cryopreserved by vitrification at the blastocyst stage on Day 6 post ICSI, was successfully thawed 16 months later and transferred in an unstimulated cycle; no pregnancy resulted.

5.4.2. Case 2

5.4.2.1. IVF and Biopsy

Eight oocytes were retrieved, of which six were mature second meiotic division (MII) oocytes suitable for ICSI. The first polar body (PB1) was biopsied from each of the six oocytes. Following ICSI, six normally fertilised 2PN zygotes were produced and the second polar body (PB2) was removed.

5.4.2.2. PGS

Array CGH analysis of PB1 and PB2 revealed a normal pattern in zygotes 1 and 4 with chromosome 22 gain (PB1) and loss (PB2) in embryo 2; in embryos 3 and 5 a normal pattern in PB1 contrasted with gain of chromosome 15 and 22 respectively in PB2 (Table 5.3).

Table 5.3: Comparison of Analyses by Mutation, Linkage, Array CGH and Karyomapping

Embryo ID	SLO Status by mini-sequencing and linkage analysis	SLO status by Karyomapping (see Figure 2.2 and Table 2.4)	PB1 by aCGH	PB2 by aCGH	Karyotype by Karyomapping	Comment
1	Unaffected	-	Normal	Normal	-	Transferred
2	Paternal carrier	Paternal carrier	Chr 22 gain	Chr 22 loss	Normal	Not transferred
3	Unaffected	Unaffected	Normal	Chr 15 gain	Maternal monosomy 15, Paternal monosomy 7	Not transferred
4	Affected	Affected	Normal	Normal	Normal	Not transferred
5	Normal	Normal	Normal	Chr 22 gain	Maternal monosomy 22, paternal deletion 15q	Not transferred
6	No result	No result	Normal	Chrs 12 and 14 gain	Arrested, no result	Not transferred

Each embryo had one blastomere biopsied and a combination of mini-sequencing plus analysis of linked markers made the initial diagnosis of Smith Lemli Opitz status. Maternal aneuploidy analysis was done by array CGH on both polar bodies. Karyomapping diagnosed both Smith Lemli Opitz status and chromosome copy number simultaneously. (NB family and clinic agreed that no Karyomapping information on transferred embryo would be communicated.)

5.4.2.3. PGD

Five of six 2PN zygotes formed embryos, which were biopsied. Mutation analysis revealed a normal pattern in embryos 1, 3 and 5 (Table 5.3). Embryo 1 was thus transferred. Concurrently, Karyomapping confirmed the *DHCR*7 status in all embryos examined (Figure 5.3, Table 5.4) (NB after discussions with the family, they made it clear they did not want us to disclose any Karyomapping result on the transferred embryo but were happy for results on all their other embryos to be disclosed) and the aneuploidy results were largely concordant with results following aCGH of the polar bodies (Table 5.3).

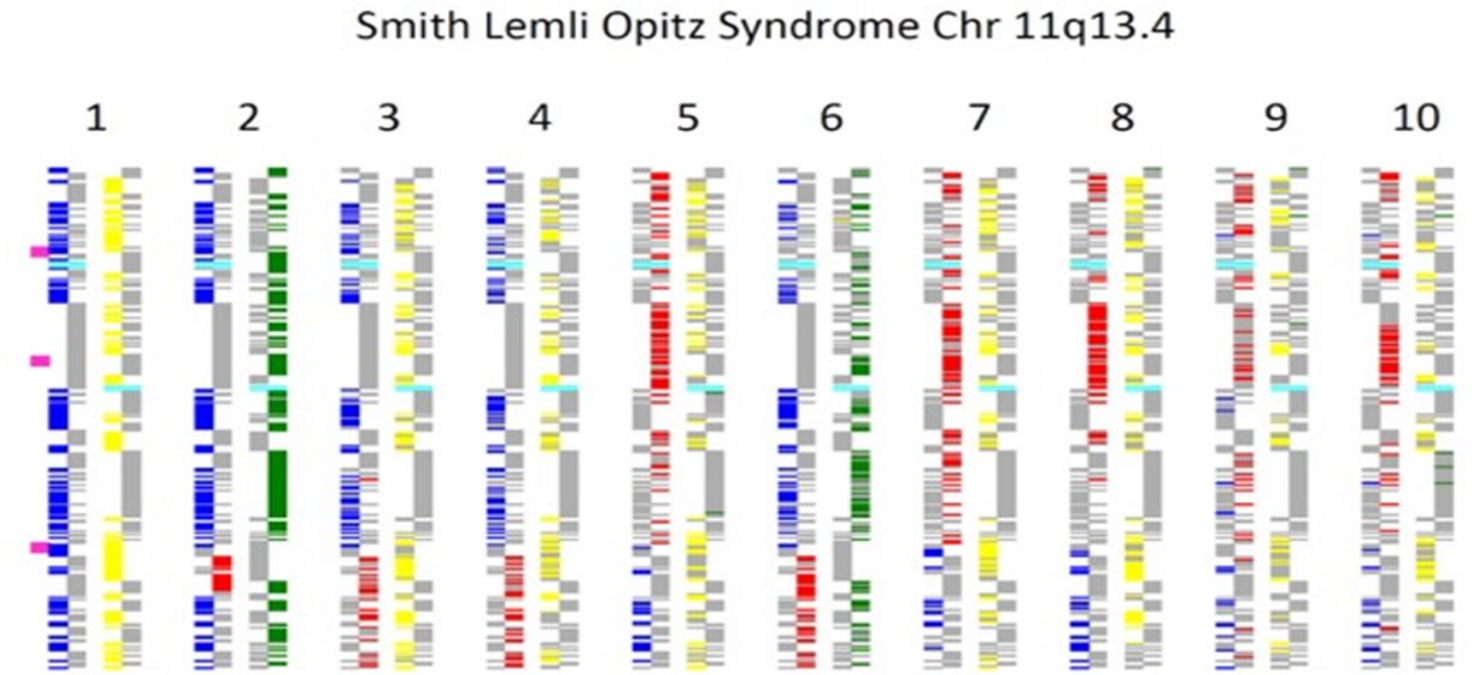

Figure 5.3. Karyomapping analysis of embryos and blastomeres (Bm).

The multiple blue, red, green and yellow bars each indicate informative SNPs. Together they denote which parental chromosome has been inherited (blue and red are paternal chromosomes, yellow and green are maternal chromosomes). The horizontal light blue lines denote the position of the SLO disease locus on each chromosome. In this case it is the blue (paternal) chromosome and green (maternal chromosome) that carry the SLO disease alleles (same pattern as affected foetus; 2). Red-yellow is thus the “unaffected-non-carrier” pattern, blue-yellow denotes a paternal carrier of SLO, red-green is a maternal carrier of SLO.

Table 5.4: Interpretation of Results from Figure 5.3

	Description	Pattern observed around SLO locus	Diagnosis
1	Child (reference)	Blue - Yellow	Paternal carrier
2	Affected fetus	Blue - Green	Affected
3	Embryo 2 blastomere 1	Blue - Yellow	Paternal carrier
4	Embryo 2 blastomere 2	Blue - Yellow	Paternal carrier
5	Embryo 3 blastomere 1	Red - Yellow	Unaffected
6	Embryo 4 blastomere 1	Blue - Green	Affected
7	Embryo 5 blastomere 1	Red - Yellow	Unaffected
8	Embryo 3 blastomere 2	Red - Yellow	Unaffected
9	Embryo 3 blastomere 3	Red – Yellow	Unaffected
10	Embryo 3 blastomere 4	Red – Yellow	Unaffected

5.4.2.4. Clinical Outcome

A pregnancy ensued leading to the live birth of a healthy male infant free of Smith-Lemli Opitz syndrome and with no apparent chromosome abnormality.

5.5. Discussion

Case 2 was the first published clinical use of Karyomapping leading to a live birth of a healthy PGD baby. Specifically the use of Karyomapping confirmed the primary diagnoses of SLO status (by mini-sequencing) and chromosome copy number (by aCGH on polar bodies). Karyomapping was nonetheless performed 'in real time' alongside the standard analyses providing proof of principle of its efficacy in a clinical setting. Concordance with established gold standards attest comprehensively that Karyomapping can detect monogenic disease. Analysis of polar bodies by aCGH and blastomeres by Karyomapping permitted the comparison of aneuploidy results from both polar bodies and the subsequent embryos. One advantage of Karyomapping over aCGH is that it distinguishes the parent and phase of origin of meiotic chromosome error. For example, as shown in Table 2.1, embryo 3, the gain of chromosome 15 in the PB2 suggested a meiosis II error, which was confirmed as a reciprocal loss of chromosome 15 in the embryo. This was also mirrored in embryo 5 for chromosome 22 and the normal diagnosis of embryo 4 matched in both polar bodies and blastomere. In embryos 3 and 5, Karyomapping confirmed that the further abnormalities were paternal in origin and thus would not have been detected in the polar bodies. In embryo 2 a reciprocal gain and loss of chromosome 22 in PB1 and PB2 respectively was not reflected as an abnormality in the embryo, thereby invoking the widely reported mechanism of precocious separation of sister chromatids in the first meiotic division, resulting in a euploid conceptus (Angell *et al.* 1991; Kuliev *et al.* 2011; Gabriel *et al.* 2011; Handyside *et al.* 2012).

The results of these cases demonstrate the clinical utility of a novel, comprehensive approach for PGD (Karyomapping) that combines detection of any monogenic disorder (potentially) with comprehensive chromosome screening in a single test that requires no *a priori* development.

Comparison with a well-established strategy (minisequencing for direct mutation detection combined with linked STR marker analysis) suggests that Karyomapping could be applied clinically for the autosomal dominant condition, Marfan syndrome and the autosomal recessive condition, SLO syndrome. Specifically after whole genome amplification of single blastomeres biopsied from cleavage-stage embryos, both methods (performed in parallel) identified unaffected and affected embryos with high efficiency and accuracy. Karyomapping however had the added advantage of not requiring the clinical work-up of a specific test beforehand (only the SNP array information from the parents and a relative of known carrier status was needed).

For Case 1 (published the following year – Thornhill *et al.* 2015) minisequencing in combination with the analysis of several STR markers, yielded results within 24 hours for all six embryos in which whole genome amplification of the single cells was successful. Furthermore, in all cases, each locus was successfully re-amplified from the MDA products with no detectable ADO. However, because STR analysis in this way is not quantitative, and two of the markers were only semi-informative, ADO cannot be completely excluded in the unaffected embryos (Figure 5.1). In the affected embryo, single paternal and maternal repeat alleles were detected for all three STR markers and both the normal and mutant alleles were detected by minisequencing. Although this would, in practice, lead to a low probability of misdiagnosis, the mere presence of ADO at one or two loci might nonetheless undermine confidence in the result. Indeed, one result (Embryo 6; Table 2.2) was reported to be of lower accuracy because no paternal specific repeat alleles were detected. Karyomapping following SNP genotyping on the other hand identified 122 informative SNP loci across each of the two paternal and two maternal chromosomes in an approximately 5Mb and 6Mb region spanning the FBN1 locus on chromosome 15q21.1 (Figure 5.2). Even taking into account the significant incidence of ‘no calls’ at heterozygous loci, the density of positive informative SNPs for the chromosome present, together with the absence of positive informative markers for the other chromosome, delivered highly accurate haplotyping – significantly more accurate than haplotyping with individual loci. Conservatively, the accuracy of Karyomapping could be calculated as the probability of a double recombination between the

nearest flanking positive (or negative) informative SNP loci. For the single cells in this family, this ranged from about 0.5-1Mb across FBN1. Thus the probability of a double crossover in this region would be less than 0.25-0.5x10-4 assuming 1% recombination per megabase.

Figure 5.4 illustrates also the flexibility and utility of Karyomapping in that it can in theory be used for multiple loci simultaneously. For instance there are 11 loci corresponding to disorders licensed for PGD by the Human Fertilisation and Embryology Authority (HFEA) in the region captured in this figure, including the HLA regions used for diagnoses involving so called 'saviour siblings'.

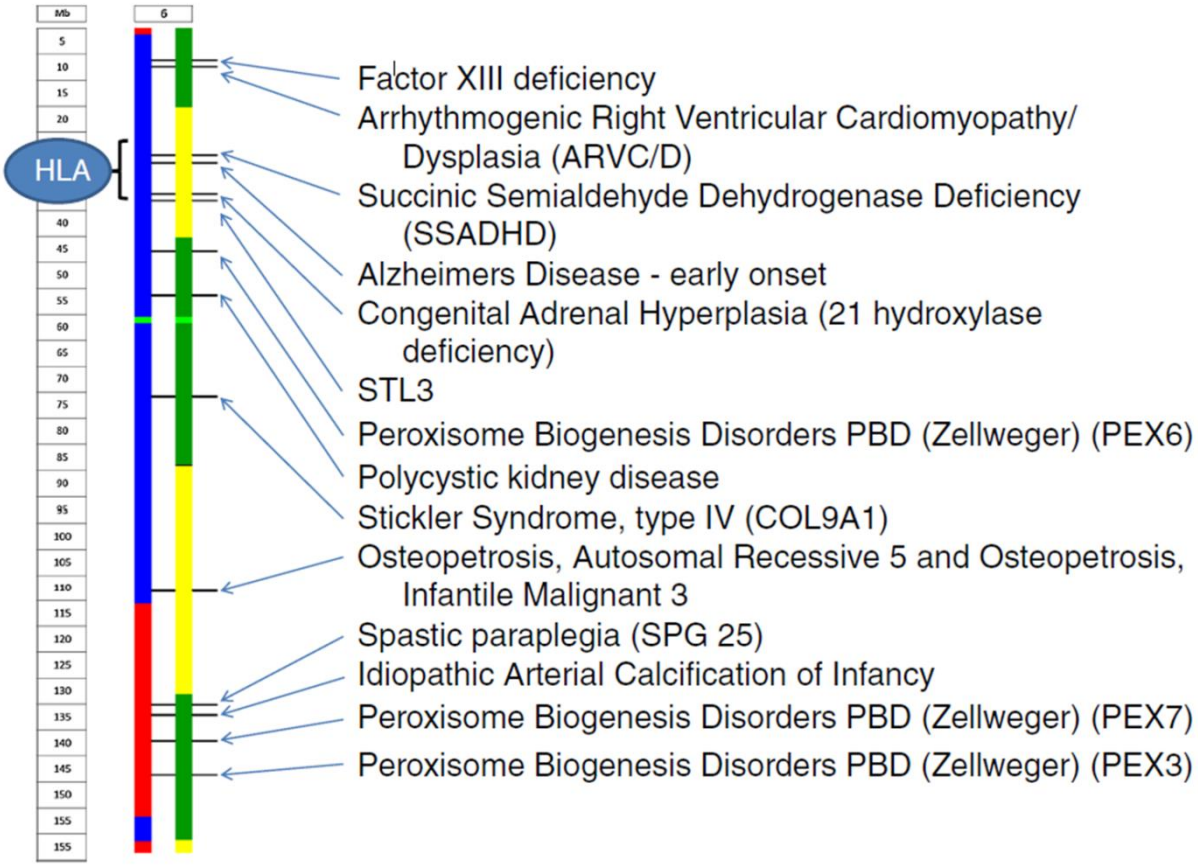

Figure 5.4. Karyomap of a single blastomere focussing on a region of chromosome 6 (Thornhill *et al.* 2014).

The image indicates that there are 11 loci in this region corresponding to disorders currently licensed for PGD by the HFEA. This includes the HLA regions used for diagnoses of saviour siblings.

PGD aneuploidy screening (PGD-AS) for the purposes of improving IVF success rates has met with widespread controversy (Mastenbroek *et al.* 2007; Summers *et al.* 2009; Thornhill & Handyside 2009). One criticism, the fact that PGD-AS using fluorescent in-situ hybridisation (FISH) screened only a small proportion of the total chromosome complement (Summers *et al.* 2009; Thornhill & Handyside 2009), can also be addressed through aCGH and clinical validation of this procedure is now established (reviewed in Fiorentino *et al.* 2010). Treff *et al.* (2010) reported the use of SNP arrays for the detection of chromosome imbalance both for PGD-AS and for the screening of translocation carriers.

Karyomapping uses a similar approach (i.e. SNP arrays) to Treff *et al.* (2010) and, combined with a degree of quantitative analysis, has the ability to distinguish any numerical or structural chromosome abnormality as well as the parent and phase of origin of the abnormality. The latter has clinical implications when considering obstetric outcomes of mosaic pregnancies: mosaic trisomies of meiotic origin often lead to specific phenotypes such as pregnancy loss, intra-uterine growth retardation or excessive birth weight, whereas those of post-zygotic origin generally proceed to term without clinical consequence (Griffin 1996). Karyomapping can also detect uniparental disomy, which can lead to Prader-Willi or Angleman syndromes as well as abnormal patterns of genome duplication seen with, for example, molar pregnancies.

The primary purpose of PGD cycles is to identify embryos with a high probability of transmitting a genetic disorder. The inclusion of comprehensive chromosome screening, in addition to diagnosis of a familial mutation, is a powerful combination, especially when applied in a single assay. Given that chromosomal errors are common in embryos, leading to high rates of embryo implantation failure, miscarriage and more birth defects, there is a sound basis for including comprehensive chromosome analysis alongside PGD. Furthermore, the additional information relating to parental origin of meiotic errors provided by Karyomapping (but not derivable from array comparative genomic hybridisation data) should be particularly helpful for couples in determining which therapeutic intervention to try next (e.g. donor oocytes or donor sperm). In theory, screening for spontaneously arising aneuploidies should increase the likelihood that the embryo chosen for

transfer will establish a viable pregnancy and ultimately a healthy child. Indeed, as a selection tool, aneuploidy screening can prioritise the embryo for transfer to achieve improved implantation rates and lower miscarriage rates in fresh transfer cycles (Scott *et al.* 2013) as well as support single embryo transfer policy as part of the drive towards reducing multiple birth rates (Yang *et al.* 2012).

In these two cases, the benefits of Karyomapping over, for instance, more established molecular cytogenetic approaches (e.g. array CGH) were immediately apparent. As an example, maternal meiotic trisomy of chromosome 1 was detected in a single cell of embryo 2 from Case 1, then subsequently detected in all other cells of that embryo. Meiotic errors are more likely to lead to clinical problems as they are more likely to affect all or most of the cells in the embryo, whereas post-zygotic errors might affect fewer cells depending on the cleavage division in which they occur. For instance the detection of monosomy 21 in embryo 1 for Case 1 was clearly a post-zygotic one that affected one cell and not the rest of the embryo. The added advantage of knowing the meiotic origin of aneuploidy may thus further improve success rates of PGD following aneuploidy screening when compared to other techniques including array CGH and quantitative fluorescent PCR. The detection of structural chromosome imbalance is also currently an advantage of Karyomapping compared to state of the art use of comparative genomic hybridisation, which struggles to detect small abnormalities when using DNA amplified from single cells (e.g. Vanneste *et al.* 2009). Four structural abnormalities and their origins were clearly identified in this study, with a fifth possibly occurring in Case 1 in a single cell of an embryo that was transferred. In this case, the possibility of a deletion was only identified after a retrospective analysis of the Karyomapping data and thus, unlike the other four abnormalities discovered therefore, it cannot be certain whether the result was real or artefact. Nonetheless the absence of any congenital abnormality associated with a terminal 6q deletion in either the surviving twin or the one that perished suggests that it was not a chromosome abnormality present in the majority of the embryo. Finally, Karyomapping determined that embryo 3 of Case 1 had no paternal genome and presumably arose as a result of a parthenogenetically activated oocyte (maternal

diploid). Such conceptuses are not compatible with implantation; notably array comparative genomic hybridisation would have diagnosed such a conceptus as normal.

There are a number of limitations to Karyomapping. For instance, a suitable informative family member, usually an affected child (as well as DNA from the parents) needs to be available. Obtaining parental DNA for analysis is not usually an issue as the parents are actively involved in the whole IVF process throughout the treatment cycle; theoretically however there may be issues with consent or technical problems with the SNP array on the parental genomic DNA.

However, DNA from an informative family member can limit the use of Karyomapping; this is nonetheless the same as any PGD in which linkage analysis is involved. The higher density of markers when SNP arrays are used compared with the 'standard' PCR-based strategies means that there is a greater likelihood of the family member being informative, even if there is a crossover at or near the locus of interest. Nonetheless if a crossover in either reference individual or embryo is directly next to the locus of interest, this may (rarely) render individual diagnoses unreadable by this method. Like all PGD, Karyomapping does not *a priori* detect de-novo mutation (for demonstration of this see Rechitsky *et al.* 2011), nor the confounding effect of pseudogenes. Moreover Karyomapping does not detect post-zygotic chromosome duplication nor copy number variation. Karyomapping therefore has a number of limitations; in our view however use of Karyomapping, for the most part, represents an advancement on the current state of the art for PGD.

Several authors have reported the simultaneous detection of monogenic and chromosomal disorders – to the best of my knowledge, the first of these was a case report by Brezina *et al.* (2011) but more recently Rechitsky *et al.* (2013), which described detection of cytogenetic disorders and cystic fibrosis simultaneously. These, however, ultimately used different approaches to detect the monogenic and chromosomal disorder and the issue of having to tailor the test to the disease in question thus remains. There has been abundant literature on the use of haplotyping for the detection of monogenic and chromosomal disorders (e.g. Rechitsky *et al.* 2006; Renwick *et al.* 2006; 2010). Karyomapping is essentially an extension on this pioneering

work except that, rather than using tailored, linked markers, application of a whole genomic platform permits the use of a single test for each and every case. Karyomapping is moreover platform independent. Here I used Illumina SNP arrays, however the binary nature of the output means that any platform could potentially be used. This includes single cell whole genome sequencing where I propose that, even with the most robust whole genome amplification, sequence gaps would inevitably arise in the assembly. These could be overcome by adaptations of the Karyomapping algorithm. In a procedure where diagnostic speed is of the essence, it seems reasonable to suggest that a rudimentary whole genome sequence (which would take the shortest time) followed by Karyomapping would be the most accurate and expedient means of achieving a diagnosis. Karyomapping therefore has inherent 'future-proofing' in its design and adaptations of the algorithm could, I believe, form the basis of the majority of preimplantation genetic diagnoses worldwide.

With each application of new technology there is an inevitable ethical debate, particularly in the area of assisted reproduction. Fortunately, the law regarding PGD in the UK is very clear. The indication for performing the procedure of embryo biopsy as a precursor to diagnostic testing must meet a series of legal tests. These include the seriousness of the disorder and the likelihood that any child born would suffer from it. In addition, the condition itself for which any preimplantation test is applied must be licensed (HFEA, 1990). However, there are several additional concerns raised by the ability to obtain large amounts of genetic information from the entire genome (Hens *et al.* 2013). One frequently raised ethical concern relating to the ability to screen an ever-increasing number of genes simultaneously is the notion of designing a baby. However, the probability of selecting an 'ideal' embryo from a typical cohort of approximately 10-15 embryos is vanishingly small even when considering only five loci. Of more pragmatic concern is the very real possibility of incidental findings with unknown significance, as evidenced in this report for chromosomal disorders. The detection of hitherto unreported copy number variants as well as small or partial deletions and duplications of unknown pathological significance underlines the importance of and need for comprehensive genetic counselling throughout the PGD process.

6. Specific Aim 3: To apply Karyomapping to demonstrate its clinical utility as a genome-wide 'chromosome fingerprint' in a clinical setting

As outlined in section 2.4.3 of the General Introduction, blastocyst biopsy is now widely used for both PGS and PGD. Although this approach yields good results, variable embryo quality and rates of development remain a challenge. Here, I report a case in which a blastocyst was biopsied for PGS by array CGH on Day 6 post insemination after having hatched completely. In addition to a small trophectoderm sample, excluded cell fragments from the subzonal space from this embryo were also sampled. Unexpectedly, the array CGH results from the fragments and trophectoderm sample were non-concordant: 47,XX,+19 and 46,XY respectively. DNA fingerprinting by short tandem repeat and amelogenin analysis confirmed the sex chromosome difference but appeared to show that the two samples were related but non-identical. Genome-wide single nucleotide polymorphism genotyping and Karyomapping identified that the origin of the DNA amplified from the fragments was that of the second polar body corresponding to the oocyte from which the biopsied embryo developed. The fact that polar body DNA can persist to the blastocyst stage provides evidence that excluded cell fragments should not be used for diagnostic purposes and should be avoided when performing embryo biopsies since there is a risk of diagnostic errors. This work has been recently published as follows:

Ottolini CS, Rogers S, Sage K, Summers MC, Capalbo A, Griffin DK, Sarasa J, Wells D and Handyside AH. Karyomapping identifies second polar body DNA persisting to the blastocyst stage: implications for embryo biopsy. Reprod Biomed Online. 2015 Dec;31(6):776-82.

6.1. My Personal Contribution to the Work

I was involved in the clinical management of the published case above, conceiving and designing the clinical follow-up. I performed Single Nucleotide Polymorphism (SNP) genotyping (Karyomapping), minisequencing (short tandem repeat, STR) and array comparative genomic hybridisation (CGH) and analysis. I was involved in the writing and editing of the published

manuscript and the design and creation of the figures. What follows is an adaptation of the published manuscript.

6.2. Introduction

Blastocyst biopsy (as discussed in section 3.6), by excision of small numbers of herniating trophectoderm cells, is now widely used and is increasingly replacing cleavage stage biopsy for both preimplantation genetic screening (PGS) for aneuploidy and preimplantation genetic diagnosis (PGD) of single gene defects and other abnormalities (Thornhill *et al.* 2012). The main reasons for this are the availability of improved culture media and the widespread adoption of blastocyst culture to select normally developing embryos for transfer with improved implantation and live birth rates. Also the original protocol, which used microneedles for partial zona dissection to promote herniation as the blastocyst expands, and mechanical excision of trophectoderm cells (Dokras *et al.* 1990; 1991), has now been superseded by the use of non-contact infrared lasers (Veiga *et al.* 1997; Boada *et al.* 1998; Kokkali *et al.* 2005). Zona drilling by laser allows precise control of the position of the herniating trophectoderm cells, away from the inner cell mass, and laser assisted excision causes minimal damage to the biopsied cells and the embryo (Scott *et al.* 2013).

Nevertheless, blastocyst biopsy remains challenging because of variability in embryo quality, particularly in the number of cells in the trophectoderm layer, and the rate of development to the expanded blastocyst stage. Whereas, most normally developing embryos reach the 6- to 10-cell stage on the morning of Day 3 post insemination, allowing cleavage stage biopsy, the timing of blastocyst expansion can vary by over 24 hours and occur on Day 5, 6 or even Day 7. Increasingly, therefore, vitrification is being used to cryopreserve biopsied blastocysts, allowing more flexibility in the timing of blastocyst biopsy (Liebermann 2015). One strategy is to biopsy any embryos reaching the expanded blastocyst stage on Day 5, perform the genetic analysis within 24 hours and transfer unaffected fresh blastocysts on Day 6. Embryos reaching the expanded blastocyst stage on Day 6 or 7 are biopsied later, vitrified, tested and unaffected embryos are

transferred in a subsequent cycle. Alternatively, all biopsied blastocysts can be vitrified and replaced in subsequent cycles. Indeed, recent evidence indicates that a strategy involving trophectoderm biopsy, vitrification and PGS is highly effective clinically, since euploid blastocysts all have similarly high implantation and clinical pregnancy rates despite differences in morphology and developmental rate (Capalbo *et al.* 2014).

Here, I report a case in which a slow developing embryo only reached the blastocyst stage on Day 6 post insemination and had hatched completely before being biopsied for PGS by array CGH. Biopsy of hatched blastocysts is more difficult and because the trophectoderm sample obtained was relatively small, excluded cell fragments present in the subzonal space were also sampled. Excluded fragments and cells, some of which are nucleated, are commonly observed at the morula stage onwards and are a potential source of DNA for genetic analysis. Unexpectedly, however, the array CGH results from the fragments and trophectoderm samples were non-concordant in this case. To investigate the cause of this non-concordance, DNA fingerprinting using a panel of informative STR markers including amelogenin to determine the sex, and SNP genotyping and Karyomapping analysis was performed on all samples. The results of both tests were completely concordant and Karyomap analysis identified beyond doubt that the origin of the DNA amplified from the fragments was exclusively that of the second polar body corresponding to the fertilised oocyte that gave rise to the embryo from which the trophectoderm had been biopsied. The implications for blastocyst biopsy and the risk of diagnostic errors are discussed.

6.3. Materials and Methods

6.3.1. Patient History and IVF Treatment Cycle

Following genetic counselling, a couple (maternal age 40yr; paternal age 34yr) requested *in vitro* fertilisation (IVF) with PGS by array CGH for advanced maternal age after failing to conceive naturally for more than a year. The woman had never previously been pregnant but otherwise had no known cause for infertility. The man had never fathered a child and had a history of

surgery to correct undescended testicles. However, semen analysis showed that he was normozoospermic.

Ovarian stimulation was achieved by a standard antagonist regimen with hCG trigger after 12 days of stimulation. Oocyte collection followed 35h post hCG and six mature second meiotic division (MII) oocytes were retrieved. All oocytes underwent IVF with the male partner's sperm and all six fertilised normally with two pronuclei visible the following day (Day 1 post insemination). The embryos were cultured in a time-lapse incubator (Embryoscope; Fertilitech, Denmark) to enable continuous observation. On Day 6, three embryos had reached the expanded blastocyst stage, with one of the three embryos having hatched completely from the zona pellucida. The remaining three embryos arrested at the cleavage stage and were discarded.

6.3.2. Blastocyst Biopsy and Vitrification

The two expanded, non-hatched blastocysts were biopsied by first making a small hole in the zona pellucida using a laser (Saturn; Research Instruments, Penryn, UK) opposite to the position of the inner cell mass. Three to 10 cells were then drawn through the breach in the zona into a sampling pipette and excised using a series of laser pulses across the join between adjacent trophectoderm cells. With the hatched blastocyst, the embryo was immobilised directly by suction onto the holding pipette and biopsied by drawing a small number of trophectoderm cells into a sampling pipette as above. In addition, excluded fragments left behind in the subzonal space (Figure 6.1) were also sampled separately. Finally, all three biopsied blastocysts were vitrified using a commercial kit (Kitazato, Japan) following a previously published protocol (Kuwayama, 2007).

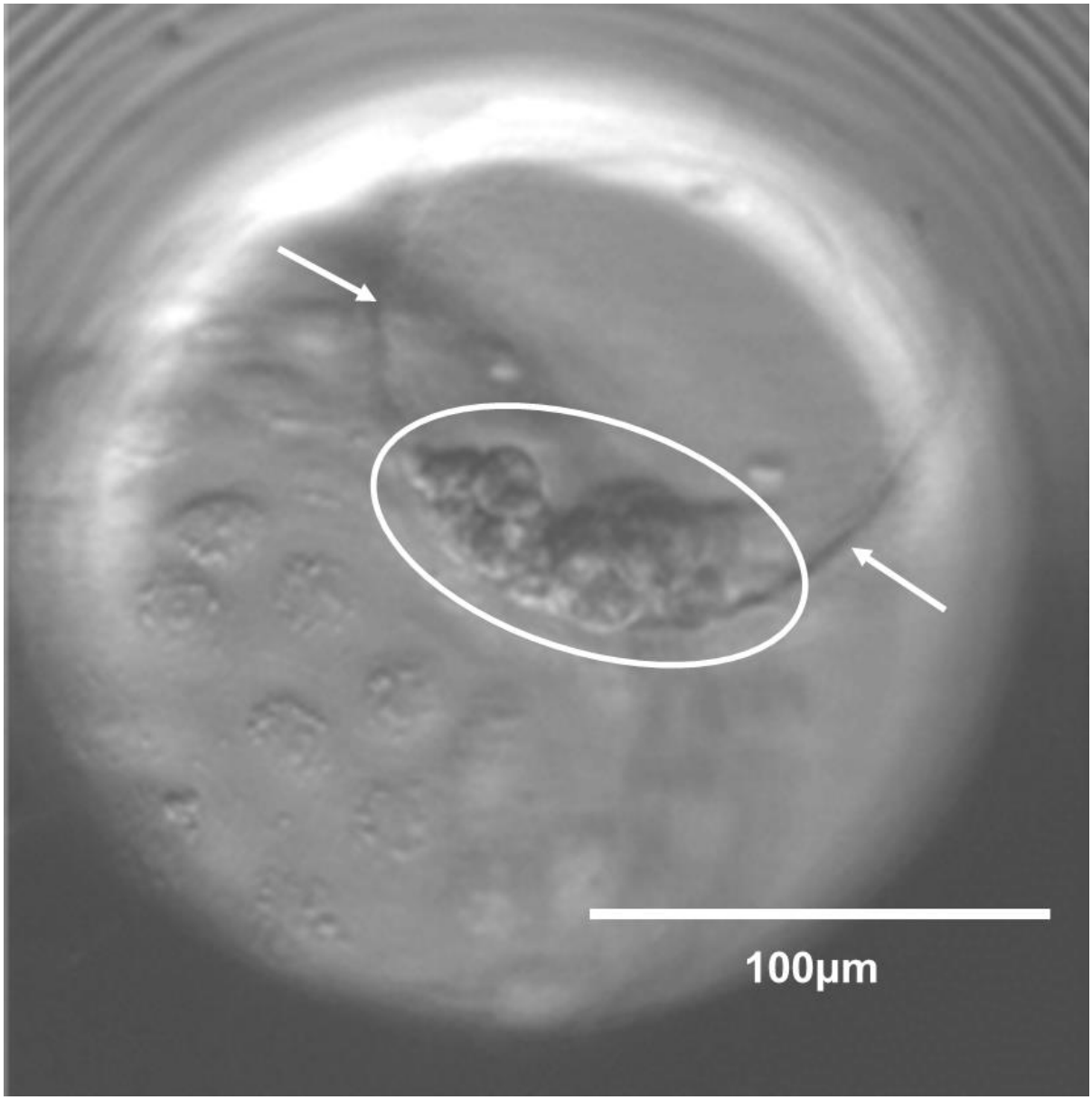

Figure 6.1. Hatched blastocyst (embryo 5) on Day 6 post insemination prior to biopsy (Ottolini *et al.* 2015a).

Note the large group of excluded cell fragments (circled) remaining within the zona pellucida (arrows).

6.3.3. Array Comparative Genomic Analysis (Array CGH)

The biopsied cells and fragments were each placed in 2µl of phosphate buffered saline (PBS) in 0.2ml PCR tubes and whole genome amplification (WGA) performed using a PCR-library based method (Sureplex, Illumina, Cambridge). The WGA products were then used for 24 chromosome copy number analysis by array CGH (24Sure; Illumina, Cambridge) with dedicated software (Bluefuse Multi v3; Illumina, Cambridge) according to the manufacturer's instructions. For detailed methodology see Fragouli *et al.* 2011.

6.3.4. DNA Fingerprinting

All of the WGA products and parental genomic DNAs were DNA fingerprinted by analysis of five Informative STR markers on different autosomes (D2S389, D3S1581, D4S2964, D7S2847, D15S659) and on the sex chromosomes (AMELX/Y). The STR markers were amplified in separate single-plex fluorescent PCRs (Hot Master Taq DNA polymerase; 5PRIME, Hilden, Germany), and the amplified fragments sized by capillary electrophoresis (3130 Genetic Analyzer (Applied Biosystems, USA) with dedicated software (GeneMapper v4.0; Applied Biosystems, USA).

6.3.5. Single Nucleotide Polymorphism (SNP) Genotyping and Karyomapping

All of the WGA products and parental genomic DNAs were also genotyped at approximately 300K SNP loci genome wide for karyomap analysis using a dedicated beadarray (Human Karyomap; Illumina, USA) as described previously (Natesan *et al.* 2014) using a 24-hour protocol (Konstandinidis *et al.* 2015). Genotype data was then exported into Microsoft Excel and karyomap analysis preformed using a dedicated Visual Basic for Applications (VBA) macro. To phase heterozygous SNPs, one of the embryo samples was used as a reference and this was then repeated using another embryo to check the analysis. Finally, the positions of meiotic

crossovers between parental chromosomes for each chromosome were located and marked (excluding reference crossovers) and other custom VBA macros used for processing.

6.4. Results

6.4.1. Array CGH

Whole genome amplification and array CGH was successful with all four samples biopsied from the three biopsied blastocysts (Table 6.1). One embryo (embryo 3) was missing a copy of chromosome 22 (monosomy 22), one embryo was euploid and the two samples from the third embryo were non-concordant. The trophectoderm biopsy (sample 5a) was euploid and male (46,XY) whereas the excluded fragment sample (sample 5b) had an extra chromosome 19 (trisomy 19) and was female (47,XX,+19) (Figure 6.2).

Table 6.1: 24 Chromosome Copy Number Analysis of Biopsied Blastocysts by Array Comparative Genomic Hybridisation (array CGH) and Single Nucleotide Polymorphism (SNP) Genotyping and Karyomapping (Ottolini *et al.* 2015a)

Sample ID	Sample type	Array CGH	Karyomapping
3	Trophectoderm	45 XX, -22	45 XX, -22 (maternal)
5a	Trophectoderm	46 XY	46 XY
5b	Excluded cell fragments	47 XX, +19	23 X haploid (maternal)
6	Trophectoderm	46 XY	46 XY

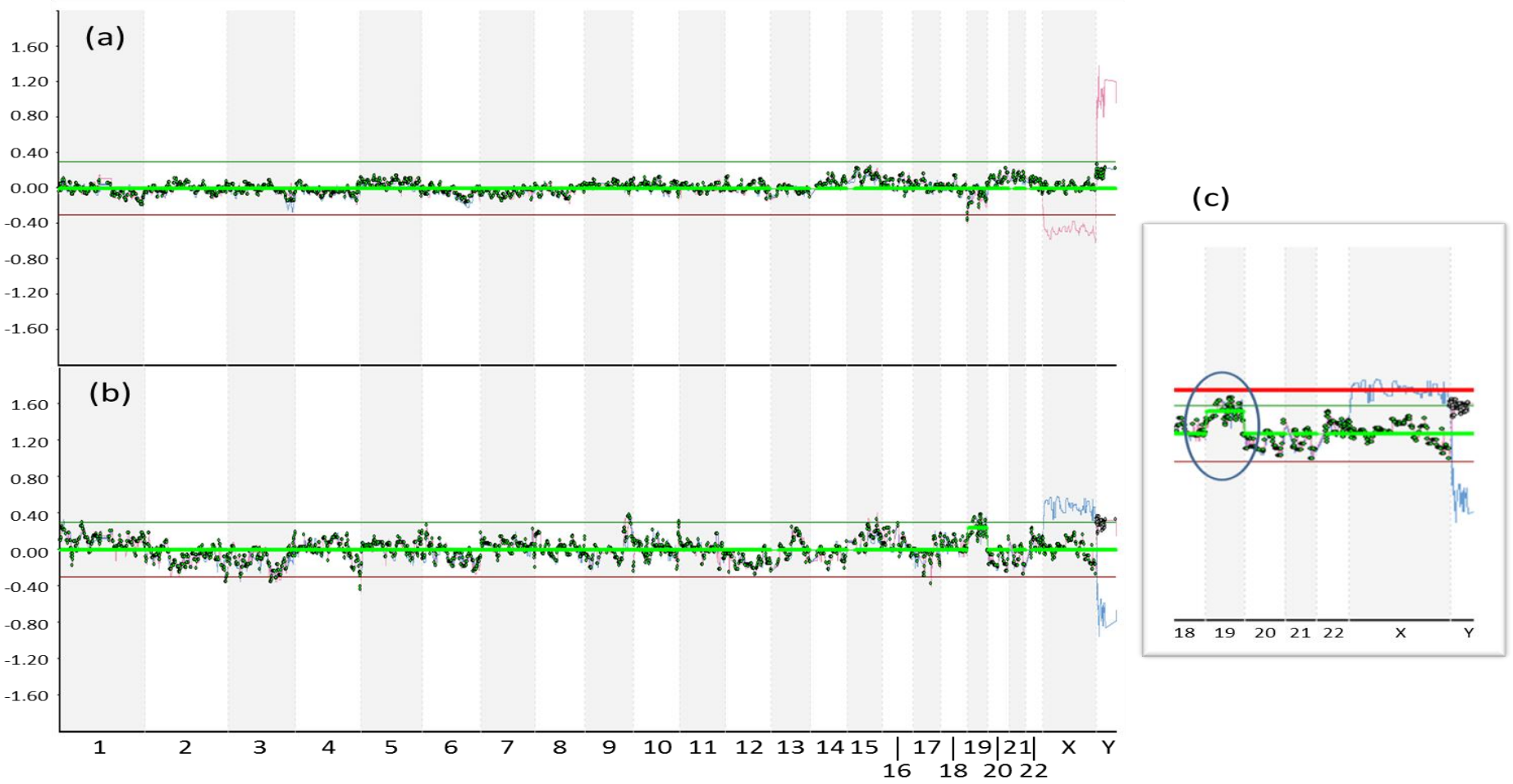

Figure 6.2. Array CGH ratio plots for the trophectoderm biopsy sample (a), and the excluded cell fragments (b) from embryo 5 (Ottolini *et al.* 2015a).

Note that both samples have normal copy number for all chromosomes except that the ratio of probes on chromosome 19 are consistently raised in (b). Also the gender of the trophectoderm sample (a) is identified as male since there is only a single copy of the X chromosome when compared to the sex-mismatched female DNA and a single Y chromosome (pink line). Whereas the fragment sample (b) is identified as female with the same copy number for autosomes and the X chromosome and missing the Y chromosome when compared with sex-mismatched male DNA (blue line). (c) Magnified portion of (b) showing the elevated ratio for chromosome 19 (circled) not reaching the level of the internal X chromosome control (bold red line) on the array.

6.4.2. DNA Fingerprinting

STR analysis at five loci on different chromosomes demonstrated that all four samples had unique combinations of parental alleles indicating they were related but distinct individuals (Table 6.2). Furthermore, amelogenin analysis confirmed the sex of each sample as originally ascertained by array CGH. There was a high allele dropout (ADO) rate across the samples, as typically observed for STR analysis applied to WGA products. In addition, however, the excluded fragment sample was anomalous because only a single maternal allele was detected at each of the three STRs which amplified and no paternal alleles were observed for any of the STRs. Furthermore, the three maternal alleles were the opposite of those seen in the corresponding trophectoderm sample.

Table 6.2: DNA Fingerprinting at Five Short Tandem Repeat (STR) Markers on Different Chromosomes and Amelogenin

	Samples											
Marker	**Paternal gDNA**		**Maternal gDNA**		**3**		**5a**		**5b**		**6**	
D2S389	197	209	199	216	209	216	197	216		199	209	216
D3S1581	113	142	142		142		142			ADO	113	142
D4S2964	179	182	187	191	ADO	187	ADO	187		ADO	182	191
D7S2847	178	184	184	192	184		178	184		192	184	
D15S659	176	200	180	192	176	192	176	192		180	ADO	192
AMELX/Y	105	110	105		105		110	105		105	105*	

Maternal alleles, blue and red; maternal alleles, green and yellow; semi informative alleles, orange; uninformative alleles, no shading. *Presumed allele dropout of AMELY (110). Samples 3, 5a and 6 are trophectoderm samples. Sample 5b is the excluded cell fragment sample related to sample 5a. Bold type highlights the opposite maternal alleles present in samples 5a and 5b.

6.4.3. Single Nucleotide Polymorphism (SNP) Genotyping and Karyomapping

SNP genotyping and Karyomapping was successful with all four WGA products. Conventional analysis of the SNPs on the X and Y chromosomes confirmed the sex indicated by array CGH in all cases. In addition, Karyomapping confirmed the absence of the maternal copy of chromosome 22 in embryo 3 (Table 6.1) and in agreement with the euploid array CGH result, failed to detect any meiotic trisomies or missing chromosomes in the trophectoderm sample from embryo 5 (sample 5a) and embryo 6. However, for the excluded fragment sample from embryo 5 (sample 5b), only maternal SNP markers for a single maternal chromosome were detected across all chromosomes (including chromosome 19) indicating that it was haploid.

Comparing the karyomaps and the positions of the crossovers in the excluded fragment sample (sample 5b) and the results for maternal chromosomes in the trophectoderm sample (sample 5a), it was clear that all 22 autosomes and the X chromosome were derived from the same maternal homologue in both samples, i.e. the maternal haplotype (yellow or green) detected around the centromere was identical (Figure 6.3). This proves that the maternal chromosome sets from the two samples are derived from the same oocyte. Moreover, the presence of only a maternal set of chromosomes and the pattern of crossovers identifies the origin of the DNA in the excluded fragment sample as being derived exclusively from the second polar body, i.e. the majority of crossovers were in different positions, except for 12 distal crossovers in closely similar positions, as would be expected for reciprocal crossovers between sister chromatids (Ottolini *et al.* 2015). This genetic data rules out the possibility of the two samples originating from sibling embryos. Similar comparisons with the maternal chromosomes in the other two embryos demonstrated that they had distinct maternal chromosome sets and crossover patterns (data not shown). Finally, the maternal haplotypes identified with Karyomapping in the two samples from embryo 5 on the relevant chromosomes were concordant with the results of the STR analysis, which showed opposite alleles at each locus.

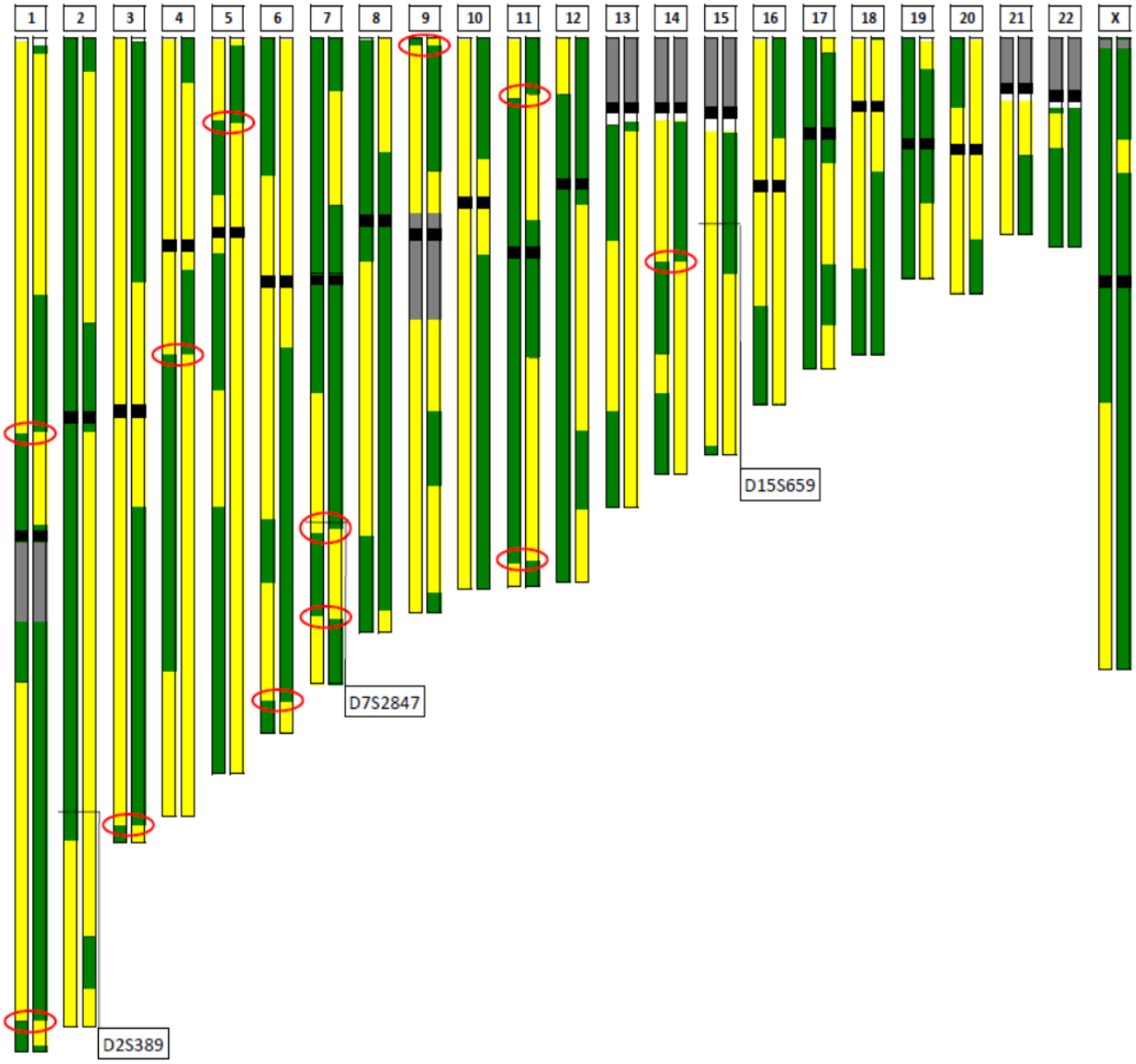

Figure 6.3. Comparison of the karyomaps for the maternal chromosome sets for the excluded cell fragments (on the left in each case) and the trophectoderm biopsy (right) (Ottolini *et al.* 2015a).

Maternal haplotypes, yellow and green; centromeres, black; satellite regions, grey. Note the crossovers from one maternal haplotype to the other are mostly different except for 12 common crossovers between sister chromatids (red ellipses). The positions of the three STR markers which amplified in both samples are indicated on the relevant chromosomes. Note that the maternal haplotypes are different at these positions.

6.5. Discussion

A major advantage of blastocyst biopsy is that multiple trophectoderm cells, in the range of 3-10 cells, can be biopsied from each embryo. Compared with genetic analysis of single cells, whole genome amplification bias and chromosome copy number artefacts are reduced in multiple cell samples and also ADO at, for example, mutation sites decreases dramatically (Handyside *et al.* 2004). On the other hand, a disadvantage is that chromosomal mosaicism arising through abnormal processes of nuclear and cell division, mainly during cleavage, can persist at the blastocyst stage. In the context of PGS of aneuploidy by any quantitative method, this can result in intermediate chromosome copy number changes, which may be difficult to interpret. Although most multiple trophectoderm biopsies are concordant, a few give results consistent with mosaicism (Capalbo *et al.* 2013b).

In the case reported here, one of the embryos only reached the blastocyst stage on Day 6 but had hatched completely from the zona prior to biopsy. Biopsy of fully hatched blastocysts is technically challenging and in this situation, the blastocyst has to be held directly by gentle suction to the holding pipette while the trophectoderm cells to be biopsied are drawn up into a sampling pipette and a laser used to excise them. The blastocyst then collapses initially preventing any second attempt to obtain more cells if deemed necessary. As only a small number of cells were biopsied from this particular embryo, a cluster of excluded cell fragments that had remained within the zona pellucida were also biopsied separately for analysis. Although there is no published evidence, these cells were sampled on the assumption that they were the remnants of arrested cells not incorporated into the developing blastocyst. The array CGH results for the fragments (47,XX,+19) and the trophectoderm sample (46,XY), however, were non-concordant. Although it was assumed that the more reliable result for this embryo was the latter, despite rigorous witnessing protocols, I could not rule out that the samples had been mixed up as the embryo biopsied following this one was also a euploid male (46,XY). To exclude this possibility, therefore, all samples were DNA fingerprinted using a panel of informative STR markers and amelogenin to determine the sex and subsequently SNP genotyped for Karyomapping.

The results of the DNA fingerprinting and amelogenin analysis confirmed the sex of three of the samples determined by array CGH and ruled out any sample mix up since the sampled fragments had a distinct set of STR alleles. In the fourth sample, only AMELX amplified from embryo 6 presumably as a result of ADO (Table 6.2). Furthermore, the absence of any paternal alleles and the presence of only a single maternal allele at each locus suggested that the DNA may have originated in a polar body with a haploid set of maternal chromosomes. Finally, genome-wide SNP genotyping and Karyomapping identified beyond doubt that the DNA from the fragments was exclusively that of the second polar body corresponding to the embryo from which the trophectoderm cells had been sampled. The evidence for this is threefold: (1) no paternal SNP markers were detected for any of the chromosomes; (2) the grandparental origin of each of the 23 maternal chromosomes in both samples was identical (theoretically the chance of an identical set is 2^{23}:1); and (3) although most crossovers were in different positions, there were 12 crossovers in identical positions in both sets of maternal chromosomes consistent with distal crossovers between sister chromatids (Ottolini *et al.* 2015) (Figure 6.3). Furthermore, the maternal haplotypes identified by Karyomapping at the STR loci are all concordant with the alleles detected by direct analysis (Table 6.2).

Interestingly, contrary to the array CGH result, only a single maternal chromosome 19 was detected by karyomap analysis in both samples from embryo 5. However, the trisomy 19 in the fragment sample was reported on the assumption that it was a multiple cell sample, which could include mosaic copy number abnormalities. Close inspection of the array CGH plot for sample 5b (Figure 6.2) reveals that this is most likely the explanation for this discrepancy. The ratio of all of the probes on chromosome 19 is raised consistently as indicated by the software (green line). However, the ratio shift is much less than the X chromosome internal control compared with the male sex mismatched control DNA that would qualify as a trisomy in a single cell sample. In this case, therefore, this may be an example of whole genome amplification bias which is known to occur with polar body samples (Christopikou *et al.* 2013; Capalbo *et al.* 2013a). Knowing that this

can occur, experienced array CGH laboratories typically employ more stringent criteria for calling aneuploidies in polar bodies, especially those affecting chromosome 19.

The persistence of polar body DNA for almost a week after extrusion following fertilisation is unexpected since both polar bodies appear to fragment and are generally not visible at the blastocyst stage. In this case, a relatively large group of excluded fragments has been shown to have DNA originating exclusively from the second polar body. The origin of most of the fragments therefore was presumably anucleate fragments, which commonly appear during cleavage divisions. Larger studies of such fragments will be needed to assess how frequently this occurs and whether there is evidence of the persistence of DNA from the first polar body also or excluded nucleated cells, which have subsequently fragmented.

The implications of the persistence of polar body DNA in excluded fragments in the sub-zonal space up to the blastocyst stage, are important for both cleavage and blastocyst stage embryo biopsy. Clearly the assumption that these fragments are representative of the embryo is not always the case. Therefore, there is a risk of misdiagnosis for several reasons. PGD for single gene defects by conventional targeted haplotype and mutation analysis, for example, may give the opposite result for maternal loci in distal regions of the affected chromosome as was demonstrated here for the three STR loci. Polar body DNA may be more prone to whole genome amplification bias artefacts for chromosome copy number analysis (Christopikou *et al.* 2013; Capalbo *et al.* 2013a). Biopsy samples which inadvertently include these fragments could be contaminated with DNA which is not representative of the embryo, potentially giving false results or appearing to be mosaic. Until further studies have been done, therefore, harvesting samples of excluded fragments for diagnostic purposes should be avoided and efforts made to prevent them contaminating any embryo biopsy samples.

7. Specific Aim 4. To investigate the use of a calcium ionophore protocol to activate human oocytes, ultimately to investigate the incidence of chromosomal aneuploidy in the activated oocytes using array CGH and Karyomapping

The results from this chapter have been accepted for publication and are in press. Capalbo A*, **Ottolini CS***, Griffin DK, Ubaldi FM, Handyside AH and Rienzi L. Artificial oocyte activation with calcium ionophore does not cause a widespread increase in chromosome segregation errors in the second meiotic division of the oocyte. Fertility and Stirility (in press) *Joint first author

7.1. My Personal Contribution to the Work

I was integral to conceiving and designing the experiments for this chapter with the help of Dr Antonio Capalbo. I performed the majority of the embryology including oocyte warming, biopsy, tubing and whole genome amplification of the samples. I performed some of the SNP genotyping and array CGH and analysed all of the CGH and SNP data. I was involved in the writing of the submitted manuscript and designed and created the figures. What follows is an adaptation of the manuscript submitted to MHR (2015).

7.2. Introduction

Failure of fertilisation resulting in few or no embryos for transfer continues to be a significant clinical challenge for a minority of patients undergoing *in vitro* fertilisation (IVF). The introduction of intra-cytoplasmic sperm injection (ICSI) in the early 1990s, significantly improved the clinical outcome for patients with male factor infertility, particularly those with low sperm counts who could not achieve normal levels of fertilisation with conventional IVF (Palermo *et al.* 1992). Typical fertilisation rates with ICSI average 70% for most patients, including those with poor semen parameters or surgically retrieved sperm. However, a significant proportion of ICSI cycles still result in fertilisation rates below 50% (Montag *et al.* 2012) with between 1% and 4% resulting in

total failed fertilisation (Esfandiari *et al.* 2005; Liu *et al.* 1995; Shinar *et al.* 2014). Although the invasive nature of the ICSI procedure itself may contribute to a proportion of oocytes not fertilising normally, most commonly the failure of an oocyte to fertilise after sperm injection is failure of oocyte activation (Flaherty *et al.* 1995; Rawe *et al.* 2000; Sousa & Tesarik 1994).

In most mammals, the mature ovulated oocyte is arrested in metaphase of the second meiotic division (meiosis II) until fertilisation by a sperm. Sperm binding with the oolemma activates the oocyte triggering a series of pulsatile increases in intracellular calcium concentration, which in turn results in the resumption and completion of the second meiotic division with the extrusion of the second polar body, and the initiation of preimplantation development (Kline & Kline 1992). PLCζ, a sperm-specific phospholipase, is considered the trigger for the molecular pathway within the oocyte resulting in the release of calcium stores from the endoplasmic reticulum (Saunders *et al.* 2002). Recent studies have shown that fertilisation failure following ICSI can be linked to sperm devoid of PLCζ or sperm with abnormal PLCζ function (Heytens *et al.* 2009; Lee *et al.* 2014; Yoon *et al.* 2008). It has also been demonstrated that oocyte factors as well as sperm factors are involved in failed fertilisation following ICSI (Tesarik *et al.* 2002).

Artificially increasing intracellular calcium with a variety of stimuli, from a brief exposure to low concentrations of ethanol to calcium ionophore exposure to allow the influx of calcium ions from the medium, triggers oocyte activation in several mammalian species (Kaufman 1982; Whittingham 1980). In assisted conception, artificial activation of human oocytes (AOA) with calcium ionophore has been used clinically in cases of failed fertilisation following ICSI, resulting in completion of normal fertilisation in a significant proportion of oocytes and live births following embryo transfer (Nasr-Esfahani, Deemeh & Tavalaee 2010). Indeed, there is evidence to show that AOA can overcome both oocyte and sperm related failed fertilisation (Heindryckx *et al.* 2005). However, information on the effect of AOA and its biosafety is limited to clinical follow-up of 21 children conceived using the technique, which demonstrated that their early development is within the expected normal range (Vanden Meerschaut *et al.* 2014). Also, because of the abnormal, sustained increase in intracellular calcium concentration, which may have effects on downstream

molecular events, it has been argued that AOA should only be used in failed fertilisation cases and not as a routine adjuvant to ICSI (Van Blerkom *et al.* 2015).

Since very little preclinical evidence about the safety of AOA has been reported in the literature, here, I have investigated the effect of AOA with calcium ionophore on the incidence of female meiotic errors resulting in abnormal chromosome copy number, or aneuploidy, in the activated oocytes. Chromosome copy number was analysed by array comparative genomic hybridisation (array CGH) and combined with genome-wide single nucleotide polymorphism (SNP) genotyping of the oocyte donors and oocytes to identify the meiotic origin of any chromosome gains. As all of the oocytes were arrested in metaphase of meiosis II prior to activation, any effect of exposure to calcium ionophore should only affect the segregation of chromosomes at anaphase of meiosis II following resumption of meiosis.

7.3. Materials and Methods

All oocytes for the study were obtained from 12 patients that had undergone IVF treatment at the Centre for Reproductive Medicine GENERA in Rome between June 2008 and May 2009 (Table 7.1). According to Italian law at the time of the patient's IVF cycles, a maximum of three oocytes could be inseminated per patient and any surplus mature oocytes were vitrified. Surplus vitrified oocytes were later recruited for the study after informed consent was obtained from the patients. Consent was also obtained from all donors to obtain buccal cell swabs for genotyping. The study was approved by the Institutional Review Board of the Clinica Valle Giulia, where the oocytes were stored, and did not influence treatment in any way.

Table 7.1: Details of Cycles with Vitrified Oocytes

Patient	Aetiology	Stimulation protocol	Maternal age at OPU/vitrification (yr)	Oocytes collected	Oocytes vitrified	Oocytes donated	Live birth from cohort
1	male factor	Agonist	33.2	12	2	2	yes
2	endometriosis	Agonist	37.9	10	7	5	yes
3	idiopathic	Agonist	37.4	10	10	4	no
4	male factor	Antagonist	40.6	12	6	5	yes
5	male factor	Antagonist	37.6	15	10	10	yes
6	male factor & tubal	Agonist	37.3	11	6	3	yes
7	male factor	Agonist	35.7	11	5	5	no
8	Tubal	Agonist	38.4	16	9	6	yes
9	male factor	Agonist	29.0	12	6	6	yes
10	male factor	Agonist	31.7	14	5	4	yes
11	male factor	Agonist	39.0	18	18	3	no
12	male factor	Agonist	36.2	6	3	3	yes
		Mean	36.2	12.3	7.3	4.6	
		±SD	3.3	3.2	4.2	2.1	
		Range	29.0-40.6	6-18	2-18	2-10	

7.3.1. Oocyte Collection, Vitrification and Warming

Ovarian hyperstimulation was achieved using long down regulation agonist or standard antagonist protocols and transvaginal oocyte collection was performed 35 hours post-human Chorionic Gonadotrophin (hCG) administration. The vitrification and warming procedures were performed according to a published protocol (Kuwayama *et al.* 2005; Kuwayama 2007) using commercially available vitrification and warming kits (Kitazato BioPharma Co., Japan). Vitrification was performed a maximum of 40h post-hCG administration and the oocytes were stored on Cryotop vitrification tools (Kitazato BioPharma Co., Japan) in liquid nitrogen.

7.3.2. Oocyte Culture and Activation

All oocyte culture was performed at 37°C in 6% CO_2 and 5% O_2. Individual oocytes were cultured separately and culture drops and wells were numbered to allow traceability throughout the experiment. Immediately after warming, the surviving oocytes were moved to 35µl microdrops of cleavage medium +10% human serum albumin (HSA) under mineral oil (Sage; Cooper Surgical, USA) and cultured for 2h prior to activation. Oocytes were activated by exposure to 100µM calcium ionophore (A23187; Sigma-Aldrich, USA) in cleavage +10% HSA from a stock solution in DMSO (Sigma-Aldrich, USA) diluted 1:40. Oocytes were transferred to 35µl drops of the activation medium under oil, for 40 min. The oocytes were then moved, after thorough washing, to separate wells of multiwell slides (Unisence Fertilitech, Denmark) in cleavage medium under oil (medium as used directly following oocyte warming). The slides were placed in the time lapse incubator (Embryoscope; Unisence Fertilitech, Denmark) for assessment of second polar body (PB2) extrusion and appearance of pronuclei.

7.3.3. Oocyte Isolation and Tubing

The zona pellucida was removed from activated oocytes and the polar bodies were isolated by micromanipulation (Narishige, Japan) on an inverted microscope (Nikon Ltd, Japan) equipped

with Hoffman Modulation contrast and a 37°C heated stage (Linkam Scientific Instruments, UK) as previously described (Capalbo *et al.* 2013). Oocytes were secured by suction with the holding pipette (TPC, Australia) and a large aperture was made in the zona pellucida with a series of laser (Saturn laser; Research Instruments, UK) pulses. The aspiration pipette (Zona drilling pipette; TPC, Australia) was then inserted through the opening and the polar bodies removed with gentle suction. The oocyte was then removed from the zona by both displacement and zona manipulation techniques using the aspiration pipette. Once free from the zona, the oocytes were washed and transferred to polymerase chain reaction (PCR) tubes ensuring the polar bodies did not contaminate the samples. Transfer of the oocytes to PCR tubes was performed using a plastic denuding pipette (COOK Medical, Ireland) with a 130µm lumen. Individually labelled PCR tubes (Cell Projects Ltd, UK) were primed with 2µl Dulbecco's phosphate buffered saline (DPBS) (Gibco; Life technologies, USA) with 0.1% poly vinyl alcohol (Sigma-Aldrich, USA). Individual oocytes were expelled into the DPBS in around 1µl of the medium containing the samples. The PCR tubes were then briefly centrifuged, snap frozen in liquid nitrogen and stored at -20°C prior to whole genome amplification.

7.3.4. Whole Genome Amplification (WGA) and Genomic DNA Extraction

DNA from all oocytes in the study were amplified by either multiple displacement amplification (MDA) (REPLI-g Single Cell Kit; Qiagen, UK) or PCR library based whole genome amplification (WGA) (SurePlex; Illumina, USA) according to the manufacturer's instructions to obtain sufficient DNA for downstream analysis. MDA was performed with a short, 2h incubation. genomic DNA (gDNA) from all oocyte donors was obtained using buccal cell swabs (Isohelix, Cell Projects Ltd, UK). Extraction of the gDNA from the buccal cells was performed using a proteinase K extraction kit to a final volume of 30µl, following the manufacturer's instructions (Isohelix, Cell Projects Ltd, UK).

7.3.5. Array CGH and SNP Genotyping

When feasible, both array CGH and SNP genotyping were performed on each sample. For array CGH analysis, 4µl aliquots of WGA products from the oocytes were processed on 24Sure microarray slides (Illumina, USA) according to the manufacturer's instructions. The data was imported and analysed using dedicated software (BlueFuse Multi v 4.0; Illumina, USA). 400ng of genomic DNA or 8µl of WGA products from the oocyte samples were processed on an SNP genotyping BeadChips for ~300K SNPs genome-wide (HumanCytoSNP-12 or HumanKaryomap-12; Illumina, USA), according to the manufacturer's instructions. The genotype data was exported as a Microsoft Excel file, using genotyping software (GenomeStudio; Illumina, USA) for analysis.

7.3.6. SNP Analysis

To detect aneuploidies of meiotic origin, each of the patients donating oocytes were genotyped and informative maternal heterozygous SNP loci were phased by reference to either a presumed haploid sibling oocyte (or PB2 if no sibling oocyte was available). In cases where the reference was itself aneuploid for a particular chromosome, a second reference was also used to confirm the status of the chromosome(s) involved. Mendelian analysis of the genotype of each of the activated oocytes at these informative SNP loci then allowed the identification of meiotic errors resulting in two chromatids instead of the normal single chromatid segregating to the oocyte (chromatid gain) by the presence of heterozygous regions. Furthermore, the distribution of these heterozygous regions allows the classification of these errors into: 1) those that occur in the first meiotic division (meiosis I) and have chromatids from both homologous chromosomes, which result in heterozygosity in the pericentromeric and more distal regions of the chromosome arms; and 2) errors in the second division (meiosis II) and have chromatids from the same homolog, which result in homozygosity in the pericentromeric region of the chromosome but are heterozygous in more distal regions. Finally the absence of any informative maternal SNPs (chromatid loss) indicates the absence of a chromosome and thus the meiotic origin of losses

cannot be determined with this methodology. Therefore, chromatid loss in the oocyte could not be used for the study.

7.4. Results

7.4.1. Artificial Oocyte Activation (AOA)

56 oocytes arrested at metaphase of the second meiotic division (meiosis II), which had been cryopreserved by vitrification, from 12 patients with a mean age of 36.2 years ± SD 3.3, most of whom had pregnancies and live births following successful IVF treatment, mainly for male factor infertility, were donated for the study (Table 7.1). 49 (88%) survived thawing and 39 (80%) activated following exposure to calcium ionophore as demonstrated by the formation of one or more pronuclei and/or the extrusion of the PB2 (Table 7.2). Most of the activated oocytes extruded the PB2 and formed a single pronucleus (2PB, 1PN: 30/39; 77%) as expected. However, five (13%) activated oocytes with a PB2 failed to form a pronucleus (2PB, 0PN) and three (8%) formed two pronuclei (2PB, 2PN). Finally, one activated oocyte failed to extrude the PB2 and formed a single normal sized pronucleus with several smaller pronuclei (1PB, >2PN).

Table 7.2: Incidence of Normal and Abnormal Patterns of Polar Body Extrusion and Pronucleus Formation Following Artificial Oocyte Activation

Patient	Oocytes thawed	Oocytes survived	Total activated	Normal activated		Abnormal activated	
				1PN, 2PB	0PN, 2PB	>2PN, 1PB	2PN, 2PB
1	2	2	2	2	0	0	0
2	5	5	5	3	1	0	1
3	4	4	2	1	1	0	0
4	5	4	4	4	0	0	0
5	10	5	3	3	0	0	0
6	3	3	3	2	0	1	0
7	5	5	5	2	2	0	1
8	6	6	5	5	0	0	0
9	6	6	1	1	0	0	0
10	4	4	4	4	0	0	0
11	3	2	2	0	1	0	1
12	3	3	3	3	0	0	0
Total (%)	56	49 (87.5)	39 (80)	30 (77)	5 (13)	1 (2.5)	3 (7.5)

7.4.2. Chromosome Copy Number Analysis

Chromosome copy number was analysed in 31 activated oocytes (2PB, 1 or 0PN n=27; 2PB, 2PN n=3; 1PB, >2PN n=1) by array CGH (n=26) and/or SNP genotyping (n=25) (Table 4.3). In total 20/31 activated oocytes were analysed by both array CGH and SNP genotyping, 6/31 were analysed by array CGH only and 5/31 were analysed by SNP genotyping only (Table 7.3). Overall, 13 (42%) activated oocytes had one or more chromosome copy number abnormalities (mean 2.0 per aneuploid oocyte; range 1-7) including two partial chromosome gains (+15qter and +8pter). In the 10 aneuploid activated oocytes analysed by both array CGH and SNP genotyping, all 17 whole chromosome aneuploidies were detected by the two methods (Table 7.3) (100% concordance). Of the two partial gains, identified as isolated heterozygous regions by SNP analysis and therefore likely to be of meiotic origin (not gonadal mosaicism), only the +15qter was confirmed by array CGH (50% concordance). However, Sample 7.4 (with the +8pter) was amplified by MDA, which is not optimised for the CGH array used, and can thus explain the non-concordance (Table 7.3).

Table 7.3: Aneuploidies Identified in Normal and Abnormal Activated Oocytes

Patient	Oocyte ID	Array CGH analysis	SNP genotyping analysis	No of polar bodies (PB) and pronuclei (PN)	Amplification type
1	1.1	-5, -10, +20	-5, -10, +20	2PB, 1PN	SurePlex
	1.2	+11, +15qter, -21	+11, +15qter, -21	2PB, 1PN	SurePlex
2	2.1	+22	+22	2PB, 1PN	SurePlex
	2.2	+15	+15	2PB, 1PN	SurePlex
	2.3	+1	+1	2PB, 0PN	SurePlex
	2.4	-13	-13	2PB, 2PN	SurePlex
	2.5	Euploid	Euploid	2PB, 1PN	SurePlex
3	3.1	Euploid	Euploid	2PB, 0PN	SurePlex
4	4.1	-4	-4	2PB, 1PN	SurePlex

Patient	Oocyte ID	Array CGH analysis	SNP genotyping analysis	No of polar bodies (PB) and pronuclei (PN)	Amplification type
	4.2	Euploid	Euploid	2PB, 1PN	SurePlex
	4.3	Euploid	Euploid	2PB, 1PN	SurePlex
	4.4	Euploid	Euploid	2PB, 1PN	SurePlex
5	5.1	Euploid	N/A	2PB, 1PN	SurePlex
	5.2	-13	N/A	2PB, 1PN	SurePlex
	5.3	Euploid	N/A	2PB, 1PN	SurePlex
6	6.1	Euploid	N/A	1PB, >2PN	MDA
	6.2	Euploid	Euploid	2PB, 1PN	MDA
	6.3	Euploid	Euploid	2PB, 1PN	MDA
7	7.1	Euploid	N/A	2PB, 2PN	MDA
	7.2	-13, +20, -22	-13, +20, -22	2PB, 0PN	MDA
	7.3	Euploid	Euploid	2PB, 1PN	MDA
	7.4	-4	-4, +8pter	2PB, 1PN	MDA
8	8.1	-6, -18, +20	-6, -18, +20	2PB, 1PN	MDA
	8.2	Euploid	Euploid	2PB, 1PN	MDA
	8.3	Euploid	Euploid	2PB, 1PN	MDA
9	9.1	N/A	Euploid	2PB, 1PN	MDA
10	10.1	N/A	-17	2PB, 1PN	MDA
	10.2	N/A	Euploid	2PB, 1PN	MDA
	10.3	N/A	Euploid	2PB, 1PN	MDA
	10.4	N/A	Euploid	2PB, 1PN	MDA
11	11.1	+1, +4, +15, +16, +17, -18, -22	N/A	2PB, 2PN	SurePlex

7.4.3. SNP Analysis of Meiotic Errors

SNP analysis of 24 activated oocytes, which extruded the PB2 and formed a single pronucleus as expected (2PB, 1PN) or which failed to form a visible pronucleus (2PB, 0PN), were all shown by SNP genotype analysis to have a haploid set of maternal chromosomes with the exception of the aneuploid chromosomes. Of the seven chromosome gains identified by SNP genotype analysis, five had patterns of heterozygosity of meiosis I type errors including the pericentromere and only two had patterns consistent with meiosis II type errors (Table 7.3; Figure 7.1). The remaining one activated oocyte analysed by SNP genotyping, which had extruded the PB2 and formed two pronuclei (2PB, 2PN), was shown to be diploid (digynic) with patterns of heterozygosity consistent with the presence of both sets of meiosis II chromosomes. The only exception was chromosome 13, which had only a single copy consistent with the loss observed with array CGH (Figure 7.2a). Similar interrogation of the array CGH plot of another oocyte that formed two pronuclei (2PB, 2PN) (oocyte 11.1) also showed that the separation of the two chromosome losses (chromosomes 18 and 21) was consistent with a single copy indicating a diploid (digynic) aneuploid oocyte (Figure 7.2b).

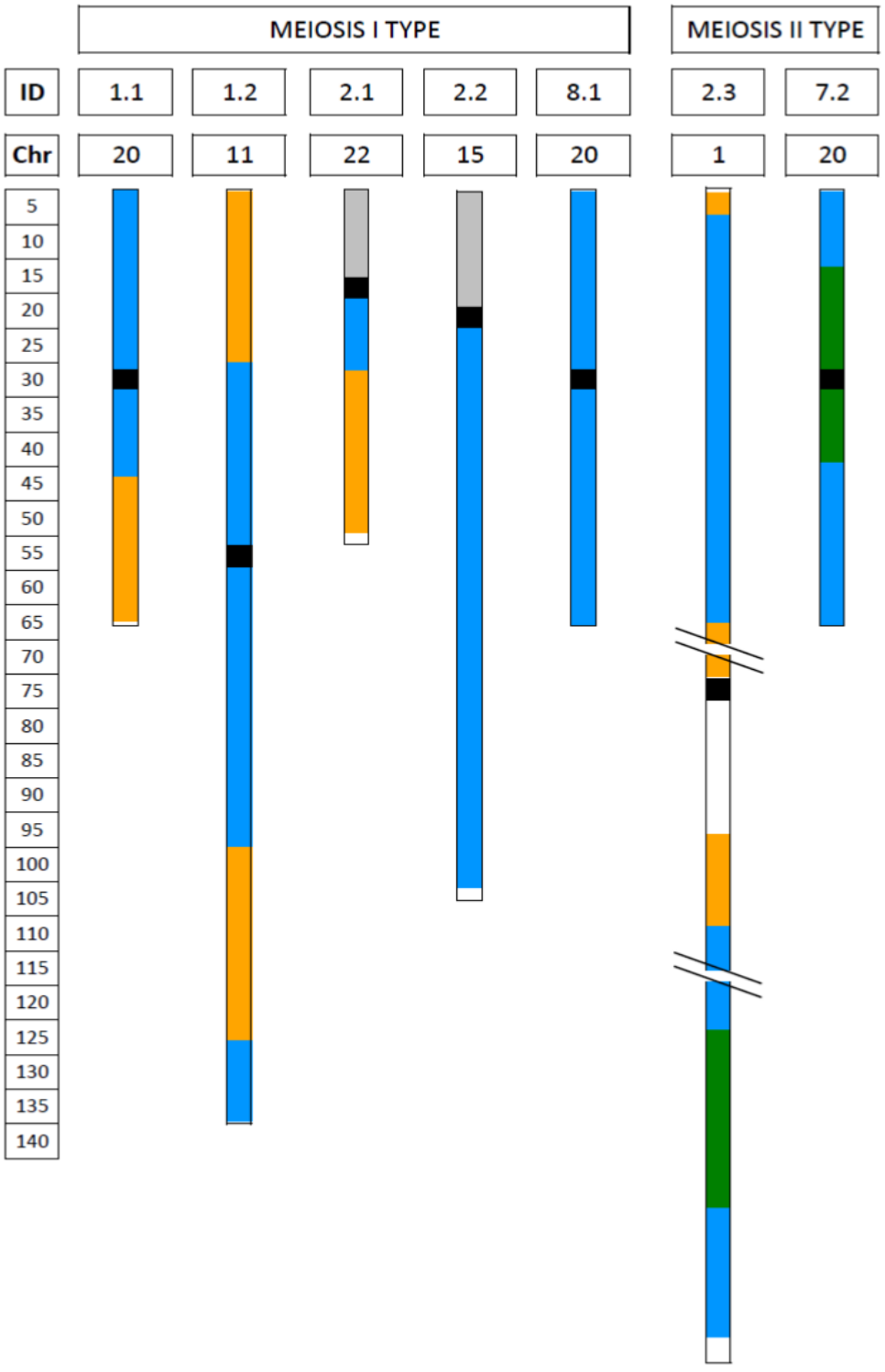

Figure 7.1. Diagrammatic representation of all chromosome gains from oocytes demonstrating single or no pronucleus formation with the extrusion of the second polar body after activation.

Homozygous regions of the chromosomes are coloured yellow or green (depending on the maternal haplotype present) and heterozygous regions in blue (both maternal haplotypes present). The centromeres are shown in black and satellite DNA is coloured grey. The scale bar to the left denotes the Megabase pair (Mbp) position along the chromosomes. The gains present with either pericentromeric heterozygosity (yellow or green around the centromere) as MI errors or pericentromeric homozygosity (blue around the centromere) as MII errors.

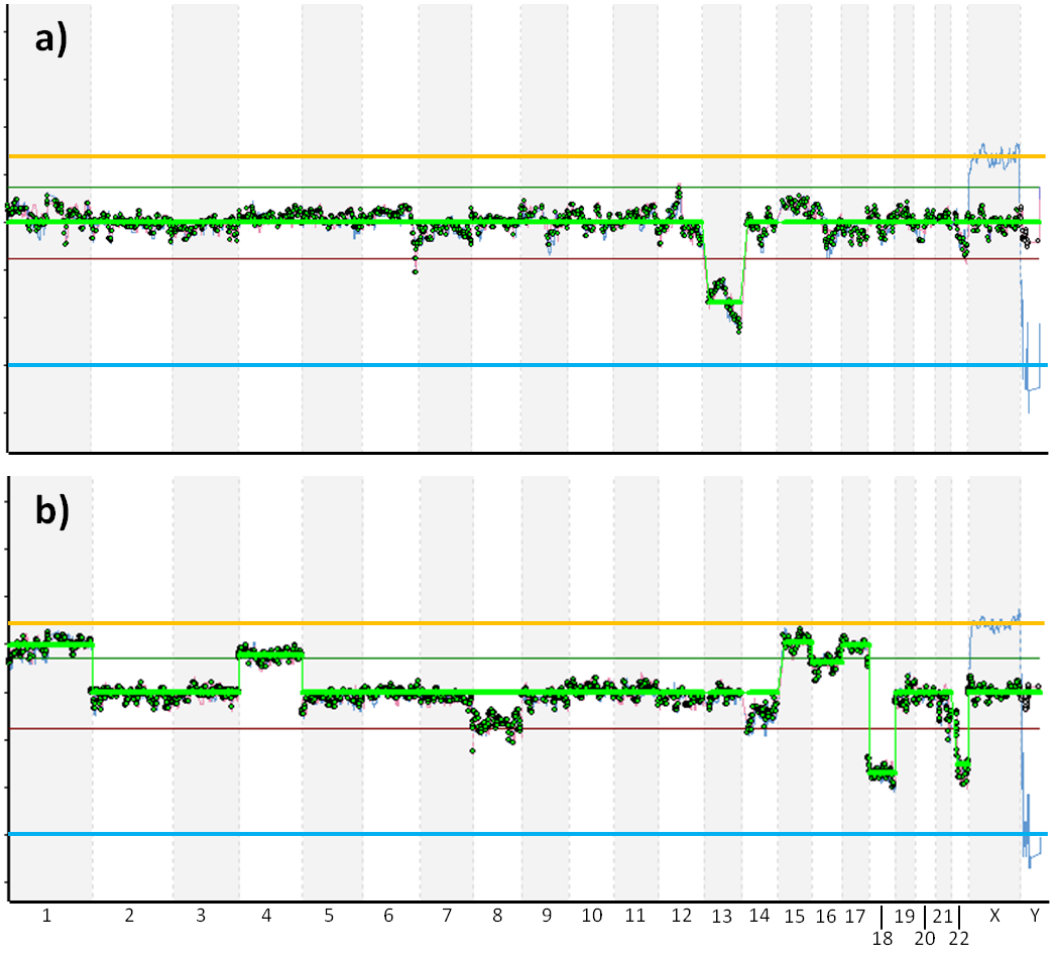

Figure 7.2. Array CHG plots of two activated diploid oocytes displaying two pronuclei consistent with diploid state.

This can be determined by the single chromatid loss (a) and multiple chromatid gains and losses (b). The Log2 separation ratio of X chromosome and Y chromosome when the diploid oocytes are compared to sex mismatched male DNA are indicated by the orange and blue lines

respectively. a) Separation for all probes on chromosome 13 do not reach the blue line, consistent with a single copy of the chromosome or chromatid loss from diploid state. b) Separation of all gains and losses do not reach the orange and blue lines respectively. The gains are consistent with three copies of the chromosome or chromatid gain from the diploid state. As in (a), the losses in (b) do not reach the blue line, consistent with chromatid losses from the diploid state.

7.5. Discussion

Artificial activation of oocytes (AOA) by exposure to calcium ionophore is being used increasingly to overcome low or failed fertilisation following ICSI and there are now several reports of pregnancies and healthy live births (Kashir *et al.* 2010; Vanden Meerschaut *et al.* 2014). Following exposure of oocytes arrested in metaphase of the second meiotic division (meiosis II) to calcium ionophore, chromosome copy number analysis of activated oocytes demonstrated a high incidence of aneuploidy of meiotic origin (13/31; 42%). However, the incidence is comparable to the incidence in normally fertilised embryos in women of a similar age range (Franasiak *et al.* 2014). Also, analysis of informative heterozygous maternal SNP loci showed that five chromosome gains in the activated oocytes had patterns of heterozygosity including the pericentromeric region of the chromosomes, indicating their origin in the first meiotic division (meiosis I) and only two with meiosis II type patterns (Table 7.3; Table 7.1). This level of second meiotic division (MII) errors is in line with studies on meiotic errors following IVF only (Capalbo *et al.* 2013). Therefore, there is no evidence in this preliminary dataset to suggest that AOA with calcium ionophore causes a global increase in meiotic chromosome segregation errors.

In contrast, SNP analysis of an activated oocyte, which had extruded PB2 but then formed two pronuclei (2PB, 2PN), clearly demonstrated that all chromosomes had a pattern of heterozygosity consistent with the presence of both sets of meiosis II chromosomes and was therefore diploid (digynic). The exception was chromosome 13 which had no regions of heterozygosity indicating the presence of a single chromosome and consistent with the log2 ratio observed by array CGH

(Figure 7.2a). Notably, array CGH does not detect the overall ploidy of a cell since it normalises copy number across the genome for comparison with individual chromosomes. As this array CGH pattern of putative single loss (and single gain) from diploid copy number was observed in a second oocyte (Figure 7.2b). It is likely therefore that all activated oocytes in our data set with two or more pronuclei were similarly digynic. This would suggest that the main risk following AOA with calcium ionophore is failure to coordinate telophase of meiosis II with extrusion of the PB2 resulting in retention of both chromosome sets in the oocyte (4/39; 10%). Thus, in clinical practice, these data suggest that a careful examination for PB2 extrusion and pronucleus formation by time-lapse imaging is essential to avoid the transfer of digynic triploid embryos following AOA. Similarly, following failed fertilisation by ICSI and AOA, measures should be taken to avoid transfer of digynic parthenotes that appear morphologically identical to normally fertilised zygotes (2PB, 2PN) and that can equally progress to the blastocyst stage and implant. To a more general extent, these data reiterate the importance of performing further evaluation of fertilised eggs following regular IVF and showing abnormal zygote pronuclear patterns (such as, but not limited to, 1PN, 3PN and micro PNs) with the use of new powerful technologies able to give a clear and unbiased picture about chromosomal segregation during female meiosis.

Although preliminary evidence has been provided that AOA is likely not to affect oocyte aneuploidy, I do not recommend it to be applied as routine practice in IVF to generally increase fertilisation rates. I agree with the recent cautionary note that suggests that further validation is necessary for the clinical use of AOA and that it should be selectively applied to patients with known aetiology (van Blerkom, Cohen, & Johnson 2015). Further to this point, there is direct evidence from our data suggesting that the clinical application of AOA may not benefit all infertility patients. Although using my activation protocol I was able to achieve a consistently high rate of normal oocyte activation in the majority of our donors, one outlier (Patient 9) had a low activation rate of 1/6 (17% activation) (Table 7.2). This is further evidence in support of previous reports demonstrating that AOA is not beneficial for all patients to maximise fertilisation rates (Vanden Meerschaut *et al.* 2012; Montag *et al.* 2012). Furthermore, oocytes used in this study belong

mostly to patients who had a successful pregnancy outcome using sibling oocytes from the same stimulation (Table 7.1).

Finally, the protocol used for activation here involved prolonged exposure (40 min) to higher concentrations of calcium ionophore (100µM) than are currently used clinically, to ensure a high level of activation (39/49; 80%). Therefore, it will be important to extend this study to normal clinical AOA protocols in failed fertilised oocytes and to analyse the incidence and meiotic origin of aneuploidies in activated oocytes/embryos by SNP genotyping of both parents using karyomap analysis (Handyside *et al.* 2010; Natesan *et al.* 2014).

8. Specific Aim 5: To develop an algorithm based on Karyomapping (termed MeioMapping) to investigate the mechanisms of human female meiosis by recovering of all three products of human female meiosis from individual oocytes (termed Trio) to allow exploration of the full extent of meiotic chromosome recombination and segregation that occurs in the female germline

For this specific aim of the thesis I have worked in collaboration with several groups to develop a highly successful oocyte activation, biopsy and genotyping protocol for creating recombination and chromosome segregation maps for the three products of human female meiosis. Following ovarian stimulation and oocyte retrieval, I am able to successfully induce arrested MII human oocytes to complete the second meiotic division and extrude the second polar body. This, in conjunction with sequential biopsy of the polar bodies, allows separate genotyping of all meiotic products without the creation of embryos from fertilised eggs for research purposes. Our unique algorithms allow simultaneous analysis of meiotic recombination and chromosome segregation across the three products of meiosis, which provides new mechanistic insight into maternally-derived aneuploidies. MeioMapping could be clinically applied to improve outcomes for infertility patients undergoing IVF. Our protocol works with a greater than 80% oocyte activation rate and segregation errors at meiosis II are not increased relative to fertilised oocytes. Oocyte activation and sequential biopsy of meiotic products has uncovered new insights into the basis of meiotic errors that may aid future reproductive therapies. The protocol from this part of my thesis was commissioned by the Editors of the Nature Protocols journal and has been submitted and accepted for publication; **Ottolini CS**, Capalbo A, Newnham L, Cimadomo C, Natesan SA, Hoffmann ER, Ubaldi FM, Rienzi L and Handyside AH. Generating maps of genome-wide recombination and chromosome segregation in human oocytes and embryos. Nature Protocols (commissioned and submitted).

8.1. My Personal Contribution to the Work

I was integral to conceiving and designing the embryological component of the submitted protocol with the help of Dr Antonio Capalbo and assisted Professor Alan Handyside in developing the Microsoft Excel tools based on Karyomapping (Handyside *et al.* 2010) to perform what has been termed MeioMapping. I was involved in the writing of the submitted manuscript and the design and creation of the figures. What follows is an adaptation of the manuscript commissioned by Nature Protocols (2015).

8.2. Introduction

8.2.1. Development of the Protocol

As discussed in section 2.1 of the general discussion, meiosis in the human female is exceptionally error prone with 30-70% of human adult oocytes displaying chromosome copy number abnormalities, and >90% of human aneuploidies being of maternal meiotic origin (Hassold & Hunt 2001). Chromosome segregation errors in human female meiosis are the principal cause of embryo aneuploidy leading to failed implantation, miscarriage, and live births affected with chromosomal disorders (Down syndrome). The main contributing factors to these errors are maternal age and altered genetic recombination in maternal meiosis (Nagaoka *et al.* 2012). Our knowledge of chromosome segregation in human female meiosis is largely based on linkage analysis on trisomic conceptions and quantitative chromosome analysis of the polar bodies and embryo biopsies following *in vitro* fertilisation (IVF) treatment.

Until recently, nondisjunction of chromosomes (homologs) in the first meiotic division was thought to be the predominant mechanism by which chromosome imbalances arose in embryos. Population studies as well as cytological observations on foetal oocytes are historically the only sources of information on recombination and position of crossovers. Generating complete genome-wide maps of recombination requires all three products of meiosis, which up until

recently has been unattainable owing to difficulty sourcing adult material and the need for fertilisation to complete the second meiotic division. Here I describe my approach that overcomes the need to fertilise oocytes in order to obtain complete 'MeioMaps' of recombination and chromosome segregation (Ottolini *et al.* 2015). Obtaining MeioMaps is important for fully understanding the differences in recombination as well as their effects on chromosome segregation, for genome evolution as well as the genesis of human aneuploidies. Moreover, MeioMaps also reveal the meiotic origin of monosomies, which until now have been limited to copy number analyses of polar bodies.

The MeioMap protocol was developed as a tool to study patterns of meiotic segregation and recombination in human oocytes. To fully study genome-wide crossover patterns and chromosome segregation in adult oocytes from human females, one must recover all three products of a single meiosis (Figure 8.1). I set out to develop a protocol which would enable us to obtain and separate the three products of human female meiosis (polar body 1, polar body 2 and oocyte).

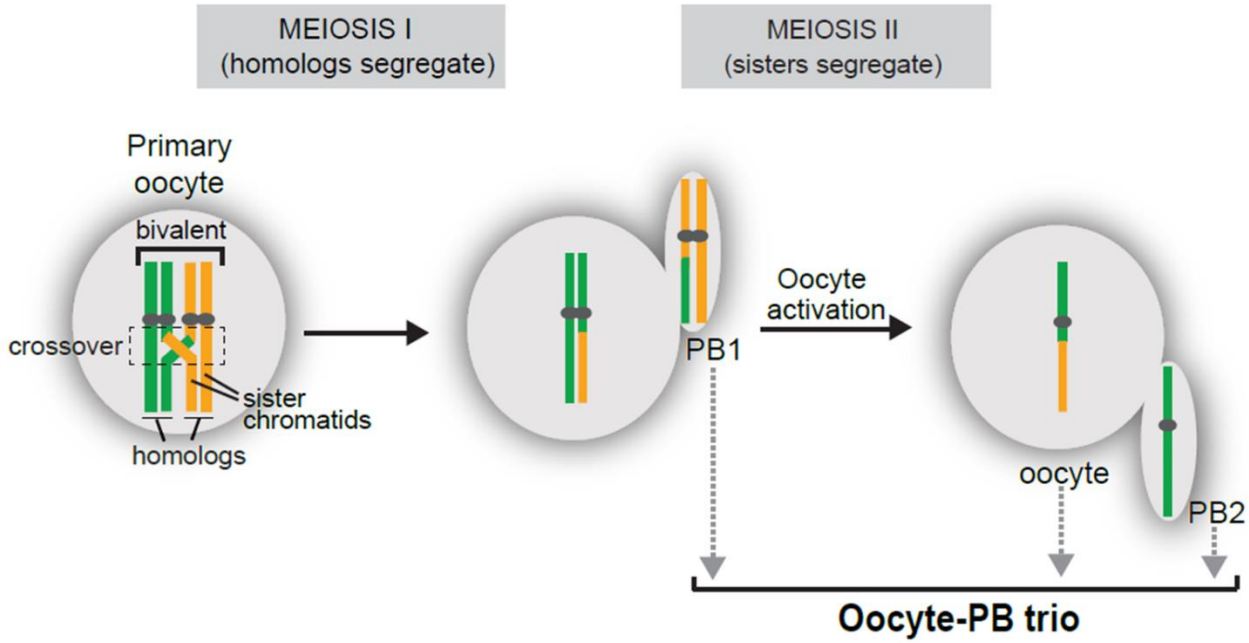

Figure 8.1. Schematic showing an adult oocyte completing the first and second meiotic divisions.

In the adult ovary, primary oocytes contain 23 pairs of homologous chromosomes held together by crossovers in the 'bivalent' configuration. Oocytes complete meiosis I *in vivo* and extrude one set of homologs into the first polar body (PB1), the mature oocyte then arrests at metaphase II. Completion of meiosis II normally only occurs upon fertilisation, but I utilise a calcium ionophore to trigger meiosis II without fertilisation by sperm. At meiosis II one set of sister chromatids are extruded to the second polar body (PB2) resulting in a haploid oocyte. The first and second polar bodies are biopsied sequentially, followed by tubing of the activated oocyte.

To this end, I obtained donated human oocytes that had extruded polar body 1 (PB1) *in vivo* and were arrested at metaphase II (MII). I biopsied the PB1, followed by exposure of the oocyte to a calcium ionophore (A23187), which mimics fertilisation thereby activating the oocyte to complete meiosis II and extrude the polar body 2 (PB2). I then separated the PB2 and oocyte and performed whole genome amplification (WGA) on the three individually recovered meiotic products (Figure 8.2). The WGA products as well as extracted genomic DNA from the oocyte donor were Single Nucleotide Polymorphism (SNP) genotyped and the heterozygous SNPs were used to perform genome-wide inheritance analysis of maternal haplotypes. With these data, I was able create genome-wide genetic recombination and chromosome segregation MeioMaps of the trios, detecting crossovers at a resolution of around 100kb.

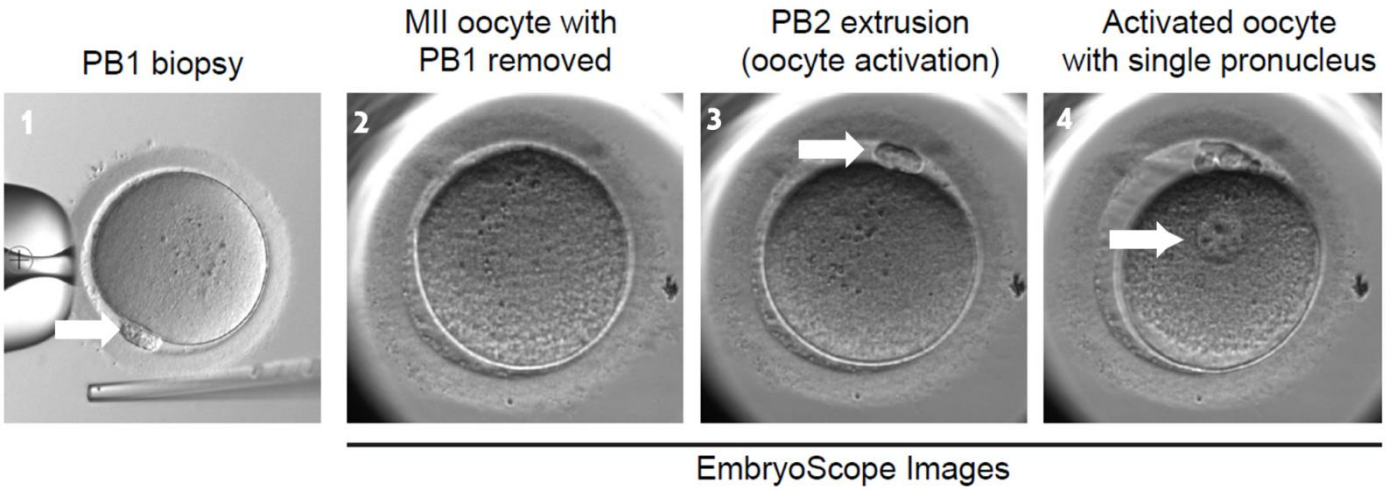

Figure 8.2. Images showing set up for the first polar body (PB1; arrow in image 1) biopsy and oocyte activation culture (Sections 8.3.1. to 8.3.3 and 8.3.5).

The mature oocyte with biopsied PB1 is activated using a calcium ionophore and PB2 is then biopsied (not shown). Note the appearance of the PB2 and a single pronucleus in the activated oocyte (arrows in images 3 and 4 respectively).

The first aim was to obtain high quality genotype data. With this in mind I explored avenues to parthenogenically activate oocytes to eliminate the need for fertilisation by sperm, which contaminates the egg with the sperm DNA. It was first discovered in the 1970s that increasing the intracellular free Ca^{2+} in mammalian oocytes could induce the sequence of events normally following fertilisation, including the completion of meiosis II and subsequent cell division (Fulton & Whittingham 1978). Since then, many groups have published their findings using a calcium ionophore for either parthenogenic activation of human oocytes or assisted activation of human oocytes following poor fertilisation outcomes in IVF (Nasr-Esfahani *et al.* 2010). Instead of direct injection of Ca^{2+} the ionophore binds with the cell membrane allowing passage of ions across the membrane therefore creating the influx of Ca2+ (Saunders *et al.* 2002). Using my protocol I was able to induce the extrusion of PB2 in >80% oocytes without perturbing the second meiotic division.

The second aim was to ensure proper identification of the polar bodies and oocytes for downstream applications. I did this by integrating an adapted clinical strategy, which uses the sequential biopsy of the two polar bodies). Using this technique, I was able to ensure that there was no sample mix up or cross contamination between samples (Capalbo *et al.* 2013).

The final aim was to genotype the separated products of meiosis and apply algorithms for detecting heterozygosity and haplotype changes to analyse recombination and chromosome/chromatid segregation across the PB1, PB2 and the oocyte. I term this MeioMapping (Ottolini *et al.* 2015). To map the positions of crossovers in the two polar bodies (PB1, PB2) and the corresponding activated oocyte (oocyte-PB trio), a simple Mendelian algorithm is used to phase heterozygous (AB) maternal SNPs distributed across each chromosome (including the non-PAR region of the X chromosome and excluding the Y chromosome) using a haploid PB2 or activated oocyte as a reference. This results in two notional maternal haplotypes at consecutive loci across each chromosome: Maternal haplotype 1 (reference) and 2 (non-reference) colour coded in yellow and green respectively (Table 5.1). The genotypes at all of these informative loci are then examined in each of the other trio samples and

compared to the reference. If the sample genotype is homozygous and identical to the reference it is Maternal haplotype 1 (yellow). If homozygous for the other SNP allele then it is Maternal haplotype 2 (green). Finally, if heterozygous it is colour coded in red or if there is no call for that SNP in grey (Table 8.1).

Table 8.1: Table Showing Representation of Phasing of Maternal SNPs in Oocyte-PB Trios

						MeioMap		
		Haplotype				PB1	PB2	OOCYTE
		1				Haplotype	Haplotype	Haplotype
SNP no.	MAT	REF	PB1	PB2	OOCYTE	1 2	1 2	1 2
1	AA			Not informative				
2	BB			Not informative				
3	AB	AA	AB	AA	BB	A B	A	B
4	AB	BB	BB	NC	AA	B		A
5	AB	AA	AB	AA	NC	A B	A	
6	AB	AA	AB	AA	BB	A B	A	B
7	AB	AA	NC	BB	AA		B	A
8	AB	BB	AB	NC	BB	B A		B
9	AB	AA	BB	BB	NC	B	B	
10	AB	BB	AB	NC	BB	B A		B
11	AB	BB	BB	AA	AA	B	A	A
12	AB	AA	AA	BB	NC	A	B	
13	AB	BB	BB	AB	AA	B	B A	A
14	AB	BB	BB	AA	AA	B	A	A
15	AB	AA	AA	BB	BB	A	B	B
16	AB	AA	AA	NC	BB	A		B
17	AB	BB	BB	AA	BB	B	A	B
18	AB	BB	BB	AA	AA	B	A	A

Only heterozygous maternal SNPs are informative for phasing. Where the sample SNP matches the reference it is assigned maternal haplotype 1 and is coloured yellow in the MeioMap. Where the sample SNP differs from the reference, it is assigned maternal haplotype 2 and coloured green. Where both SNPs are present (AB) the region is heterozygous and is coloured red. When no SNP calls, the SNP is coloured grey. Crossovers between homozygous regions of PB2 and oocyte occur at SNP 6 and 14. A crossover between heterozygous and homozygous regions in PB1 and oocyte occurs at SNP 10. A 'common crossover' (see text for full explanation) occurs at SNP 14. Examples of allele drop out (ADO) and allele drop in (ADI) are as follows: ADO in homozygous region (grey cell, SNP 4 PB2) leads to loss of resolution; ADO in heterozygous region (SNP 4 or 9 in PB1) leads to loss of heterozygosity and creates 'noise' in the data; Double ADO (SNP 7 in PB1) results in no call and a reduced resolution; ADI without ADO (SNP 13 in PB2) results in erroneous heterozygous calls and 'noise' in the data; ADI with ADO (SNP 17 in oocyte) leads to erroneous call of opposing haplotype and 'noise' in the data.

Theoretically, all maternal heterozygous SNPs should be informative. In practice, however, selecting heterozygous maternal SNPs, which are, as an additional requirement, genotyped as homozygous in the chosen reference, significantly improves the consistency of haplotype calling. Note that because of the principle of independent segregation, each chromosome in the reference has a random grandparental origin.

When the colour coded SNPs are displayed in columns as a consecutive series for each chromosome, the transitions which occur as a result of recombination are evident. For PB1, each recombination is marked by a transition from a heterozygous (red) region to a homozygous region for one of the two maternal haplotypes (yellow or green) or vice versa. For PB2 and the activated oocyte, the transitions occur between the two homozygous maternal haplotypes (yellow to green or green to yellow; Figure 8.3). At this stage, the reference sample, which for phasing purposes is assumed to have no recombination, displays only one maternal haplotype i.e. all SNPs coded yellow. However, in most cases the reference chromosome will in fact be recombinant. This assumption has the effect of creating an apparent recombination in all of the other samples at that position (common recombination), though it will not be observed in the heterozygous regions of PB1. Each sample, therefore, has a combination of true recombinations and common recombinations. Secondary analysis is then required to identify the common recombinations, restore them to the reference sample and remove them from all of the others (Figure 8.4).

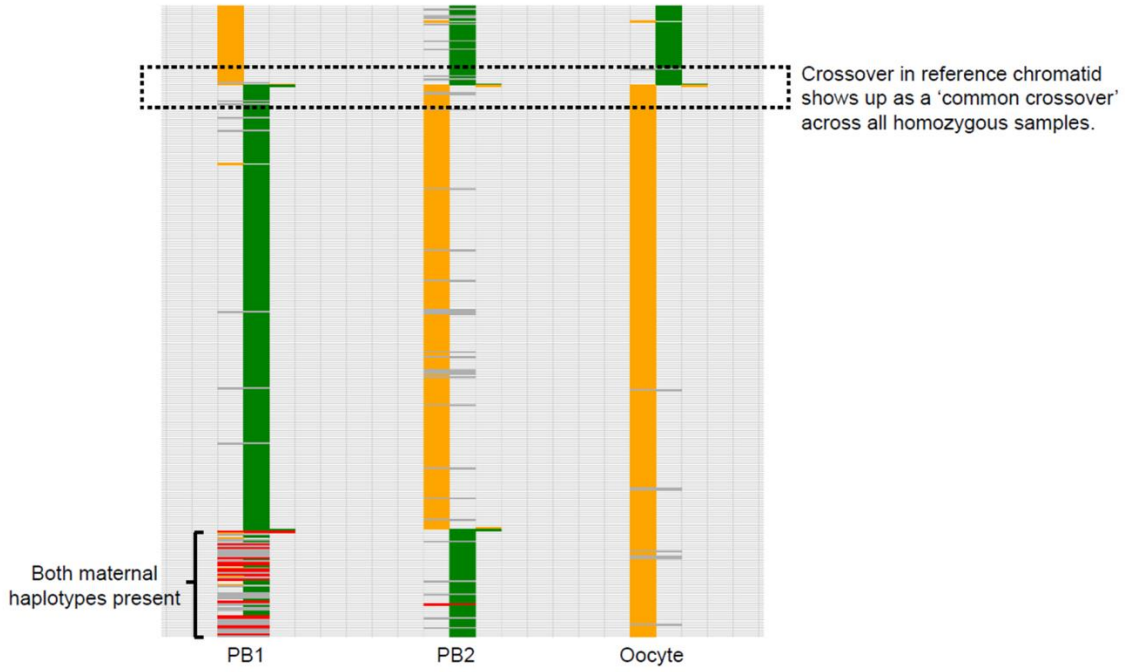

Figure 8.3. Screenshot of SNP patterns in an oocyte-polar body trio.

Opposing grandparental SNPs are shown as yellow or green cells. When both grandparental SNPs are present (i.e. in heterozygous regions) the cells are coloured red. Grey cells denote SNPs that have failed to call (ADO). Transitions between haplotypes mark points of crossovers. Crossovers are 'tagged' (step X) by copying the two SNPs flanking a crossover into the right-hand adjacent column. The dashed box illustrates where a crossover has occurred in the reference resulting in a 'common crossover' at the same position across all homozygous samples. Screenshot is from data imported into a Microsoft Excel worksheet.

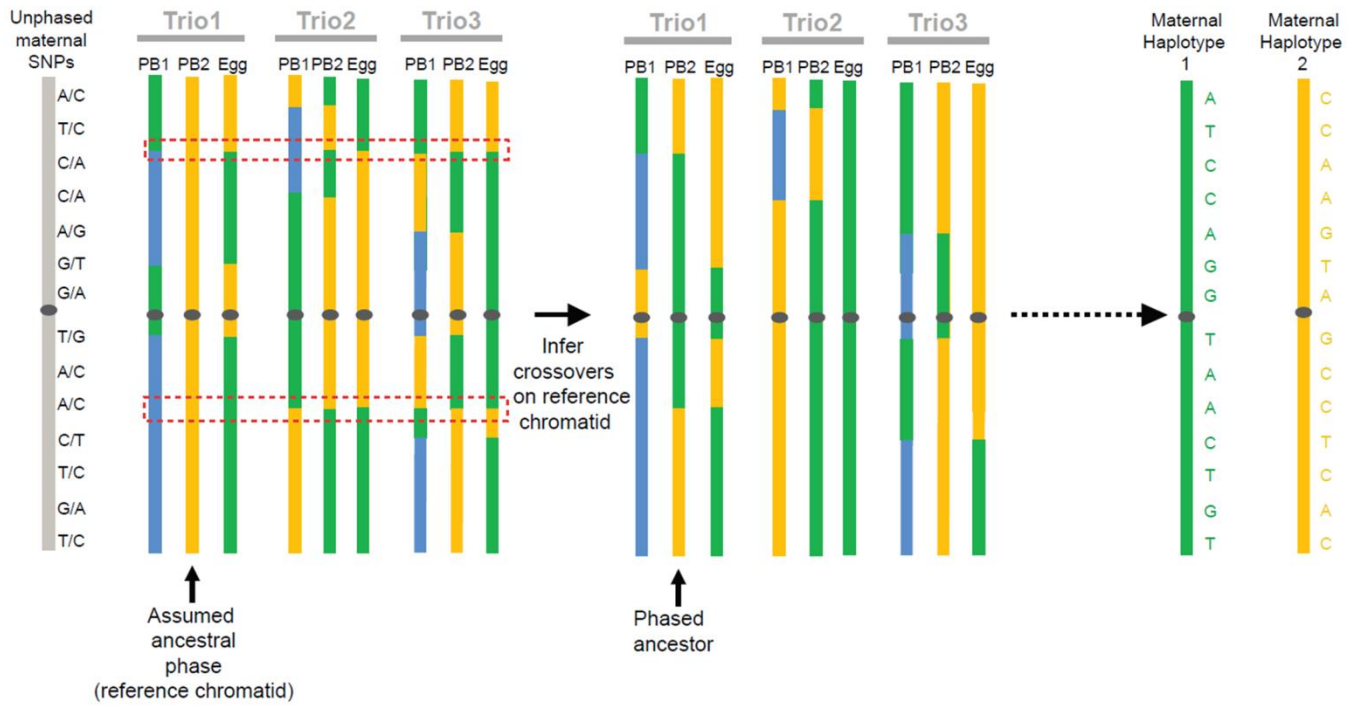

Figure 8.4. Informative SNPs are phased using a reference chromatid to reveal positions of haplotype switches (crossovers).

A haploid cell containing a single chromatid (either PB2 or oocyte) with a good call rate is chosen as the reference chromatid. Oocyte-PB trios from the same individual are compared to the reference chromatid and crossovers are mapped at positions where the haplotypes switch from the 'assumed ancestral phasing' in the reference. When a crossover occurs on the reference chromatid, this manifests as a 'common crossover' that appears across all homozygous samples at the same position (dotted red boxes). These common crossovers are identified, removed and replaced to the reference chromatid using a macro. This process is repeated with a second reference to confirm crossover positions.

8.2.2. Applications of the Method

This protocol is an important advance to human oocyte research within an ethical framework that facilitates a new era of investigation into various aspects of female meiosis. It does not require the creation or destruction of fertilised human embryos and the protocol was paramount to uncovering several novel findings (Ottolini *et al.* 2015). These include a previously undescribed meiotic segregation pattern termed 'reverse segregation' which has shed new light on the meiotic origin of both monosomies and trisomies. It has led to direct evidence showing that lower, genome-wide recombination rates are associated with increased mis-segregation of chromosomes in human female meiosis, suggesting that higher recombination rates are selected for in the female germline. The studies also revealed the first direct evidence of meiotic drive, in which non-recombinant chromatids are preferentially excluded from the oocyte. Moving forward this protocol is central for further oocyte-PB trio analysis and is the protocol devised by the Human MeioMap Project (www.sussex.ac.uk/lifesci/hoffmannlab/research/meiomap) to explore human female meiosis on a broader population scale.

The protocol outlined below is theoretically platform-independent, relying only on the detection of genetic variation. Therefore, with minor adaptation, the protocol will move forward with advances in single cell technology, including next generation sequencing, which will increase the resolution and may enable the detection of *de novo* gene conversions.

Currently the protocol is optimised for oocytes arrested at metaphase II. However, with further development it could be employed to utilise surplus immature (MI or GV) oocytes from human IVF cycles that are otherwise unused. This is a potentially large resource that could enable easy and ethical access to material for the study of human female meiosis. Application of this method will also allow assessment of the efficacy of the first meiotic division following the *in vitro* maturation process.

MeioMapping of female meioses can also be done by analysing the SNP genotype of PB1, PB2 and the fertilised embryo (embryo-PB trio). For embryo-PB trios, the presence of the paternal genome in the embryo samples has to be taken into account. One option is to use the

Karyomapping algorithm, which is designed to identify four sets of informative SNPs for the four parental chromosomes, using an embryo sample, for example, as a reference (Handyside *et al.* 2010). This has the advantage that recombinations between the paternal chromosomes can be identified in the same embryos. However, the resolution is lower because distinct sets of informative SNPs are used to define each haplotype and the number of these SNP loci is significantly reduced. Alternatively, exactly the same algorithm as used for oocyte-PB trios can be used with either a PB2 or embryo as reference, with the requirement that the reference SNP genotype is homozygous. In comparison with oocyte-PB trios, the number of informative SNP loci will be reduced because the paternal contribution will result in heterozygosity at some loci. However, the resolution is significantly higher than with Karyomapping as all of these informative loci identify both maternal haplotypes. For purposes of simplicity I have concentrated on oocyte-trios only for this protocol. Modifications to the protocol required for MeioMapping embryo-trios are available on request.

8.2.3. Comparison to Other Methods

Until the introduction of MeioMapping, the relationship between recombination and meiotic chromosome segregation in humans were confined to population-based studies (Zaragoza *et al.* 1994; Hassold *et al.* 1995; Oliver *et al.* 2008; Middlebrooks *et al.* 2013; Kong *et al.* 2004). This type of analysis is limited to trisomies that are compatible with *in utero* development. By its nature, this could not be performed on aneuploidies that are incompatible with *in utero* development and so excludes embryos that fail to give rise to clinically recognised pregnancies. Furthermore, by only examining one product of meiosis, chromosome mis-segregation patterns and total recombination rates can only be inferred.

One major advantage of MeioMapping is its power to detect global recombination rates in human oocytes. Previously, the only method of detecting recombination across all 23 homologs was through cytological analysis of Mlh1 (that marks crossovers) in foetal oocytes (Gruhn *et al.* 2013;

Tease *et al.* 2002). However, this method cannot determine crossovers that may have arisen through Mlh1-independent pathways (e.g. Mus81-dependent crossovers).

The second major advantage of MeioMapping is its capacity to reveal the chromosome segregation patterns that result in aneuploidy. Previously this could only be inferred from the SNPs surrounding the pericentromere in trisomic conceptions (Zaragoza *et al.* 1994; Hassold *et al.* 1995), which are potentially subject to interpretation errors. More recently however, chromosome copy number analysis of polar bodies such as array comparative genomic hybridisation (CGH) has enabled new insight into the prevalence of segregation errors in preimplantation embryos following IVF (Handyside *et al.* 2012; Capalbo *et al.* 2013; Christopikou *et al.* 2013). However, this quantitative analysis is also subject to interpretation errors regarding the meiotic origins of aneuploidy.

To obtain similar results to our protocol, Hou *et al.* used intracytoplasmic sperm injection (ICSI) to induce resumption of the second meiotic division in mature (MII arrested) human oocytes (Hou *et al.* 2013). The female pro-nucleus was then removed from the resulting normally fertilised zygotes (human embryos) thus destroying them. Our oocyte activation protocol is less technically involved and does not result in the creation or destruction of human embryos for research purposes. Furthermore, my protocol results in an activation rate equal to or higher than performing ICSI in an clinical IVF setting (Palermo *et al.* 1995).

An advantage of the simple Mendelian approach compared to other advanced bioinformatic algorithms, which identify haplotypes by analysing multiple reference samples (Hou *et al.* 2013) is that a single reference is sufficient to detect recombination and chromosome segregation patterns. However, running the analysis with a second reference, ideally from another trio, can be helpful to resolve rare ambiguous recombinations (for example at the extreme ends of chromosomes). It becomes necessary to use a second reference if there are one or more aneuploidies in the original reference. This also provides an opportunity to check that the common recombinations restored to the reference sample are correct (see step 46).

Finally, different platforms exist for detecting SNPs across the genome that can be applied to this type of analysis. In contrast to Hou *et al.* who used a sequencing-based approach (Hou *et al.* 2013) I validated the protocol using genome-wide SNP arrays. Although my method could be adapted to a sequencing-based approach, the efficacy and resolution depends on the read depth and level of SNP overlap across all samples (including maternal and reference genotypes). At present, the depth of sequencing required for my approach is not cost-effective and thus has not been explored.

8.2.4. Level of Expertise Needed

Clinical:

- Registered medical practitioner licensed for oocyte collection from the donors

Molecular biology:

- Basic molecular biology skills are required to amplify single cell DNA and extract gDNA from tissue samples. Knowledge of array scanners and their software is also required.

Embryology:

- Advanced micromanipulation and basic cell culture skill. Mammalian embryologists with embryo biopsy expertise recommended as operators.

Data analysis:

- Advanced knowledge of Microsoft Excel to create and run macros (or other relevant software knowledge).

8.2.5. Limitations

As a minimum, this strategy requires that the reference is from a second trio and therefore requires more than one oocyte-PB trio per donor. Otherwise, reciprocal recombinations between

the sister chromatids in PB2 and the activated oocyte will not be detectable (see Figure 8.4). If this requirement is fulfilled, the complete pattern of recombinations for each trio can be identified (or inferred in any trio with the genotypes of only two out of the three products of meiosis). At present the protocol does not allow for the separation of the two sister chromatids in the PB1. Reciprocal crossovers in the PB1 are unidentifiable as they exist in heterozygous regions of PB1 that cannot be phased (Ottolini *et al.* 2015).

Perhaps the largest limitation of the protocol is obtaining the oocytes themselves. This relies upon patients undergoing an invasive medical procedure to retrieve oocytes directly from the ovarian follicles prior to ovulation. Obtaining material relies on patients either donating oocytes as part of a clinical IVF cycle (Ottolini *et al.* 2015), or a specific donation for research purposes (Hou *et al.* 2013).

This protocol also relies upon single cell WGA, which results in a certain level of amplification error (Findlay *et al.* 1995). Random failure to amplify one of the parental SNPs (known as 'allele dropout'; ADO) will reduce resolution in haploid homozygous regions and result in erroneous homozygous calls in heterozygous regions (Table 8.1). WGA can also introduce random erroneous amplification of the incorrect allele at certain loci. This is known as allele drop in and will introduce low-level 'noise' to the data (Table 8.1).

8.3. Materials

8.3.1. Essential Equipment

- A dedicated tissue culture facility suitable for the culture of human gametes and embryos
- Class 2 flow cabinet work station with a stereo microscope and 37°C heated work surface
- Incubators for embryo media equilibration and embryo activation culture
- Time lapse incubator (e.g. EmbryoScope; Unisence Fertilitech, Denmark) for cell culture and tracking

- Micromanipulators (e.g. Narishige, Japan) fitted with a single hand operated aspirator and a mouth pipette to control micro-pipette
- Inverted microscope (e.g. Eclipse TS100; Nikon Ltd, Japan) equipped with Hoffman Modulation contrast, 37°C heating stage and a laser objective (e.g. Saturn laser; Research Instruments, UK)
- Holding micro-pipette (Holding pipette; TPC, Australia) and aspiration micro-pipette for biopsy (zona drilling pipette; TPC, Australia)
- Stripper hand piece and plastic denuding pipette tips with 130µm lumen (COOK Medical, Ireland)
- Culture Dishes appropriate for applications
- PC running Microsoft Excel

8.3.2. Essential Reagents

- Oocyte culture medium (e.g. Quinn's Advantage Cleavage medium; Cooper surgical, USA)
- Oocyte handling medium (e.g. Quinn's Advantage Medium w/HEPES; Cooper surgical, USA)
- Human serum albumen (e.g. HSA, Cooper surgical, USA)
- Mineral oil (e.g. Oil; Cooper surgical, USA)
- Calcium ionophore (Sigma-Aldrich, USA)
- DMSO (Sigma-Aldrich, USA)

8.3.3. Reagent Set-up

- Prepare Calcium ionophore stock solution
    - Dilute 20.94mg of calcium ionophore in 10ml of DMSO to make 4mM stock solution
    - Store at -20°C for up to three months
- Supplement all media with 10% HSA
    - Store at 3-5°C for up to a week
- Prepare working activation culture medium
    - Add 100µl of stock solution to 3.9ml of Sage cleavage +10% HSA for a final 100uM working solution
    - Use within 12 hours
- Dish preparation and equilibration
    - Prepare culture medium drops within dishes and cover with mineral oil
    - Allow to equilibrate in gassed incubator for a minimum of three hours prior to use
- Prepare handling medium drops (for biopsy) within dishes and cover with mineral oil
    - Allow to equilibrate on heated stage (37°C) for a minimum of 20 minutes prior to use

8.3.4. Preparation

Obtaining mature (MII) human oocytes:

Oocytes can be obtained from a natural menstrual cycle or after a period of any standard clinical ovarian hyperstimulation protocol. Oocytes should be collected by surgical means ~35 hours post

LH surge or administration of HCG trigger. All collected oocytes must undergo enzymatic and mechanical removal of all cumulus cells and the cells of the corona radiata.

Critical step – incomplete removal of all maternal somatic cell surrounding the oocyte could result in contamination of downstream applications. At this point oocytes may be vitrified for batching purposes prior to starting the protocol. For best results the protocol should begin 38-40 hours post LH surge (natural cycle) or administration of HCG trigger (stimulated cycle). In the case of vitrified oocytes, the protocol should begin 1-2 hours post oocyte warming.

All oocyte culture is performed in a humidified incubator set at 37°C in 6% CO_2 and 5% O_2.

To enable tracking of the oocytes and their corresponding PBs throughout the protocol, individual samples must remain separated. Thus, all culture drops, wells and tubes should be uniquely numbered and recorded to allow traceability throughout the experiment.

The protocol requires genomic DNA from all egg donors. In our experience, the genomic DNA can be easily obtained in three ways for the protocol. Depending on when and how the oocytes are obtained: 1) Washed cumulus cell can be used from the donated oocytes collected at the time of oocyte denuding; 2) Blood samples can be taken from the donor at any time; 3) Buccal cell swabs can be taken from the donor at any time. **N.B: This is especially useful if the oocytes are donated retrospectively as buccal cell swab kits can be sent in the post.** DNA extraction can be performed at any time as per the instructions accompanying commercially available kits.

8.4. Step-by-Step Protocol

8.4.1. First Polar Body (PB1) Biopsy

N.B: The activation and biopsy steps below could feasibly be performed by a single operator. However, it is recommended that two operators work in tandem at time points where certain activities can be performed in parallel (e.g. biopsy and tubing) to avoid

delays in processing to preserving the sample's integrity especially when performing the protocol on more than six oocytes at a time.

1. At a stereo microscope work station, move the oocytes to a biopsy dish with individually numbered 10µl microdrops of HEPES medium +10% HSA under Sage oil. Use a wash drop per oocyte to ensure that each oocyte is free from any cellular debris before allocating them to their biopsy drop. The number of oocytes per dish is dependent on the skill of the operator. I recommend that no more than 15 minutes should pass between the oocytes entering the dish and them being removed after biopsy (from 1-6 oocytes per dish).
2. Place the dish containing the oocytes on the inverted microscope (with micromanipulators and laser attached) to give a clear view of the PB and secure the oocyte by suction with the holding pipette ensuring that the oocyte is just above the bottom of the dish.
3. Rotate the oocyte using the aspiration pipette until the PB is clearly in focus at around 12 or six o'clock orientation. If done correctly, the zona pellucida should also be clearly in focus (Figure 8.2). It is essential to maintain a gentle yet constantly full seal between the holding pipette and the oocyte as even a small break in the seal could result in a poor outcome.
4. Once the oocyte is correctly positioned for biopsy make a small aperture with a series of laser pulses in the zona pellucida, no larger than the diameter of the aspiration pipette, adjacent to the PB on the side of the aspiration pipette. Work inwards from the outer surface of the zona. Attention must be given so as not to fire a laser pulse at the cytoplasm of the oocyte or PB.
5. Insert the aspiration pipette through the opening in the zona and position the lumen of the pipette adjacent to the PB.
6. Use the aspirator to create a small amount of suction and slowly withdraw to remove the PB. If avoidable, the PB should not entirely enter the pipette as this could result in lysis.

Laser assistance may be required if the PB is still attached to the oocyte to break the intercellular bond. A single laser pulse, on the lowest intensity setting, can be used at the cell junction to release the bond. If PB1 is fragmented, or fragments during biopsy, ensure all fragments are removed for tubing.

7. Once successfully removed, separate the PB and oocytes to separate areas of the drop to ensure safe transfer of the oocyte to further culture without disturbing the PB. Make a note of the position of the PB in each drop for future reference.

8.4.2. Activation Culture

8. Move the dish containing the biopsied oocytes to a stereo microscope work station.
9. Identify both the PB and the oocyte down the microscope. Use a stripper pipette to transfer the oocytes to activation culture drops making sure not to disturb the PB. Care must be taken from this point onwards not to excerpt too much pressure on the biopsied oocytes when pipetting. Slow pipetting with gentle aspiration and expulsion is recommended.
10. Move the oocytes to individually numbered activation culture drops, leaving the biopsied PB1 behind in the biopsy dish for immediate tubing. Use a wash drop to gently wash each oocyte before allocating them to their activation culture drop. Begin a 40 minute timer from the time the last oocyte is transferred to activation culture and put the dish in the incubator until the timer ends.

At this point, further PB1 biopsy can be performed following the steps above (steps 1-10). If so a second operator should perform the tubing procedure below in parallel.

8.4.3. PB1 Tubing

11. Prime the appropriate number of 0.2ml, RNase and DNase free thin walled, flat cap polymerase chain reaction (PCR) tubes with 1ul of phosphate buffered saline (PBS) for the number of polar bodies to be tubed and label each tube appropriately.
12. To avoid evaporation and contamination, close the cap on the tubes gently (loose cap). Caps should be closed but easily releasable for depositing the samples. The 1µL of PBS should remain at the bottom of the tubes. If not, or small drops form on the side of the tube, give the tubes a quick spin on the micro centrifuge prior to depositing the samples.
13. Focus on the polar body with the stereo microscope using the mirror to create contrast for best visibility.
14. Set the stripper pipette to 1µL and using a 120µm pipette tip prime as much as possible with PBS. Depress the plunger all the way, aspirating PBS into the pipette until the plunger is entirely released. For best results change to a new stripper tip for each sample.
15. Enter the drop with the pipette tip whilst gently expelling a small amount of PBS to ensure no oil blocks the tip. If any oil droplets are visible in the pipette tip, try to clear it by vigorous aspiration in clean PBS or replace it and restart from step 14.
16. Place the pipette tip over and adjacent to the PB and release the plunger entirely (PB should enter the pipette and remain there). Ensure that the plunger and the pipette are not knocked at this stage as the sample could be lost.
17. Open a pre-primed and labelled PCR tube and hold the tube between thumb and index finger so as to have a clear view through the tube from top to bottom.
18. Insert the pipette containing the sample into the tube so that the tip enters the PBS. Avoid touching the sides of the tube or the bottom if possible.
19. Expel the contents of the pipette into the tube stopping when 1µL mark is reached. This should be when a point of more resistance is felt when depressing the plunger.

20. Keep the plunger depressed to this point and re-enter the sample drop, expelling the remaining PBS whilst observing any objects exiting the pipette. Pipette up and down once or twice with the media in the drop to ensure the PB is not stuck to the pipette wall. If no PB is observed, tightly cap the tube.

Move on to the remaining samples following the same instructions.

21. Once all samples have been tubed, briefly centrifuge them to ensure the samples and all the media are in the bottom of the tubes.
22. Submerge the bottom of every tube (not the entire tube) in a shallow LN2 bath to snap freeze and store tubes in racks at -20°C.

8.4.4. Post Activation Culture

Ideally, post activation culture should be performed within a time lapse incubator for easy assessment of PB2 extrusion and pronuclear formation. For my protocol I specifically use the EmbryoScope system that has its own proprietary dishes called EmbryoScope Slides.

23. After 40 minutes of activation culture, remove the dish containing the oocytes from the incubator and move it to the stereo microscope work station.
24. Move each oocyte to a separate well of an EmbryoScope slide with a 170µm pipette tip. Wash using gentle pipetting in the provided wash well prior to depositing in the final culture well. Ensure each oocyte is positioned in the centre of the micro-well for best visibility on the time lapse system.
25. Move the EmbryoScope slide to the EmbryoScope incubator unit and insert following the prompts. It is important that the slide is seated in its position securely using substantial downward force.

If time lapse is not available, move the oocytes to a dish containing individually labelled 30µl drops of post activation culture medium. Wash thoroughly (yet gently) through a series of wash

drops (2) in the dish prior to depositing in the final culture drop. Place the dish in the standard incubator.

8.4.5. Assessing activation

Assessment of PB2 extrusion should be performed around 16 hours after the oocytes are moved to post activation culture.

26. Use the EmbryoScope time lapse viewer to scroll through the images of each oocyte whilst the EmryoScope slide containing the oocytes remains in the incubator unit. Scrolling at different focal depths may be necessary to properly identify PB2 extrusion. Pronuclei may also become visible by this time however normal activation is not dependent on it (Figure 8.2).

If time lapse is not available, move the dish containing the oocytes to the inverted microscope work station. Gradually focus through the oocytes to identify the presence of PB2. Again, pronuclei may also be visible by this time; however normal activation is not dependent on it.

8.4.6. PB2 Biopsy

27. Repeat steps 1-7 ensuring extra care is taken when pipetting (step 1) and that suction with the holding pipette (steps 2-3) avoids the existing aperture in the zona pellucida.

If PB2 biopsy is to be performed on more than one dish of activated oocytes (maximum six oocytes) a second operator should perform the tubing procedure below in parallel.

8.4.7. PB2 Tubing

28. Repeat steps 11-20 whist the oocyte remains in the drop with the PB2. It is important that the oocyte and PB2 are well separated in the drop and that the oocyte is avoided when pipettes enter the drop (steps 15-16 & 20).

29. Leave the biopsy dish, now containing only the oocytes (devoid of their PB1 and PB2), on the heated stage of the stereo microscope if working alone. If working in tandem with another operator, move biopsy dish to inverted microscope for zona removal procedure (step 31).

30. Repeat steps 21-22 with tubed PB2 samples.

8.4.8. Zona removal

31. Place the dish containing the oocytes on the inverted microscope (with micromanipulators and laser attached) to give a clear view of the zona pellucida and secure the oocyte by suction with the holding pipette ensuring that the oocyte is just above the bottom of the dish. Be careful to avoid the two existing apertures in the zona.

32. Once in position, make a large aperture in the zona pellucida using a series of laser pulses. The aperture should be between a quarter and half of the zona around. Ablate the zona using laser pulses approximately the same diameter of the zona thickness, working in a circular fashion.

33. Insert the aspiration pipette under the zona and gently expel medium to displace the oocyte so that it is free from the zona. Ensure that the pipette is well primed and be careful not to blow any bubbles. Gentle manual manipulation with the aspiration pipette to move the oocyte may also be necessary to help the displacement process.

34. Whilst still attached to the zona move the holding pipette to the edge of the drop and deposit the zona there leaving the oocyte in the centre of the drop.

8.4.9. Oocyte tubing

35. Repeat steps 11-22 to complete the tubing of the oocyte. Try to avoid the Zona pellucida when aspirating the oocyte (steps 15-16).

8.4.10. Whole Genome Amplification (WGA) and Genotyping

N.B. The following two points are performed following the clinical Karyomapping protocol for single cells provided by Illumina within the Karyomapping product. For further details refer to Natesan *et al.* (Karyomapping validation paper). Briefly;

36. The PCR tubes containing the trios samples were brought to an end volume of 4µl with PBS and multiple displacement amplification (MDA) protocol performed according to the instructions provided (SureMDA, Illumina).

37. 400ng of the donor's genomic DNA or 8µl of the WGA products from the trio's samples (PB1, PB2 or oocyte) were processed on SNP genotyping beadchips (Human CytoSNP-12 or Human Karyomapping beadarray; Illumina, San Diego, CA, USA) for ~300K SNPs, following the instructions provided.

N.B. This part of the protocol can be performed by a third party if necessary. If so, the samples can be shipped in racks on ice to the commissioned laboratory.

Key point. Do not ship on dry ice. Insure care is taken with the parcel and shipping time does not exceed three hours.

8.4.11. MeioMapping

38. The SNP genotypes for maternal genomic DNA, and the WGA products for PB1, PB2 and activated oocyte for each trio are exported from Genomestudio (Illumina, USA) as a text file along with the chromosome location and base pair position.

39. This data is then imported into Microsoft Excel and sorted according to (1) chromosome and (2) base pair (bp) position. This file is then saved and archived following step 38.

Steps 38 onwards are carried out using a series of Visual Basic for Applications (VBA) macros in Microsoft Excel.

40. The SNP genotype data for each of the 23 chromosomes is imported separately into a second Excel spreadsheet for MeioMapping and arranged in blocks side-by-side. Note that the original data and processed data are stored in separate Excel workbooks to keep the size of the files to a manageable size.

41. The call rates and heterozygous call rates are calculated for all samples.

42. A reference sample (either a PB2 or activated oocyte) is selected. Note that to maximise the number of informative SNP loci a reference sample with a high call rate and low heterozygous call rate should be selected.

43. Informative maternal heterozygous SNP loci for each chromosome, which genotype as homozygous in the reference sample (AA or BB), are identified and defined as Maternal haplotype 1 (yellow) (Table 8.1).

44. Sample genotypes at informative maternal SNP loci for each chromosome are compared to the reference genotype and identified as: (1) homozygous for the same allele – Maternal haplotype 1 (yellow); (2) homozygous for the other allele – Maternal haplotype 2 (green); (3) heterozygous – combination of Maternal haplotypes 1 and 2 (red); or (4) no call (grey). See Figure 8.3 and Table 8.1.

45. The results of (6) are displayed as a consecutive series of informative SNPs in vertical columns, colour coded with their bp position, for each chromosome, again in separate blocks arranged side-by-side in a separate worksheet (Figure 8.3).

46. The positions of any recombinations indicated by the transitions described above are tagged either manually or using a macro. For manual tagging, the informative SNPs flanking the recombination are copied and pasted into the adjacent right-hand column, including the colour coding and bp position (Figure 8.3).

Notes:

(1) Each recombination should always be present in two out of three of the products of meiosis at the same position.

(2) Regions of heterozygosity which indicate the presence of two non-sister chromatids, typically in PB1 may, depending on amplification efficiency, have variable levels of ADO and 'no calls' (Table 8.1). The transition from these regions to homozygous regions of sister chromatids is generally clearly evident but less well defined for this reason. Whereas transitions between homozygous maternal haplotypes are sharply defined since they are not affected by ADO and have lower no call rates than heterozygous loci. The nearest flanking heterozygous (red) SNP and homozygous SNP (yellow or green) should therefore be tagged and the corresponding transition in PB2 or the activated oocyte used to define the position of the recombination event.

47. The flanking tags for each recombination in each sample are imported into a separate worksheet.

48. 'Common crossovers' are identified by their presence in all homozygous samples at the same position (Figure 8.4), defined by an overlapping range for the two flanking tags in each sample. Note that common crossovers cannot be identified in heterozygous regions, typically in PB1. Reciprocal recombination between segregated sister chromatids in PB2 and the activated oocyte, one of which is the reference, will not be identified in the non-reference component and needs to be added back to this component also (Figure 8.4).

49. Common crossovers are removed from each non-reference sample and added to the reference sample (Figure 8.4).

50. The position of all crossovers is calculated as an average of the base pair position of the flanking tags.

51. The haplotype colours across each true recombination are corrected following the removal of the common crossovers.

52. The pattern of recombinations in each component of each trio is displayed according to its position to generate the MeioMap (Figure 8.4).

Notes:

(1) Secondary analysis of the numbers and positions of the recombinations can be done either with the use of further macros within Excel or by exporting the relevant data.

(2) Segregation errors in female meiosis can be inferred by atypical patterns of homozygous and heterozygous regions in the three components in the MeioMap (Ottolini *et al.* 2015).

9. Specific Aim 6: To combine the techniques developed above and use both Karyomapping and MeioMapping to explore the full extent of meiotic chromosome recombination and segregation that occurs in the human oocyte

As outlined in sections 2.2.2 and 2.8 of the General Introduction, crossover recombination reshuffles genes and prevents errors in segregation that lead to extra or missing chromosomes (aneuploidy) in human eggs, a major cause of pregnancy failure and congenital disorders. To explore this further, I generated genome-wide maps of crossovers and chromosome segregation patterns by recovering all three products of single female meiosis (as described in Specific Aim 5). Genotyping>4 million informative SNPs from 23 complete meioses allowed us to map 2,032 maternal and 1,342 paternal crossovers and to infer the segregation patterns of 529 chromosome pairs. I uncover: a) a novel reverse chromosome segregation pattern in which both homologs separate their sister chromatids at meiosis I; b) detect selection for higher recombination rates in the female germline by the elimination of aneuploid embryos; and c) report chromosomal drive against non-recombinant chromatids at meiosis II. Collectively, the findings of this specific aim reveal that recombination not only affects homolog segregation at meiosis I but also the fate of sister chromatids at meiosis II. This work has been recently published as follows:

Ottolini CS, Newnham LJ, Capalbo A, Natesan SA, Joshi HA, Cimadomo D, Griffin DK, Sage K, Summers MC, Thornhill AR, Housworth E, Herbert AD, Rienzi L, Ubaldi FM, Handyside AH, and Hoffmann ER, *Genome-wide maps of recombination and chromosome segregation in human oocytes and embryos show selection for maternal recombination rates.* Nat Genet. 2015 Jul;47(7):727-35.

9.1. My Personal Contribution to the Work

I was integral to conceiving and designing the experiments for this chapter. I performed the majority of the embryology including oocyte warming and oocyte and embryo biopsy as well as tubing and whole genome amplification of the samples. I performed some of the SNP genotyping and array CGH and analysed all of the CGH and SNP data. I was involved in the writing and editing of the published manuscript and the design and creation of the figures. What follows is an adaptation of the published manuscript.

9.2. Introduction

Errors in chromosome segregation during the meiotic divisions in human female meiosis are a major cause of aneuploid conceptions, leading to implantation failure, pregnancy loss and congenital disorders (Nagaoka *et al.* 2012). The incidence of human trisomies increases exponentially in women from ~35 years of age, but despite conservative estimates that 10-30% of natural conceptions are aneuploid (Hassold & Hunt 2001), the underlying causes and their relative contributions are still unclear. In addition to maternal age, one important factor that predisposes to mis-segregation in both sexes is altered recombination. Recombinant chromosomes in the offspring are the result of crossovers, the reciprocal exchange of DNA between homologous chromosomes (homologs). Together with sister chromatid cohesion, crossovers physically link the homolog pair together during the prophase stage of meiosis (Figure 9.1a), which takes place during foetal development in females. The linkages have to be maintained for decades, because the two rounds of chromosome segregation only occur in the adult woman. By following the pattern of genetic markers such as single nucleotide polymorphisms (SNPs) on the two chromosomes inherited from the mother in trisomic conceptions, it has been inferred that some crossovers occur too close to centromeres (Hassold *et al.* 1980; Hassold & Jacobs 1984; Zaragoza *et al.* 1994; Freeman *et al.* 2007; Nagaoka *et al.* 2012), where they may disrupt the cohesion between the two sister chromatids (Koehler *et al.* 1996; Rockmill *et al.* 2006). Other crossovers have been suggested to be too far from the

centromeres to mediate correct attachment, or to be lacking altogether (non-exchange, E_0) (Hassold *et al.* 1980; Hassold & Jacobs 1984; Zaragoza *et al.* 1994; Freeman *et al.* 2007; Nagaoka *et al.* 2012). If these inferences are correct, it follows that events that shape the recombination landscape in oocytes during foetal development affect the risk of women having an aneuploid conception decades later in adult life.

A limitation of these extensive population-based studies, however, is that only one of the products of meiosis is analysed (the oocyte). This prevents direct identification of the origin of chromosome segregation errors and provides only partial information on the crossovers during prophase of meiosis I. The 'missing data' problem is so significant that even the meiotic origin of age-related trisomies has been challenged recently (Hulten *et al.* 2010). Another confounding factor is that spontaneous miscarriages, still and live births on which our current knowledge is based represent only a minor fraction of the aneuploid embryos at conception. The majority of affected embryos are lost throughout pregnancy resulting in major preclinical and clinical losses (Hassold & Hunt 2001). Thus, to understand the origin of human aneuploidies, I need to assess all three meiotic products in unselected oocytes and embryos.

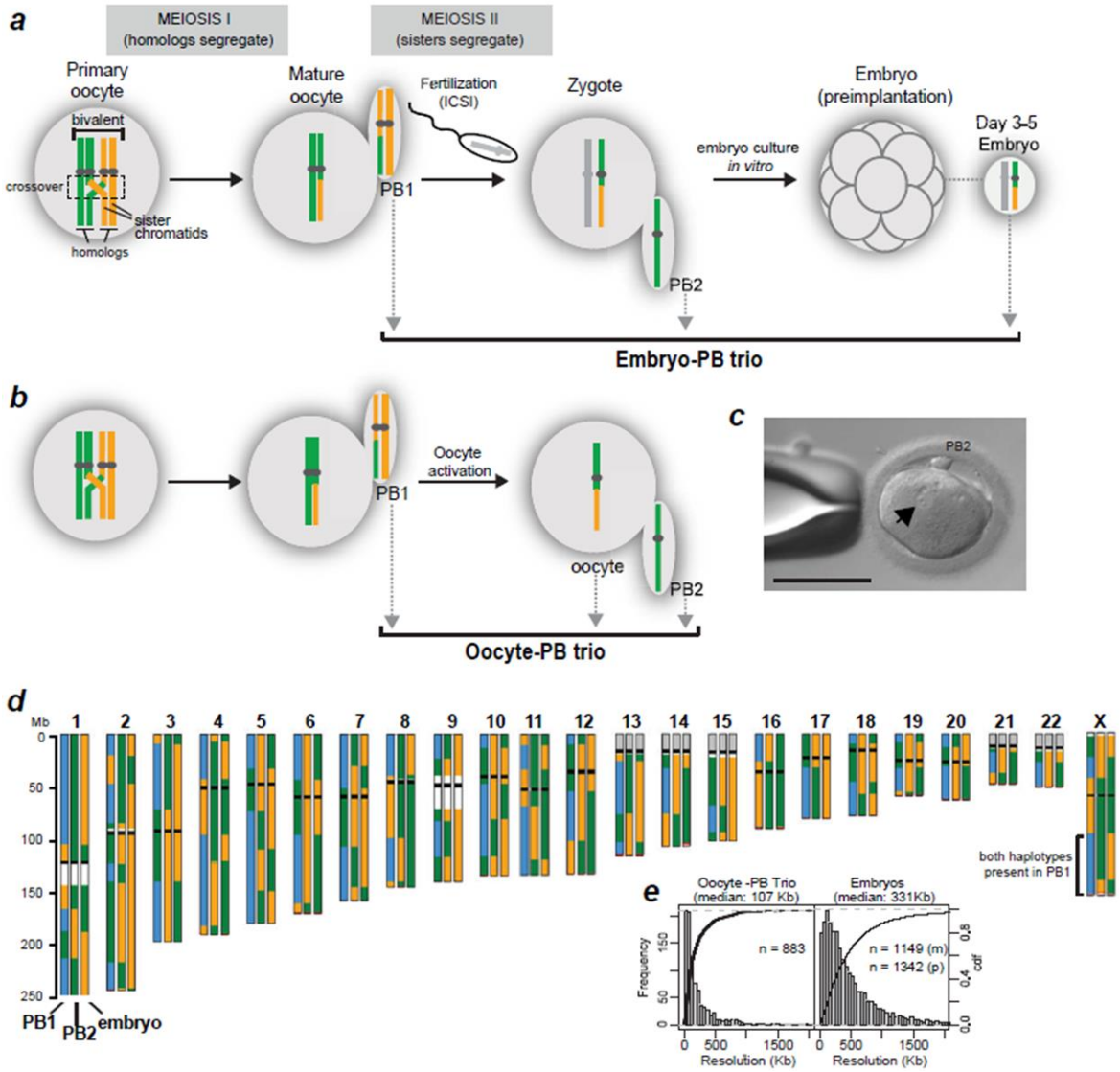

Figure 9.1. Human MeioMaps from embryos and oocytes together with their corresponding polar bodies (Ottolini *et al.* 2015).

(a,b) The genotypes of the two maternal chromosomes are shown as green and yellow. Crossovers, shown in the dashed box, occur during foetal development. The two polar bodies were sequentially biopsied (grey arrows) to avoid misidentification. Maternal MeioMaps were deduced from the embryo following intracytoplasmic sperm injection (ICSI) or directly assessed in the haploid oocyte, after artificial activation *(b)*.

(c) An activated oocyte with a single pronucleus (arrow) and PB2. Scale bar: 110µm.

(d) An example of a MeioMap after genome-wide SNP detection and phasing (see Methods). Each chromosome is represented by three vertical columns representing the three cells of the trio (PB1, PB2, and embryo or oocyte). The two phased maternal haplotypes are represented by green and yellow. Blue represents the detection of both haplotypes. Regions where SNPs are not available on the array are shown in white (repetitive sequences on chr. 1 and 9) or gray (rDNA). Black bars illustrate the position of the centromere. Red bars show the last informative SNPs to call. Crossovers are manifested as reciprocal breakpoints in haplotypes (green to yellow, blue to green, etc.) in two of the three cells. Note that the colours of the haplotype blocks between different chromosomes are not necessarily derived from the same grandparent. Histograms of the resolution of the crossovers are shown in **(*e*)**. The resolution was 352kb and 311kb for maternal (m) and paternal (p) crossovers in the embryos respectively.

9.3. Methods

The processing of oocytes for this section was performed following the protocol developed in Specific Aim 5. A brief overview is provided below. For more details please refer to Specific Aim 5.

9.3.1 Ethics

All material for the study was ethically sourced with fully informed patient consent. All oocytes for the study were obtained from donors after completion of their *in vitro* fertilisation (IVF) treatment and were destroyed for analysis. The oocytes used were vitrified in accordance with Italian law in place at the time of oocyte retrieval for IVF treatment. Use of the oocytes for the study was approved by the Institutional Review Board of the Valle Giulia Clinic where the oocytes were stored and did not influence patient treatment. All embryo samples for the study were either obtained by tubing embryos in their entirety (destroyed) for analysis following a previous abnormal outcome in clinical tests or reanalysis of clinical biopsy samples after embryos were

transferred, stored or discarded depending on the clinical result. SNP genotyping was performed as clinical follow up/validation of clinical genetic analysis and covered by the Human Fertilisation and Embryology Authority (HFEA) code of practice. All primary data were encoded such that informative SNPs were represented as A and B. Only secondary data with informative SNPs encoded A and B were used for data analysis.

9.3.2. Oocyte-PB Trios

9.3.2.1. Patient Participation and Consent

All second meiotic division (MII) oocytes for the study were obtained from patients undergoing intra-cytoplasmic sperm injection (ICSI) treatment in the Centre for Reproductive Medicine GENERA in Rome between 2 September 2008 and 15 May 2009 following controlled ovarian hyperstimulation performed using two different protocols: GnRH-agonist long protocol and GnRH-antagonist protocol. According to the Italian law in force when these oocytes were collected, a maximum of three oocytes could be inseminated per patient. The remaining MII oocytes were vitrified and later recruited for the study after informed consent was obtained from the patients. The study and the informed consent were approved by the Institutional Review Board of the Valle Giulia Clinic and did not influence patient treatment.

9.3.2.2. Oocyte Collection

Oocyte collection was performed at 35h post-human Chorionic Gonadotrophin (hCG) administration. Removal of the cumulus mass was performed by brief exposure to 40IU/ml hyaluronidase solution in Sage fertilisation medium +10% human serum albumin (HSA) (Cooper Surgical, USA), followed by mechanical removal of the corona radiata with the use of plastic 'denuding' pipettes of defined diameters (COOK Medical, Ireland) in a controlled 6% CO_2 and 37°C environment. This procedure was performed between 37h and 40h post-hCG administration. MII oocytes were then identified for vitrification.

9.3.2.3. Oocyte Vitrification and Warming

The vitrification and warming procedures were performed according to Kuwayama *et al.* (Kuwayama *et al.* 2005; Kuwayama 2007). Commercially available vitrification and warming kits were used (Kitazato BioPharma Co., Japan). The vitrification procedure was performed a maximum of 40 hours post-hCG administration. The oocytes were stored on a cryotop vitrification tool (Kitazato BioPharma Co., Japan) with a plastic cap for protection during storage in liquid nitrogen. All oocytes were stored submerged in liquid nitrogen until warming was performed. Following oocyte warming degenerated oocytes were discarded and the surviving oocytes were cultured before biopsy of the first polar body (PB1) and activation.

9.3.2.4. Oocyte Culture and Activation

All oocyte culture was performed at 37°C in 6% CO_2 and 5% O_2. To enable tracking of the oocytes and PBs, individual culture was performed and culture drops and wells were numbered to allow traceability throughout the experiment.

Immediately after warming, the surviving oocytes were allocated to individually numbered 35µl microdrops of Sage cleavage medium +10% HSA under mineral oil (Cooper Surgical, USA) and cultured for two hours prior to PB1 biopsy and activation.

Oocytes were activated by exposure to activation medium: 100µM calcium ionophore (A23187, C7522 Sigma-Aldrich) in Sage cleavage +10% HSA (Cooper Surgical, USA) from a stock solution in DMSO (Sigma-Aldrich) diluted 1:40. Oocytes were transferred to 35µl drops of the activation medium under Sage oil, numbered appropriately. Activation culture was performed for 40-120 mins. The oocytes were then moved to post activation culture.

Post activation culture was performed in separate wells of EmbryoScope slides (Unisence Fertilitech, Denmark) in cleavage medium – medium as used in post warm culture under Sage oil. The slides were placed in the EmbryoScope time lapse incubator (Unisence Fertilitech, Denmark)

for assessment of second polar body (PB2) extrusion and appearance of pronuclei prior to PB2 biopsy.

9.3.2.5. Polar Body Biopsy

Polar bodies were biopsied sequentially in order to discriminate between the three products of meiosis using micromanipulators (Narishige, Japan) on an inverted microscope (Nikon Ltd, Japan) equipped with Hoffman Modulation contrast and a 37°C heating stage (Linkam Scientific Instruments, UK). The PB1 was biopsied prior to oocyte activation and the PB2 was biopsied following its extrusion, post activation as previously described by Capalbo *et al.* (Capalbo *et al.* 2013). All biopsies were performed in individually numbered 10µl microdrops of HEPES medium +10% HSA under Sage oil (Cooper Surgical, USA) for tractability. For both PB1 and PB2 biopsies, oocytes were positioned on the microscope to give a clear view of the PB and secured by suction with the holding pipette (TPC, Australia). An aperture was made in the zona pellucida with a series of laser pulses (Saturn laser; Research Instruments, UK) working inwards from the outer surface of the zona. The aspiration pipette (zona drilling pipette; TPC, Australia) was then inserted through the opening and the PB removed with gentle suction. PB1 biopsy: Once biopsied the oocytes were moved to activation culture leaving the biopsied PB1 in the microdrop for immediate transfer to a 0.2ml, RNase and DNase free thin walled, flat cap polymerase chain reaction (PCR) tube (Corning, Sigma-Aldrich) for DNA amplification. PB2 biopsy: once biopsied the PB2 was immediately transferred to a PCR tube for DNA amplification with the oocyte still in the microdrop. The oocyte was then returned to the micromanipulator for full zona removal. The zonae were removed from the oocytes using the same setup for the biopsy procedure. The oocyte was anchored to the holding pipette and a larger aperture was made in the zona using laser pulses. The oocyte was removed from the zona using both displacement and zona manipulation techniques with the aspiration pipette. Once free from the zonae, the oocytes were transferred to PCR tubes for DNA amplification.

Transfer of the samples to PCR tubes was performed using a plastic denuding pipette (COOK Medical, Ireland) with a 130µm lumen. Individually labelled PCR tubes were primed with 2µl Dulbecco's phosphate buffered saline (DPBS) (Gibco, Life technologies) with 0.1% polyvinyl alcohol (Sigma-Aldrich). Individual samples were expelled into the DPBS in around 1µl of the medium containing the samples, leaving a final volume of no more than 4µl of medium with the sample in the PCR tubes. The PCR tubes were then briefly centrifuged, snap frozen in liquid nitrogen and stored at -20°C prior to whole genome amplification (WGA).

9.3.3. DNA Extraction and Whole Genome Amplification (WGA)

Genomic DNA (gDNA) from all oocyte donors was obtained using buccal cell swabs (Isohelix, Cell Projects Ltd). Extraction of the gDNA from the swabs was performed using a proteinase K extraction kit to a final volume of 30µl, following the manufacturer's instructions. DNA from all three products of meiosis was obtained by lysis of the cells and WGA. The PCR tubes containing the samples were brought to an end volume of 4µl with phosphate buffered saline (PBS) and REPLI-g Single Cell Kit multiple displacement amplification (SureMDA, Illumina) or PCR library based SurePlex amplification (Illumina) was performed according to the manufacturer's instructions. Multiple displacement amplification (MDA) was performed with a short 2h incubation.

9.3.4. Embryos and Embryo-PB Trios

9.3.4.1. Embryo Samples

35 embryos diagnosed as affected and/or aneuploid were analysed from four clinical cases for either preimplantation genetic diagnosis (PGD) of single gene defects or preimplantation genetic screening (PGS) for aneuploidy following standard IVF protocols at The Bridge Centre, London with patients' informed consent. SNP genotyping was performed for quality control purposes following clinical biopsy and genetic testing of the embryos under the HFEA clinic licence L0070-14-a using similar methods to those described for the processing of the oocyte-PB trios.

In one of the PGD cases, two surplus denuded first meiotic division (MI) oocytes were allowed to mature *in vitro* by overnight culture in Sage fertilisation medium +10% HSA under mineral oil (Cooper Surgical). Biopsy of PB1, tubing and WGA of the oocyte and PB1 were then performed as described for the oocyte-PB trios.

9.3.4.2. Embryo-PB Trios

In another PGS case, in which array comparative genomic hybridisation (CGH) had been used to detect aneuploidy by copy number analysis of both polar bodies, the WGA products (Sureplex; Illumina, San Diego, CA, USA) from both polar bodies were SNP genotyped along with parental genomic DNAs and, with patients' informed consent, WGA products (SureMDA; Illumina, San Diego, CA, USA) of nine corresponding fertilised embryos which had all been diagnosed as aneuploid.

9.3.5. Array CGH, SNP Bead Array and Data Analysis

For array CGH analysis, 4µl aliquots of Sureplex single cell amplified DNA Products (PB1, PB2, oocyte or blastomere) were processed on microarray slides (24Sure; Illumina, USA). The data was imported and analysed using dedicated software (BlueFuse Multi v 4.0; Illumina, USA).

For SNP genotyping, 400ng of genomic DNA or 8µl of WGA products from the single cell and embryo samples (PB1, PB2, oocyte, single blastomere or whole embryo) were processed on a SNP genotyping beadarray (Human CytoSNP-12 or Human Karyomapping beadarray; Illumina, San Diego, CA, USA) for ~300K SNPs, using a shortened protocol and the genotype data analysed using a dedicated software programme for Karyomapping (Bluefuse Multi v4.0; Illumina, San Diego, CA, USA) or exported as a text file for analysis in Microsoft Excel (Natesan, Bladon *et al.* 2014).

9.3.6. MeioMap Analysis

Following SNP genotyping, MeioMaps were constructed and displayed by importing the data into Microsoft Excel and processing using custom macros written in Visual Basic for Applications. For the oocyte-PB trios, a simple algorithm was used to phase all heterozygous maternal SNP loci using a haploid PB2 or oocyte sample as a reference. This defined a reference set of homozygous SNP loci (haplotype) genome-wide (AA or BB), across each chromosome. The genotype of each of the samples including the reference were then interrogated at each of these informative SNP loci and displayed as either the same as the reference (yellow) or opposite to the reference (green) or heterozygous (blue) indicating the presence of both maternal haplotypes. Phase transitions at crossovers were then manually tagged in Excel by copying the closest SNP calls bracketing the crossover and the type and position of these SNPs imported into a second spreadsheet for further processing. Because phasing is achieved using a reference sample, any phase transitions caused by crossovers in that particular sample appear in identical positions in all other samples analysed (with the exception of any crossover between the reference and the PB2 or oocyte in that trio). Macros in the second spreadsheet therefore identified these common crossovers, restored them to the reference sample and removed them from all of the other samples. The MeioMaps were then displayed, checked and further edited manually as necessary. All oocyte-PB trios were run with at least two references to MeioMap any aneuploid chromosomes in the reference trio and to double-check all crossovers.

For embryo-PB trios, two methods were used. Where the SNP genotype of a close relative or, in some cases, a sibling embryo was available, the samples were Karyomapped using the standard algorithm which identifies informative SNP loci for all four parental haplotypes in either Excel or using dedicated software (Bluefuse Multi v4.0; Illumina, San Diego, CA) (Handyside *et al.* 2010; Natesan *et al.* 2014). Alternatively to improve resolution, a modified Karyomapping algorithm with a PB2 or oocyte as reference was used. This algorithm identified all combinations of parental genotypes that were informative for the maternal haplotype only. In either case, the phase

transitions were manually tagged and imported into the second spreadsheet for further processing, display and final editing as above.

The workflow was validated on single cells by comparing recombination maps in 15 individual cells from a donor to the genomic DNA of the child, and by assessing 10 individual blastomeres from the same embryo for direct comparison. In all cases, concordance of recombination rates and positions was >99% (data not shown).

9.3.7. Simulation: Crossover Distribution Amongst Chromosomes and Distances Between Crossovers Along Chromosomes

Simulations were performed to allocate a specified number of crossover events to set of chromosomes. Chromosomes were allocated a specified length using the minimum and maximum crossover locations mapped within the experimental dataset. Crossovers were allocated randomly to chromosomes with weighted probability using the chromosome length, thus longer chromosomes receive more crossovers. The allocation was either totally random (non-obligate) or random following allocation of one crossover per chromosome (obligate). For each chromosome the positions of the allocated crossovers was determined iteratively by randomly selecting an available location. The available locations were all possible positions not within a minimum distance (107kb) from the existing crossover positions. The simulation reported the total number of crossovers per chromosome and the inter-crossover distances. The distance from the outermost crossover to the chromosome termini was not included. 10,000 simulations were performed to create the distributions.

To estimate the fraction of missed crossovers, 125 crossovers were randomly distributed amongst chromosomes with a minimum distance of 0kb between them. A cumulative distribution of inter-crossover distances was constructed, ignoring crossover distances that were adjacent to telomeres. The cumulative frequencies were 0.04% at 10kb, 0.15% at 30kb, 0.52% at 107kb, 0.75% at 150kb, and 1% at 200kb.

9.3.8. Chromatid Interference

To detect chromatid interference, I identified 134 chromosome pairs with two crossovers and I asked whether the same two chromatids were less or more likely to be involved in both crossover events compared to random participation. I was unable to reject the null hypothesis of no chromatid interference ($p>0.5$; t-test for proportions), consistent with reports that negative chromatid interference is weak (Hou et al. 2013).

9.3.9. Statistics, Modelling, and Graphics

All statictical analysis, modelling and graphics in this specific aim were performed on the advice of Dr Eva Hoffmann and Professor Alan Handyside and were either performed by them or following their direct instructions. Specifically, Statistical tests and modelling were carried out in Perl or R. All tests were permutation and non-parametric tests, or logistic regression analysis as indicated throughout the manuscript. For logistic regression, the AIC was used to choose the appropriate link function. Binomial distribution of error variances were assessed using the plot (model) function of R. Residual variance and degrees of freedom was tested using chi-square and rejected if below 5%. Two-sided tests were employed, unless otherwise indicated. The lme4, lmPerm, psperman libraries were used in R. Graphics were rendered using the basic functions in R or the ggplot2 library (Wickham 2009).

9.4. Results

9.4.1. MeioMaps of Single Meioses in Oocytes and Embryos

To follow genome-wide recombination and chromosome segregation simultaneously, I recovered all three products of female meiosis, which include the first and second polar bodies (PB1 and PB2) and the corresponding activated oocytes (as described in Specific Aim 5) or fertilised embryos. These are referred to as oocyte-PB or embryo-PB trios (Figure 9.1a-c). 10 embryo-PB trios were obtained after fertilisation of the oocyte following ICSI. The embryos reached various

stages of preimplantation development and originated from a single donor having preimplantation genetic screening for recurrent miscarriage and who consented to follow up genetic analysis of her embryos (Figure 9.1a, Table 9.1).

Table 9.1: Donor Information for Embryos[a] (Ottolini *et al.* 2015)

Donor ID	Age	Oocytes Retrieved	No. Embryos Analysed	Stage of pre-implantation embryo development			Permission to biopsy PBs	No. Embryos Transferred	Live Birth Outcome[d]	Reason for karyomapping
				Cleavage	Morula	Blastocyst				
LB01	38	8	4	2	1	1	no	1	Live birth	PGD for single gene disorder and PGS for advanced maternal age
LB02[b]	35	10	6	2	0	4	no	2	Twin live birth	PGD for single gene disorder
LB03	38	21	10	5	1	4	9[c]	1	None	PGS for recurrent miscarriage
LB04	34	23	8	5	3	0	no	1	None	PGD for paternal translocation
LB05[e]	41	27	10	10	0	0	no	1	Live Birth	PGS for advanced maternal age
		Total:	**38**				**9**	**5**	**3**	

[a] From The Bridge Centre, UK. Diagnostic follow-up in compliance with the code of practice (HFEA)

[b] Donor of the two MII-arrested oocyte-PB1 duos (see Methods)

[c] Corresponding embryo with both polar bodies analysed for MeioMapping

[d] embryo giving rise to live births not mapped

[e] Paternal translocation chromosomes were excluded from the analysis

A further 13 trios were generated following the protocol developed in Specific Aim 5 of this thesis, without fertilisation by activating mature MII-arrested oocytes with a calcium ionophore, which induced completion of MII and extrusion of the PB2 (Figure 9.1b,c). This protocol was highly successful (85%, n=40, Table 9.2) and did not alter the rate of meiosis II errors in the activated oocytes compared to embryos generated by ICSI (six of 299 versus four of 230; Table 9.3) (see also Specific Aim 4). The oocyte-PB trios were obtained from five healthy female donors, who had cryopreserved unfertilised eggs in the course of fertility treatment. Four of the five donors had achieved a pregnancy and live birth following IVF and all five consented to their remaining eggs being activated and undergoing genome analyses. The principle of isolating all three meiotic products is similar to the approach of using the polar bodies and recovering the female pronucleus from zygotes (Hou *et al.* 2013).

Table 9.2: Donor Information for Oocyte-PB Trios (Ottolini *et al.* 2015)

StudyID	oocytes collected	oocytes vitrified	Oocytes used for study	Oocytes after warming	Activated oocytes	Complete trios amplified	Patient age	Pregnancy from cycle	Reason for infertility
G01	10	10	4	4	2	0	37.4	no	idiopathic
G02	6	3	3	3	3	0	36.2	yes	male factor
G03	15	10	10	5	3	0	37.6	yes	male factor
G04*	11	5	5	5	5	3	35.7	no	male factor
G05	11	6	3	3	3	0	37.3	yes	idiopathic
G06*	12	6	6	5	4	4	40.6	yes	male factor
G07*	16	9	6	6	5	1	38.4	yes	tubal
G08*	10	7	5	5	5	3	37.9	yes	endometriosis
G09*	12	fresh	2	2	2	2	33.2	yes	male factor
G10	18	18	3	2	2	0	39.0	no	male factor
			Total:	**40**	**34**	**13**	**37.3**		

* Trios used to generate MeioMaps. Average age: 37.2 years

Table 9.3: Origin and Incidence of Maternal Aneuploidies (Ottolini *et al.* 2015)

				Chromosome mis-segregation events[d]						
Dataset:	**Mean maternal age[a]**	**n[b]**	**% aneuploid oocytes**	**All events**	**Aneuploid outcome in oocyte**	**Gain in oocyte**		**Loss in oocyte**		**Total chr**
						MI	**MII**	**MI**	**MII**	
Oocyte-PB trios	37.3 (33-41)	13	62%	26	12	2	4	4	2	299
Embryo-PB trios	38.3	10	70%	19	8	4	1	0	3	230
Embryo only	37.1 (34-42)	29[c]	54%	n.d.	19	5	4	n.d	n.d.	667

[a] Mean age and range

[b] Number of trios or embryos analysed

[c] 28 embryos and 1 chorionic villus sample

[d] Statistical test for significance of MII nondisjunction rates in oocyte-PB and embryo-PB trios: 6 out of 299 compared to 4 out of 230, respectively, G-test with Williams' correction, p=0.82

n.d. not determined since no information from polar bodies.

The trio datasets were complemented with data on recombination and aneuploidy rates from 29 embryos (without polar bodies) in which SNP genotyping and Karyomapping (Handyside *et al.* 2010) had previously been used for preimplantation genetic diagnosis. Because informative SNPs were available from both the mother and father, I was able to compare recombination in paternal and maternal chromosomes and their association with aneuploidy in embryos (Table 9.4).

Table 9.4: Recombination Frequencies in Embryos (Ottolini *et al.* 2015)

EMBRYO ID	Donor	Embryo Ref	Type	Event	Sex	Chr 1	Chr 2	Chr 3	Chr 4	Chr 5	Chr 6	Chr 7	Chr 8	Chr 9	Chr 10	Chr 11	Chr 12	Chr 13	Chr 14	Chr 15	Chr 16	Chr 17	Chr 18	Chr 19	Chr 20	Chr21	Chr 22	Chr X	Chr Y	Total
1	LB02	*1.1	Embryo	Recombination	Mother	4	2	3	1	3	2	2	2	2	3	2	2	2	1	3	2	1	2	3	2		2	1	NA	47
1	LB02	*1.1	Embryo	Recombination	Father	2	0	2	1	2	2	0	1	0	2	2	1	2	1	0	0	1	0	2	0	1	0	NA	0	22
2	LB02	*1.2	Embryo	Recombination	Mother	4	2	3	1	3	2	2	2	2	3	2	2	2	1	3	2	1	2	3	2	0	2	1	NA	47
2	LB02	*1.2	Embryo	Recombination	Father	2	0	2	1	2	2	0	1	0	2	2	1	2	1	0	0	1	0	2	0	1	0	NA	0	22
3	LB02	2	Embryo	Recombination	Mother	7	2	1	2	1	3	4	5	3	1	0	3	2	1	2	2	1	1	1	2	0	0	2	NA	46
3	LB02	2	Embryo	Recombination	Father	2	2	0	1	2	1	2	1	0	2	1	1	1	1	1	2	2	0	1	2	1	1	NA	0	27
4	LB02	3	Embryo	Recombination	Mother	2	1	2	1	2	2	3	2	2	2	1	1	1	4	3	1	1	0		0	0	0	1	NA	32
4	LB02	3	Embryo	Recombination	Father	NA	NA	NA	NA	NA	NA	NA	NA	NA	NA	NA	NA	NA	NA	NA	NA	NA	NA	NA	NA	NA	NA	NA	0	0
5	LB02	4	Embryo	Recombination	Mother	4	1	3	3	1	5	2	2	2	2	3	1	3	1	2	2	2	2	2	2	1	2	4	NA	52
5	LB02	4	Embryo	Recombination	Father	1	2	2	0	2	2	2	2	1	0	2	1	2	1	1	2	2	0	2	0	0	0	0		27
6	LB02	*5.1	Embryo	Recombination	Mother	0	5	4	2	1	3	1	0	3	3	3	3	2	1	1	1	1	1	0	2	1	0	4	NA	42
6	LB02	*5.1	Embryo	Recombination	Father	3	2	2	3	3		2	1	2	1	2	1	1	2	1	2	1	1	1	3	1	1	0	0	36
7	LB02	6	Embryo	Recombination	Mother	4	1	4	4	2	2	0	4	0	1	2	2	0	2	2	0	1	2	1	2	0	1	1	NA	38
7	LB02	6	Embryo	Recombination	Father	3	2	1	1	4	0	1	0	1	3	1	3	1	1		1	2	0	1	2	1	2	0	0	31
8	LB02	7	Embryo	Recombination	Mother	1	3	5	2	2	2	1	0	3	1	2	3	0	1	0	0	2	2	1	2	0	0	1	NA	34
8	LB02	7	Embryo	Recombination	Father	3	3	0	0	0	3	2	3	1	1	2	2	1	1	1	2	1	0	1	1	1	1	0	0	30

					Sex	Chr 1	Chr 2	Chr 3	Chr 4	Chr 5	Chr 6	Chr 7	Chr 8	Chr 9	Chr 10	Chr 11	Chr 12	Chr 13	Chr 14	Chr 15	Chr 16	Chr 17	Chr 18	Chr 19	Chr 20	Chr21	Chr 22	Chr X	Chr Y	Total
9	LB01		Daughter	Recombination	Mother	6	4	4	2	4	4	1	1	1	4	5	3	2	1	2	0	3	0	1	0	0	0	3	NA	51
9	LB01		Daughter	Recombination	Father	2	3	1	2	0	2	2	1	0	2	3	2	1	1	2	1	2	2	0	0	1	1	0	0	31
10	LB01	CVS	CVS	Recombination	Mother	7	1	4	0	1	2	3	1	0	3	4	0	1	1	1	2	3	1	2	2	0	1	4	NA	44
10	LB01	CVS	CVS	Recombination	Father	2	3	1	2	0	2	2	1	0	2	3	2	1	1	2	1	2	2	0	0	1	1	0	0	31
11	LB01	*2.1	Embryo	Recombination	Mother	4	4	2	6	4	5	4	2	2	0	1	3	1	2	1	2	1	1	1	1	0	1	3	NA	51
11	LB01	*2.1	Embryo	Recombination	Father	2	2	0	1	0	1	1	1	1	1	0	1	0	1	0	2	1	0	1	1	0	0	0	0	17
12	LB01	*2.2	Embryo	Recombination	Mother	4	4	2	6	4	5	4	2	2	0	1	3	1	2	1	2	1	1	1	1		1	3	NA	51
12	LB01	*2.2	Embryo	Recombination	Father	2	2	0	1	0	1	1	1	1	1	0	1	0	1	0	2	1	0	1	1	0	0	0	0	17
13	LB01	*3.1	Embryo	Recombination	Mother	8	3	4	2	2	4	1	4	1	5	2	5	3	2		2	3	2	1	2	2	0	2	NA	60
13	LB01	*3.1	Embryo	Recombination	Father	4	3	3	1	2	2		2	1	2	2	2	2	2	1	1	1	2	0	1	1	0	0	0	35
16	LB01	*3.2	Embryo	Recombination	Mother	8	3	4	2	2	4	1	4	1	5	2	5	3	2		2	3	2	1	2	2	0	2	NA	60
16	LB01	*3.2	Embryo	Recombination	Father	4	3	3	1	2	2		2	1	2	2	2	2	2	1	1	1	2	0	1	1	0	0	0	35
14	LB01	4	Embryo	Recombination	Mother	5	4	3	2	2	0	2	3	2	3	2	1	1	1	1	0	1	1	1	1	1	1	0	NA	38
14	LB01	4	Embryo	Recombination	Father	2	2	1	3	2	1	2	1	3	2	2	1	0	2	1	1	1	1	2	1	0	1	0	0	32
15	LB01	5	Embryo	Recombination	Mother	6	5	2	5	5	1	2	2	3	4	2	3	0	2	3	1	1	3	0	0	1		3	NA	54
15	LB01	5	Embryo	Recombination	Father	1	1	2	1	3	0	1	2	0	2	2	1	1	0	1	1	1	1	1	1	1	1	0	0	25
17	LB03	2	Embryo	Recombination	Mother	2	3	2	4	3	2	3	1	0	3	3	1	2	1	0	1	0	3	2	1	1	1	3	NA	42
17	LB03	2	Embryo	Recombination	Father	2	2	1	1	1	1	0	1	0	2	2	0	2	0	1	1	0	0	1	1	0	0	0	0	19
18	LB03	5	Embryo	Recombination	Mother	7	2	3	5	0	3	1	3	3	1	0	3	1	2	1	2	3	3	2	0		1	1	NA	47

					Sex	Chr 1	Chr 2	Chr 3	Chr 4	Chr 5	Chr 6	Chr 7	Chr 8	Chr 9	Chr 10	Chr 11	Chr 12	Chr 13	Chr 14	Chr 15	Chr 16	Chr 17	Chr 18	Chr 19	Chr 20	Chr21	Chr 22	Chr X	Chr Y	Total
18	LB03	5	Embryo	Recombination	Father	2	0	2	1	1	2	3	1	1	2	1	1	0	0	2	2	0	0	0	2	0	0	0	0	23
19	LB03	6	Embryo	Recombination	Mother	3	3	NA	NA	NA	NA	NA	NA	NA	NA	NA	NA	NA	NA	NA	NA	NA	NA	NA	NA	NA	NA	NA	NA	6
19	LB03	6	Embryo	Recombination	Father	2	1		1	2	1	1		1	2		2	1	2	2	2	2	2	2	2	1	1		0	30
20	LB03	7	Embryo	Recombination	Mother	2	2	3	3	3	3		1	2	2		2	1	1	2	2	2	0	0	1	1		2	NA	35
20	LB03	7	Embryo	Recombination	Father	0	0	2	2	2	1	2	1	0	0	2	2	2	1	1	1	1	1	0	0	1	1	0	0	23
21	LB03	8	Embryo	Recombination	Mother	3	4	2	3	3	3	2	4	3	3	0	1	2	2	0	2	3	1	1	3	1	1	3	NA	50
21	LB03	8	Embryo	Recombination	Father	3	0	3	0	2	1	2	1	0	2	1	2	0	0	0	1	1	0	0	2	1	0	0	0	22
22	LB03	10	Embryo	Recombination	Mother	2	0	5	3	2	0	3	1	2	1	2	1	1	1	2	1	2	2	0	2	1	0	3	NA	37
22	LB03	10	Embryo	Recombination	Father	3	0	2	1	1	1	1	0	1	1	1	1	2	0	0	2	2	2	1	1	1	0		0	24
23	LB03	11	Embryo	Recombination	Mother	1	2	4	4	2	0	2	0	1	1	1	3	0	2	1	2	0	0	0	1	2	1	1	NA	31
23	LB03	11	Embryo	Recombination	Father	3	2	1	1	1	2	0	1	1	2	0	0	1	1	0	1	1	1	0	0	0	0	0	0	19
24	LB03	12	Embryo	Recombination	Mother	5	4	4	6	5	3	7	4	6	3	2	4	0	1	3	3	1	4	1	0	2	1	2	NA	71
24	LB03	12	Embryo	Recombination	Father	1	3	3	2	1	1	1	3	1	1	1	1	2	1	1	1	0	2	2	0	0	0	0	0	28
25	LB03	14	Embryo	Recombination	Mother	4	5	2	4	3	1	3	1	1	2	3	3	3	3	1	3	1	2		0	1	0	1	NA	47
25	LB03	14	Embryo	Recombination	Father	1	3	3	2	3	1	1	0	3	1	1	2	1	1	1	1	1	1	0	1	0	0	0	0	28
26	LB03	16	Embryo	Recombination	Mother	3	3	3	1	2	2	4	1	1	1	1	1	1	2	3	1	2	2	0	2		0	0	NA	36
26	LB03	16	Embryo	Recombination	Father	2	2	1	0	2	1	2	1	1	3	0	1	1	0	1	1	1	1	3	2	0	1	0	0	27
27	LB04	1	Embryo	Recombination	Mother	3	2	2	4	2	0	3	0	1	2	1	2	2	1	2	1	2	1	0	0	0	0	0	NA	31
27	LB04	1	Embryo	Recombination	Father	2	3	1	1	0	0	2	2	1	0	1	2	1	0	2	1	0	1	0	2	1	1	0	0	24

					Sex	Chr 1	Chr 2	Chr 3	Chr 4	Chr 5	Chr 6	Chr 7	Chr 8	Chr 9	Chr 10	Chr 11	Chr 12	Chr 13	Chr 14	Chr 15	Chr 16	Chr 17	Chr 18	Chr 19	Chr 20	Chr21	Chr 22	Chr X	Chr Y	Total
28	LB04	2	Embryo	Recombination	Mother	5	3	3	3	3	2	3	1	1	2	3	2	0	2	2		1	2	0	1			1	NA	40
28	LB04	2	Embryo	Recombination	Father	3	4	3	2	2	1	1	1	1	2	1	1	1	1	2	0	0	1	1	1	1	2	0	0	32
29	LB04	3	Embryo	Recombination	Mother	5	2	6	1	2	1	4	2	3	4	0	3	1	4	3	2	2	1	0	1	2	1	1	NA	51
29	LB04	3	Embryo	Recombination	Father	1	3	2	0	2	1	1	1	0	1	1	2	0	2	1	2	0	0	2	0	0	2	0	0	24
34	LB04	4	Embryo	Recombination	Mother	2	4	3	1	0	3	2	3	4	3	1	0	1	1	0	1	2	1	0	2	1	0	1	NA	36
34	LB04	4	Embryo	Recombination	Father	1	1	1	1	1	0	1	2	0	0	2	2	1	0	0	1	1	1	0	0	0	2	0	0	18
30	LB04	5	Embryo	Recombination	Mother	2	2	4	4	3	4	4	0	2	1	3	2	2	2	3		1	1	1	1	1	0	1	NA	44
30	LB04	5	Embryo	Recombination	Father	1	1	2	1	2	2	0	2	2	0	2	0	0	2	1	2	0	1	1	0	0	1	0	0	23
31	LB04	6	Embryo	Recombination	Mother	3	1	3	2	0	1	4	2	3	1	2	1	2	0	1	3	1	1	1	1	2	1	4	NA	40
31	LB04	6	Embryo	Recombination	Father	2	3	3	1	0	0	2	0	1	1	1	1	0	1	0	2	2	0	0	1	0	2	0	0	23
32	LB04	7	Embryo	Recombination	Mother	2	3	3	1	2	0	1	2	3	0	1	2	1	1	1	3	3	1	1	0	2	0	3	NA	36
32	LB04	7	Embryo	Recombination	Father	2	0	1	1	1	1	1	0	0	0	2	1	0	0	1	0	0	1	2	1	0	3	0	0	18
33	LB04	8	Embryo	Recombination	Mother	1	4	1	2	2	2	1	2	2	2	3	2	1	2	2	0	2	1	2	2	1	1	0	NA	38
33	LB04	8	Embryo	Recombination	Father	1	2	1	2	3	1	1	0	1	2	2	0	1	2	1	2	1	1	2	1	0	0	0	0	27
35	LB05	1	Embryo	Recombination	Mother	4	0	2	2	3	1	0	2		1	1	2	0	1	1	1	0	0	1	1		0	1	NA	24
35	LB05	1	Embryo	Recombination	Father	2	1	0	2	1	2	2	2	1	1	1	3	2	2	1	1	0	0	1	2	0	0	0	0	27
36	LB05	2	Embryo	Recombination	Mother	5	2	2	3	1	3	3	2	3	2	3	3	1	3	1	0	0	3	0	2	1	1	2	NA	46
36	LB05	2	Embryo	Recombination	Father	2	2	1	1	3	1	2	3	3	1	1	0	1	1	2	1	1	1	1	2	1	0	0	0	31
37	LB05	3	Embryo	Recombination	Mother	2	3	1	2	1	3	0	3	1	0	2	2	1		1	2	3	1	1	1	1	1	1	NA	33

					Sex	Chr 1	Chr 2	Chr 3	Chr 4	Chr 5	Chr 6	Chr 7	Chr 8	Chr 9	Chr 10	Chr 11	Chr 12	Chr 13	Chr 14	Chr 15	Chr 16	Chr 17	Chr 18	Chr 19	Chr 20	Chr21	Chr 22	Chr X	Chr Y	Total
37	LB05	3	Embryo	Recombination	Father	1	3	1	2	1	1	0	2	1	1	1	1	2	1	2	2	1	0	2	1	1	0	0	0	27
38	LB05	4	Embryo	Recombination	Mother	0		0	0	0		0					0	0		0	0			0	0				NA	0
38	LB05	4	Embryo	Recombination	Father	4	1	1	1	0	2	1	0	0	1	2	0	0	1	1	1	0	2	0	1	0	1	0	0	20
39	LB05	5	Embryo	Recombination	Mother	NA	NA	NA	NA	NA	NA	NA	NA	NA	NA	NA	NA	NA	NA	NA	NA	NA	NA	NA	NA	NA	NA	NA	NA	0
39	LB05	5	Embryo	Recombination	Father	1	0	3	0	2	1	1	2	1	2	1	1	1	1	1	1	1	1	1	0	1	1	0	0	24
40	LB05	6	Embryo	Recombination	Mother	4	3	2	4	3	3	5	1	1	1	2	0	3	1	1	3	0	1	2	2	0	1	0	NA	43
40	LB05	6	Embryo	Recombination	Father	1	1	2	0	2	0	2	2	1	1	1	2	1	1	0	1	1	1	2	0	0	0	0	0	22
41	LB05	7	Embryo	Recombination	Mother	3	3	3	2	2	4	3	3	3	2	3	1	1	1	3	3	1	1	0	2	0	1	2	NA	47
41	LB05	7	Embryo	Recombination	Father	2	1	0	1	0	0	2	0	0	2	0	2	1	0	0	2	0	0	1	0	1	1	0	0	16
42	LB05	8	Embryo	Recombination	Mother	3	4	2	5	4	4	3	3	3	1	2	4	2	1	1	2	2	1	1	0	1	2	1	NA	52
42	LB05	8	Embryo	Recombination	Father	1	0	1	0	0	1	1	1	0	0	1	1	0	1	0	2	1	0	2	1	0	0	0	0	14
43	LB05	9	Embryo	Recombination	Mother	4	4	1	3	2	2	1	4	0	4	1	1	2	0	1	3	0	1	2	1	0	2	4	NA	43
43	LB05	9	Embryo	Recombination	Father	1	3	1	1	2	2	1	0	2	1	0	1	0	1		2	0	0	0	1	0	1	0	0	20
44	LB05	10	Embryo	Recombination	Mother	3	5	3	1	4	3	2	2	1	1	2	3	2	2		2	0	2	2	1	1	1	1	NA	44
44	LB05	10	Embryo	Recombination	Father	3	1	2	2	1	0	2	1	2	1	0	0	1	1	2	1	1	0	0	1	0	1	0	0	23
Combined Recombination						242	154	157	133	130	116	120	103	94	120	108	118	78	86	82	91	87	76	63	73	43	44	63	0	2,339
N			sex combined			86	86	85	85	85	85	85	85	85	85	85	85	85	85	85	85	85	85	85	85	85	85	82	44	
Population-average CO/chr			sex combined			2.81	1.79	1.85	1.56	1.53	1.36	1.41	1.21	1.11	1.41	1.27	1.39	0.92	1.01	0.96	1.07	1.02	0.89	0.74	0.86	0.51	0.52	0.77	0.00	36.08
N			Maternal			43	43	42	42	42	42	42	42	42	42	42	42	42	42	42	42	42	42	42	42	42	42	42	0	

		Sex	Chr 1	Chr 2	Chr 3	Chr 4	Chr 5	Chr 6	Chr 7	Chr 8	Chr 9	Chr 10	Chr 11	Chr 12	Chr 13	Chr 14	Chr 15	Chr 16	Chr 17	Chr 18	Chr 19	Chr 20	Chr21	Chr 22	Chr X	Chr Y	Total
N	Paternal		43	43	43	43	43	43	43	43	43	43	43	43	43	43	43	43	43	43	43	43	43	43	40	44	
Population-average CO/chr	Maternal		3.65	2.74	2.83	2.71	2.29	2.36	2.31	2.00	1.88	2.00	1.81	2.12	1.36	1.48	1.45	1.52	1.43	1.40	0.93	1.21	0.71	0.67	1.76	NA	85.57
Population-average CO/chr	Paternal		1.98	1.70	1.49	1.14	1.47	1.14	1.26	1.16	0.88	1.35	1.28	1.26	0.98	0.98	0.88	1.30	0.91	0.74	0.98	0.93	0.49	0.70	0.00	0.00	51.14
Hou *et al.* (2013)	Maternal		5.72	5.44	4.76	4.44	4.21	4.03	3.65	3.56	3.32	3.68	3.26	3.46	2.50	2.37	2.37	2.79	2.65	2.60	2.26	2.21	1.32	1.31	3.04	-	74.96
Gruhn *et al.*	Oocyte	Mlh1 foci	5.9 ± 0.18	NA	NA	NA	NA	3.7 ± 0.19	NA	NA	2.8 ± 0.05	NA	NA	NA	2.6 ± 0.07	2.2 ± 0.1	2.3 ± 0.15	2.5 ± 0.07	NA	2.3 ± 0.07	NA	NA	1.2 ± 0.03	1.4 ± 0.04	NA	NA	69± 0.29
	Sperm	Mlh1 foci	3.7 ± 0.06	NA	NA	NA	NA	2.6± 0.05	NA	NA	2.5 ± 0.08	NA	NA	NA	1.9 ± 0.03	1.9 ± 0.04	2.0 ± 0.03	2.0 ± 0.02	NA	1.8 ± 0.03	NA	NA	1.0 ± 0.01	1.2 ± 0.02	NA	NA	49 ± 0.07

* More than one sample per embryo analysed. Key below.

NA Not applicable or not available

Non-recombinant (R0)

Monosomy

Trisomy- maternal

Trisomy- paternal

All samples were amplified by whole genome amplification and genotyped at ~300,000 SNP loci genome-wide (Handyside *et al.* 2010). Across the 23 complete trios (meioses), >4 million informative SNPs were detected at high stringency with an average resolution of 30kb. The SNPs spanned >92% of the genome. For the oocyte-PB trios, genomic DNA from each donor was also genotyped to identify informative heterozygous SNP loci (hetSNPs). For the oocyte-PB trios, all hetSNPs in the mother's genomic DNA are informative, whereas in embryos, maternal and paternal hetSNPs may be shared. Hence, the pattern of recombination in the paternal chromosomes was analysed by Karyomapping (Handyside *et al.* 2010; Natesan *et al.* 2014) and only the two subsets of SNP loci which were heterozygous in the father and homozygous in the mother (or vice versa) were identified and used to phase the two haplotypes from the given parent in the embryo (Handyside *et al.* 2010; Natesan *et al.* 2014). The informative SNPs were phased using 'siblings' (Hou *et al.* 2013) that contain only a single chromatid from their mother (PB2, oocytes or maternal chromatid in embryo) or father (embryos). The informative SNPs were phased by selecting a PB2 or oocyte/embryo as a reference (also known as 'assumed ancestor') (Hou *et al.* 2013) and inferring the crossover positions in the assumed offspring (i.e. trios from the same parent; Figure 9.2). Crossovers in the same position in the assumed offspring are highly unlikely to occur and these common crossovers can therefore be used to re-form the reference genome from which the two haplotypes can be deduced as described in Specific Aim 5 (Figure 9.2). Since many of the samples were single cells, the workflow was validated by comparing recombination maps in 15 individual cells from a donor to the genomic DNA of the child, and by assessing 10 individual blastomeres from the same embryo for direct comparison. In all cases, concordance of recombination frequencies and their positions was >99%.

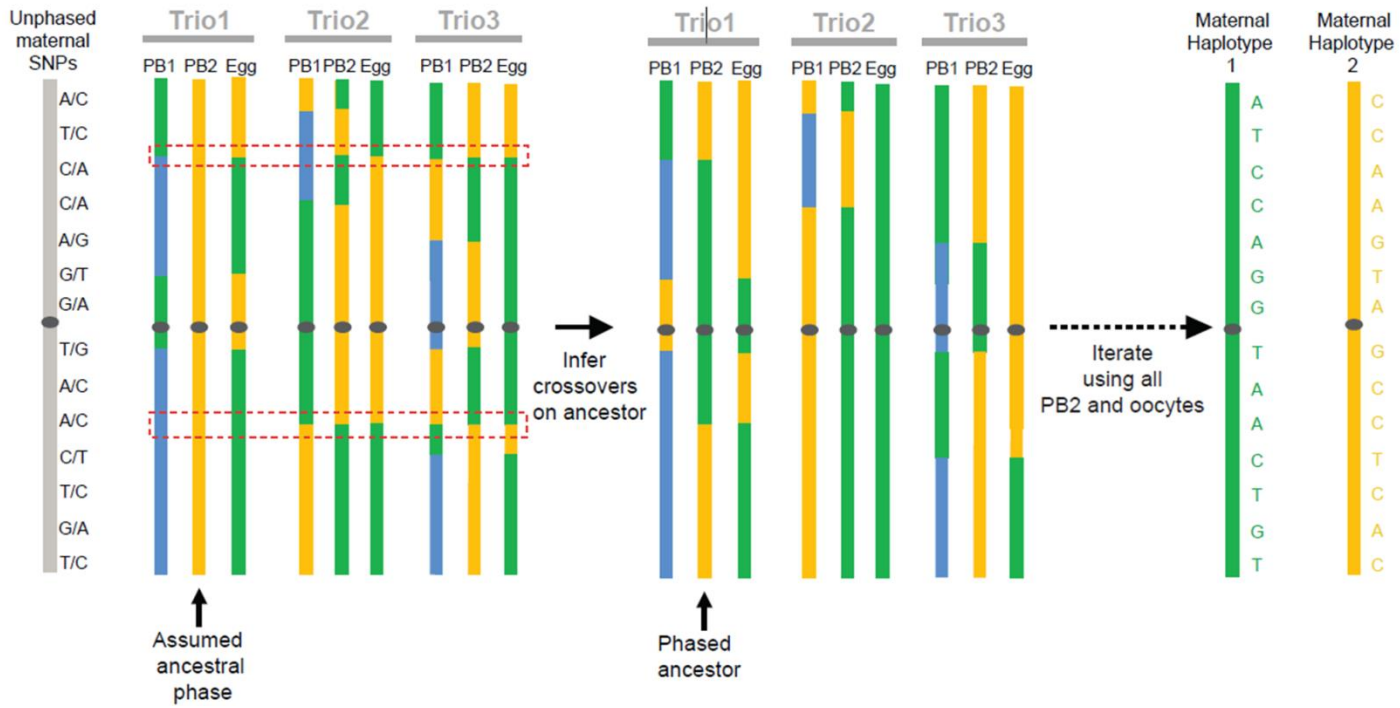

Figure 9.2. Phasing of maternal haplotypes (Ottolini *et al.* 2015).

Informative SNPs are phased using the assumed ancestor method (Hou *et al.* 2013). A haploid cell containing a single chromatid (1C; either PB2 or Egg) is chosen as the 'assumed ancestor', also known as the reference. Trios from the same mother (or embryos from the same father) are 'assumed offspring'. Using the reference, crossovers in all other assumed offspring are mapped where haplotypes change in comparison to the assumed ancestral phasing. Crossovers shared by sibling trios (or assumed offspring; red boxes) can be used to infer crossovers in the assumed ancestor. Iterative phasing using all available oocytes and PB2 allows deduction of the maternal haplotypes.

A typical MeioMap from a normal embryo-PB trio is shown in Figure 9.1d. MeioMaps reveal Mendelian segregation of sequence polymorphisms (green and yellow segregate 2:2 across haplotype regions) and independent assortment of different chromosomes in meiosis I (pericentromeric SNPs are used as a chromosome's fingerprint). Crossovers, which result in recombinant chromosomes, are evident by transitions between the two maternal haplotypes (green or yellow) in the PB2 and oocyte, or between a single maternal haplotype and heterozygous regions (PB1). 39 cases of aneuploidy were detected by the absence or presence of SNPs from an entire chromosome (Table 9.3). The inferred chromosomal aneuploidies can be observed by array CGH (Figure 9.3). I also detected three gross structural rearrangements to chromosomes. Since two of the three meiotic products were affected (reciprocal gain and loss), it rules out that these rearrangements occurred during germline development and demonstrates that such rearrangements can occur during meiosis (Table 9.5). Aneuploidy rates and the contribution of MI and MII errors were similar to those expected for this age range (33-41 years; Table 9.3) (Alfarawati *et al.* 2011; Gutierrez-Mateo *et al.* 2011; Kuliev *et al.* 2011; Capalbo *et al.* 2013; Franasiak *et al.* 2014).

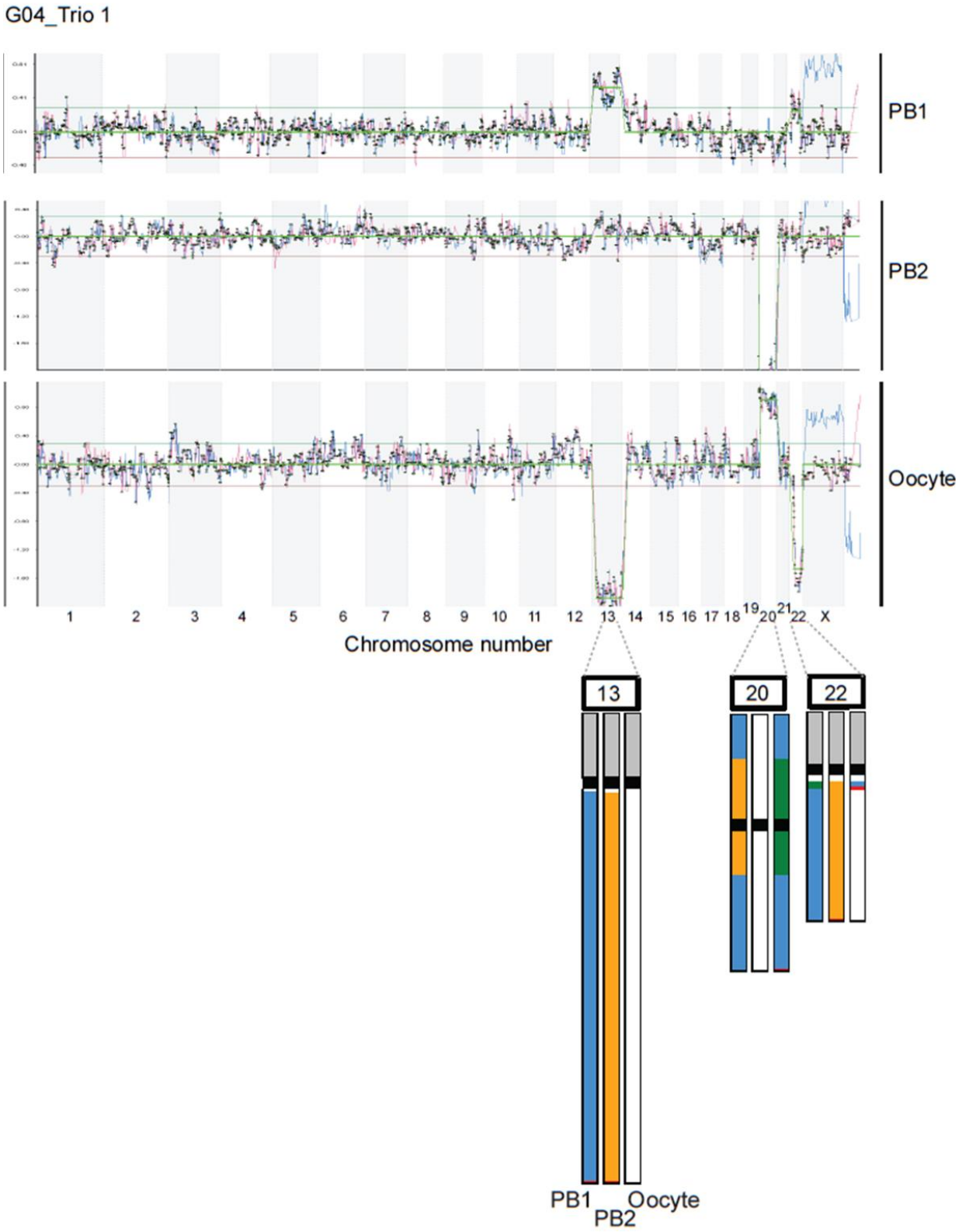

Figure 9.3. Validation of whole-chromosome aneuploidy by aCGH (Ottolini *et al.* 2015).

An example of chromosome segregation abnormalities inferred from the SNP array patterns in oocyte-PB trios and confirmed by aCGH of the same amplified DNA from all three samples. In the

aCGH output, the green and pink lines are the internal female samples and the blue trace indicates the male reference. The log2 ratios of the X chromosomes of the reference genomes are used for internal calibration of whole-chromosome loss or gain. The MeioMaps for three chromosomes in the same oocyte-PB trio are shown below the aCGH traces (G04_1). For chromosome 13, three chromatids segregated to the first polar body, and a single chromatid was present in the second polar body and missing in the oocyte. This is consistent with precocious separation of sister chromatids (PSSC) at meiosis I. Chromosome 20 segregated normally at meiosis I (normal PB1), but there was a gain in the oocyte and a corresponding loss in the PB2, consistent with meiosis II nondisjunction. Chromosome 22 underwent a partial gain in PB1 and a corresponding loss in the oocyte. This is consistent with a gross structural rearrangement whereby the majority of chromosome 22 segregated to the PB1 along with the intact homolog (Table 9.5). In the SNP representations, yellow and green blocks represent the two different grandparental haplotypes and blue blocks denote regions where both haplotypes are present. All aneuploidies in the oocyte-PB trio data set were verified using aCGH. Validation for embryos has been published previously (Natesan *et al.* 2014).

Table 9.5: Gross Structural Rearrangements in Meiosis Detected by MeioMapping (Ottolini *et al.* 2015)

Donor ID	Chromosome	Breakpoint position (Mb)	Description
G04_1	22q	18.6 Mb	Loss of large section of q-arm in oocyte, reciprocal gain in PB1
G04_3	8p	9.6 Mb	Gain of small region at p-Ter in oocyte, reciprocal loss in PB1
G09_2	15q	44.1 Mb	Gain of region of q-arm in oocyte, reciprocal loss in PB1
LB03_13	4q	83.07 Mb	Deletion of large region in PB2 only

All gains and losses were reciprocal and involved two meiotic products, such that a gain in the oocyte was matched by the loss of the chromosome in the PB1 or PB2. Of the 529 chromosome pairs assessed in the trios, I did not detect any deviation from the four chromatids expected to participate in meiosis. These observations firmly establish meiotic errors as the main contributor of aneuploid conceptions and do not support germline mosaicism in chromosome number prior to meiosis (Hulten *et al.* 2010) as a significant factor in the maternal age-related increase in human trisomies.

9.4.2. A Novel, Reverse Segregation Pattern in Human Meiosis

To understand the nature of mis-segregation, I inferred chromosome segregation from the trios by following the informative SNPs at the pericentromere. Trisomies that occur at a high rate in the natural population of women of advanced maternal age (Hassold & Jacobs 1984) were originally hypothesised to arise by MI nondisjunction (MI NDJ) where both homologs segregate to the oocyte at meiosis I, followed by a normal second division (Reiger, Michaelis *et al.* 1968) (Figure 9.4a; Figure 9.5a). However, cytological examination of human oocytes that failed to fertilise in IVF clinics suggested that PSSC was the major cause of human age-related trisomies (Angell 1991), at least in a clinical setting (Figure 9.4a; Figure 9.5b). Having the genetic identity of the chromatids not only from the embryos or oocytes but also their matched polar bodies allows the two segregation patterns to be distinguished, because the chromosome signatures in the two

PBs will differ (Figure 9.4a). Confirming previous studies using array CGH for copy number analysis in trios (Handyside *et al.* 2012), classical meiosis I nondisjunction was relatively rare and precocious separation of sister chromatids was more frequent, at least in stimulated IVF-treated patients (Figure 9.4a-c). The preponderance of PSSC compared to meiosis I nondisjunction is consistent with findings in oocytes from younger Chinese donors, although aneuploidy rates are much lower in this age group (Figure 9.4b) (Hou *et al.* 2013).

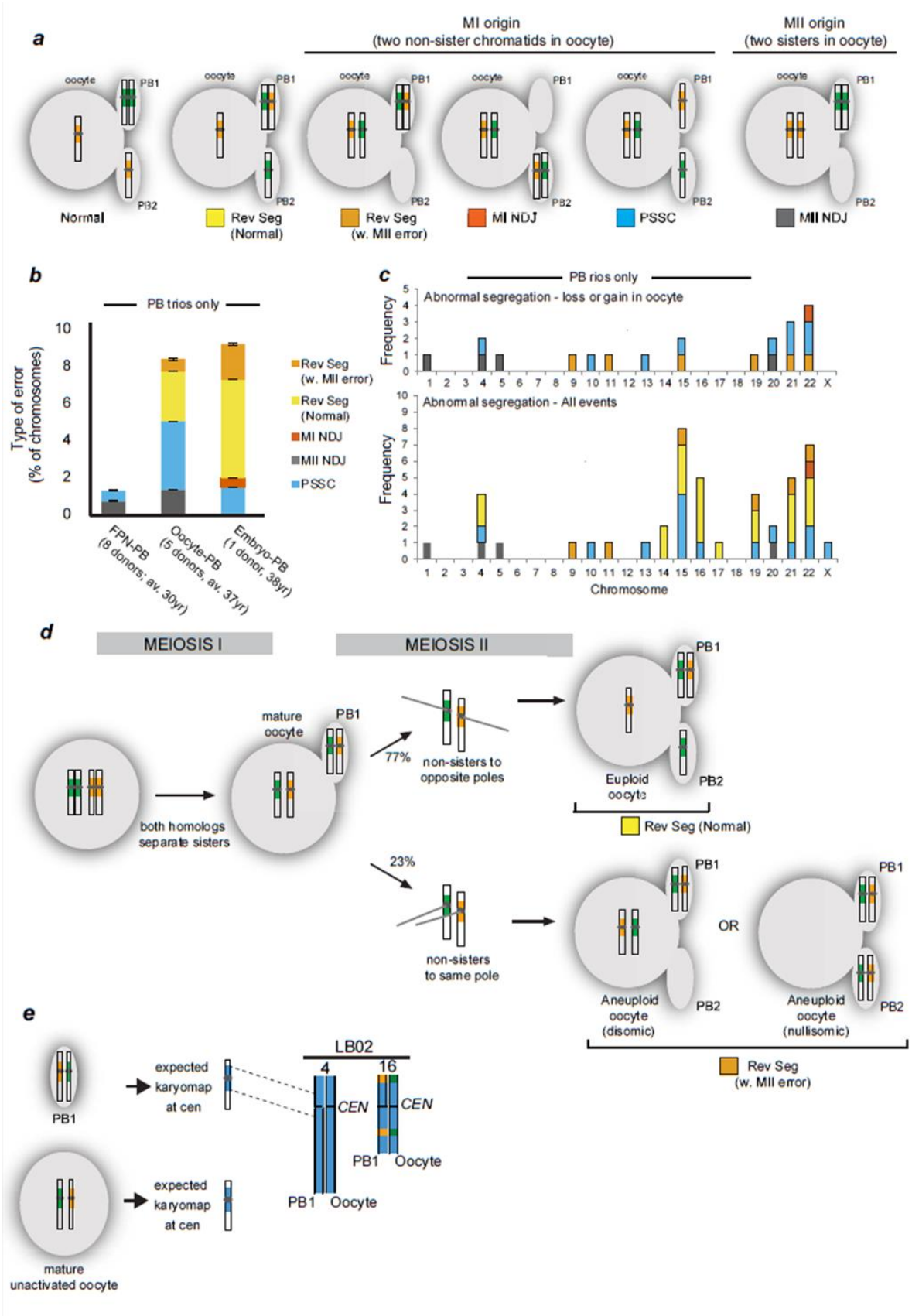

Figure 9.4. MeioMaps reveal origin of aneuploidies and a novel chromosome segregation pattern (Ottolini *et al.* 2015).

(*a*) Segregation patterns revealed from following the pericentromeric haplotypes (yellow and green around centromere) in all three products of female meiosis. Only examples leading to trisomic conceptions are shown. For all possible segregation patterns detected by MeioMapping see Figure 9.5. MI NDJ: meiosis I nondisjunction; Rev Seg reverse segregation; PSSC: precocious separation of sister chromatids; MII NDJ: meiosis II nondisjunction.

(*b*) Incidence and type of segregation errors in oocyte-PB and embryo-PB trios. Errors detected in MeioMaps generated from the female pronucleus (FPN-PB) from a younger donor population (Hou, Fan *et al.* 2013) are shown for comparison. The number of donors and average (av.) age are shown. Age ranges were 25-35 for FPN-PB (Hou *et al.* 2013) and 33-41 for oocyte-PB trios. The embryo donor was 38 years (Table 9.1 and 9.2). Bars: standard error of a proportion.

(*c*) Chromosome abnormalities resulting in aneuploid oocytes or embryos (upper panel) and all non-canonical segregation patterns (lower panel).

(*d*) Inferred mode of reverse segregation (Rev Seg). Frequencies are shown in Table 9.6. Alternative segregation outcomes at meiosis II (euploid and aneuploid, n=26; $p<0.025$; binomial exact test with correction for continuity).

(e) Detection of the inferred intermediate of reverse segregation, a mature oocyte and PB1 containing two non-sister chromatids each. Two mature oocytes that contained a PB1 but were unactivated were biopsied and the SNPs detected genome-wide. The expected chromosome fingerprints that contained heterozygous SNPs around the centromeres are shown in blue. Two examples were found in this egg (chromosomes 4 and 16; Table 9.6).

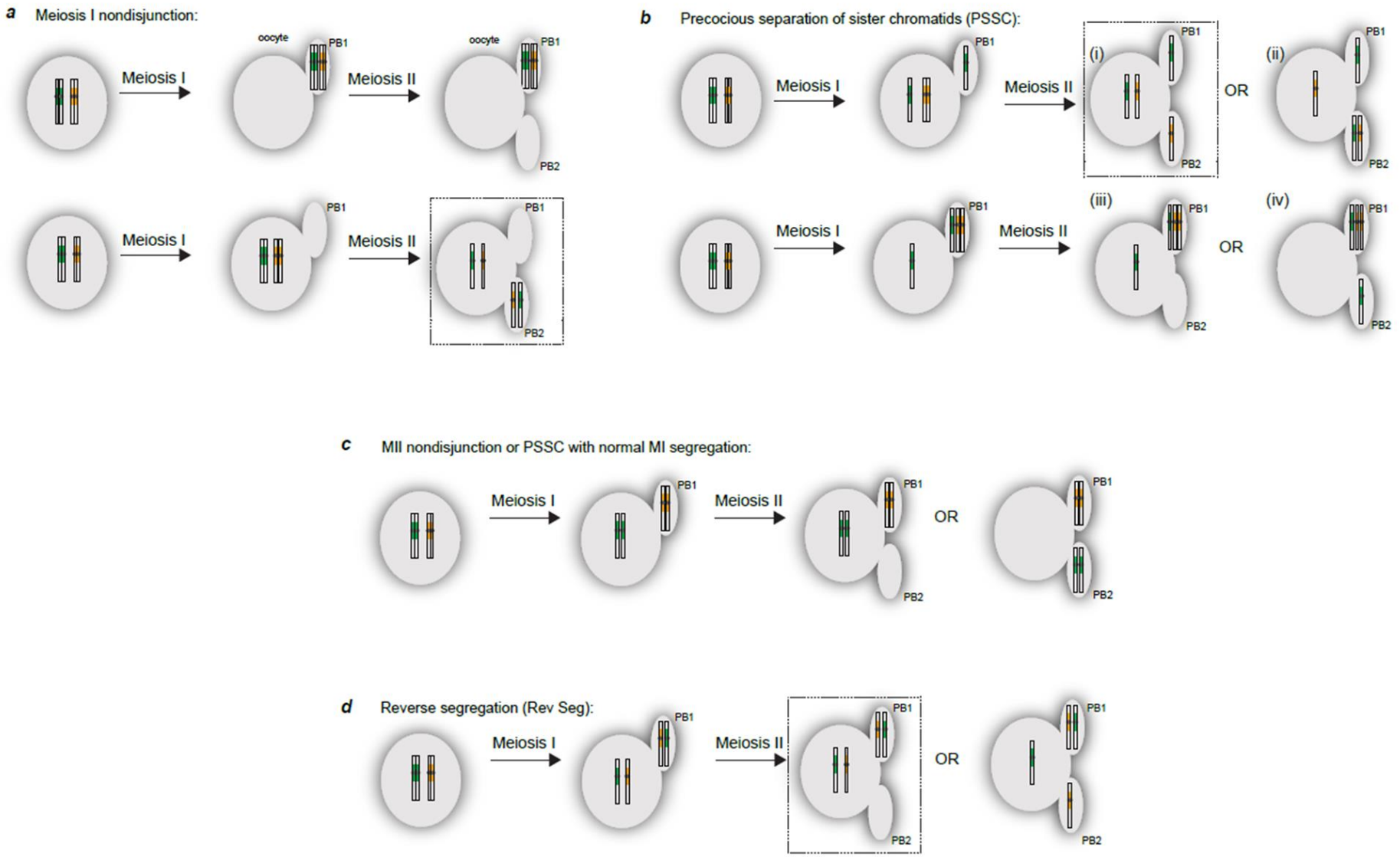

Figure 9.5. Non-canonical segregation patterns (Ottolini *et al.* 2015).

(a) Meiosis I nondisjunction yields a PB1 containing all four chromatids and an empty oocyte and PB2 (top) or an empty first polar body and two non-sister chromatids in the oocyte and PB2 (bottom).

(b) PSSC has four possible segregation outcomes (i–iv). The green homolog has separated precociously at meiosis I, and the yellow homolog segregates normally either to the oocyte (top) or the PB1 (bottom). At meiosis II, the green chromatid segregates randomly to the oocyte (i) and (iii), or to the PB2 (ii) and (iv). Note that one of the nine PSSC events involved a structural change in combination with the precocious separation of the sister chromatids in meiosis I.

(c) Meiosis II nondisjunction results in two sister chromatids in either the oocyte or PB2 (shown for green only). This pattern could also arise from an earlier PSSC event, where the two sister chromatids have come apart and both stay in the oocyte at meiosis I.

(d) Reverse segregation. Both homologs segregate their sister chromatids at meiosis I, giving rise to an intermediate where both the oocyte and PB1 contain the correct content but two non-sister chromatids (Figure 9.4e). At meiosis II, the two non-sister chromatids either segregate into the PB2 and oocyte, remain in the oocyte or both segregate to the PB2 (Figure 9.4d). Dotted boxes highlight three different segregation errors that would give rise to the same pattern of maternal pericentromeric SNPs in a trisomic conception (i.e. two non-sister chromatids). Without the information from the polar bodies, these three patterns are indistinguishable.

Unexpectedly, the most frequent non-canonical segregation pattern gave rise to a PB1 that contained two non-sister chromatids (green and yellow fingerprints around the centromere, n=26). In 20 of the 26 instances, both the oocyte and the PB2 contained a normal chromosome content, but with non-sisters instead of sister chromatids (Figure 9.4a, Rev Seg). This pattern cannot be detected by copy number analysis used previously (Handyside *et al.* 2012), since the complement of chromosomes in the three cells is normal. I refer to this novel pattern as reverse segregation, since I infer that sister chromatids of both homologs separated first in meiosis I, followed by non-sister chromatids in meiosis II (Figure 9.4d). The equational division at MI is unlikely to be the result of two independent PSSC events, because the observed frequency of both homologs separating their sister chromatids is more than 100× greater than the predicted frequency based on two independent PSSC events ($p<0.001$). Consistent with equational divisions of both homologs at meiosis I, I observed the predicted intermediate of reverse segregation, a mature oocyte and PB1 that contain two non-sister chromatids (Figure 9.4e; Table 9.6). Both acrocentric and larger metacentric chromosomes displayed this reverse segregation pattern (Figure 9.4c; Table 9.6), which was observed in all donors, ruling out that it was specific to certain women (Table 9.7). In the remaining six cases, the two non-sister chromatids mis-segregated into the egg or the PB2, resulting in an aneuploid oocyte (Figure 9.4a, Rev Seg w. MII; Figure 9.5d). In summary, I have observed a novel segregation pattern where both homologs undergo an equational division at meiosis I, followed by a weak preference for accurate disjunction of the two non-sister chromatids at meiosis II. This is reminiscent of 'inverted meiosis' in organisms with holocentric chromosomes (Viera *et al.* 2009; Cabral *et al.* 2014; Heckmann *et al.* 2014).

Table 9.6: Incidence of Reverse Segregation (Ottolini *et al.* 2015)

Sample type	Incidence	Chromosomes involved
Oocyte-PB1 duos (unactivated)[a]	8.7 ± 4.2% (n=46)	4, 13, 14, 16
Oocyte-PB1-PB2 trios	3.7 ± 1.1% (n=299)	4, 11, 14, 15, 16, 19, 22
Embryo-PB1-PB2 trios	7.2 ± 1.8% (n=207)	4, 9, 16, 17, 19, 21, 22

[a] See Figure 9.4e. Reverse segregation was observed in all donors (Table 9.7).

Table 9.7: Summary of Recombination and Chromosome Segregation in all Trios (Ottolini *et al.* 2015)

Donor	Trio		Chromosome																							Total
			1	2	3	4	5	6	7	8	9	10	11	12	13	14	15	16	17	18	19	20	21	22	X	
Oocyte-PB Trios:																										
G04	3	PB1	6	4	4	3	3	2	3	3	3	3	2	2	0	1	1	3	1	1	2	2	1	1	3	54
		PB2	3	1	3	1	1	1	2	1	2	1	1	3	0	0	0	2	0	0	0	n/a	0	0	3	25
		Egg	3	3	1	2	2	1	1	2	1	2	1	1	n/a	1	1	1	1	1	2	2	1	0	0	30
		Total	6	4	4	3	3	2	3	3	3	3	2	3	0	1	1	3	1	1	2	2	1	1	3	55
G04	4	PB1	6	5	4	3	4	4	3	5	4	2	2	3	2	2	0	2	3	3	3	2	1	1	3	67
		PB2	3	2	1	5	4	2	2	2	4	3	3	2	4	1	0	2	3	4	1	0	0	0	2	50
		Egg	5	7	3	4	2	2	1	5	0	1	3	1	2	1	1	0	0	1	2	2	1	1	3	48
		Total	7	7	4	6	5	4	3	6	4	3	4	3	4	2	1	2	3	4	3	2	1	1	4	83
G04	5	PB1	5	6	5	4	4	5	5	3	4	4	3	4	2	2	3	5	3	2	3	2	1	1	4	80
		PB2	3	5	2	4	2	2	0	1	4	3	3	3	4	0	2	2	2	2	0	0	0	0	3	47
		Egg	2	3	3	n/a	2	5	5	4	0	1	0	1	2	2	3	3	1	2	3	2	1	1	3	49
		Total	5	7	5	4	4	6	5	4	4	4	3	4	4	2	4	5	3	3	3	2	1	1	5	88

Donor	Trio		Chromosome																							Total
			1	2	3	4	5	6	7	8	9	10	11	12	13	14	15	16	17	18	19	20	21	22	X	
G06	1	PB1	4	5	4	0	5	7	2	2	5	2	2	4	3	3	2	2	4	2	3	2	2	1	0	66
		PB2	4	5	3	0	3	3	1	3	4	2	0	2	2	0	0	1	3	2	0	1	1	1	n/a	41
		Egg	0	0	1	n/a	2	4	1	1	1	4	2	2	1	3	2	1	1	0	3	1	1	0	0	31
		Total	4	5	4	0	5	7	2	3	5	4	2	4	3	3	2	2	4	2	3	2	2	1	0	69
G06	2	PB1	6	6	5	5	4	5	3	4	4	5	3	3	4	0	3	3	3	2	2	2	1	2	6	81
		PB2	5	6	4	7	6	2	4	4	3	3	1	1	1	1	2	2	2	3	0	3	1	2	5	68
		Egg	3	4	5	2	6	3	5	2	1	2	2	2	3	1	1	1	1	3	2	1	0	0	1	51
		Total	7	8	7	7	8	5	6	5	4	5	3	3	4	1	3	3	3	4	2	3	1	2	6	100
G06	3	PB1	6	8	6	4	5	4	5	2	3	5	3	4	4	3	2	2	5	2	2	2	1	1	5	79
		PB2	5	4	6	4	2	2	4	1	0	5	0	4	1	3	2	0	3	3	1	0	0	0	1	50
		Egg	3	6	4	4	3	4	1	1	3	2	3	4	3	0	2	2	2	1	1	2	1	1	4	53
		Total	7	9	8	6	5	5	5	2	3	6	3	6	4	3	3	2	5	3	2	2	1	1	5	96
G06	4	PB1	5	6	3	2	4	4	3	3	2	2	3	3	3	1	3	3	2	2	0	2	1	2	2	59
		PB2	2	8	1	3	1	2	0	1	1	3	2	1	2	1	1	1	2	1	1	1	0	1	2	36
		Egg	3	4	2	3	3	2	3	2	3	3	1	2	3	2	2	2	0	1	1	3	1	1	0	47
		Total	5	9	3	4	4	4	3	3	3	4	3	3	4	2	3	3	2	2	1	3	1	2	2	73

Donor	Trio		Chromosome																							Total
			1	2	3	4	5	6	7	8	9	10	11	12	13	14	15	16	17	18	19	20	21	22	X	
G07	2	PB1	3	5	7	4	3	5	2	3	4	5	4	2	1	2	0	3	3	2	2	3	2	1	2	68
		PB2	1	3	3	2	2	2	2	2	2	1	3	1	1	0	n/a	0	2	2	0	2	1	1	2	33
		Egg	2	2	4	2	1	3	0	1	2	4	1	1	0	2	0	3	1	0	2	1	1	0	0	35
		Total	3	5	7	4	3	5	2	3	4	5	4	2	1	2	0	3	3	2	2	3	2	1	2	68
G08	1	PB1	3	3	4	0	2	2	2	2	2	3	2	3	1	2	1	3	1	2	2	2	1	1	2	46
		PB2	2	3	1	4	0	1	1	1	1	1	3	2	1	1	3	1	0	1	1	1	1	0	1	31
		Egg	1	2	3	4	2	1	3	1	1	4	1	1	0	1	2	2	1	3	1	1	0	1	1	37
		Total	3	4	4	4	2	2	3	2	2	4	3	3	1	2	3	3	1	3	2	2	1	1	2	57
G08	2	PB1	4	6	5	4	4	2	2	2	3	3	5	2	2	1	0	3	2	2	2	2	1	1	3	61
		PB2	1	3	2	1	3	3	3	1	2	2	2	1	0	1	n/a	0	3	0	0	1	0	1	4	34
		Egg	3	3	3	3	1	5	1	1	3	1	3	3	2	2	0	3	1	2	2	1	1	2	1	47
		Total	4	6	5	4	4	5	3	2	4	3	5	3	2	2	0	3	3	2	2	2	1	2	4	71
G08	3	PB1	5	2	7	4	6	4	2	2	5	3	3	4	4	2	3	3	3	2	2	2	2	1	2	73
		PB2	n/a	2	3	1	3	1	1	0	3	2	0	2	3	0	1	1	2	1	0	1	1	1	0	29
		Egg	5	2	4	3	3	3	1	2	2	1	3	2	1	2	2	2	1	1	2	1	1	0	2	46
		Total	5	3	7	4	6	4	2	2	5	3	3	4	4	2	3	3	3	2	2	2	2	1	2	74

Donor	Trio		Chromosome																							Total
			1	2	3	4	5	6	7	8	9	10	11	12	13	14	15	16	17	18	19	20	21	22	X	
G09	1	PB1	3	2	3	2	3	2	2	2	2	0	2	1	3	3	1	0	1	1	1	0	1	1	1	37
		PB2	2	2	3	2	3	1	0	1	1	1	2	0	2	1	2	n/a	1	0	1	1	1	1	0	28
		Egg	3	2	2	2	n/a	1	2	1	1	n/a	0	1	2	3	3	0	0	1	0	1	0	0	1	26
		Total	4	3	4	3	3	2	2	2	2	1	2	1	4	4	3	0	1	1	1	1	1	1	1	47
G09	2	PB1	3	4	2	2	5	3	3	2	4	2	3	3	1	1	1	1	2	2	1	3	0	1	2	51
		PB2	1	2	0	1	1	1	2	0	2	0	n/a	1	1	0	0	0	1	1	0	3	0	1	1	19
		Egg	2	2	2	1	4	2	1	2	2	2	3	2	0	1	1	1	1	1	1	0	n/a	0	1	32
		Total	3	4	2	2	5	3	3	2	4	2	3	3	1	1	1	1	2	2	1	3	0	1	2	51
Embryo-PB Trios:																										
LB03	2	PB1	4	6	3	3	2	3	2	3	3	3	3	3	3	2	2	2	1	2	3	2	2	1	3	61
		PB2	2	5	1	3	3	1	3	2	3	2	2	2	1	1	2	1	1	1	1	1	1	0	2	41
		Embryo	2	3	2	4	3	2	3	1	0	3	3	1	2	1	0	1	0	3	2	1	1	1	3	42
		Total	4	7	3	5	4	3	4	3	3	4	4	3	3	2	2	2	1	3	3	2	2	1	4	72
LB03	7	PB1	5	2	3	3	3	3	2	2	2	2	3	2	2	1	1	2	3	2	2	3	1	1	2	52
		PB2	2	2	2	1	2	0	1	3	0	2	2	2	1	2	1	0	1	1	1	2	0	1	0	29
		Embryo	3	2	3	2	3	3	1	1	2	2	1	2	1	1	2	2	2	1	1	1	1	0	2	39
		Total	5	3	4	3	4	3	2	3	2	3	3	3	2	2	2	2	3	2	2	3	1	1	2	60

Donor	Trio		Chromosome																							Total
			1	2	3	4	5	6	7	8	9	10	11	12	13	14	15	16	17	18	19	20	21	22	X	
LB03	8	PB1	7	7	4	4	6	5	4	5	3	2	2	4	3	2	n/a	3	5	3	2	2	1	2	2	78
		PB2	4	3	2	4	3	2	2	1	0	3	1	4	1	0	n/a	1	2	2	1	0	0	1	3	40
		Embryo	3	4	2	2	3	3	2	4	3	3	1	2	2	2	3	2	3	1	1	2	1	1	3	53
		Total	7	7	4	5	6	5	4	5	3	4	2	5	3	2	3	3	5	3	2	2	1	2	4	87
LB03	10	PB1	4	4	4	5	2	5	2	4	5	2	3	3	2	2	1	0	4	2	0	2	2	1	6	65
		PB2	4	3	2	3	3	4	4	5	1	1	1	4	1	2	3	1	2	2	0	0	3	1	3	53
		Embryo	2	1	4	2	3	1	4	1	4	1	2	1	1	2	2	1	2	2	0	2	1	0	3	42
		Total	5	4	5	5	4	5	5	5	5	2	3	4	2	3	3	1	4	3	0	2	3	1	6	80
LB03	11	PB1	2	5	3	4	3	3	2	4	2	3	3	2	2	1	2	2	3	2	2	2	1	n/a	2	55
		PB2	2	3	1	1	4	2	2	4	1	3	1	2	2	2	1	0	2	2	1	1	1	1	1	40
		Embryo	2	2	4	3	1	1	2	0	1	2	2	2	0	3	1	2	1	0	1	1	2	1	1	35
		Total	3	5	4	4	4	3	3	4	2	4	3	3	2	3	2	2	3	2	2	2	2	1	2	65
LB03	12	PB1	9	10	6	6	9	5	5	7	5	5	5	6	1	2	3	4	3	3	2	3	2	1	3	105
		PB2	5	6	5	3	4	2	2	3	4	4	3	6	1	4	2	1	2	1	3	3	0	0	3	67
		Embryo	4	4	5	5	5	3	7	4	7	3	2	4	0	2	3	3	1	4	1	0	2	1	2	72
		Total	9	10	8	7	9	5	7	7	8	6	5	8	1	4	4	4	3	4	3	3	2	1	4	122

Donor	Trio		Chromosome																							Total
			1	2	3	4	5	6	7	8	9	10	11	12	13	14	15	16	17	18	19	20	21	22	X	
LB03	13	PB1	3	3	2	2	2	3	3	2	2	2	2	2	3	1	1	2	2	2	2	2	0	0	2	45
		PB2	3	2	2	1	1	1	2	1	1	0	0	2	2	3	2	1	1	2	0	0	0	0	3	30
		Embryo	2	3	0	1	3	2	1	1	3	2	2	0	1	2	1	1	1	2	2	2	0	0	1	33
		Total	4	4	2	2	3	3	3	2	3	2	2	2	3	3	2	2	2	3	2	2	0	0	3	54
LB03	14	PB1	5	3	3	4	5	5	5	2	2	3	2	3	3	3	1	4	1	3	0	2	1	0	3	63
		PB2	1	4	3	1	2	4	4	1	3	1	3	2	0	0	0	3	2	1	0	2	0	0	4	41
		Embryo	4	5	2	3	3	1	3	1	1	2	3	3	3	3	1	3	1	2	0	0	1	0	1	46
		Total	5	6	4	4	5	5	6	2	3	3	4	4	3	3	1	5	2	3	0	2	1	0	4	75
LB03	16	PB1	7	2	5	2	4	3	5	4	3	2	3	2	2	3	3	3	2	2	2	2	0	1	2	64
		PB2	6	2	2	2	2	3	2	3	2	1	1	2	1	1	0	2	2	0	2	0	0	1	2	39
		Embryo	3	2	3	0	2	2	3	1	1	1	2	2	1	2	3	1	2	2	0	2	0	0	0	35
		Total	8	3	5	2	4	4	5	4	3	2	3	3	2	3	3	3	3	2	2	2	0	1	2	69

Key

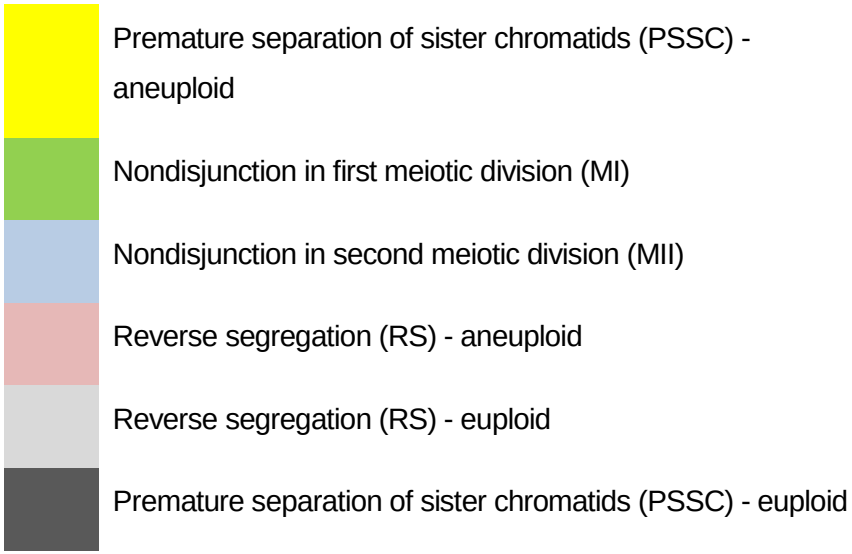
Premature separation of sister chromatids (PSSC) - aneuploid
Nondisjunction in first meiotic division (MI)
Nondisjunction in second meiotic division (MII)
Reverse segregation (RS) - aneuploid
Reverse segregation (RS) - euploid
Premature separation of sister chromatids (PSSC) - euploid

9.4.3. Variation in Global Recombination Rates in Adult Oocytes

Variation in recombination in foetal oocytes has been hypothesised to give rise to vulnerable crossover configurations that predispose chromosome pairs to mis-segregation decades later in the adult woman. To assess recombination in adult oocytes and embryos, I mapped 883 maternal crossovers in the oocyte-PB trios and 1,149 and 1,342 maternal and paternal crossovers, respectively, in the embryos (Figure 9.6a; Tables 9.7-9.11). 12% of the reciprocal crossover events mapped to non-sister chromatids in the PB2 and oocyte, whilst the PB1 was heterozygous for the SNPs. A similar proportion would be expected to be present in the PB1 and are undetectable, since the two DNA strands cannot currently be separated and phased individually (Hou *et al.* 2013). Using the 300K SNP arrays gave median resolutions of 107kb and 331kb for crossovers in the oocyte-PB and embryos, respectively (Figure 9.1e). This is similar to high-resolution population-based studies employing SNP arrays (Kong *et al.* 2002; Coop *et al.* 2008; Middlebrooks *et al.* 2013).

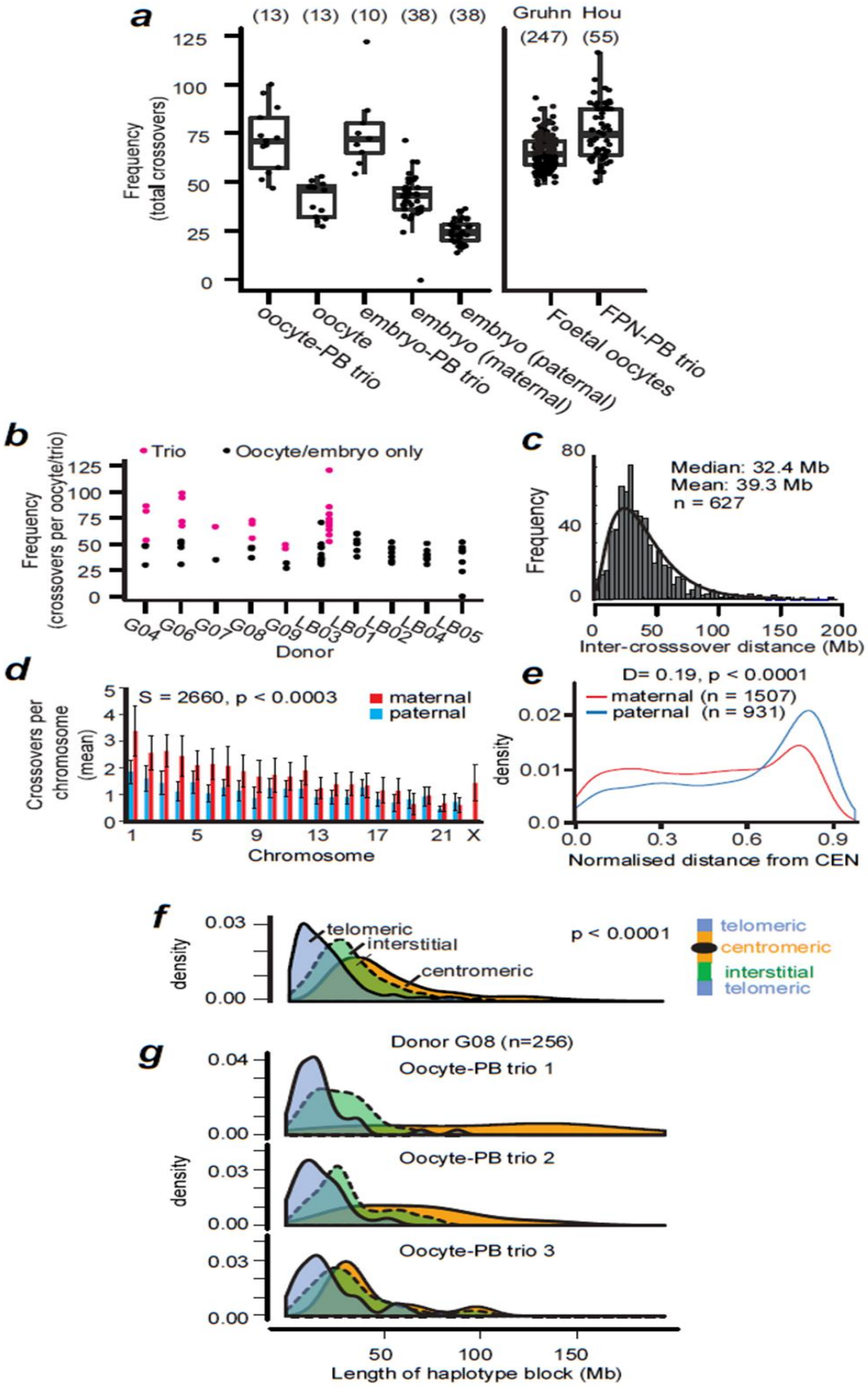

Figure 9.6. Variation in genome-wide recombination rates between/within individuals (Ottolini *et al.* 2015).

(a) Boxplot of global recombination rates showing the interquartile range (box), median (horizontal bar), and whiskers (1.5× IQR). Numbers analysed are in parentheses. Rates from foetal oocytes ('Gruhn')(Gruhn, Rubio *et al.* 2013) and female pronucleus-PB trios ('Hou') (Hou, Fan *et al.* 2013).

(b) Recombination rates for the 10 donors. Black: rates using information from oocyte or embryo only. Magenta: rates using the information from the complete oocyte-PB trios.

(c) Inter-crossover distances, excluding centromeric distances. The fitted curve is based on maximum likelihood estimation of the gamma distribution, shape: 2.6141 ± 0.14 (S.E.), rate 0.066 ± 0.0039 (S.E.). Estimated fitted mean: 39.3Mb, log-likehood of fitting: -2802.738; AIC: 5609.476.

(d) Average and standard deviation of chromosome-specific recombination (Table 9.4). GLM analysis revealed that chromosome size had a significant effect on sex-specific recombination frequencies. Spearman correlation test is shown for the p-value for individual, pair-wise comparisons between maternal and paternal recombination frequencies per chromosome. As chromosome size decreases, the contribution of sex to crossover frequencies decreases (see Source Data for Figure 9.6d).

(e) Crossover position relative to centromeres (CEN), normalised to chromosome length. Statistics: Two-sided Kolmogorov-Smirnov test of normalised and absolute lengths; $p<0.0005$; X chr. excluded; Figure 9.8).

(f) Length of haplotype blocks (not inter-crossover distances), according to position relative to telomeres (blue), centromeres (yellow), or interstitial (green). Statistics: non-parametric ANOVA ($p<0.0001$). Centromeric blocks excluded the ~3×10^6 base pairs of alpha-satellite DNA.

(g) Variation in centromere repression of crossovers in oocyte-PB trios from the same donor.

Table 9.8: Map Distances in Embryos (Ottolini *et al.* 2015)

				Chr 1	Chr 2	Chr 3	Chr 4	Chr 5	Chr 6	Chr 7	Chr 8	Chr 9	Chr 10	Chr 11	Chr 12	Chr 13	Chr 14	Chr 15	Chr 16	Chr 17	Chr 18	Chr 19	Chr 20	Chr 21	Chr 22	Chr X	Chr Y	Total	Mean
Embryo Ref	**Type**	**Event**	**Sex**																										
1.1	Embryo	Recombination	Mother	1.60	0.80	1.20	0.40	1.20	0.80	0.80	0.80	0.80	1.20	0.80	0.80	0.80	0.40	1.20	0.80	0.40	0.80	1.20	0.80	NA	0.80	0.40	NA	18.81	0.82
1.1	Embryo	Recombination	Father	0.80	0.00	0.80	0.40	0.80	0.80	0.00	0.40	0.00	0.80	0.80	0.40	0.80	0.40	0.00	0.00	0.40	0.00	0.80	0.00	0.40	0.00	NA	0.00	8.80	0.38
1.2	Embryo	Recombination	Mother	1.60	0.80	1.20	0.40	1.20	0.80	0.80	0.80	0.80	1.20	0.80	0.80	0.80	0.40	1.20	0.80	0.40	0.80	1.20	0.80	0.00	0.80	0.40	NA	18.81	0.82
1.2	Embryo	Recombination	Father	0.80	0.00	0.80	0.40	0.80	0.80	0.00	0.40	0.00	0.80	0.80	0.40	0.80	0.40	0.00	0.00	0.40	0.00	0.80	0.00	0.40	0.00	NA	0.00	8.80	0.38
2	Embryo	Recombination	Mother	2.80	0.80	0.40	0.80	0.40	1.20	1.60	2.00	1.20	0.40	0.00	1.20	0.80	0.40	0.80	0.80	0.40	0.40	0.40	0.80	0.00	0.00	0.80	NA	18.41	0.80
2	Embryo	Recombination	Father	0.80	0.80	0.00	0.40	0.80	0.40	0.80	0.40	0.00	0.80	0.40	0.40	0.40	0.40	0.40	0.80	0.80	0.00	0.40	0.80	0.40	0.40	NA	0.00	10.80	0.47
3	Embryo	Recombination	Mother	0.80	0.40	0.80	0.40	0.80	0.80	1.20	0.80	0.80	0.80	0.40	0.40	0.40	1.60	1.20	0.40	0.40	0.00	0.00	0.00	0.00	0.00	0.40	NA	12.80	0.56
3	Embryo	Recombination	Father	NA	NA	NA	NA	NA	NA	NA	NA	NA	NA	NA	NA	NA	NA	NA	NA	NA	NA	NA	NA	NA	NA	NA	0.00	0.00	0.00
4	Embryo	Recombination	Mother	1.60	0.40	1.20	1.20	0.40	2.00	0.80	0.80	0.80	0.80	1.20	0.40	1.20	0.40	0.80	0.80	0.80	0.80	0.80	0.80	0.40	0.80	1.60	NA	20.81	0.90
4	Embryo	Recombination	Father	0.40	0.80	0.80	0.00	0.80	0.80	0.80	0.80	0.40	0.00	0.80	0.40	0.80	0.40	0.40	0.80	0.80	0.00	0.80	0.00	0.00	0.00	0.00	0.00	10.80	0.47
5.1	Embryo	Recombination	Mother	0.00	2.00	1.60	0.80	0.40	1.20	0.40	0.00	1.20	1.20	1.20	1.20	0.80	0.40	0.40	0.40	0.40	0.40	0.00	0.80	0.40	0.00	1.60	NA	16.81	0.73
5.1	Embryo	Recombination	Father	1.20	0.80	0.80	1.20	1.20	0.00	0.80	0.40	0.80	0.40	0.80	0.40	0.40	0.80	0.40	0.80	0.40	0.40	0.40	1.20	0.40	0.40	0.00	0.00	14.41	0.63
6	Embryo	Recombination	Mother	1.60	0.40	1.60	1.60	0.80	0.80	0.00	1.60	0.00	0.40	0.80	0.80	0.00	0.80	0.80	0.00	0.40	0.80	0.40	0.80	0.00	0.40	0.40	NA	15.21	0.66
6	Embryo	Recombination	Father	1.20	0.80	0.40	0.40	1.60	0.00	0.40	0.00	0.40	1.20	0.40	1.20	0.40	0.40	0.00	0.40	0.80	0.00	0.40	0.80	0.40	0.80	0.00	0.00	12.40	0.54
REF	Embryo	Recombination	Mother	0.40	1.20	2.00	0.80	0.80	0.80	0.40	0.00	1.20	0.40	0.80	1.20	0.00	0.40	0.00	0.00	0.80	0.80	0.40	0.80	0.00	0.00	0.40	NA	13.61	0.59
REF	Embryo	Recombination	Father	1.20	1.20	0.00	0.00	0.00	1.20	0.80	1.20	0.40	0.40	0.80	0.80	0.40	0.40	0.40	0.80	0.40	0.00	0.40	0.40	0.40	0.40	0.00	0.00	12.00	0.52
REF	Daughter	Recombination	Mother	2.40	1.60	1.60	0.80	1.60	1.60	0.40	0.40	0.40	1.60	2.00	1.20	0.80	0.40	0.80	0.00	1.20	0.00	0.40	0.00	0.00	0.00	1.20	NA	20.41	0.89

				Chr 1	Chr 2	Chr 3	Chr 4	Chr 5	Chr 6	Chr 7	Chr 8	Chr 9	Chr 10	Chr 11	Chr 12	Chr 13	Chr 14	Chr 15	Chr 16	Chr 17	Chr 18	Chr 19	Chr 20	Chr 21	Chr 22	Chr X	Chr Y	Total	Mean
REF	Daughter	Recombination	Father	0.80	1.20	0.40	0.80	0.00	0.80	0.80	0.40	0.00	0.80	1.20	0.80	0.40	0.40	0.80	0.40	0.80	0.80	0.00	0.00	0.40	0.40	0.00	0.00	12.40	0.54
CVS		Recombination	Mother	2.80	0.40	1.60	0.00	0.40	0.80	1.20	0.40	0.00	1.20	1.60	0.00	0.40	0.40	0.40	0.80	1.20	0.40	0.80	0.80	0.00	0.40	1.60	NA	17.61	0.77
CVS		Recombination	Father	0.80	1.20	0.40	0.80	0.00	0.80	0.80	0.40	0.00	0.80	1.20	0.80	0.40	0.40	0.80	0.40	0.80	0.80	0.00	0.00	0.40	0.40	0.00	0.00	12.40	0.54
2.1	Embryo	Recombination	Mother	1.60	1.60	0.80	2.40	1.60	2.00	1.60	0.80	0.80	0.00	0.40	1.20	0.40	0.80	0.40	0.80	0.40	0.40	0.40	0.40	0.00	0.40	1.20	NA	20.41	0.89
2.1	Embryo	Recombination	Father	0.80	0.80	0.00	0.40	0.00	0.40	0.40	0.40	0.40	0.40	0.00	0.40	0.00	0.40	0.00	0.80	0.40	0.00	0.40	0.40	0.00	0.00	0.00	0.00	6.80	0.30
2.2	Embryo	Recombination	Mother	1.60	1.60	0.80	2.40	1.60	2.00	1.60	0.80	0.80	0.00	0.40	1.20	0.40	0.80	0.40	0.80	0.40	0.40	0.40	0.40	0.00	0.40	1.20	NA	20.41	0.89
2.2	Embryo	Recombination	Father	0.80	0.80	0.00	0.40	0.00	0.40	0.40	0.40	0.40	0.40	0.00	0.40	0.00	0.40	0.00	0.80	0.40	0.00	0.40	0.40	0.00	0.00	0.00	0.00	6.80	0.30
3.1	Embryo	Recombination	Mother	3.20	1.20	1.60	0.80	0.80	1.60	0.40	1.60	0.40	2.00	0.80	2.00	1.20	0.80	0.00	0.80	1.20	0.80	0.40	0.80	0.80	0.00	0.80	NA	24.01	1.04
3.1	Embryo	Recombination	Father	1.60	1.20	1.20	0.40	0.80	0.80	0.00	0.80	0.40	0.80	0.80	0.80	0.80	0.80	0.40	0.40	0.40	0.80	0.00	0.40	0.40	0.00	0.00	0.00	14.01	0.61
3.2	Embryo	Recombination	Mother	3.20	1.20	1.60	0.80	0.80	1.60	0.40	1.60	0.40	2.00	0.80	2.00	1.20	0.80	0.00	0.80	1.20	0.80	0.40	0.80	0.80	0.00	0.80	NA	24.01	1.04
3.2	Embryo	Recombination	Father	1.60	1.20	1.20	0.40	0.80	0.80	0.00	0.80	0.40	0.80	0.80	0.80	0.80	0.80	0.40	0.40	0.40	0.80	0.00	0.40	0.40	0.00	0.00	0.00	14.01	0.61
4	Embryo	Recombination	Mother	2.00	1.60	1.20	0.80	0.80	0.00	0.80	1.20	0.80	1.20	0.80	0.40	0.40	0.40	0.40	0.00	0.40	0.40	0.40	0.40	0.40	0.40	0.00	NA	15.21	0.66
4	Embryo	Recombination	Father	0.80	0.80	0.40	1.20	0.80	0.40	0.80	0.40	1.20	0.80	0.80	0.40	0.00	0.80	0.40	0.40	0.40	0.40	0.80	0.40	0.00	0.40	0.00	0.00	12.80	0.56
5	Embryo	Recombination	Mother	2.40	2.00	0.80	2.00	2.00	0.40	0.80	0.80	1.20	1.60	0.80	1.20	0.00	0.80	1.20	0.40	0.40	1.20	0.00	0.00	0.40	0.00	1.20	NA	21.61	0.94
5	Embryo	Recombination	Father	0.40	0.40	0.80	0.40	1.20	0.00	0.40	0.80	0.00	0.80	0.80	0.40	0.40	0.00	0.40	0.40	0.40	0.40	0.40	0.40	0.40	0.40	0.00	0.00	10.00	0.43
2	Embryo	Recombination	Mother	0.80	1.20	0.80	1.20	1.20	0.80	1.20	0.00	0.00	1.20	1.20	0.40	0.80	0.40	0.00	0.40	0.00	1.20	0.80	0.40	0.40	0.40	1.20	NA	16.01	0.70
2	Embryo	Recombination	Father	0.80	0.80	0.40	0.40	0.40	0.40	0.00	0.40	0.00	0.80	0.80	0.00	0.80	0.00	0.40	0.40	0.00	0.00	0.40	0.40	0.00	0.00	0.00	0.00	7.60	0.33
5	Embryo	Recombination	Mother	2.80	0.80	1.20	2.00	0.00	1.20	0.40	1.20	1.20	0.40	0.00	1.20	0.40	0.80	0.40	0.80	1.20	1.20	0.80	0.00	0.00	0.40	0.40	NA	18.81	0.82
5	Embryo	Recombination	Father	0.80	0.00	0.80	0.40	0.40	0.80	1.20	0.40	0.40	0.80	0.40	0.40	0.00	0.00	0.80	0.80	0.00	0.00	0.00	0.80	0.00	0.00	0.00	0.00	9.20	0.40
6	Embryo	Recombination	Mother	1.20	1.20	NA	NA	NA	NA	NA	NA	NA	NA	NA	NA	NA	NA	NA	NA	NA	NA	NA	NA	NA	NA	NA	NA	2.40	0.10

				Chr 1	Chr 2	Chr 3	Chr 4	Chr 5	Chr 6	Chr 7	Chr 8	Chr 9	Chr 10	Chr 11	Chr 12	Chr 13	Chr 14	Chr 15	Chr 16	Chr 17	Chr 18	Chr 19	Chr 20	Chr 21	Chr 22	Chr X	Chr Y	Total	Mean
6	Embryo	Recombination	Father	0.80	0.40	0.00	0.40	0.80	0.40	0.40	0.00	0.40	0.80	0.00	0.80	0.40	0.80	0.80	0.80	0.80	0.80	0.80	0.80	0.40	0.40	0.00	0.00	12.00	0.52
7	Embryo	Recombination	Mother	0.80	0.80	1.20	1.20	1.20	1.20	0.00	0.40	0.80	0.80	0.00	0.80	0.40	0.40	0.80	0.80	0.80	0.00	0.00	0.40	0.40	0.00	0.80	NA	14.01	0.61
7	Embryo	Recombination	Father	0.00	0.00	0.80	0.80	0.80	0.40	0.80	0.40	0.00	0.00	0.80	0.80	0.80	0.40	0.40	0.40	0.40	0.40	0.00	0.00	0.40	0.40	0.00	0.00	9.20	0.40
8	Embryo	Recombination	Mother	1.20	1.60	0.80	1.20	1.20	1.20	0.80	1.60	1.20	1.20	0.00	0.40	0.80	0.80	0.00	0.80	1.20	0.40	0.40	1.20	0.40	0.40	1.20	NA	20.01	0.87
8	Embryo	Recombination	Father	1.20	0.00	1.20	0.00	0.80	0.40	0.80	0.40	0.00	0.80	0.40	0.80	0.00	0.00	0.00	0.40	0.40	0.00	0.00	0.80	0.40	0.00	0.00	0.00	8.80	0.38
10	Embryo	Recombination	Mother	0.80	0.00	2.00	1.20	0.80	0.00	1.20	0.40	0.80	0.40	0.80	0.40	0.40	0.40	0.80	0.40	0.80	0.80	0.00	0.80	0.40	0.00	1.20	NA	14.81	0.64
10	Embryo	Recombination	Father	1.20	0.00	0.80	0.40	0.40	0.40	0.40	0.00	0.40	0.40	0.40	0.40	0.80	0.00	0.00	0.80	0.80	0.80	0.40	0.40	0.40	0.00	0.00	0.00	9.60	0.42
11	Embryo	Recombination	Mother	1.14	0.57	0.23	0.51	0.57	0.74	1.26	0.97	0.57	0.57	0.17	0.51	0.40	1.09	0.74	0.57	0.57	-0.11	-0.06	0.34	NA	-0.06	0.40	NA	13.10	0.57
11	Embryo	Recombination	Father	1.10	0.59	0.10	0.53	0.50	0.73	1.39	1.01	0.59	0.50	0.07	0.49	0.33	1.21	0.76	0.59	0.60	-0.21	-0.24	0.31	0.08	-0.14	NA	0.00	13.07	0.57
12	Embryo	Recombination	Mother	1.06	0.60	-0.03	0.54	0.43	0.71	1.51	1.06	0.60	0.43	-0.03	0.46	0.26	1.34	0.77	0.60	0.63	-0.31	-0.43	0.29	0.05	-0.23	0.40	NA	13.04	0.57
12	Embryo	Recombination	Father	1.01	0.61	-0.16	0.56	0.36	0.70	1.64	1.10	0.61	0.36	-0.13	0.43	0.19	1.47	0.79	0.61	0.66	-0.41	-0.61	0.26	0.01	-0.31	NA	0.00	13.00	0.57
14	Embryo	Recombination	Mother	0.97	0.63	-0.29	0.57	0.29	0.69	1.77	1.14	0.63	0.29	-0.23	0.40	0.11	1.60	0.80	0.63	0.69	-0.51	-0.80	0.23	-0.02	-0.40	0.80	NA	12.97	0.56
14	Embryo	Recombination	Father	0.93	0.64	-0.41	0.59	0.21	0.67	1.90	1.19	0.64	0.21	-0.33	0.37	0.04	1.73	0.81	0.64	0.71	-0.61	-0.99	0.20	-0.06	-0.49	NA	0.00	12.94	0.56
16	Embryo	Recombination	Mother	0.89	0.66	-0.54	0.60	0.14	0.66	2.03	1.23	0.66	0.14	-0.43	0.34	-0.03	1.86	0.83	0.66	0.74	-0.71	-1.17	0.17	-0.09	-0.57	0.40	NA	12.91	0.56
16	Embryo	Recombination	Father	NA	NA	NA	NA	NA	NA	NA	NA	NA	NA	NA	NA	NA	NA	NA	NA	NA	NA	NA	NA	NA	NA	NA	0.00	12.87	0.56
1	Embryo	Recombination	Mother	1.22	0.58	0.78	1.02	0.78	0.65	0.64	0.78	0.48	1.04	0.56	0.74	0.41	0.48	0.39	0.54	0.38	0.65	0.35	0.31	0.24	0.13	0.27	NA	12.84	0.56
1	Embryo	Recombination	Father	1.21	0.56	0.77	1.03	0.79	0.64	0.64	0.79	0.48	1.06	0.54	0.73	0.40	0.48	0.39	0.54	0.37	0.66	0.35	0.30	0.24	0.12	0.26	0.00	12.81	0.56
2	Embryo	Recombination	Mother	1.21	0.54	0.76	1.04	0.79	0.62	0.64	0.80	0.47	1.07	0.53	0.73	0.40	0.47	0.39	0.54	0.36	0.68	0.34	0.29	0.24	0.11	0.24	NA	12.78	0.56
2	Embryo	Recombination	Father	1.20	0.53	0.75	1.05	0.79	0.61	0.64	0.80	0.47	1.09	0.51	0.72	0.39	0.47	0.39	0.54	0.34	0.69	0.34	0.28	0.24	0.11	0.23	0.00	12.74	0.55
3	Embryo	Recombination	Mother	1.20	0.51	0.74	1.06	0.79	0.59	0.64	0.81	0.47	1.10	0.49	0.72	0.38	0.47	0.38	0.54	0.33	0.70	0.34	0.27	0.24	0.10	0.21	NA	12.71	0.55

				Chr 1	Chr 2	Chr 3	Chr 4	Chr 5	Chr 6	Chr 7	Chr 8	Chr 9	Chr 10	Chr 11	Chr 12	Chr 13	Chr 14	Chr 15	Chr 16	Chr 17	Chr 18	Chr 19	Chr 20	Chr 21	Chr 22	Chr X	Chr Y	Total	Mean
3	Embryo	Recombination	Father	1.19	0.49	0.73	1.07	0.79	0.58	0.64	0.82	0.47	1.12	0.48	0.71	0.38	0.47	0.38	0.54	0.31	0.71	0.34	0.26	0.25	0.09	0.20	0.00	12.68	0.55
4	Embryo	Recombination	Mother	1.19	0.47	0.72	1.08	0.80	0.56	0.64	0.83	0.47	1.13	0.46	0.71	0.37	0.47	0.38	0.54	0.30	0.72	0.33	0.24	0.25	0.08	0.19	NA	12.65	0.55
4	Embryo	Recombination	Father	1.18	0.45	0.71	1.09	0.80	0.55	0.64	0.83	0.46	1.15	0.44	0.71	0.37	0.46	0.38	0.54	0.29	0.73	0.33	0.23	0.25	0.08	0.17	0.00	12.61	0.55
5	Embryo	Recombination	Mother	1.18	0.43	0.70	1.10	0.80	0.53	0.64	0.84	0.46	1.16	0.43	0.70	0.36	0.46	0.38	0.54	0.27	0.74	0.33	0.22	0.25	0.07	0.16	NA	12.58	0.55
5	Embryo	Recombination	Father	1.17	0.41	0.69	1.11	0.80	0.52	0.64	0.85	0.46	1.18	0.41	0.70	0.36	0.46	0.38	0.54	0.26	0.75	0.33	0.21	0.25	0.06	0.14	0.00	12.55	0.55
6	Embryo	Recombination	Mother	1.17	0.40	0.68	1.12	0.80	0.50	0.64	0.86	0.46	1.19	0.39	0.69	0.35	0.46	0.37	0.54	0.25	0.76	0.32	0.20	0.25	0.05	0.13	NA	12.52	0.54
6	Embryo	Recombination	Father	1.17	0.38	0.67	1.13	0.80	0.49	0.64	0.86	0.45	1.21	0.38	0.69	0.35	0.45	0.37	0.54	0.23	0.77	0.32	0.19	0.25	0.04	0.11	0.00	12.48	0.54
7	Embryo	Recombination	Mother	1.16	0.36	0.66	1.14	0.81	0.47	0.64	0.87	0.45	1.22	0.36	0.68	0.34	0.45	0.37	0.54	0.22	0.78	0.32	0.18	0.25	0.04	0.10	NA	12.45	0.54
7	Embryo	Recombination	Father	1.16	0.34	0.65	1.15	0.81	0.46	0.64	0.88	0.45	1.24	0.34	0.68	0.34	0.45	0.37	0.54	0.20	0.79	0.32	0.17	0.25	0.03	0.08	0.00	12.42	0.54
8	Embryo	Recombination	Mother	1.15	0.32	0.64	1.15	0.81	0.44	0.64	0.89	0.45	1.25	0.33	0.68	0.33	0.45	0.37	0.54	0.19	0.80	0.31	0.16	0.25	0.02	0.07	NA	12.39	0.54
8	Embryo	Recombination	Father	1.15	0.30	0.63	1.16	0.81	0.43	0.64	0.89	0.44	1.27	0.31	0.67	0.32	0.44	0.37	0.54	0.18	0.81	0.31	0.15	0.25	0.01	0.05	0.00	12.35	0.54
1	Embryo	Recombination	Mother	1.14	0.28	0.62	1.17	0.81	0.41	0.64	0.90	0.44	1.28	0.29	0.67	0.32	0.44	0.36	0.55	0.16	0.82	0.31	0.13	0.25	0.01	0.04	NA	12.32	0.54
1	Embryo	Recombination	Father	1.14	0.27	0.61	1.18	0.82	0.40	0.64	0.91	0.44	1.30	0.28	0.66	0.31	0.44	0.36	0.55	0.15	0.83	0.31	0.12	0.25	0.00	0.02	0.00	12.29	0.53
2	Embryo	Recombination	Mother	1.13	0.25	0.60	1.19	0.82	0.38	0.64	0.92	0.44	1.31	0.26	0.66	0.31	0.44	0.36	0.55	0.13	0.85	0.30	0.11	0.25	-0.01	0.01	NA	12.26	0.53
2	Embryo	Recombination	Father	1.13	0.23	0.59	1.20	0.82	0.37	0.64	0.92	0.43	1.33	0.24	0.65	0.30	0.43	0.36	0.55	0.12	0.86	0.30	0.10	0.25	-0.02	-0.01	0.00	12.22	0.53
3	Embryo	Recombination	Mother	1.12	0.21	0.58	1.21	0.82	0.35	0.64	0.93	0.43	1.34	0.23	0.65	0.30	0.43	0.36	0.55	0.11	0.87	0.30	0.09	0.25	-0.03	-0.02	NA	12.19	0.53
3	Embryo	Recombination	Father	1.12	0.19	0.57	1.22	0.82	0.34	0.64	0.94	0.43	1.36	0.21	0.64	0.29	0.43	0.36	0.55	0.09	0.88	0.30	0.08	0.25	-0.03	-0.04	0.00	12.16	0.53
4	Embryo	Recombination	Mother	1.11	0.17	0.56	1.23	0.83	0.32	0.64	0.95	0.43	1.37	0.19	0.64	0.29	0.43	0.35	0.55	0.08	0.89	0.29	0.07	0.25	-0.04	-0.05	NA	12.13	0.53
4	Embryo	Recombination	Father	1.11	0.16	0.55	1.24	0.83	0.31	0.64	0.96	0.42	1.39	0.18	0.64	0.28	0.42	0.35	0.55	0.06	0.90	0.29	0.06	0.25	-0.05	-0.06	0.00	12.09	0.53
5	Embryo	Recombination	Mother	1.11	0.14	0.54	1.25	0.83	0.29	0.64	0.96	0.42	1.40	0.16	0.63	0.28	0.42	0.35	0.55	0.05	0.91	0.29	0.05	0.25	-0.06	-0.08	NA	12.06	0.52

				Chr 1	Chr 2	Chr 3	Chr 4	Chr 5	Chr 6	Chr 7	Chr 8	Chr 9	Chr 10	Chr 11	Chr 12	Chr 13	Chr 14	Chr 15	Chr 16	Chr 17	Chr 18	Chr 19	Chr 20	Chr 21	Chr 22	Chr X	Chr Y	Total	Mean
5	Embryo	Recombination	Father	1.10	0.12	0.53	1.26	0.83	0.28	0.64	0.97	0.42	1.42	0.14	0.63	0.27	0.42	0.35	0.55	0.04	0.92	0.29	0.03	0.25	-0.06	-0.09	0.00	12.03	0.52
6	Embryo	Recombination	Mother	1.10	0.10	0.52	1.27	0.83	0.26	0.64	0.98	0.42	1.43	0.13	0.62	0.26	0.42	0.35	0.55	0.02	0.93	0.28	0.02	0.25	-0.07	-0.11	NA	12.00	0.52
6	Embryo	Recombination	Father	1.09	0.08	0.51	1.28	0.83	0.25	0.64	0.99	0.41	1.45	0.11	0.62	0.26	0.41	0.35	0.55	0.01	0.94	0.28	0.01	0.25	-0.08	-0.12	0.00	11.96	0.52
7	Embryo	Recombination	Mother	1.09	0.06	NA	NA	NA	NA	NA	NA	NA	NA	NA	NA	NA	NA	NA	NA	NA	NA	NA	NA	NA	NA	NA	NA	11.93	0.52
7	Embryo	Recombination	Father	1.08	0.04	1.60	0.63	0.57	0.23	0.97	0.46	0.51	0.46	0.69	0.34	0.57	0.00	0.00	0.51	0.74	0.63	0.06	0.69	0.40	-0.06	0.57	0.00	11.90	0.52
8	Embryo	Recombination	Mother	1.08	0.03	1.76	0.60	0.50	0.14	1.06	0.46	0.51	0.41	0.77	0.27	0.59	-0.10	-0.10	0.49	0.74	0.67	0.01	0.70	0.40	-0.11	0.60	NA	11.87	0.52
8	Embryo	Recombination	Father	1.07	0.01	1.92	0.57	0.43	0.06	1.14	0.46	0.51	0.37	0.86	0.20	0.60	-0.20	-0.20	0.46	0.74	0.71	-0.03	0.71	0.40	-0.17	0.63	0.00	11.83	0.51
9	Embryo	Recombination	Mother	1.07	-0.01	2.07	0.54	0.36	-0.03	1.23	0.46	0.51	0.33	0.94	0.13	0.61	-0.30	-0.30	0.43	0.74	0.76	-0.07	0.73	0.40	-0.23	0.66	NA	11.80	0.51
9	Embryo	Recombination	Father	1.06	-0.03	2.23	0.51	0.29	-0.11	1.31	0.46	0.51	0.29	1.03	0.06	0.63	-0.40	-0.40	0.40	0.74	0.80	-0.11	0.74	0.40	-0.29	0.69	0.00	11.77	0.51
10	Embryo	Recombination	Mother	1.06	-0.05	2.39	0.49	0.21	-0.20	1.40	0.46	0.51	0.24	1.11	-0.01	0.64	-0.50	-0.50	0.37	0.74	0.84	-0.16	0.76	0.40	-0.34	0.71	NA	11.74	0.51
10	Embryo	Recombination	Father	1.06	-0.07	2.54	0.46	0.14	-0.29	1.49	0.46	0.51	0.20	1.20	-0.09	0.66	-0.60	-0.60	0.34	0.74	0.89	-0.20	0.77	0.40	-0.40	0.74	0.00	11.70	0.51
Chromosome size (Mb) hGRCb37 (full length)				250	243	198	192	181	171	159	146	141	136	135	134	115	107	103	90.4	81.5	78.1	59.4	63.0	48.2	51.3	155	59.4	3038.7	132.12
Population-average		sex combined	Embryo	1.13	0.74	0.93	0.81	0.85	0.80	0.89	0.82	0.78	1.04	0.94	1.04	0.80	0.94	0.94	1.18	1.26	1.15	1.25	1.36	1.06	1.01	0.49	NA	22.20	0.97
Population-average		Maternal	Embryo	1.46	1.13	1.43	1.40	1.26	1.38	1.45	1.35	1.33	1.48	1.34	1.58	1.18	1.38	1.42	1.69	1.75	1.80	1.56	1.93	1.52	1.30	1.13	NA	33.24	1.45
Population-average		Paternal	Embryo	0.79	0.70	0.75	0.59	0.81	0.67	0.79	0.79	0.62	1.00	0.95	0.94	0.85	0.91	0.86	1.44	1.11	0.95	1.64	1.48	1.01	1.36	NA	NA	21.02	0.96
Population-average		Rec rate	Oocyte	1.03	1.36	1.34	1.31	1.32	1.33	1.13	1.13	1.33	1.53	1.22	1.32	1.37	1.07	1.24	1.40	1.65	1.82	1.75	1.95	1.28	1.20	0.97	NA	31.06	1.30
deCODE		Maternal	Population	1.34	1.28	1.35	1.35	1.37	1.36	1.38	1.39	1.32	1.52	1.39	1.47	1.27	1.15	1.36	1.65	1.87	1.75	1.94	1.75	1.39	1.29	1.11	NA	33.05	1.40
HapMap		Paternal	Population	1.15	1.10	1.13	1.12	1.13	1.12	1.18	1.15	1.18	1.34	1.17	1.30	1.09	1.12	1.38	1.48	1.58	1.50	1.81	1.71	1.29	1.44	1.16	NA	29.63	1.23
Hou *et al.* 2013		Maternal	Oocyte	1.33	1.32	1.39	1.36	1.30	1.39	1.30	1.45	1.33	1.52	1.38	1.41	1.32	1.28	1.41	1.76	1.86	1.82	2.05	1.79	1.60	1.38	1.14	NA	33.88	1.47

Table 9.9: Crossovers in Oocytes (Ottolini *et al.* 2015)

Donor	G04	G04	G04	G06	G06	G06	G06	G07	G08	G08	G08	G09	G09	Combined	Population-average	Hou *et al.* (2013)	Gruhn *et al.* (2014)
Trio	3	4	5	1	2	3	4	1	1	2	3	1	2				Table S5
Type	Oocyte	Oocyte	Oocyte	Oocyte	Oocyte	Oocyte	Oocyte	Oocyte	Oocyte	Oocyte	Oocyte	Oocyte	Oocyte	Oocyte			Oocyte
Event	Crossovers	Crossovers	Crossovers	Crossovers	Crossovers	Crossovers	Crossovers	Crossovers	Crossovers	Crossovers	Crossovers	Crossovers	Crossovers	Crossovers			Mlh1 foci
Chr1	6	7	5	4	7	7	5	3	3	4	5	4	3	63	4.85	5.72	5.9 ± 0.18
Chr2	4	7	7	5	8	9	9	5	4	6	3	3	4	74	5.69	5.44	NA
Chr3	4	4	5	4	7	8	3	7	4	5	7	4	2	64	4.92	4.76	NA
Chr4	3	6	4	NA	7	6	4	4	4	4	4	3	2	51	4.25	4.44	NA
Chr5	3	5	4	5	8	5	4	3	2	4	6	3	5	57	4.38	4.21	NA
Chr6	2	4	6	7	5	5	4	5	2	5	4	2	3	54	4.15	4.03	3.7 ± 0.19
Chr7	3	3	5	2	6	5	3	2	3	3	2	2	3	42	3.23	3.65	NA
Chr8	3	6	4	3	5	2	3	3	2	2	2	2	2	39	3.00	3.56	NA
Chr9	3	4	4	5	4	3	3	4	2	4	5	2	4	47	3.62	3.32	2.8 ± 0.05
Chr10	3	3	4	4	5	6	4	5	4	3	3	1	2	47	3.62	3.68	NA
Chr11	2	4	3	2	3	3	3	4	3	5	3	2	3	40	3.08	3.26	NA

Chr12	3	3	4	4	3	6	3	2	3	3	4	1	3	42	3.23	3.46	NA
Chr13	NA	4	4	3	4	4	4	1	1	2	4	4	1	36	3.00	2.50	2.6 ± 0.07
Chr14	1	2	2	3	1	3	2	2	2	2	2	4	1	27	2.08	2.37	2.2 ± 0.1
Chr15	1	1	4	2	3	3	3	NA	3	NA	3	3	1	27	2.45	2.37	2.3 ± 0.15
Chr16	3	2	5	2	3	2	3	3	3	3	3	NA	1	33	2.75	2.79	2.5 ± 0.07
Chr17	1	3	3	4	3	5	2	3	1	3	3	1	2	34	2.62	2.65	NA
Chr18	1	4	3	2	4	3	2	2	3	2	2	1	2	31	2.38	2.60	2.3 ± 0.07
Chr19	2	3	3	3	2	2	1	2	2	2	2	1	1	26	2.00	2.26	NA
Chr20	2	2	2	2	3	2	3	3	2	2	2	1	3	29	2.23	2.21	NA
Chr21	1	1	1	2	1	1	1	2	1	1	2	1	NA	15	1.25	1.32	1.2 ± 0.03
Chr22	1	1	1	1	2	1	2	1	1	2	1	1	1	16	1.23	1.31	1.4 ± 0.04
ChrX	3	4	5	NA	6	5	2	2	2	4	2	1	2	38	3.45	3.04	NA
ChrY	NA	NA	NA	NA	NA	NA	NA	NA	NA	NA	NA	NA	NA	NA	-	-	NA
Total	55	83	88	69	100	96	73	68	57	71	74	47	51	932	71.69	74.96	69± 0.29

Table 9.10: Recombination Frequencies in Oocytes (Ottolini *et al.* 2015)

				Chr 1	Chr 2	Chr 3	Chr 4	Chr 5	Chr 6	Chr 7	Chr 8	Chr 9	Chr 10	Chr 11	Chr 12	Chr 13	Chr 14	Chr 15	Chr 16	Chr 17	Chr 18	Chr 19	Chr 20	Chr 21	Chr 22	Chr X	Total
Donor	**Trio**	**Cell**	**Type**																								
G04	3	PB2	Recombination rate	3	1	3	1	1	1	2	1	2	1	1	3	0	0	0	2	0	0	0	0	0	0	3	25
G04	3	Egg	Recombination rate	3	3	1	2	2	1	1	2	1	2	1	1	0	1	1	1	1	1	2	2	1	0	0	30
G04	4	PB2	Recombination rate	3	2	1	5	4	2	2	2	4	3	3	2	4	1	0	2	3	4	1	0	0	0	2	50
G04	4	Egg	Recombination rate	5	7	3	4	2	2	1	5	0	1	3	1	2	1	1	0	0	1	2	2	1	1	3	48
G04	5	PB2	Recombination rate	3	5	2	4	2	2	0	1	4	3	3	3	4	0	2	2	2	2	0	0	0	0	3	47
G04	5	Egg	Recombination rate	2	3	3	0	2	5	5	4	0	1	0	1	2	2	3	3	1	2	3	2	1	1	3	49
G06	1	PB2	Recombination rate	4	5	3	0	3	3	1	3	4	2	0	2	2	0	0	1	3	2	0	1	1	1	0	41
G06	1	Egg	Recombination rate	0	0	1	0	2	4	1	1	1	4	2	2	1	3	2	1	1	0	3	1	1	0	0	31
G06	2	PB2	Recombination rate	5	6	4	7	6	2	4	4	3	3	1	1	1	1	2	2	2	3	0	3	1	2	5	68
G06	2	Egg	Recombination rate	3	4	5	2	6	3	5	2	1	2	2	2	3	1	1	1	1	3	2	1	0	0	1	51

				Chr 1	Chr 2	Chr 3	Chr 4	Chr 5	Chr 6	Chr 7	Chr 8	Chr 9	Chr 10	Chr 11	Chr 12	Chr 13	Chr 14	Chr 15	Chr 16	Chr 17	Chr 18	Chr 19	Chr 20	Chr 21	Chr 22	Chr X	Total
G06	3	PB2	Recombination rate	5	4	6	4	2	2	4	1	0	5	0	4	1	3	2	0	3	3	1	0	0	0	3	53
G06	3	Egg	Recombination rate	3	6	4	4	3	4	1	1	3	2	3	4	3	0	2	2	2	1	1	2	1	1	2	55
G06	4	PB2	Recombination rate	2	8	1	3	1	2	0	1	1	3	2	1	2	1	1	1	2	1	1	1	0	1	0	36
G06	4	Egg	Recombination rate	3	4	2	3	3	2	3	2	3	3	1	2	3	2	2	2	0	1	1	3	1	1	0	47
G07	1	PB2	Recombination rate	1	3	3	2	2	2	2	2	2	1	3	1	1	0	0	0	2	2	0	2	1	1	0	33
G07	1	Egg	Recombination rate	2	2	4	2	1	3	0	1	2	4	1	1	0	2	0	3	1	0	2	1	1	0	2	35
G08	1	PB2	Recombination rate	2	3	1	4	0	1	1	1	1	1	3	2	1	1	3	1	0	1	1	1	1	0	1	31
G08	1	Egg	Recombination rate	1	2	3	4	2	1	3	1	1	4	1	1	0	1	2	2	1	3	1	1	0	1	1	37
G08	2	PB2	Recombination rate	1	3	2	1	3	3	3	1	2	2	2	1	0	1	0	0	3	0	0	1	0	1	4	34
G08	2	Egg	Recombination rate	3	3	3	3	1	5	1	1	3	1	3	3	2	2	0	3	1	2	2	1	1	2	1	47
G08	3	PB2	Recombination rate	0	2	3	1	3	1	1	0	3	2	0	2	3	0	1	1	2	1	0	1	1	1	0	29
G08	3	Egg	Recombination rate	5	2	4	3	3	3	1	2	2	1	3	2	1	2	2	2	1	1	2	1	1	0	2	46
G09	1	PB2	Recombination rate	2	2	3	2	3	1	0	1	1	1	2	0	2	1	2	0	1	0	1	1	1	1	0	28

				Chr 1	Chr 2	Chr 3	Chr 4	Chr 5	Chr 6	Chr 7	Chr 8	Chr 9	Chr 10	Chr 11	Chr 12	Chr 13	Chr 14	Chr 15	Chr 16	Chr 17	Chr 18	Chr 19	Chr 20	Chr 21	Chr 22	Chr X	Total
G09	1	Egg	Recombination rate	3	2	2	2	0	1	2	1	1	0	0	1	2	3	3	0	0	1	0	1	1	0	1	27
G09	2	PB2	Recombination rate	1	2	0	1	1	1	2	0	2	0	0	1	1	0	0	0	1	1	0	3	0	1	1	19
G09	2	Egg	Recombination rate	2	2	2	1	4	2	1	2	2	2	3	2	0	1	1	1	1	1	1	0	0	0	1	32
Total				67	86	69	65	62	59	47	43	49	54	43	46	41	30	33	33	35	37	27	32	16	16	39	1029
GRC_h37 (Total Lengths)				249.9	243.2	198.02	191.54	180.92	171.12	159.32	146.44	141.7	135.53	135.05	133.85	115.17	107.35	102.53	90.355	81.53	78.082	59.381	63.026	48.158	51.305	155.27	3038.7
Rec. rate (cM/Mb)-build 37				1.0311	1.3600	1.3407	1.3054	1.3188	1.3264	1.1342	1.1297	1.3304	1.5329	1.2245	1.3218	1.3692	1.0748	1.2378	1.4047	1.6511	1.8225	1.7488	1.9528	1.2778	1.1994	0.9660	1.3024

Table 9.11: Map Distances in Oocytes (Ottolini *et al.* 2015)

				Chr 1	Chr 2	Chr 3	Chr 4	Chr 5	Chr 6	Chr 7	Chr 8	Chr 9	Chr 10	Chr 11	Chr 12	Chr 13	Chr 14	Chr 15	Chr 16	Chr 17	Chr 18	Chr 19	Chr 20	Chr 21	Chr 22	Chr X	Total	Average
Donor	**Trio**	**Cell**	**Type**																									
G04	3	PB2	Recombination rate	1.20	0.41	1.51	0.52	0.55	0.58	1.26	0.68	1.41	0.74	0.74	2.24	0.00	0.00	0.00	2.21	0.00	0.00	0.00	0.00	0.00	0.00	1.93	0.82	0.70
G04	3	Egg	Recombination rate	1.20	1.23	0.50	1.04	1.11	0.58	0.63	1.37	0.71	1.48	0.74	0.75	0.00	0.93	0.98	1.11	1.23	1.28	3.37	3.17	2.08	0.00	0.00	0.99	1.11
G04	4	PB2	Recombination rate	1.20	0.82	0.50	2.61	2.21	1.17	1.26	1.37	2.82	2.21	2.22	1.49	3.47	0.93	0.00	2.21	3.68	5.12	1.68	0.00	0.00	0.00	1.29	1.65	1.66
G04	4	Egg	Recombination rate	2.00	2.88	1.51	2.09	1.11	1.17	0.63	3.41	0.00	0.74	2.22	0.75	1.74	0.93	0.98	0.00	0.00	1.28	3.37	3.17	2.08	1.95	1.93	1.58	1.56
G04	5	PB2	Recombination rate	1.20	2.06	1.01	2.09	1.11	1.17	0.00	0.68	2.82	2.21	2.22	2.24	3.47	0.00	1.95	2.21	2.45	2.56	0.00	0.00	0.00	0.00	1.93	1.55	1.45
G04	5	Egg	Recombination rate	0.80	1.23	1.51	0.00	1.11	2.92	3.14	2.73	0.00	0.74	0.00	0.75	1.74	1.86	2.93	3.32	1.23	2.56	5.05	3.17	2.08	1.95	1.93	1.61	1.86
G06	1	PB2	Recombination rate	1.60	2.06	1.51	0.00	1.66	1.75	0.63	2.05	2.82	1.48	0.00	1.49	1.74	0.00	0.00	1.11	3.68	2.56	0.00	1.59	2.08	1.95	0.00	1.35	1.38
G06	1	Egg	Recombination rate	0.00	0.00	0.50	0.00	1.11	2.34	0.63	0.68	0.71	2.95	1.48	1.49	0.87	2.79	1.95	1.11	1.23	0.00	5.05	1.59	2.08	0.00	0.00	1.02	1.24
G06	2	PB2	Recombination rate	2.00	2.47	2.02	3.65	3.32	1.17	2.51	2.73	2.12	2.21	0.74	0.75	0.87	0.93	1.95	2.21	2.45	3.84	0.00	4.76	2.08	3.90	3.22	2.24	2.26
G06	2	Egg	Recombination rate	1.20	1.64	2.52	1.04	3.32	1.75	3.14	1.37	0.71	1.48	1.48	1.49	2.60	0.93	0.98	1.11	1.23	3.84	3.37	1.59	0.00	0.00	0.64	1.68	1.63
G06	3	PB2	Recombination rate	2.00	1.64	3.03	2.09	1.11	1.17	2.51	0.68	0.00	3.69	0.00	2.99	0.87	2.79	1.95	0.00	3.68	3.84	1.68	0.00	0.00	0.00	1.93	1.74	1.64
G06	3	Egg	Recombination rate	1.20	2.47	2.02	2.09	1.66	2.34	0.63	0.68	2.12	1.48	2.22	2.99	2.60	0.00	1.95	2.21	2.45	1.28	1.68	3.17	2.08	1.95	1.29	1.81	1.85

				Chr 1	Chr 2	Chr 3	Chr 4	Chr 5	Chr 6	Chr 7	Chr 8	Chr 9	Chr 10	Chr 11	Chr 12	Chr 13	Chr 14	Chr 15	Chr 16	Chr 17	Chr 18	Chr 19	Chr 20	Chr 21	Chr 22	Chr X	Total	Average
G06	4	PB2	Recombination rate	0.80	3.29	0.50	1.57	0.55	1.17	0.00	0.68	0.71	2.21	1.48	0.75	1.74	0.93	0.98	1.11	2.45	1.28	1.68	1.59	0.00	1.95	0.00	1.18	1.19
G06	4	Egg	Recombination rate	1.20	1.64	1.01	1.57	1.66	1.17	1.88	1.37	2.12	2.21	0.74	1.49	2.60	1.86	1.95	2.21	0.00	1.28	1.68	4.76	2.08	1.95	0.00	1.55	1.67
G07	1	PB2	Recombination rate	0.40	1.23	1.51	1.04	1.11	1.17	1.26	1.37	1.41	0.74	2.22	0.75	0.87	0.00	0.00	0.00	2.45	2.56	0.00	3.17	2.08	1.95	0.00	1.09	1.19
G07	1	Egg	Recombination rate	0.80	0.82	2.02	1.04	0.55	1.75	0.00	0.68	1.41	2.95	0.74	0.75	0.00	1.86	0.00	3.32	1.23	0.00	3.37	1.59	2.08	0.00	1.29	1.15	1.23
G08	1	PB2	Recombination rate	0.80	1.23	0.50	2.09	0.00	0.58	0.63	0.68	0.71	0.74	2.22	1.49	0.87	0.93	2.93	1.11	0.00	1.28	1.68	1.59	2.08	0.00	0.64	1.02	1.08
G08	1	Egg	Recombination rate	0.40	0.82	1.51	2.09	1.11	0.58	1.88	0.68	0.71	2.95	0.74	0.75	0.00	0.93	1.95	2.21	1.23	3.84	1.68	1.59	0.00	1.95	0.64	1.22	1.32
G08	2	PB2	Recombination rate	0.40	1.23	1.01	0.52	1.66	1.75	1.88	0.68	1.41	1.48	1.48	0.75	0.00	0.93	0.00	0.00	3.68	0.00	0.00	1.59	0.00	1.95	2.58	1.12	1.09
G08	2	Egg	Recombination rate	1.20	1.23	1.51	1.57	0.55	2.92	0.63	0.68	2.12	0.74	2.22	2.24	1.74	1.86	0.00	3.32	1.23	2.56	3.37	1.59	2.08	3.90	0.64	1.55	1.73
G08	3	PB2	Recombination rate	0.00	0.82	1.51	0.52	1.66	0.58	0.63	0.00	2.12	1.48	0.00	1.49	2.60	0.00	0.98	1.11	2.45	1.28	0.00	1.59	2.08	1.95	0.00	0.95	1.08
G08	3	Egg	Recombination rate	2.00	0.82	2.02	1.57	1.66	1.75	0.63	1.37	1.41	0.74	2.22	1.49	0.87	1.86	1.95	2.21	1.23	1.28	3.37	1.59	2.08	0.00	1.29	1.51	1.54
G09	1	PB2	Recombination rate	0.80	0.82	1.51	1.04	1.66	0.58	0.00	0.68	0.71	0.74	1.48	0.00	1.74	0.93	1.95	0.00	1.23	0.00	1.68	1.59	2.08	1.95	0.00	0.92	1.01
G09	1	Egg	Recombination rate	1.20	0.82	1.01	1.04	0.00	0.58	1.26	0.68	0.71	0.00	0.00	0.75	1.74	2.79	2.93	0.00	0.00	1.28	0.00	1.59	2.08	0.00	0.64	0.89	0.92
G09	2	PB2	Recombination rate	0.40	0.82	0.00	0.52	0.55	0.58	1.26	0.00	1.41	0.00	0.00	0.75	0.87	0.00	0.00	0.00	1.23	1.28	0.00	4.76	0.00	1.95	0.64	0.63	0.74
G09	2	Egg	Recombination rate	0.80	0.82	1.01	0.52	2.21	1.17	0.63	1.37	1.41	1.48	2.22	1.49	0.00	0.93	0.98	1.11	1.23	1.28	1.68	0.00	0.00	0.00	0.64	1.05	1.00

				Chr 1	Chr 2	Chr 3	Chr 4	Chr 5	Chr 6	Chr 7	Chr 8	Chr 9	Chr 10	Chr 11	Chr 12	Chr 13	Chr 14	Chr 15	Chr 16	Chr 17	Chr 18	Chr 19	Chr 20	Chr 21	Chr 22	Chr X	Total	Average
		Total	Recombination rate	26.81	35.36	34.84	33.94	34.27	34.48	29.50	29.36	34.58	39.84	31.84	34.37	35.60	27.95	32.19	36.52	42.93	47.39	45.47	50.77	33.22	31.19	25.12	33.86	35.11
			GRC_h37 (Total Lengths)	249.90	243.20	198.02	191.54	180.92	171.12	159.32	146.44	141.70	135.53	135.05	133.85	115.17	107.35	102.53	90.35	81.53	78.08	59.38	63.03	48.16	51.30	155.27	3038.74	132.12
Population average (oocyte)			Recombination rate (cM/Mb)	1.08	1.27	1.44	1.20	1.32	1.62	1.21	1.31	1.09	1.53	1.31	1.32	1.27	1.50	1.50	1.79	1.04	1.67	2.85	2.20	1.60	1.05	0.84	33.00	1.43
deCODE				1.34	1.28	1.35	1.35	1.37	1.36	1.38	1.39	1.32	1.52	1.39	1.47	1.27	1.15	1.36	1.65	1.87	1.75	1.94	1.75	1.39	1.29	1.11	33.05	1.44
HapMap				1.15	1.10	1.13	1.12	1.13	1.12	1.18	1.15	1.18	1.34	1.17	1.30	1.09	1.12	1.38	1.48	1.58	1.50	1.81	1.71	1.29	1.44	1.16	29.63	1.29
Hou *et al.* 2013				1.37	1.29	1.43	1.29	1.30	1.34	1.33	1.36	1.32	1.52	1.30	1.46	1.23	1.32	1.30	1.68	1.76	1.84	2.00	1.83	1.53	1.51	1.10	33.41	1.45

Several observations support the conclusion that recombination rates in the adult oocytes and embryos are highly variable, like those seen in unselected, foetal oocytes (Lenzi *et al.* 2005; Cheng *et al.* 2009; Gruhn *et al.* 2013). At the same time, the average recombination frequencies are reminiscent of those reported for human populations. The average number of maternal crossovers in the oocyte or embryos was 41.6 ± 11.3 S.D. (n=51; Tables 9.7-9.11). This rate is consistent with estimates from foetal oocytes and population-based assessments (Broman *et al.* 1998; Kong *et al.* 2002; Tease *et al.* 2002; Kong *et al.* 2004; Myers *et al.* 2005; Coop *et al.* 2008; Kong *et al.* 2008; Hou *et al.* 2013; Kong *et al.* 2014) and those detected in the female pronucleus (42.5 ± 9.0 S.D., n=52) (Kong *et al.* 2010). The frequencies of crossovers detected in the egg correlated well with those in the PB1 or PB2 (Figure 9.7). The maternal recombination rates and the lengths of haplotype blocks were highly variable between donors as well as within donors (Lenzi *et al.* 2005; Cheng *et al.* 2009; Chowdhury *et al.* 2009; Kong *et al.* 2010), varying by as much as two-fold (Figure 9.6b, f and g; Figure 9.7). Using the oocyte-PB trios, maternal crossovers displayed a median distance of 32.4Mb, which was in excess of the 18.3Mb predicted by random distribution of crossovers along chromosomes described in the Methods section 9.3.8. This is consistent with crossover interference along homolog pairs (Hou *et al.* 2013).

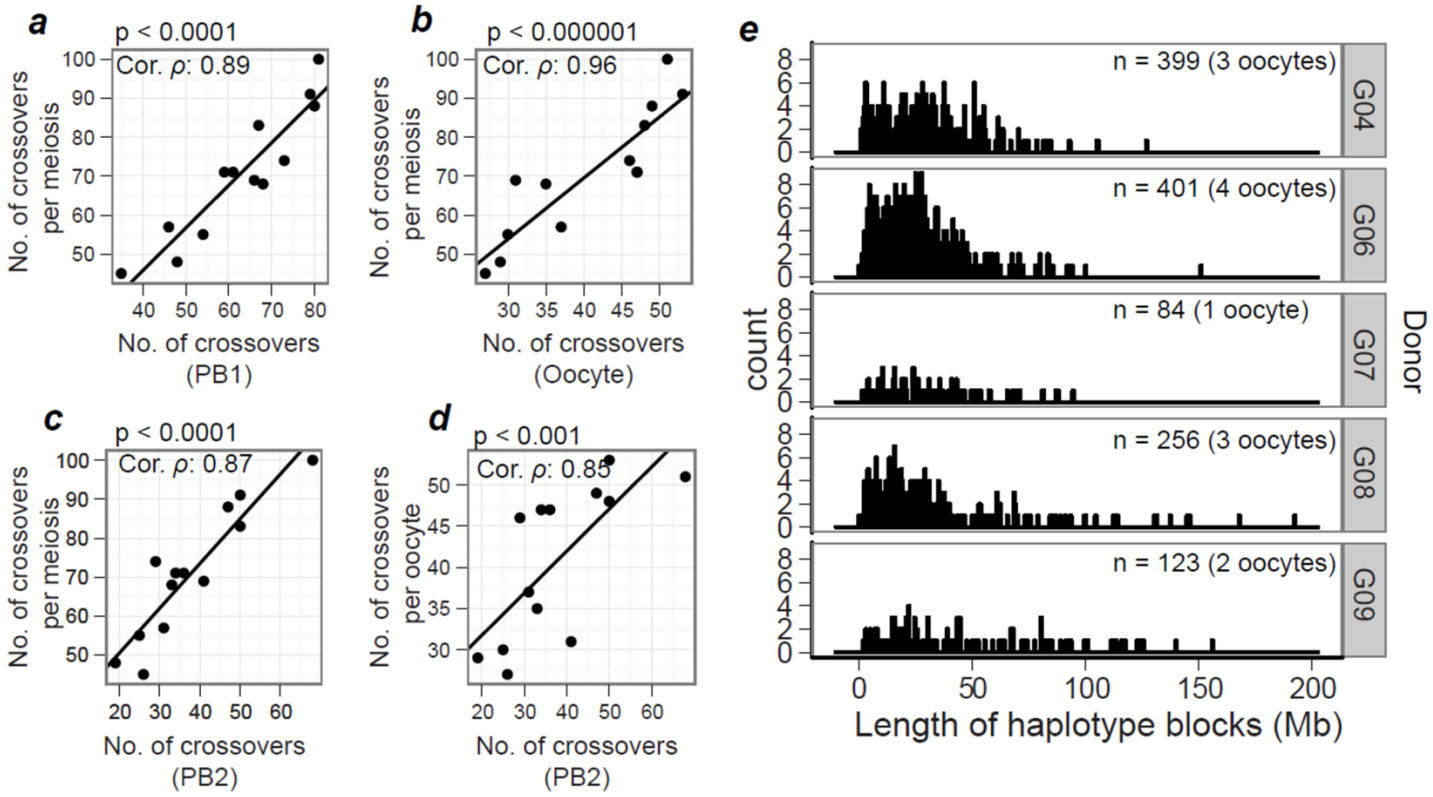

Figure 9.7. Correlation of recombination detected in the oocytes and polar bodies (Ottolini *et al.* 2015).

(a–c) Spearman correlation (ρ) between crossover frequencies per meiosis estimated from the oocyte-PB trio and correlated with counts in PB1 only (a), oocyte only (b) and PB2 (c).

(d) Correlation of crossover events detected in the oocyte as compared to the PB2. (n=13; 5 donors).

(e) Heterogeneity in haplotype lengths in the five different oocyte-PB donors.

Embryos contain informative markers of both maternal and paternal origin. This allows us to assess recombination of both sexes in unselected embryos for the first time. Maternal recombination rates were 1.63-fold higher than paternal rates in the embryos, consistent with population-based studies and molecular approaches on single sperm and foetal oocytes (Kong *et al.* 2002; Lenzi *et al.* 2005; Cheng *et al.* 2009; Gruhn *et al.* 2013; Broman *et al.* 1998; Tease, Hartshorn & Hulten 2002; Kong *et al.* 2004). The additional maternal recombination events are in part from female-only recombination along the X chromosome and in part from higher crossover frequencies on larger autosomes (Figure 9.6d). Maternal recombination was more centromeric compared to paternal events (Figure 9.6e; Figure 9.8), although centromeres tended to suppress nearby recombination (Hou *et al.* 2013; Kong *et al.* 2002; Lenzi *et al.* 2005; Cheng *et al.* 2009; Gruhn *et al.* 2013; Broman *et al.* 1998; Tease, Hartshorn & Hulten 2002; Kong *et al.* 2004) (Figure 9.6f). However, the suppression of centromeric crossovers varied amongst oocyte-PB trios, even within the same woman (Figure 9.6g). This variation may predispose some oocytes to crossovers positioned too close to centromeres that may interfere with segregation. Collectively, these observations reveal that the variation in total crossover numbers detected in adult oocytes is analogous to the variation in Mlh1 counts observed in foetal oocytes (Lenzi *et al.* 2005; Cheng *et al.* 2009; Gruhn *et al.* 2013), suggesting that Mlh1 foci serve as a good proxy for crossover recombination events in human oocytes.

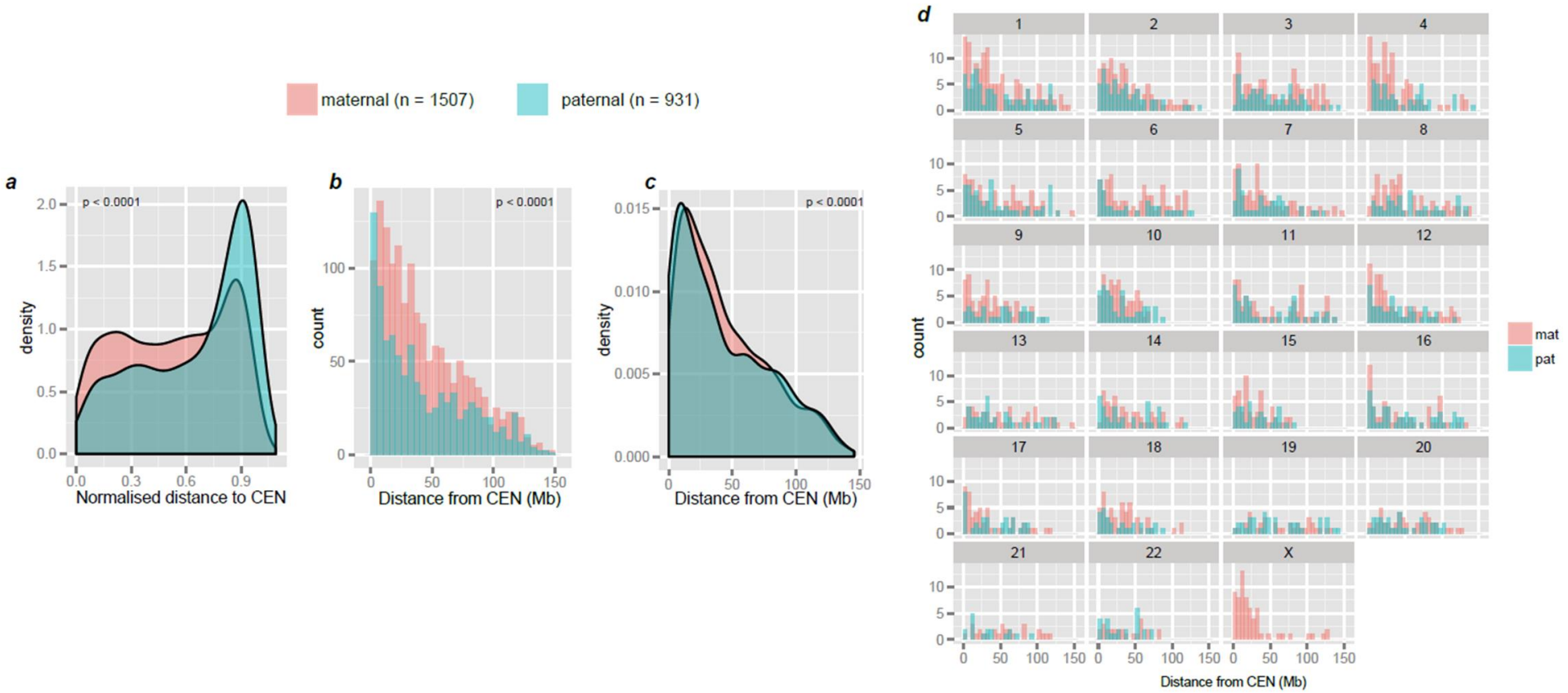

Figure 9.8. Chromosome-specific responses to recombination rates and positions in male and female meiosis (Ottolini *et al.* 2015).

(a) Density curves of the normalised distance of crossovers to centromeres (CEN). Statistics: Kolmogorov-Smirnov test, two-sided. **(b,c)** Histograms and density curves of absolute distances of crossovers to centromeres. Statistics: Kolmogorov-Smirnov test, two-sided. **(d)** Chromosome-specific responses in crossover position along chromosomes in the two sexes.

Simultaneously, the average recombination rates are reminiscent of those in the human population. This validates our approach and lends support to the hypothesis that the variability in the rates and distribution of recombination events between and within individuals give rise to vulnerable crossover configurations in foetal oocytes that are propagated to adult oocytes and, ultimately, embryos.

9.4.4. Global Recombination Rates as a Risk Factor for Aneuploidy

To understand how the variability of maternal recombination rates affects human aneuploidy, I addressed whether the global, genome-wide recombination rates were correlated with the incidence of aneuploidy in individual oocytes and embryos. Indeed, the global recombination rate was a strong predictor of aneuploidy (Figure 9.9a), even when I excluded an outlier embryo, which contained 12 aneuploidies and no detectable crossovers amongst any of the chromosome pairs. The recombination rate is an important factor, accounting for 18% of the variation in the incidence of aneuploidy (outlier excluded; permutation test).

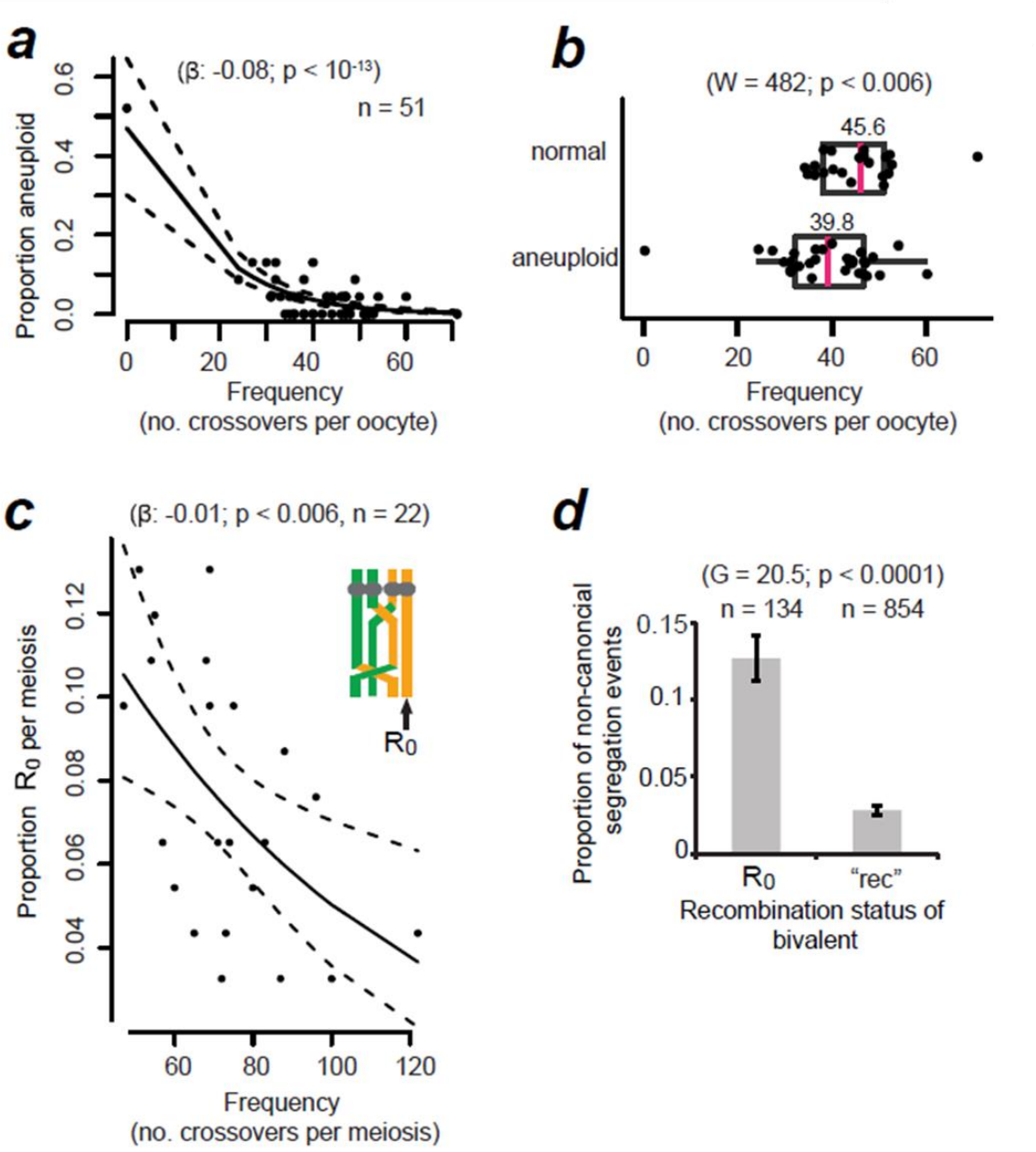

Figure 9.9. Higher global recombination rates protect against aneuploidy and are selected for in the human female germline (Ottolini *et al.* 2015).

(*a*) Logistic regression of the frequency of aneuploid chromosomes as a function of global recombination rate in the embryo or oocyte. Black lines shows logistic regression model and 95% confidence interval (dashed line; binomial family). When the outlier with 0 recombination events was omitted, the regression coefficient β was -0.06 and still highly significant ($p<0.003$). The outlier was omitted from all subsequent statistical analyses.

(*b*) Recombination rates in normal versus aneuploid oocytes and embryos. The arithmetic mean is shown above of the median (magenta, vertical bar). Statistics: Mann-Whitney-Wilcoxon test; one-sided.

(*c*) Incidence of bivalents containing at least one non-recombinant chromatid (R_0) as a function of global recombination rates in oocyte-PB and embryo-PB trios. Statistics as in (*a*).

(*d*) Segregation errors amongst chromosomes that contained one or more R_0 or where all four chromatids had recombined ('rec'). p-values from G-test of heterogeneity (two-sided) are shown. Bars represent standard errors of a proportion ($\sqrt{[p \times (1-p)/n]}$).

If lower global recombination rates predispose oocytes to meiotic chromosome segregation errors, then normal euploid embryos should contain chromosomes that underwent higher maternal genome-wide recombination frequencies than those of aneuploid embryos. To examine whether this was the case, I divided the embryos and oocytes into two groups (euploid or aneuploid) and determined their respective recombination rates (Figure 9.9b). Normal, euploid oocytes and embryos had on average 5.8 recombination events more than aneuploid ones. This difference was significant even when I accounted for crossovers that may not be detected due to the presence of two chromosomes in the aneuploid oocyte (Hou *et al.* 2013). Notably, the overlap in the distribution of recombination rates between the euploid and aneuploid groups is consistent with the presence of other factors that influence the fidelity of chromosome segregation (Nagaoka *et al.* 2012). The findings suggest that higher global recombination frequencies, which are determined during foetal development, protect against errors in chromosome segregation decades later in the adult woman. When errors do occur, they give rise to aneuploidy, many of which are selected against prior to the implantation of the embryo (Capalbo *et al.* 2014). One implication of this is that recombination rates may be under selection in women as they enter their 30s, increasing rates by as much as 14% in women of advanced maternal age (5.8/41.5, the overall average).

9.4.5. Non-Recombinant Chromatids Are at Risk of PSSC

How do global recombination rates affect the segregation outcomes of individual homolog pairs? I hypothesised that lower global recombination rates might increase the risk of generating vulnerable crossover configurations. I first considered non-exchange E_0 homolog pairs, which would give rise to trios, where the PB1 contains one homolog (green or yellow) and the oocyte and PB2 one sister each from the other homolog (Figure 9.10a). Of 529 chromosome pairs, no such example was observed in our data, although one case was observed by Hou *et al.* (personal communication, Hou *et al.* 2013). E_0 may be extremely rare, or another possibility is that they mis-segregate. Indeed, I observed 13 putative E_0 from the 529 chromosome pairs across the 23 trios

(Figure 9.10d-g). The overall incidence (2.6%, n=506) and the overrepresentation of the two smallest chromosomes (21 and 22) are reminiscent of observations of cytological markers for crossovers on foetal chromosomes in meiotic prophase (Lenzi *et al.* 2005; Cheng *et al.* 2009; Gruhn *et al.* 2013). The observed incidence of presumed E_0 was much lower than expected if crossovers were randomly distributed amongst chromosomes (Figure 6.10h), suggestive of crossover assurance mechanism(s) in human oocytes. None of the presumed E_0 chromosomes followed a classical meiotic segregation pattern. Instead they all underwent PSSC or reverse segregation (with or without MII mis-segregation; Figure 9.10). This is consistent with the bi-orientation of sister chromatids of univalent chromosomes at meiosis I in model organisms (LeMaire-Adkins & Hunt 2000; Kouznetsova *et al.* 2007).

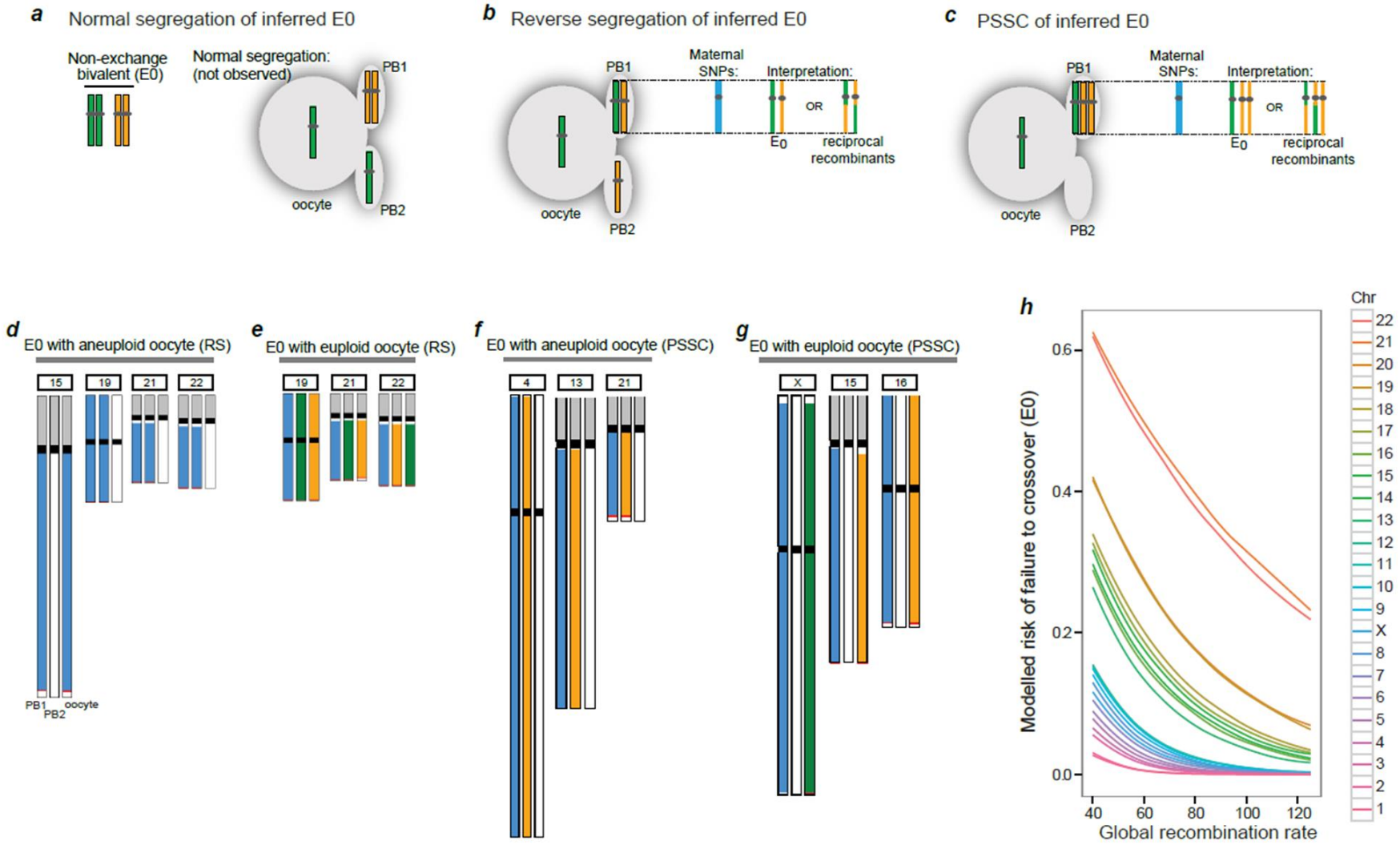

Figure 9.10. Crossover assurance in human female meiosis (Ottolini *et al.* 2015).

(a) A non-exchange or exchange-less chromosome pair (E0) (left). In normal meiosis, non-exchange chromosome pairs can be detected by a single haplotype in the PB1 and the other haplotype in the oocyte and PB2.

(b) E0 chromosomes that undergo reverse segregation cannot be detected directly. This is because the informative SNPs on the two chromatids in the PB1 cannot be phased; hence, potential crossovers (far right) cannot be detected.

(c) PSSC events can result in three chromatids in the PB1. Both maternal SNPs will be present and detected (blue). Since reciprocal crossovers cannot be mapped, the lack of crossovers can only be presumed.

(d-g) Trios with chromosomal content consistent with presumed or putative exchange-less (E0) homologs due to reverse segregation (RS) resulting in two aneuploid cells (d), reverse segregation resulting in normal chromosomal content in all three cells (e), or precocious separation of sister chromatids (PSSC) with an aneuploid (f) or euploid (g) oocyte.

(h) Modelled risk of a chromosome pair failing to receive a crossover (E_0) as a function of global recombination rates, using the range of rates observed in our data sets. Crossovers were allocated randomly to chromosomes with weighted probability using chromosome length; thus, longer chromosomes receive more crossovers. Data are from 10,000 simulations (see Methods section 9.3.9).

Informative SNPs on mis-segregated chromosomes cannot be phased, making crossovers undetectable (Figure 9.11). However, most of the presumed E_0 contained non-recombinant chromatids (R_0). Figure 9.9c shows that global recombination rates are important for determining the generation of R_0, which in turn are at increased risk of mis-segregation compared to fully recombinant bivalents (all four chromatids engaged in recombination; 'rec', Figure 9.9d). Bivalents that contained a R_0 were preferentially involved in PSSC, suggesting that non-recombinant chromatids are at risk of precociously separating from their sister at meiosis I. It is possible that non-recombinant chromatids are at elevated risk of becoming dissociated from the rest of the bivalent during the decades-long dictyate arrest (Wolstenholme & Angell, 2000; Garcia-Cruz *et al.* 2010). I conclude that recombination affects not only the generation and segregation of putative non-exchange homolog pairs, but also influences the dynamics of sister chromatid segregation.

9.4.6. Meiotic Drive for Recombinant Chromatids at Meiosis II

Nonrecombinant chromatids are not only at risk of PSSC, but their segregation at meiosis II is also affected by the lack of recombination. The MeioMaps revealed 135 chromatids in the oocyte or PB2 that were non-recombinant and had segregated normally (Figure 9.11a). These R_0 are expected to be randomly distributed amongst the oocyte and the PB2. Contrary to this expectation, R_0 were nearly twice as likely to be found in the PB2 than the oocyte. The selection appears to be against non-recombinant chromatids, because when both sisters recombined, their segregation was random and the recombination rates were similar in the oocyte and PB2 (Table 9.7). I infer that when the two sister chromatids segregated at meiosis II, non-recombinant chromatids were preferentially driven into the PB2 and thus eliminated from the human germline (Figure 9.11b,c). The use of the asymmetric cell divisions during oogenesis for the preferential inclusion of an allele (Sandler & Novitski 1957) or even whole chromosomes (Dawe & Cande 1996; Pardo-Manuel de Villena & Sapienza 2001; Bongiorni *et al.* 2004) is referred to as meiotic or chromosomal drive. The meiotic drive against non-recombinant chromatids resulted in a 6.6% elevation in the recombination rates in oocytes compared to the PB2s (Table 9.7). These findings

imply that recombination is not only important for the accurate segregation of homologs at meiosis I, but also acts as a driving force during sister chromatid segregation at meiosis II. Selection against non-recombinant chromatids may prevent entire chromosomes from being inherited as a single haplotype block, thereby reducing the probability of inbreeding or propagation of segregation distorters (Haig & Grafen 1991; Brandvain & Coop 2012; Chmatal *et al.* 2014). This may be significant in terms of population structure and the genomic health of children. The difference in genome structure between the PB2 and oocyte is particularly relevant, because the PB2 has been proposed for use in treatment of mitochondrial disease (Wang *et al.* 2014).

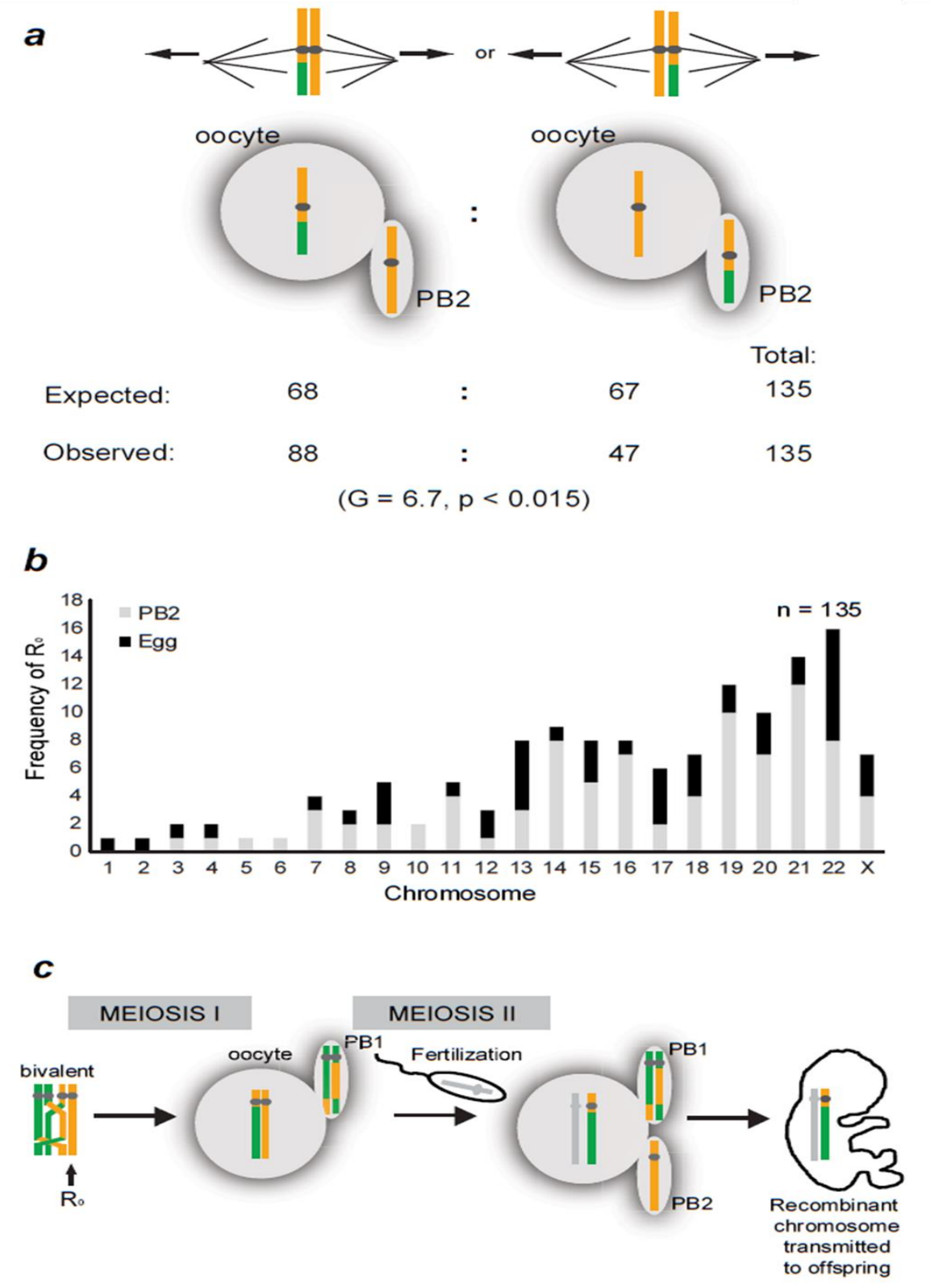

Figure 9.11. Meiotic drive for recombinant chromatids at meiosis II increases recombination rates in the human female germline (Ottolini *et al.* 2015).

(a) Sister chromatids are expected to segregate randomly at meiosis II. However, when chromosomes that contained one non-recombinant chromatid and one recombinant one segregated, the recombinant chromatid was twice as likely to segregate to the oocyte. G-test for proportions (two-sided).

(b) Chromosome-specific frequencies of R_0 chromatids segregating to the PB2 or oocyte.

(c) Diagrammatic representation of meiotic drive against non-recombinant chromatids at meiosis II in the human female germline. Paternal chromosome is shown in grey.

9.5. Discussion

Until recently, recombination and chromosome segregation were studied in populations, where missing polar body information was not available; or in foetal oocytes, which arise decades prior to the segregation events being studied. MeioMaps from unselected adult oocytes, the female pronucleus in zygotes (Hou *et al.* 2013), and embryos, now provide a 'missing link' between events that occur during foetal development and their influence on chromosome segregation outcomes decades later in the adult oocyte.

Recombination rates in the unselected oocytes were 1.6-fold higher than in males and showed a broad distribution, similar to the high degree of variation in foetal oocytes (Lenzi *et al.* 2005; Cheng *et al.* 2009; Gruhn *et al.* 2013). Sex-specific differences in chromosome structure during meiotic prophase have been suggested to explain this difference, with female chromosomes having a longer axis and shorter chromatin loops (Lynn *et al.* 2002). The increased loop number correlates with the increased recombination rate in female meiosis (Lynn *et al.* 2002; Gruhn *et al.* 2013). Although the mean female recombination rates were similar to those seen in populations, the range was substantially broader. I found that lower genome-wide recombination rates were selected against because they were less likely give rise to a euploid oocyte. This is consistent with findings that Down Syndrome individuals have lower genome-wide recombination rates compared to their euploid siblings (Middlebrooks *et al.* 2013). The degree of selection is not observed in younger women (Hou *et al.* 2013) and could contribute to the higher recombination rates in children as mothers age (Kong *et al.* 2004; Coop *et al.* 2008; Campbell *et al.* 2015). This model predicts that children born to younger mothers should display a broader range in recombination frequencies compared to those born to women of advanced maternal age.

Lower genome-wide recombination rates increase the risk of at least two types of vulnerable crossover configurations: non-recombinant chromatids (R_0) and putative non-exchange homologs (E_0). R_0 are a risk factor for PSSC and their preferential segregation to the second polar body at meiosis II (meiotic drive). The putative E_0 either underwent PSSC or a novel reverse segregation pattern, where sister chromatids of both homologs separated at meiosis I, followed by a weak

preference of accurate division of the two non-sister chromatids at meiosis II. The reverse segregation pattern is not limited to E_0 and could be the result of centromeric crossovers that fall at or within 1-2Mb of the centromeres, the positions of the last informative SNPs (Table 9.12). Centromeric crossovers interfere with segregation of sister chromatids in *Drosophila* and budding yeast (Rockmill *et al.* 2006), and are associated with an increased risk of aneuploidy in humans (Nagaoka *et al.* 2012). The relatively high incidence of MII nondisjunction (23%, n=26) associated with reverse segregation could be explained by crossover in the extreme vicinity of centromeres.

Table 9.12: Heterozygous SNP (or Informative SNP) Resolution Near Centromeres of Chromosomes Undergoing Reverse Segregation (Ottolini *et al.* 2015)

Donor ID	chr	Genome Build	pCEN (p-arm)	Closest pCEN SNP on mothers gDNA	Nearest SNP where both haplotypes call in PB1 (p-arm)	Distance (Mb) to last informative SNP (p-arm)	Distance (Mb) to CEN boundary (HCG v37/36)	crossover position on p-arm (Mb)	Distance (Mb) to nearest crossover (p-arm)	pCEN + 3Mb (q-arm)	Closest qCEN SNP on mothers gDNA	Nearest SNP where both haplotypes call in PB1 (q-arm)	Distance (Mb) to last informative SNP (p-arm)	Distance (Mb) to CEN boundary (HCG v37/36)	crossover position on q-arm (Mb)	Distance (Mb) to nearest crossover (q-arm)	no. of CO
G04 - Trio 1	16	GRCh37	35.336	35.070	33.910	1.160	1.426	24.926	10.143	38.336	47.018	47.379	0.361	9.043	78.929	31.911	3
G04 - Trio 3	15	GRCh37	n/a	n/a	n/a	n/a	n/a	n/a	n/a	20.000	20.192	22.870	2.678	2.870	29.194	9.002	4
G06 - Trio 2	14	GRCh37	n/a	n/a	n/a	n/a	n/a	n/a	n/a	19.000	20.296	20.503	0.207	1.503	97.164	76.868	1
G06 - Trio 3	14	GRCh37	n/a	n/a	n/a	n/a	n/a	n/a	n/a	19.000	20.296	20.373	0.077	1.373	51.414	31.119	3
G06 - Trio 3	15	GRCh37	n/a	n/a	n/a	n/a	n/a	n/a	n/a	20.000	22.779	22.837	0.058	2.837	38.007	15.228	3
G08 - Trio 1	4	GRCh37	49.660	48.749	48.749	0.000	0.911	25.598	22.846	52.660	52.991	54.194	1.202	1.534	170.819	118.133	3
G08 - Trio 1	19	GRCh37	24.682	24.468	24.468	0.000	0.214	n/a	n/a	27.682	28.002	28.175	0.174	0.493	37.489	4.904	2
G08 - Trio 2	15	GRCh37	n/a	n/a	n/a	n/a	n/a	n/a	n/a	20.000	20.176	20.176	0.000	0.176	n/a	n/a	n/a
G09 - Trio 2	11	GRCh36	51.451	51.369	48.966	2.403	2.484	24.795	n/a	54.451	55.039	55.708	0.669	1.257	95.106	40.067	3
G09 - Trio 2	15	GRCh36	n/a	n/a	n/a	n/a	n/a	n/a	n/a	18.260	19.970	20.556	0.586	2.296	44.246	24.276	3
G09 - Trio 2	22	GRCh36	n/a	n/a	n/a	n/a	n/a	n/a	n/a	14.330	15.468	15.468	0.000	1.138	26.000	10.532	1
LB03 - Trio 7	16	GRCh37	35.336	34.928	33.910	1.018	1.426	10.422	n/a	38.336	47.379	48.978	1.599	10.643	78.622	31.243	2

Donor ID	chr	Genome Build	pCEN (p-arm)	Closest pCEN SNP on mothers gDNA	Nearest SNP where both haplotypes call in PB1 (p-arm)	Distance (Mb) to last informative SNP (p-arm)	Distance (Mb) to CEN boundary (HCG v37/36)	crossover position on p-arm (Mb)	Distance (Mb) to nearest crossover (p-arm)	pCEN + 3Mb (q-arm)	Closest qCEN SNP on mothers gDNA	Nearest SNP where both haplotypes call in PB1 (q-arm)	Distance (Mb) to last informative SNP (p-arm)	Distance (Mb) to CEN boundary (HCG v37/36)	crossover position on q-arm (Mb)	Distance (Mb) to nearest crossover (q-arm)	no. of CO
LB03 - Trio 7	21	GRCh37	n/a	n/a	n/a	n/a	n/a	n/a	n/a	14.288	14.880	15.617	0.737	1.329	41.202	25.708	1
LB03 - Trio 8	9	GRCh37	47.368	38.757	38.721	0.036	8.647	6.309	32.412	50.368	71.036	71.310	0.274	20.942	113.346	42.302	3
LB03 - Trio 10	16	GRCh37	35.336	34.928	33.837	1.092	1.499	n/a	n/a	38.336	47.379	47.379	0.000	9.043	83.935	36.556	1
LB03 - Trio 10	19	GRCh37	24.682	24.060	23.763	0.297	0.919	none	n/a	27.682	28.485	28.485	0.000	0.803	none	n/a	0
LB03 - Trio 10	21	GRCh37	n/a	n/a	n/a	n/a	n/a	n/a	n/a	14.288	14.880	14.880	0.000	0.592	16.417	1.537	3
LB03 - Trio 10	22	GRCh37	n/a	n/a	n/a	n/a	n/a	n/a	n/a	16.000	17.133	17.203	0.069	1.203	37.081	19.948	1
LB03 - Trio 11	4	GRCh37	49.660	49.054	48.995	0.058	0.665	38.306	10.689	52.660	52.732	52.732	0.000	0.072	97.943	45.211	4
LB03 - Trio 13	16	GRCh37	35.336	34.928	34.428	0.501	0.908	16.987	17.441	38.336	47.379	47.755	0.376	9.419	69.587	21.832	2
LB03 - Trio 13	21	GRCh37	n/a	n/a	n/a	n/a	n/a	none	n/a	14.288	14.880	15.495	0.615	1.207	none	n/a	0
LB03 - Trio 13	22	GRCh37	n/a	n/a	n/a	n/a	n/a	none	n/a	16.000	17.133	17.203	0.069	1.203	none	n/a	0
LB03 - Trio 14	17	GRCh37	22.263	22.099	22.013	0.085	0.250	18.279	3.735	25.263	25.376	25.376	0.000	0.113	55.403	30.027	2
LB03 - Trio 14	19	GRCh37	24.682	24.060	24.060	0.000	0.622	none	n/a	27.682	28.485	28.485	0.000	0.803	none	n/a	0
LB03 - Trio 14	22	GRCh37	n/a	n/a	n/a	n/a	n/a	none	n/a	16.000	17.133	17.203	0.069	1.203	none	n/a	0
LB03 - Trio 16	21	GRCh37	n/a	n/a	n/a	n/a	n/a	none	n/a	14.288	14.880	15.538	0.658	1.250	none	n/a	0

Another possible mechanism that seems particularly plausible for the larger metacentric chromosomes where two crossovers would have to occur within 1Mb on both sides of the centromere, is that homologs segregated their sister chromatids in an equational fashion in MI, followed by a weak preference for accurate non-sister chromatid segregation at MII (77% compared to 50% expected from random; n=26; $p<0.05$). It is possible that failure to establish crossovers (E_0) or maintain the bivalent structure during the extended dictyate arrest may predispose to the equational division at meiosis I. This could occur by deterioration of cohesion between sister chromatids, sister kinetochores, or bivalents falling apart into univalents. There is evidence for the latter in human MI oocytes (Angell 1997; Garcia-Cruz *et al.* 2010), but it is unknown whether their frequencies and chromosome-specific effects match the maternally-derived, age-related component underlying human aneuploidies. In mouse oocytes, univalents preferentially segregate sister chromatids at meiosis I (LeMaire-Adkins & Hunt 2000; Kouznetsova *et al.* 2007) and this may also be case in humans. At meiosis II, non-sister chromatids could be physically attached by unresolved recombination intermediates (joint molecules) (Copsey *et al.* 2013), other threads (Hughes *et al.* 2009; Cabral *et al.* 2014; Heckmann *et al.* 2014), or the oocyte may use segregation mechanisms that do not rely on physical attachment between chromosomes (Hughes-Schrader 1969). The relative contributions of reverse segregation mechanisms and centromeric crossovers remain to be determined, but in either case demonstrate that events attributed to mistakes in chromosome segregation in meiosis II can have their origin at meiosis I in human female meiosis.

10. General Discussion

Since the introduction of molecular cytogenetics into the field of human preimplantation embryos, much information has been gathered on the incidence, origin and aetiology of aneuploidy. However, research into the origin of human aneuploidy is still clearly much needed and will continue to provide new and exciting insights in the field. This thesis has helped to provide some such insight as well as developing tools that could prove useful in both clinical and research areas of preimplantation genetics. In this thesis:

1. State of the art standard protocol set have been produced as frames of reference for embryo biopsy and array CGH.
2. Karyomapping has been confirmed as a tool to detect monogenic disorders (phase and parent of origin), chromosome copy number (including parent of origin of aneuploidies) and meiotic origin of trisomies simultaneously, and be used to pinpoint points of meiotic recombination in preimplantation embryos.
3. The utility of Karyomapping as a genome-wide fingerprint was demonstrated by presenting the first data that polar body DNA can persist to the blastocyst stage of embryo development.
4. By investigating calcium ionophore for oocyte activation, sequential biopsy protocols and adapting the principals of Karyomapping a novel tool was developed to investigate the mechanisms of human female meiosis. This tool was termed MeioMapping.
5. Finally, and most importantly, MeioMapping was used to demonstrate;
    a. Reverse segregation in human oocytes, a pattern of meiotic segregation previously undescribed.
    b. Selection for higher recombination rates in the female germline.
    c. Associations between recombination rates and chromosome mis-segregation (aneuploidy).

d. Meiotic drive for recombinant chromatids at meiosis II in human female meiosis.

The improvement of current technology, including SNP genotyping and MeioMapping-related techniques, will further improve our knowledge of preimplantation aneuploidy. Hopefully the information provided (and published) in this thesis brings these techniques to further application.

What has not been discussed in this thesis is that it has been hypothesised that the high rates of aneuploidy and mosaicism following *in vitro* fertilisation (IVF) procedures may in fact be an iatrogenic artefact of the procedure itself. Ovarian hyperstimulation (Baart *et al.* 2007), fertilisation *in vitro* (Bean *et al.* 2002) and *in vitro* culture environments (IVC) (Carrell *et al.* 2005; Sabhnani *et al.* 2011; Xu *et al.* 2011) appear to affect embryo aneuploidy. A recent randomised controlled trial (RCT) of ovarian stimulation protocols revealed that minimal stimulation, although associated with a reduced number of oocytes, results in higher proportion of chromosomally 'normal' embryos. It was hypothesised that conventional stimulation protocols result mainly in an increase of post zygotic chromosome segregation errors. Altered ovarian function (recruitment of follicles), gonadotrophin dose and GnRH analogue have been offered as potential correlates for further investigation. Furthermore, mouse studies have shown increased meiotic and post zygotic error rates following IVF and IVC respectively (Bean *et al.* 2002; Sabhnani *et al.* 2011). The sensitivity of mouse oocytes to different culture regimens resulting in differing aneuploidy rates corroborates the hypothesis that IVF affects aneuploidy (Carrell *et al.* 2005). In humans, follicle stimulating hormone (FSH) levels associated with *in vitro* maturation correlate with chromosome mal-segregation in the first meiotic division (Xu *et al.* 2011). Animal models could be further employed for manipulation of IVF parameters in an effort to induce or suppress aneuploidy, although clinical IVF itself may provide the best 'experiment' to gain a better understanding of the mechanisms involved in human aneuploidy.

Full genetic sequencing seems the logical next technological advance for preimplantation genetic screening (PGS) and appears technically possible following successful genomic sequencing of microbial single cells (Zhang *et al.* 2006; Lasken 2007). Additional data at the highest possible resolution should inevitably prove more reliable for chromosome copy number analysis and, as

with SNP genotyping, points of recombination as well as points of partial aneuploidy along chromosomes could be analysed with more precision. Currently, increased resolution of PGS is limited by the whole genome amplification (WGA) step (Ling *et al.* 2009). Achieving the highest possible resolution is directly restricted by the phenomenon of allele dropout (ADO) when amplifying single or very few cells. Thus it necessary to invest effort in improving WGA technology before the full benefits of genomic sequencing could be realised. It should be noted at this point that the Karyomapping and MeioMapping work performed in this thesis would adapt easily to sequencing technologies providing a platform with which to move forward for future investigations into the genome of human gametes and preimplantation embryos.

With the increasing amount of data obtained from PGS technologies comes the issue of an increasing amount of 'incidental' findings of unknown pathological significance. Careful considerations of the social, ethical and legal aspects of these findings are required to combat potential problems prior to implementing higher resolution technologies.

The ultimate goal of PGS is to provide maximum benefit (in terms of information to the parent/healthcare provider) with minimal cost to the embryo. The possibility of gaining chromosome copy number information with no cost to the embryo would enable PGS to be used routinely as an embryo selection tool for IVF. An indirect aneuploidy screening test was first explored by associations with conventional embryo morphology scoring. However, morphological embryo grading is apparently at its limits to improve IVF success rates and has only shown very limited correlation with aneuploidy (Munné 2006; Gianaroli *et al.* 2007; Alfarawati *et al.* 2011a).

The implementation of time-lapse imaging to embryo culture has facilitated high-resolution morphokinetic analysis of embryo development in an attempt to improve IVF success rates and eliminate potentially abnormally developing embryos. Morphokinetic analysis involves continual analysis of the morphological state and rates of change during oocyte and embryo development and provides evidence of developmental milestones that can predict embryo implantation (Meseguer *et al.* 2011). Since, cells of different genotypes are known to have slightly different cell cycle times (Varrela *et al.* 1989), it follows that algorithms involving multiple developmental time

points could be used to predict embryo aneuploidy at no cost to the embryo. Embryos with an abnormal karyotype (particularly those with multiple abnormalities) may have aberrant cell cycles, detectable by morphokinetic analysis, compared with normal embryos. New studies into the morphological rates of change, including such developmental markers as PB extrusion, syngamy and early mitotic divisions, could find more significant correlations with chromosome mal-segregation than embryo morphology alone. However investigators must be sure to perform the correct analysis of results as premature implementation of new screening tests may end up creating a similar situation to Fluorescent In-situ Hybridisation (FISH) in the mid-2000s. It is potentially easy to fall into the trap of publishing unsound data in the rush to uncover a non-invasive chromosome screening test that would revolutionise the field of IVF.

Take for example two recently published papers demonstrating the utility of algorythms using time-lapse imaging for aneuploidy detection. These two articles by Campbell *et al.* (2013a, b) prematurely describe an algorithm using time-lapse imaging for aneuploidy risk classification of human preimplantation embryos. What follows is adapted from a published commentary (Ottolini, Capalbo & Rienzi 2013). On the basis of their results, the authors of these two papers postulated that by using specific morphokinetic markers they could reliably select euploid embryos for transfer. Thus, increasing pregnancy rates and reducing miscarriage rates due to aneuploidy. Although I believe that the authors have identified developmental time points – time from insemination to blastulation (tSB) and time of insemination to full blastocyst (tB) – that can be used to establish an embryo's implantation potential in their culture system, I believe that the study is underpowered and that maternal age rather than specifically embryo aneuploidy is likely to be the causative factor. First, it is my opinion that there may be no need to analyse both tSB and tB since these time points appear to be highly linked, as shown by the authors (Campbell *et al.* 2013a). The apparent linear relationship between the two variables, from the point of insemination, suggests that using only one of the variables would likely result in similar statistically significant findings. I conclude that the two articles by Campbell *et al.* are based on the premise that faster developing blastocysts are more likely to be euploid and hence implant and result in a

pregnancy. Kroener *et al.* (2012) clearly show that delayed blastulation is not associated with increased aneuploidy rates. Based on these data, and some observations from the work in this thesis, I believe that there is no evidence to suggest that Day 6 blastocysts have a higher rate of aneuploidy and lower rate of implantation when compared with Day 5 blastocysts (at least when comparing embryos within the same IVF cycle or from an age-matched population), rendering any screening test for early blastocyst formation impractical as a risk assessment for embryo aneuploidy. I therefore postulate that the observed difference in implantation in the author's data set could be attributed to factors other than chromosome copy number. A recent meta-analysis of data from the Society for Assisted Reproductive Technologies in the USA highlighted the significant difference in success rates of IVF when treating patients of differing age groups (Cohen *et al.* 2012). It is well established in human IVF that implantation potential of embryos from patients of advanced maternal age are reduced when compared with younger patient groups (Scott *et al.* 2012) and that blastocyst formation and hatching are negatively correlated with maternal age (Porter *et al.* 2002). It is also well established that embryo aneuploidy levels increase with advancing maternal age (Munné *et al.* 2007). Thus, in a non-age-controlled study population, there should always be higher aneuploidy rates in slower developing blastocysts. In the paper by Campbell *et al.* in which they modelled the risk classification (Campbell *et al.* 2013a), the reader was informed that 25 couples were enrolled in the study group, with an age range of 31-47 years. No data was provided about maternal age of the 97 analysed embryos that fell within the three aneuploidy risk classifications (low, medium and high). As no maternal age data of the embryos within each risk classification was provided, it is logical to assume (from the evidence presented above) that the differential of embryo development and rates of aneuploidy between younger and older patients have created a bias in the findings. This is a confounding factor in the study and a serious statistical flaw resulting in potential bias in the results. It is therefore possible that the algorithm is predictive of maternal age alone. In order for this retrospective study to rule out an age-related affect, the authors needed to perform a logistic regression analysis adjusted for maternal age to see if the algorithm was predictive of aneuploidy alone. I conclude that using their algorithm, the authors are in fact able to predict the

chromosome copy number of any one particular embryo from their study group as a whole. However, the authors have failed to demonstrate whether the algorithm has the same predictive value of aneuploidy and implantation potential when applied within a cohort of embryos from a single IVF cycle or a controlled patient population. Likewise in the retrospective implantation analysis paper (Campbell *et al.* 2013b), no age data were presented for the embryos that were within the three risk classification groups. I propose that, although the implantation rates between the three classification groups were found to be significantly different, the large maternal age range of patients enrolled in the study (from 25 to 47 years) creates a bias. Maternal age must be considered as a potential confounder of these observed differences. Again, as we know that embryos from younger patients have a greater change of implantation, the authors should provide age data for the classification groups. This is the only way to rule out the possibility that they are not merely separating their study group into three age classifications (low, medium and high). It should be also noted that both studies – the one in which the algorithm was developed (Campbell *et al.* 2013a) and the one in which it was applied retrospectively (Campbell *et al.* 2013b) – are based on a relatively small sample size (97 and 88 blastocysts respectively) with significant overlap within the low and medium classification groups. In the retrospective analysis, the only group without overlapping was the high-risk group where only four embryos were included, making this classification totally underpowered to be of statistical and clinical relevance. I fundamentally disagree with the author's statements that their algorithm has the ability to screen out embryos with the highest risk for aneuploidy, and could be offered to patients as an alternative to PGS with potentially as much as a 3-fold increase in implantation rate. Making such conclusions are misleading without data from a larger, age-matched study group or a prospective, randomised controlled trial to confirm their findings. In fact, in more recently published data on a larger patient population, using logistic regression analysis adjusted for the maternal age effect, no evidence of association between blastocyst aneuploidy and morphokinetic assessment was observed (Rienzi *et al.* 2015).

There are however potentially more promising approaches to non-invasive assessment of embryo viability include the measurement of what is used by or what is secreted by the oocyte or embryo. All culture media contain substances that are required for embryo development. Culture media will also contain all products secreted by the oocyte or embryo. Levels of these can be measured in a variety of ways to establish embryo viability (for review see Aydiner *et al.* 2010).

Analysis of spent culture media is an area already being explored as potential for a new indirect PGS platform. A recent study analysing uptake patterns of amino acids has shown that regulation of amino acid metabolism correlates with embryo aneuploidy. The study using FISH analysis of five chromosomes (13, 18, 21, X and Y) demonstrated altered amino acid turnover in embryos with grossly abnormal karyotypes when compared to genetically normal embryos (Picton *et al.* 2010). Although promising, this early data lacks specificity and further work is needed to more accurately establish how embryo metabolism may be indicative of its chromosomal complement. Precise metabolic profiling of embryos with known copy number aberrations is proposed as a specific experiment to establish more meaningful correlations.

A further approach is based on the hypothesis of altered gene expression and protein synthesis of chromosomally abnormal embryos. One study, using a proteomic approach, has identified the first protein secreted by human blastocysts – Lipocalin-1 that is associated with generic chromosome aneuploidy (McReynolds *et al.* 2011) – promising the biggest step to date towards a non-invasive PGS test.

Although the idea of a non-invasive aneuploidy screening test for embryos is very appealing, the reality is that embryo biopsy is likely to remain the only viable option for many years to come and PGS is likely to continue to be one of the most controversial areas of reproductive medicine. However, the entire community is united in its collective will to improve IVF success, reduce miscarriage rates and ensure that couples avoid children with developmental abnormalities. Thus, advancing our knowledge of aneuploidy in the preimplantation embryo remains key. The means by which this is achieved remains the subject of intense debate. What can be clear however is

that the controversy will serve to increase the interest in PGS, hopefully leading to new and radical future treatments.

11. Bibliography

(2008a) A long term analysis of the HFEA Register data (1991-2006). HFEA Website 1.

Agca Y, Monson RL, Northey DL, Peschel DE, Schaefer DM, Rutledge JJ (1998). Normal calves from transfer of biopsied, sexed and vitrified IVP bovine embryos. Theriogenology. 50(1):129-45.

Alfarawati S, Fragouli E, Colls P & Wells D (2011a). First births after preimplantation genetic diagnosis of structural chromosome abnormalities using comparative genomic hybridisation and microarray analysis. Hum Reprod 26, 1560-74.

Alfarawati S, Fragouli E, Colls P, Stevens J, Gutierrez-Mateo C, Schoolcraft WB, Katz-Jaffe MG & Wells D (2011b). The relationship between blastocyst morphology, chromosomal abnormality, and embryo gender. Fertil Steril 95, 520-4.

Alfarawati S, E Fragouli *et al.* (2011). 'The relationship between blastocyst morphology, chromosomal abnormality, and embryo gender.' Fertility and sterility 95(2): 520-524.

Almeida PA & Bolton VN (1996). The relationship between chromosomal abnormality in the human preimplantation embryo and development in vitro. Reprod Fertil Dev 8, 235-41.

American Society of Reproductive Medicine (ASRM) Practice Committee (2008). Preimplantation genetic testing: a Practice Committee opinion. Fertil Steril 90, S136-43.

Anderson RA & Pickering S (2008). The current status of preimplantation genetic screening: British Fertility Society Policy and Practice Guidelines. Hum Fertil (Camb) 11, 71-5.

Angell R (1997). 'First-meiotic-division nondisjunction in human oocytes.' American journal of human genetics 61(1): 23-32.

Angell RR (1991). Predivision in human oocytes at meiosis I: a mechanism for trisomy formation in man. Hum Genet 86, 383-387.

Angell RR, Templeton AA & Aitken RJ (1986). Chromosome studies in human in vitro fertilization. Hum.Genet. 72, 333-9.

Angell RR, Xian J & Keith J (1993). Chromosome anomalies in human oocytes in relation to age. Hum.Reprod 8, 1047-54.

Angell RR, Xian J, Keith J, Ledger W & Baird DT (1994). First meiotic division abnormalities in human oocytes: mechanism of trisomy formation. Cytogenet.Cell Genet. 65, 194-202.

Antczak M, Van Blerkom J (1997). Oocyte influences on early development: the regulatory proteins leptin and STAT3 are polarised in mouse and human oocytes and differentially distributed within the cells of the preimplantation stage embryo. Mol Hum Reprod 3: 1067-86.

Ao A, Handyside AH (1995). Cleavage stage human embryo biopsy. Hum Reprod Update 1: 3.

Aydiner F, Yetkin CE & Seli E (2010). Perspectives on emerging biomarkers for non-invasive assessment of embryo viability in assisted reproduction. Curr Mol Med 10, 206-15.

Baart EB, Martini E, Eijkemans MJ, Van Opstal D, Beckers NG, Verhoeff A, Macklon NS & Fauser BC (2007). Milder ovarian stimulation for in-vitro fertilization reduces aneuploidy in the human preimplantation embryo: a randomized controlled trial. Hum Reprod 22, 980-8.

Baart EB, Martini E, van den Berg I, Macklon NS, Galjaard RJ, Fauser BC *et al.* (2006). Preimplantation genetic screening reveals a high incidence of aneuploidy and mosaicism in embryos from young women undergoing IVF. Hum Reprod. 21(1):223-33.

Banerjee I, Shevlin M, Taranissi M, Thornhill A, Abdalla H, Ozturk O, Barnes J, Sutcliffe A (2008). Health of children conceived after preimplantation genetic diagnosis: a preliminary outcome study. Reprod Biomed Online. 16(3):376-81.

Baranyai B, Bodo S, Dinnyes A, Gocza E (2005). Vitrification of biopsied mouse embryos. Acta Vet Hung. 53(1):103-12.

Bean CJ, Hassold TJ, Judis L & Hunt PA (2002). Fertilization in vitro increases non-disjunction during early cleavage divisions in a mouse model system. Hum Reprod 17, 2362-7.

Bean CJ, Hunt PA, Millie EA & Hassold TJ (2001). Analysis of a malsegregating mouse Y chromosome: evidence that the earliest cleavage divisions of the mammalian embryo are non-disjunction-prone. Hum Mol Genet 10, 963-72.

Bielanska M, Tan SL, Ao A (2002). Chromosomal mosaicism throughout human preimplantation development in vitro: incidence, type, and relevance to embryo outcome. Hum Reprod. 17(2):413-9.

Bisignano A, Wells D, Harton G, Munné S (2011). PGD and aneuploidy screening for 24 chromosomes: advantages and disadvantages of competing platforms. Reprod Biomed Online. 23(6):677-85.

Blockeel C, Schutyser V, De Vos A, Verpoest W, De Vos M, Staessen C, Haentjens P, Van der Elst J & Devroey P (2008). Prospectively randomized controlled trial of PGS in IVF/ICSI patients with poor implantation. Reprod Biomed Online 17, 848-54.

Boada M, Carrera M, De La Iglesia C, Sandalinas M, Barri PN, Veiga A (1998). Successful use of a laser for human embryo biopsy in preimplantation genetic diagnosis: report of two cases. J Assist Reprod Genet 15: 302–7.

Bongiorni, S, P Fiorenzo *et al.* (2004). 'Inverted meiosis and meiotic drive in mealybugs.' Chromosoma 112(7): 331-341.

Brandvain Y and G Coop (2012). 'Scrambling eggs: meiotic drive and the evolution of female recombination rates.' Genetics 190(2): 709-723.

Braude P, Bolton V & Moore S (1988). Human gene expression first occurs between the four- and eight-cell stages of preimplantation development. Nature 332, 459-61.

Brezina PR, Benner A, Rechitsky S, Kuliev A, Pomerantseva E, Pauling D & Kearns WG (2011). Single-gene testing combined with single nucleotide polymorphism microarray preimplantation genetic diagnosis for aneuploidy: a novel approach in optimising pregnancy outcome. Fertil Steril 95, 1786 e5-8.

Broman KW, Weber JL (2000). Characterisation of human crossover interference. Am J Hum Genet;66:1911-26.

Broman, KW, JC Murray *et al.* (1998). 'Comprehensive human genetic maps: individual and sex-specific variation in recombination.' American journal of human genetics 63(3): 861-869.

Cabral, G, A Marques *et al.* (2014). 'Chiasmatic and achiasmatic inverted meiosis of plants with holocentric chromosomes.' Nature communications 5: 5070.

Campbell A, Fishel S, Bowman N, Duffy S, Sedler M, Hickman CF (2013a). Modelling a risk classification of aneuploidy in human embryos using non-invasive morphokinetics. Reprod Biomed Online. 26(5):477-85.

Campbell, A, Fishel, S, Bowman, N, Duffy, S, Sedler, M, Thornton, S (2013b). Retrospective analysis of outcomes after IVF using an aneuploidy risk model derived from time-lapse imaging without PGS. Reprod. Biomed. Online. 27, 140–146.

Campbell, CL, NA Furlotte *et al.* (2015). 'Escape from crossover interference increases with maternal age.' Nature communications 6: 6260.

Capalbo A, Wright G, Themaat L, Elliott T, Rienzi L, Nagy ZP (2011). FISH reanalysis of inner cell mass and trophectoderm samples of previously arrayCGH screened blastocysts reveals high accuracy of diagnosis and no sign of mosaicism or preferential allocation. Fertil Steril 96 (3) S22

Capalbo A, Bono S, Spizzichino L, Biricik A, Baldi M, Colamaria S, Ubaldi FM, Rienzi L, and Fiorentino F (2013). Sequential comprehensive chromosome analysis on polar bodies, blastomeres and trophoblast: insights into female meiotic errors and chromosomal segregation in the preimplantation window of embryo development. Hum Reprod 28, 509-18.

Capalbo A, Rienzi L, Cimadomo D, Maggiulli R, Elliott T, Wright G, Nagy ZP, and Ubaldi FM (2014). Correlation between standard blastocyst morphology, euploidy and implantation: an

observational study in two centres involving 956 screened blastocysts. Hum Reprod 29, 1173-81.

Capalbo A, Wright G, Elliott T, Ubaldi FM, Rienzi L and Nagy ZP (2013b). FISH reanalysis of inner cell mass and trophectoderm samples of previously array-CGH screened blastocysts shows high accuracy of diagnosis and no major diagnostic impact of mosaicism at the blastocyst stage. Hum Reprod 28, 2298-307.

Carrell DT, Liu L, Huang I & Peterson CM (2005). Comparison of maturation, meiotic competence, and chromosome aneuploidy of oocytes derived from two protocols for in vitro culture of mouse secondary follicles. J Assist Reprod Genet 22, 347-54.

Chatzimeletiou K, Mossison E, Panagiotidis Y, Prapas N, Prapas Y, Rutherford AJ, Grudzinskas G, Handyside AH (2005). Comparison of effects of zona drilling by non-contact infrared laser or acid Tyrode's on the development of human biopsied embryos as revealed by blastomere viability, cytoskeletal analysis and molecular cytogenetics. Reprod BioMed Online 11: 697–710.

Chatzimeletiou K, Picton HM, Handyside AH (2001). Use of a non-contact, infrared laser for zona drilling of mouse embryos: assessment of immediate effects on blastomere viability. Reprod BioMed Online 2: 178–87.

Chavez S, Loewke K, Han J, Moussavi F, Colls P, Munné S, Behr B, Reijo Pera RA (2012). Dynamic blastomere behaviour reflects human embryo ploidy by the four-cell stage. Nature Comm 3:1251

Chen SU, Chao KH, Wu MY, Chen CD, Ho HN, Yang YS (1998). A simplified two-pipette technique is more efficient than the conventional three-pipette method for blastomere biopsy in human embryos. Fertil Steril 69: 569–75.

Cheng EY, PA Hunt *et al.* (2009). 'Meiotic recombination in human oocytes.' PLoS genetics 5(9): e1000661.

Chmatal L, SI Gabriel *et al.* (2014). 'Centromere strength provides the cell biological basis for meiotic drive and karyotype evolution in mice.' Current biology : CB 24(19): 2295-2300.

Cho CK & Diamandis EP (2011). Application of proteomics to prenatal screening and diagnosis for aneuploidies. Clin Chem Lab Med 49, 33-41.

Chowdhury R, PR Bois *et al.* (2009). 'Genetic analysis of variation in human meiotic recombination.' PLoS genetics 5(9): e1000648.

Christopikou D, E Tsorva, K Economou, P Shelley, S Davies, M Mastrominas and AH Handyside (2013). 'Polar body analysis by array comparative genomic hybridisation accurately predicts aneuploidies of maternal meiotic origin in cleavage stage embryos of women of advanced maternal age.' Human reproduction 28(5): 1426-1434.

Cieslak J, Ivakhnenko V, Wolf G, Sheleg S, Verlinsky Y (1999). Three-dimensional partial zona dissection for preimplantation genetic diagnosis and assisted hatching. Fertil Steril 71: 308–13.

Cieslak-Janzen J, Tur-Kaspa I, Ilkevitch Y, Bernal A, Morris R, Verlinsky Y (2006). Multiple micromanipulations for preimplantation genetic diagnosis do not affect embryo development to the blastocyst stage. Fertil Steril. 85(6):1826-9.

Cohen J, Alikani M, Bisignano A (2012). Past performance of assisted reproduction technologies as a model to predict future progress: a proposed addendum to Moore's law. Reprod. Biomed. Online 25, 585–590.

Cohen J, Malter H, Wright G, Kort H, Massey J, Mitchell D (1989). Partial zona dissection of human oocytes when failure of zona pellucida penetration is anticipated. Hum Reprod 4: 435–42.

Cohen J, Wells D, Munné S (2007). Removal of 2 cells from cleavage stage embryos is likely to reduce the efficacy of chromosomal tests that are used to enhance implantation rates. Fertil Steril. 87(3):496-503.

Cohen J & Grifo JA (2007). Multicentre trial of preimplantation genetic screening reported in the New England Journal of Medicine: an in-depth look at the findings. Reprod Biomed Online 15, 365-6.

Cohen J, Wells D, Howles CM & Munné S (2009). The role of preimplantation genetic diagnosis in diagnosing embryo aneuploidy. Curr Opin Obstet Gynecol 21, 442-9.

Coonen E, Derhaag JG, Dumoulin JCM, Wissen LCP van, Bras M, Janssen M, Evers JLH, Geraedts JPM. Anaphase lagging mainly explains chromosomal mosaicism in human preimplantation embryos. Hum Reprod [Internet] 2004;19:316–324.

Coop G, X Wen *et al.* (2008). 'High-resolution mapping of crossovers reveals extensive variation in fine-scale recombination patterns among humans.' Science 319(5868): 1395-1398.

Copsey A, S Tang *et al.* (2013). 'Smc5/6 coordinates formation and resolution of joint molecules with chromosome morphology to ensure meiotic divisions.' PLoS genetics 9(12): e1004071.

Corveleyn A, Morris MA, Dequeker E, Sermon K, Davies JL, Antiñolo G *et al.* (2008). Provision and quality assurance of preimplantation genetic diagnosis in Europe. Eur J Hum Genet. 16(3):290-9.

Coutelle C, Williams C, Handyside A, Hardy K, Winston R, Williamson R (1989). Genetic analysis of DNA from single human oocytes: a model for preimplantation diagnosis of cystic fibrosis. Br Med J 299: 22–4.

Dailey T, Dale B, Cohen J & Munné S (1996a). Association between nondisjunction and maternal age in meiosis-II human oocytes. Am J Hum Genet 59, 176-84.

Dailey T, Dale B, Cohen J & Munné S (1996b). Association between nondisjunction and maternal age in meiosis-II human oocytes. Am.J.Hum.Genet. 59, 176-84.

Daphnis DD, Delhanty JD, Jerkovic S, Geyer J, Craft I & Harper JC (2005). Detailed FISH analysis of day 5 human embryos reveals the mechanisms leading to mosaic aneuploidy. Hum Reprod 20, 129-37.

Dawe RK and WZ Cande (1996). 'Induction of centromeric activity in maize by suppressor of meiotic drive 1.' Proceedings of the National Academy of Sciences of the United States of America 93(16): 8512-8517.

de Boer KA, Catt JW, Jansen RP, Leigh D, McArthur S (2004). Moving to blastocyst biopsy for preimplantation genetic diagnosis and single embryo transfer at Sydney IVF. Fertil Steril. 82(2):295-8.

Deans Z, Fiorentino F, Biricik A, Traeger-Synodinos J, Moutou C, De Rycke M, Renwick P, Sengupta S, Goossens V, Harton G (2013). The experience of 3 years of external quality assessment of preimplantation genetic diagnosis for cystic fibrosis. Eur J Hum Genet. 21(8):800-6.

Debrock S, Melotte C, Spiessens C, Peeraer K, Vanneste E, Meeuwis L, Meuleman C, Frijns JP, Vermeesch JR & D'Hooghe TM (2010). Preimplantation genetic screening for aneuploidy of embryos after in vitro fertilization in women aged at least 35 years: a prospective randomized trial. Fertil Steril 93, 364-73.

Delhanty JD (2005). Mechanisms of aneuploidy induction in human oogenesis and early embryogenesis. Cytogenet Genome Res 111, 237-44.

Delhanty JDA. Inherited aneuploidy: germline mosaicism. Cytogenet Genome Res [Internet] 2011;133:136–140.

Derhaag JG, Coonen E, Bras M, Bergers Janssen JM, Ignoul-Vanvuchelen R, Geraedts JP, Evers JL, Dumoulin JC (2003). Chromosomally abnormal cells are not selected for the extra-embryonic compartment of the human preimplantation embryo at the blastocyst stage. Hum Reprod. 18(12):2565-74.

Dokras A, Sargent IL, Ross C, Gardner RL, Barlow DH (1990). Trophectoderm biopsy in human blastocysts. Hum Reprod 5: 821–5.

Dokras A, Sargent IL, Ross C, Gardner RL, Barlow DH (1991). The human blastocyst: morphology and human chorionic gonadotrophin secretion in vitro. Hum Reprod 6: 1143–51.

Dreesen JC, Geraedts JP, Dumoulin JC, Evers JL, Pieters MH (1995). RS46(DXS548) genotyping of reproductive cells: approaching preimplantation testing of the fragile-X syndrome. Hum Genet. 96(3):323-9.

Dreesen JC, Jacobs LJ, Bras M, Herbergs J, Dumoulin JC, Geraedts JPM, Evers JLH, Smeets HJM (2000). Multiplex PCR of polymorphic markers flanking the CFTR gene; a general approach for preimplantation genetic diagnosis of cystic fibrosis. Mol Hum Reprod;6:391-396.

Dumoulin JC, Bras M, Coonen E, Dreesen J, Geraedts JP, Evers JL (1998). Effect of Ca2+/Mg2+-free medium on the biopsy procedure for preimplantation genetic diagnosis and further development of human embryos. Hum Reprod 13: 2880-3.

Egozcue S, Blanco J, Vidal F & Egozcue J (2002). Diploid sperm and the origin of triploidy. Hum Reprod 17, 5-7.

Eldadah ZA, Grifo JA, Dietz HC (1995). Marfan syndrome as a paradigm for transcript-targeted preimplantation diagnosis of heterozygous mutations. Nat Med. 1(8):798-803.

Esfandiari N, Javed MH, Gotlieb L & Casper RF (2005). Complete failed fertilisation after intracytoplasmic sperm injection – analysis of 10 years' data. International Journal of Fertility and Women's Medicine, 50(4), 187-92. Retrieved from http://www.ncbi.nlm.nih.gov/pubmed/16405104

Evsikov S, Verlinsky Y (1998). Mosaicism in the inner cell mass of human blastocysts. Hum Reprod. 13(11):3151-5.

Findlay I, P Ray, P Quirke, A Rutherford and R Lilford (1995). 'Allelic drop-out and preferential amplification in single cells and human blastomeres: implications for preimplantation diagnosis of sex and cystic fibrosis.' Hum Reprod 10(6): 1609-1618.

Fiorentino F, Biricik A, Nuccitelli A, De Palma R, Kahraman S, Iacobelli M, Trengia V, Caserta D, Bonu MA, Borini A, Baldi M (2006). Strategies and clinical outcome of 250 cycles of Preimplantation Genetic Diagnosis for single gene disorders. Hum Reprod;21:670-84.

Fiorentino F, Kahraman S, Karadayi H, Biricik A, Sertyel S, Karlikaya G, Saglam Y, Podini D, Nuccitelli A, Baldi M (2005). Short tandem repeats haplotyping of the HLA region in preimplantation HLA matching. Eur J Hum Genet;13:953-8.

Fiorentino F, Kokkali G, Biricik A, Stavrou D, Ismailoglu B, De Palma R, Arizzi L, Harton G, Sessa M, Pantos K (2010). Polymerase chain reaction-based detection of chromosomal imbalances on embryos: the evolution of preimplantation genetic diagnosis for chromosomal translocations. Fertil Steril;94:2001-11, 2011.e1-6.

Fiorentino F (2012a). Array comparative genomic hybridisation: its role in preimplantation genetic diagnosis. Curr Opin Obstet Gynecol. 24(4):203-9.

Fiorentino F (2012b). Molecular genetic analysis of single cells. Semin Reprod Med. 30(4):267-82.

Flaherty SP, Payne D, Swann NJ, & Mattews CD (1995). Aetiology of failed and abnormal fertilisation after intracytoplasmic sperm injection. Human Reproduction (Oxford, England), 10(10), 2623–9. Retrieved from http://www.ncbi.nlm.nih.gov/pubmed/8567782

Fonseka KGL, Griffin DK. Is there a paternal age effect for aneuploidy? Cytogenet Genome Res [Internet] 2011;133:280–291.

Fragouli E, Alfarawati S, Goodall NN, Sanchez-Garcia JF, Colls P & Wells D (2011). The cytogenetics of polar bodies: insights into female meiosis and the diagnosis of aneuploidy. Mol Hum Reprod.

Fragouli E, Wells D, Thornhill A, Serhal P, Faed MJ, Harper JC & Delhanty JD (2006). Comparative genomic hybridization analysis of human oocytes and polar bodies. Hum Reprod 21, 2319-28.

Fragouli E, Alfarawati S, Spath K, Jaroudi S, Sarasa J, Enciso M, Wells D (2013). The origin and impact of embryonic aneuploidy. Hum Genet. Apr 26. [Epub ahead of print]

Fragouli E, Lenzi M, Ross R, Katz-Jaffe M, Schoolcraft WB, Wells D (2008). Comprehensive molecular cytogenetic analysis of the human blastocyst stage. Hum Reprod. 23:2596-608.

Fragouli E, Alfarawati S, Daphnis DD, Goodall NN, Mania A, Griffiths T, Gordon A, Wells D (2011). Cytogenetic analysis of human blastocysts with the use of FISH, CGH and aCGH: scientific data and technical evaluation. Hum.Reprod. 26, 480-490.

Franasiak JM, Forman EJ, Hong KH, Werner MD, Upham KM, Treff NR, & Scott RT (2014). The nature of aneuploidy with increasing age of the female partner: a review of 15,169 consecutive trophectoderm biopsies evaluated with comprehensive chromosomal screening. Fertility and Sterility, 101(3), 656–663.e1. doi:10.1016/j.fertnstert.2013.11.004

Freeman SB, EG Allen *et al.* (2007). 'The National Down Syndrome Project: design and implementation.' Public health reports 122(1): 62-72.

Fritz MA. Perspectives on the efficacy and indications for preimplantation genetic screening: where are we now? Hum Reprod [Internet] 2008;23:2617–2621.

Fulton BP and DG Whittingham (1978). 'Activation of mammalian oocytes by intracellular injection of calcium.' Nature 273(5658): 149-151.

Gabriel AS, Hassold TJ, Thornhill AR, Affara NA, Handyside AH & Griffin DK (2011). An algorithm for determining the origin of trisomy and the positions of chiasmata from SNP genotype data. Chromosome Res 19, 155-63.

Gabriel AS, Thornhill AR, Ottolini CS, Gordon A, Brown APC, Taylor J, Griffin DK (2011). Array comparative genomic hybridisation on first polar bodies suggests that nondisjunction is not

the predominant mechanism leading to aneuploidy in humans. Journal of Medical Genetics, 48(7), 433-7.

Garcia-Cruz R, A Casanovas *et al.* (2010). 'Cytogenetic analyses of human oocytes provide new data on nondisjunction mechanisms and the origin of trisomy 16.' Human reproduction 25(1): 179-191.

Garcia-Cruz R, MA Brieno *et al.* (2010). 'Dynamics of cohesin proteins REC8, STAG3, SMC1 beta and SMC3 are consistent with a role in sister chromatid cohesion during meiosis in human oocytes.' Human reproduction 25(9): 2316-2327.

Gardner RL, Edwards RG. Control of the sex ratio at full term in the rabbit by transferring sexed blastocysts. Nature [Internet] 1968;218:346–349.

Geber S, Winston RM, Handyside AH (1995). Proliferation of blastomeres from biopsied cleavage stage human embryos in vitro: an alternative to blastocyst biopsy for preimplantation diagnosis. Hum Reprod 10: 1492–6.

Geraedts J, Handyside A, Harper J, Liebaers I, Sermon K, Staessen C *et al.* (1999). ESHRE Preimplantation Genetic Diagnosis (PGD) Consortium: preliminary assessment of data from January 1997 to September 1998. ESHRE PGD Consortium Steering Committee. Hum Reprod. 14(12):3138-48.

Geraedts J, Montag M, Magli MC, Repping S, Handyside A, Staessen C, Harper J, Schmutzler A, Collins J, Goossens V, van der Ven H, Vesela K & Gianaroli L (2011). Polar body array CGH for prediction of the status of the corresponding oocyte. Part I: clinical results. Hum Reprod. 26(11):3173-80

Germond M, Nocera D, Senn A, Rink K, Delacrétaz G, Fakan S (1995). Microdissection of mouse and human zona pellucida using a 1.48-microns diode laser beam: efficacy and safety of the procedure. Fertil Steril. 64(3):604-11.

Gianaroli L (2000). Preimplantation genetic diagnosis: polar body and embryo biopsy. Hum Reprod 15 Suppl 4, 69-75.

Gianaroli L, Magli MC, Ferraretti AP, Lappi M, Borghi E & Ermini B (2007). Oocyte euploidy, pronuclear zygote morphology and embryo chromosomal complement. Hum Reprod 22, 241-9.

Glujovsky D, Blake D, Farquhar C, Bardach A (2012). Cleavage stage versus blastocyst stage embryo transfer in assisted reproductive technology. Cochrane Database of Systematic Reviews Issue 7. [DOI: 10.1002/ 14651858.CD002118.pub4]

Goossens V, De Rycke M, De Vos A, Staessen C, Michiels A, Verpoest W *et al.* (2008). Diagnostic efficiency, embryonic development and clinical outcome after the biopsy of one or two blastomeres for preimplantation genetic diagnosis. Hum Reprod. 23(3):481-92.

Gordon JW, Talansky BE (1986). Assisted fertilisation by zona drilling: a mouse model for correction of oligospermia. J Exp Zool 239: 347–54.

Griffin DK, Abruzzo MA, Millie EA, Sheean LA, Feingold E, Sherman SL & Hassold TJ (1995). Non-disjunction in human sperm: evidence for an effect of increasing paternal age. Hum Mol Genet 4, 2227-32.

Griffin DK, Wilton LJ, Handyside AH, Winston RM & Delhanty JD (1992). Dual fluorescent in situ hybridisation for simultaneous detection of X and Y chromosome-specific probes for the sexing of human preimplantation embryonic nuclei. Hum.Genet. 89, 18-22.

Griffin DK. (1996) The incidence, origin and etiology of aneuploidy. Int Rev Cytol;167:263-296

Grossmann M, Calafell JM, Brandy N, Vanrell JA, Rubio C, Pellicer A, Egozcue J, Vidal F & Santalo J (1997). Origin of tripronucleate zygotes after intracytoplasmic sperm injection. Hum Reprod 12, 2762-5.

Gruhn JR, C Rubio, KW Broman, PA Hunt and T Hassold (2013). 'Cytological studies of human meiosis: sex-specific differences in recombination originate at, or prior to, establishment of double-strand breaks.' PloS one 8(12): e85075.

Gutierrez-Mateo C, Benet J, Wells D, Colls P, Bermudez MG, Sanchez-Garcia JF, Egozcue J, Navarro J & Munné S (2004). Aneuploidy study of human oocytes first polar body comparative genomic hybridisation and metaphase II fluorescence in situ hybridization analysis. Hum Reprod 19, 2859-68.

Gutierrez-Mateo C, Colls P, Sanchez-Garcia J, Escudero T, Prates R, Ketterson K, Wells D & Munné S (2011). Validation of microarray comparative genomic hybridisation for comprehensive chromosome analysis of embryos. Fertil Steril 95, 953-8.

Haig D and A Grafen (1991). 'Genetic scrambling as a defence against meiotic drive.' Journal of theoretical biology 153(4): 531-558.

Han TS, Sagoskin AW, Graham JR, Tucker MJ, Liebermann J (2003). Laser-assisted human embryo biopsy on the third day of development for preimplantation genetic diagnosis: two successful case reports. Fertil Steril 80: 453–5.

Handyside AH, Harton GL, Mariani B, Thornhill AR, Affara N, Shaw MA & Griffin DK (2010). Karyomapping: a universal method for genome wide analysis of genetic disease based on mapping crossovers between parental haplotypes. J Med Genet 47, 651-8.

Handyside AH, Montag M, Magli MC, Repping S, Harper JC, Schmutzler A, Vesela K, Gianaroli L, Geraedts J (2012). Multiple meiotic errors caused by predivision of chromatids in women of advanced maternal age undergoing in vitro fertilisation. Eur J Hum Genet;20(7):742-7.

Handyside AH & Thornhill AR (2007). In vitro fertilisation with preimplantation genetic screening. N Engl J Med 357, 1770; author reply -1.

Handyside AH, Xu K (2012). Preimplantation genetic diagnosis comes of age. Semin Reprod Med;30:255-8.

Handyside AH (2013). 24-chromosome copy number analysis: a comparison of available technologies. Fertil Steril. 100(3):595-602

Handyside AH, Delhanty JD (1997). Preimplantation genetic diagnosis: strategies and surprises. Trends Genet 13: 270–5.

Handyside AH, Kontogianni EH, Hardy K, Winston RM (1990). Pregnancies from biopsied human preimplantation embryos sexed by Y-specific DNA amplification. Nature (London) 344: 768–70.

Handyside AH, Lesko JG, Tarín JJ, Winston RM, Hughes MR (1992). Birth of a normal girl after in vitro fertilisation and preimplantation diagnostic testing for cystic fibrosis. [see comments]. N Engl J Med;327(13):905–909

Handyside AH, Robinson MD, Simpson RJ, Omar MB, Shaw MA, Grudzinskas JG, Rutherford A (2004). Isothermal whole genome amplification from single and small numbers of cells: a new era for preimplantation genetic diagnosis of inherited disease. Mol Hum Reprod;10:767-72.

Handyside AH, Thornhill AR (1998). Cleavage stage embryo biopsy for preimplantation genetic diagnosis. In: Kempers RD, Cohen J, Haney AF, Younger JB, eds. Fertility and Reproductive Medicine. Amsterdam: Elsevier, 223–9.

Handyside AH, Thornhill AR, Harton GL, Mariani B, Shaw MA, Affara N, Griffin DK (2010). Karyomapping: a novel molecular karyotyping method based on mapping crossovers between parental haplotypes with broad applications for preimplantation genetic diagnosis of inherited disease. J Med Genet;47:651-658.

Hardarson T, Hanson C, Lundin K, Hillensjo T, Nilsson L, Stevic J, Reismer E, Borg K, Wikland M & Bergh C (2008). Preimplantation genetic screening in women of advanced maternal age caused a decrease in clinical pregnancy rate: a randomized controlled trial. Hum Reprod 23, 2806-12.

Hardy K, Martin KL, Leese HJ, Winston RML, Handyside AH (1990). Human preimplantation development in vitro is not adversely affected by biopsy at the 8-cell stage. Hum Reprod 5: 708–14.

Harper JC, Boelaert K, Geraedts J, Harton G, Kearns WG, Moutou C, Muntjewerff N, Repping S, SenGupta S, Scriven PN, Traeger-Synodinos J, Vesela K, Wilton L & Sermon KD (2006). ESHRE PGD Consortium data collection V: cycles from January to December 2002 with pregnancy follow-up to October 2003. Hum Reprod 21, 3-21.

Harper JC, Coonen E, Handyside AH, Winston RM, Hopman AH, Delhanty JD (1995). Mosaicism of autosomes and sex chromosomes in morphologically normal, monospermic preimplantation human embryos. Prenat Diagn. 15(1):41-9

Harper JC, Coonen E, Ramaekers FC *et al.* (1994). Identification of the sex of human preimplantation embryos in two hours using an improved spreading method and fluorescent in-situ hybridisation (FISH) using directly labelled probes. Hum Reprod 9: 721–4.

Harper JC, Wilton L, Traeger-Synodinos J, Goossens V, Moutou C, SenGupta SB, Pehlivan Budak T, Renwick P, De Rycke M, Geraedts JP, Harton G (2012). The ESHRE PGD Consortium: 10 years of data collection. Hum Reprod Update. 18(3):234-47

Harrison RH, Kuo HC, Scriven PN, Handyside AH & Ogilvie CM (2000). Lack of cell cycle checkpoints in human cleavage stage embryos revealed by a clonal pattern of chromosomal mosaicism analysed by sequential multicolour FISH. Zygote 8, 217-24.

Harton GL, De Rycke M, Fiorentino F, Moutou C, SenGupta S, Traeger-Synodinos J, Harper JC (2011). European Society for Human Reproduction and Embryology (ESHRE) PGD Consortium. ESHRE PGD consortium best practice guidelines for amplification-based PGD. Hum Reprod.;26(1):33-40

Harton GL, Magli MC, Lundin K, Montag M, Lemmen J, Harper JC; European Society for Human Reproduction and Embryology (ESHRE) PGD Consortium/Embryology Special Interest Group (2011) ESHRE PGD Consortium/Embryology Special Interest Group--best practice guidelines for polar body and embryo biopsy for preimplantation genetic diagnosis/screening (PGD/PGS) Hum Reprod. 26(1):41-6

Harton GL, Munné S, Surrey M, Grifo J, Kaplan B, McCulloh DH, Griffin DK, Wells D. Diminished effect of maternal age on implantation after preimplantation genetic diagnosis with array comparative genomic hybridisation. Fertil Steril [Internet] 2013;100:1695–1703.

Hassold T, Hall H & Hunt P (2007). The origin of human aneuploidy: where we have been, where we are going. Hum Mol Genet 16 Spec No. 2, R203-8.

Hassold T and P Hunt (2001). 'To err (meiotically) is human: the genesis of human aneuploidy.' Nature reviews. Genetics 2(4): 280-291.

Hassold TJ and PA Jacobs (1984). 'Trisomy in man.' Annual review of genetics 18: 69-97.

Hassold T, M Merrill, K Adkins, S Freeman and S Sherman (1995). 'Recombination and maternal age-dependent nondisjunction: molecular studies of trisomy 16.' American journal of human genetics 57(4): 867-874.

Hassold T, N Chen *et al.* (1980). 'A cytogenetic study of 1000 spontaneous abortions.' Annals of human genetics 44(Pt 2): 151-178.

Hassold TJ (1986). Chromosome abnormalities in human reproductive wastage. Trends Genet. 2, 105-10.

Heckmann S, M Jankowska *et al.* (2014). 'Alternative meiotic chromatid segregation in the holocentric plant Luzula elegans.' Nature communications 5: 4979.

Heindryckx B, Van der Elst J, De Sutter P & Dhont, M (2005). Treatment option for sperm- or oocyte-related fertilisation failure: assisted oocyte activation following diagnostic heterologous ICSI. Human Reproduction (Oxford, England), 20(8), 2237-41. doi:10.1093/humrep/dei029

Hellani A, Abu-Amero K, Azouri J & El-Akoum S (2008). Successful pregnancies after application of array-comparative genomic hybridisation in PGS-aneuploidy screening. Reprod Biomed Online 17, 841-7.

Henningsen AK, Pinborg A, Lidegaard O, Vestergaard C, Forman JL, Andersen AN (2011). Perinatal outcome of singleton siblings born after assisted reproductive technology and spontaneous conception: Danish national sibling-cohort study. Fertil Steril 95(3):959-63

Hens K, Dondorp W, Handyside AH, Harper J, Newson AJ, Pennings G, Rehmann-Sutter C, de Wert G (2013). Dynamics and ethics of comprehensive preimplantation genetic testing: a review of the challenges. Hum Reprod Update.;19(4):366-75.

Heytens E, Parrington J, Coward K, Young C, Lambrecht S, Yoon S-Y, De Sutter P (2009). Reduced amounts and abnormal forms of phospholipase C zeta (PLCzeta) in spermatozoa from infertile men. Human Reproduction (Oxford, England), 24(10), 2417–28. doi:10.1093/humrep/dep207

Holding C, Bentley D, Roberts R, Bobrow M, Mathew C (1993). Development and validation of laboratory procedures for preimplantation diagnosis of Duchenne muscular dystrophy. J Med Genet. 30(11):903-9.

Holding C, Monk M (1989). Diagnosis of b-thalassaemia by DNA amplification in single blastomeres from mouse preimplantation embryos. Lancet 2: 532–5.

Hou Y, W Fan, L Yan, R Li, Y Lian, J Huang, J Li, L Xu, F Tang, XS Xie and J Qiao (2013). 'Genome analyses of single human oocytes.' Cell 155(7): 1492-1506.

Hughes SE, WD Gilliland *et al.* (2009). 'Heterochromatic threads connect oscillating chromosomes during prometaphase I in Drosophila oocytes.' PLoS genetics 5(1): e1000348.

Hughes-Schrader S (1969). 'Distance segregation and compound sex chromosomes in mantispids (Neuroptera:Mantispidae).' Chromosoma 27(2): 109-129.

Hulten MA, S Patel *et al.* (2010). 'On the origin of the maternal age effect in trisomy 21 Down syndrome: the Oocyte Mosaicism Selection model.' Reproduction 139(1): 1-9.

Human Fertilisation and Embryology Act 1990 (as amended 2008)

Inzunza J, Iwarsson E, Fridstrom M *et al.* (1998). Application of single-needle blastomere biopsy in human preimplantation genetic diagnosis. Prenat Diagn. 8(13):1381-8.

Ioannou D, Meershoek EJ, Thornhill AR, Ellis M & Griffin DK (2011). Multicolour interphase cytogenetics: 24 chromosome probes, 6 colours, 4 layers. Mol Cell Probes.

Isachenko V, Montag M, Isachenko E, van der Ven H (2005). Vitrification of mouse pronuclear embryos after polar body biopsy without direct contact with liquid nitrogen. Fertil Steril. 84(4):1011-.

James R, West J (1994). A chimaeric animal model for confined placental mosaicism. Hum Genet. 93(5):603-4.

Janny L & Menezo YJ (1996). Maternal age effect on early human embryonic development and blastocyst formation. Mol Reprod Dev 45, 31-7.

Javed R & Mukesh (2010). Current research status, databases and application of single nucleotide polymorphism. Pak J Biol Sci 13, 657-63.

Jericho H, Wilton L, Gook DA, Edgar DH (2003). A modified cryopreservation method increases the survival of human biopsied cleavage stage embryos. Hum Reprod 18: 568–71.

Johnson DS, Cinnioglu C, Ross R, Filby A, Gemelos G, Hill M, Ryan A, Smotrich D, Rabinowitz M, Murray MJ (2010a). Comprehensive analysis of karyotypic mosaicism between trophectoderm and inner cell mass. Mol Hum Reprod 16, 944-9

Johnson DS, Gemelos G, Baner J, Ryan A, Cinnioglu C, Banjevic M, Ross R, Alper M, Barrett B, Frederick J, Potter D, Behr B & Rabinowitz M (2010b). Preclinical validation of a microarray method for full molecular karyotyping of blastomeres in a 24-h protocol. Hum Reprod 25, 1066-75.

Jones A, Wright M, Kort H, Straub R, Nagy Z (2006). Comparison of laser-assisted hatching and acidified Tyrode's hatching by evaluation of blastocyst development in sibling embryos: a prospective randomised study. Fertil Steril 85: 487-491

Joris H, De Vos A, Janssens R, Devroey P, Liebaers I, Van Steirteghem A (2003). Comparison of the results of human embryo biopsy and outcome of PGD after zona drilling using acid Tyrode medium or a laser. Hum Reprod 18: 1896–902.

Joris H, Van den Abbeel E, Vos AD, Van Steirteghem A (1999). Reduced survival after human embryo biopsy and subsequent cryopreservation. Hum Reprod 14: 2833–7.

Kallioniemi A, Kallioniemi OP, Sudar D, Rutovitz D, Gray JW, Waldman F & Pinkel D (1992). Comparative genomic hybridisation for molecular cytogenetic analysis of solid tumors. Science 258, 818-21.

Kallioniemi OP, Kallioniemi A, Sudar D, Rutovitz D, Gray JW, Waldman F & Pinkel D (1993). Comparative genomic hybridisation: a rapid new method for detecting and mapping DNA amplification in tumors. Semin Cancer Biol 4, 41-6.

Kalousek D, Vekemans M (1996). Confined placental mosaicism. J Med Genet. 33(7):529-33..

Kaplan B, Wolf G, Kovalinskaya L, Verlinsky Y (1995). Viability of embryos following second polar body removal in a mouse model. J Assist Reprod Genet. 12(10):747-9.

Kashir J, Heindryckx B, Jones C, De Sutter P, Parrington J, & Coward K. Oocyte activation, phospholipase C zeta and human infertility. Human Reproduction Update, 16(6), 690–703. doi:10.1093/humupd/dmq018

Kaufman MH (1982). The chromosome complement of single-pronuclear haploid mouse embryos following activation by ethanol treatment. Journal of Embryology and Experimental Morphology, 71, 139–54. Retrieved from http://www.ncbi.nlm.nih.gov/pubmed/7153693

Khalaf Y, El-Toukhy T, Coomarasamy A, Kamal A, Bolton V, Braude P (2008). Selective single blastocyst transfer reduces the multiple pregnancy rate and increases pregnancy rates: a pre- and postintervention study. BJOG. 115(3):385-90.

Kline D & Kline JT (1992). Repetitive calcium transients and the role of calcium in exocytosis and cell cycle activation in the mouse egg. Developmental Biology, 149(1), 80–9. Retrieved from http://www.ncbi.nlm.nih.gov/pubmed/1728596

Koehler KE, CL Boulton *et al.* (1996). 'Spontaneous X chromosome MI and MII nondisjunction events in Drosophila melanogaster oocytes have different recombinational histories.' Nature genetics 14(4): 406-414.

Kokkali G, Traeger-Synodinos J, Vrettou C, Stavrou D, Jones GM, Cram DS *et al.* (2007). Blastocyst biopsy versus cleavage stage biopsy and blastocyst transfer for preimplantation genetic diagnosis of beta-thalassaemia: a pilot study. Hum Reprod. 22(5):1443-9.

Kokkali G, Vrettou C, Traeger-Synodinos J, Jones GM, Cram DS, Stavrou D *et al.* (2005). Birth of a healthy infant following trophectoderm biopsy from blastocysts for PGD of beta-thalassaemia major. Hum Reprod. 20(7):1855-9.

Kolialexi A, Tounta G, Mavrou A & Tsangaris GT (2011). Proteomic analysis of amniotic fluid for the diagnosis of fetal aneuploidies. Expert Rev Proteomics 8, 175-85.

Kong A, DF Gudbjartsson *et al.* (2002). 'A high-resolution recombination map of the human genome.' Nature genetics 31(3): 241-247.

Kong A, G Thorleifsson *et al.* (2008). 'Sequence variants in the RNF212 gene associate with genome-wide recombination rate.' Science 319(5868): 1398-1401.

Kong A, G Thorleifsson *et al.* (2010). 'Fine-scale recombination rate differences between sexes, populations and individuals.' Nature 467(7319): 1099-1103.

Kong A, G Thorleifsson *et al.* (2014). 'Common and low-frequency variants associated with genome-wide recombination rate.' Nature genetics 46(1): 11-16.

Kong A, J Barnard, DF Gudbjartsson, G Thorleifsson, G Jonsdottir, S Sigurdardottir, B Richardsson, J Jonsdottir, T Thorgeirsson, ML Frigge, NE Lamb, S Sherman, JR Gulcher

and K Stefansson (2004). 'Recombination rate and reproductive success in humans.' Nature genetics 36(11): 1203-1206.

Konstantinidis M, Prates R, Goodall N, Fischer J, Tecson V, Lemmaa T, Chua B, Jordana A, Armentia E, Wells D, Munné S (2015). Live Births following Karyomapping of Human Blastocysts – Experience from Clinical Application of the Method. Reprod Biomed Online

Kouznetsova A, L Lister *et al.* (2007). 'Bi-orientation of achiasmatic chromosomes in meiosis I oocytes contributes to aneuploidy in mice.' Nature genetics 39(8): 966-968.

Kroener L, Ambartsumyan G, Briton-Jones C, Dumesic D, Surrey M, Munné S, Hill D (2012). The effect of timing of embryonic progression on chromosomal abnormality. Fertil. Steril. 98, 876–880.

Kuliev A, Cieslak J, Ilkevitch Y & Verlinsky Y (2003). Chromosomal abnormalities in a series of 6,733 human oocytes in preimplantation diagnosis for age-related aneuploidies. Reprod Biomed Online 6, 54-9.

Kuliev A, Cieslak J & Verlinsky Y (2005). Frequency and distribution of chromosome abnormalities in human oocytes. Cytogenet Genome Res 111, 193-8.

Kuliev A, Zlatopolsky Z, Kirillova I, Spivakova J, Cieslak Janzen J (2011). Meiosis errors in over 20,000 oocytes studied in the practice of preimplantation aneuploidy testing. Reprod Biomed Online.;22(1):2-8.

Kuo HC, Ogilvie CM, Handyside AH (1998). Chromosomal mosaicism in cleavage-stage human embryos and the accuracy of single-cell genetic analysis. J Assist Reprod Genet 15: 276–80.

Kuwayama M (2007). Highly efficient vitrification for cryopreservation of human oocytes and embryos: the Cryotop method. Theriogenology 67, 73-80.

Kuwayama M, Vajta G, Kato O & Leibo SP (2005). Highly efficient vitrification method for cryopreservation of human oocytes. Reprod Biomed Online 11, 300-308.

Lamb NE, Feingold E, Savage A, Avramopoulos D, Freeman S, Gu Y, Hallberg A, Hersey J, Karadima G, Pettay D, Saker D, Shen J, Taft L, Mikkelsen M, Petersen MB, Hassold T & Sherman SL (1997). Characterisation of susceptible chiasma configurations that increase the risk for maternal nondisjunction of chromosome 21. Hum Mol Genet 6, 1391-9.

Lamb NE, Freeman SB, Savage-Austin A, Pettay D, Taft L, Hersey J, Gu Y, Shen J, Saker D, May KM, Avramopoulos D, Petersen MB, Hallberg A, Mikkelsen M, Hassold TJ & Sherman SL (1996). Susceptible chiasmate configurations of chromosome 21 predispose to non-disjunction in both maternal meiosis I and meiosis II. Nat Genet 14, 400-5.

Lanzendorf S, Ratts V, Moley K *et al.* (2007). A randomised, prospective study comparing laser-assisted hatching and assisted hatching using acidifed medium. Fertil Steril 87: 1450-7.

Lasken RS (2007). Single-cell genomic sequencing using Multiple Displacement Amplification. Curr Opin Microbiol 10, 510-6.

Lee HC, Arny M, Grow D, Dumesic D, Fissore RA, & Jellerette-Nolan T (2014). Protein phospholipase C Zeta1 expression in patients with failed ICSI but with normal sperm parameters. Journal of Assisted Reproduction and Genetics, 31(6), 749–56. doi:10.1007/s10815-014-0229-9

LeMaire-Adkins R and PA Hunt (2000). 'Nonrandom segregation of the mouse univalent X chromosome: evidence of spindle-mediated meiotic drive.' Genetics 156(2): 775-783.

Lenzi ML, J Smith *et al.* (2005). 'Extreme heterogeneity in the molecular events leading to the establishment of chiasmata during meiosis i in human oocytes.' American journal of human genetics 76(1): 112-127.

Levinson G, Fields RA, Harton GL, Palmer FT, Maddalena A, Fugger EF *et al.* (1992). Reliable gender screening for human preimplantation embryos, using multiple DNA target-sequences. Hum Reprod. 7(9):1304-13.

Li A, Gyllenstein UB, Cui X, Saiki RK, Erlich HA, Arnheim N (1988). Amplification and analysis of DNA sequences in single human sperm and diploid cells. Nature (London) 335: 414–19.

Liebermann J (2015). Vitrification: a simple and successful method for cryostorage of human blastocysts. Methods Mol Biol 1257, 305-19.

Ling J, Zhuang G, Tazon-Vega B, Zhang C, Cao B, Rosenwaks Z & Xu K (2009). Evaluation of genome coverage and fidelity of multiple displacement amplification from single cells by SNP array. Mol Hum Reprod 15, 739-47.

Liu J, Van den Abbeel E, Van Steirteghem A (1993). The in-vitro and in-vivo developmental potential of frozen and non-frozen biopsied 8-cell mouse embryos. Hum Reprod. 8(9):1481-6.

Liu J, Nagy Z, Joris H, Tournaye H, Smitz J, Camus M, Van Steirteghem A (1995). Analysis of 76 total fertilisation failure cycles out of 2732 intracytoplasmic sperm injection cycles. Human Reproduction (Oxford, England), 10(10), 2630–6. Retrieved from http://www.ncbi.nlm.nih.gov/pubmed/8567783

Lynn A, KE Koehler *et al.* (2002). 'Covariation of synaptonemal complex length and mammalian meiotic exchange rates.' Science 296(5576): 2222-2225.

Magli MC, Gianaroli L, Ferraretti AP, Toschi M, Esposito F, Fasolino MC (2004). The combination of polar body and embryo biopsy does not affect embryo viability. Hum Reprod. 19(5):1163-9.

Magli MC, Gianaroli L, Fortini D, Ferraretti AP, Munné S (1999). Impact of blastomere biopsy and cryopreservation techniques on human embryo viability. Hum Reprod 14: 770–3.

Magli MC, Gianaroli L, Grieco N, Cefalu E, Ruvolo G, Ferraretti AP (2006). Cryopreservation of biopsied embryos at the blastocyst stage. Hum Reprod. 21(10):2656-60.

Magli MC, Gianaroli L, Munné S & Ferraretti AP (1998). Incidence of chromosomal abnormalities from a morphologically normal cohort of embryos in poor-prognosis patients. J Assist Reprod Genet 15, 297-301.

Magli MC, Jones GM, Gras L, Gianaroli L, Korman I, Trounson AO (2000). Chromosome mosaicism in day 3 aneuploid embryos that develop to morphologically normal blastocysts in vitro. Hum Reprod. 15(8):1781-6.

Magli MC, Montag M, Köster M, Muzi L, Geraedts J, Collins J, Goossens V, Handyside AH, Harper J, Repiing S, Schmutzler A, Vesela K, Gianaroli L (2011). Polar body array CGH for prediction of the status of the corresponding oocyte. Part II: technical aspects. Hum Reprod 26(11) 3181-85

Mahmood R, Brierley CH, Faed MJ, Mills JA & Delhanty JD (2000). Mechanisms of maternal aneuploidy: FISH analysis of oocytes and polar bodies in patients undergoing assisted conception. Hum Genet 106, 620-6.

Malter HE, Cohen J (1989). Partial zona dissection of the human oocyte: a nontraumatic method using micromanipulation to assist zona pellucida penetration. Fertil Steril 51: 139–48.

Martin RH, Ko E & Rademaker A (1991). Distribution of aneuploidy in human gametes: comparison between human sperm and oocytes. Am J Med Genet 39, 321-31.

Mastenbroek S, Twisk M, van der Veen F, Repping S (2011). Preimplantation genetic screening: a systematic review and meta-analysis of RCTs. Hum Reprod Update. 17(4):454-66

Mastenbroek S, Twisk M, van Echten-Arends J, Sikkema-Raddatz B, Korevaar JC, Verhoeve HR, Vogel NE, Arts EG, de Vries JW, Bossuyt PM, Buys CH, Heineman MJ, Repping S, van der Veen F (2007). In vitro fertilisation with preimplantation genetic screening. N Engl J Med. Jul 5;357(1):9-17.

McReynolds S, Vanderlinden L, Stevens J, Hansen K, Schoolcraft WB & Katz-Jaffe MG (2011). Lipocalin-1: a potential marker for noninvasive aneuploidy screening. Fertil Steril 95, 2631-3.

Mersereau JE, Pergament E, Zhang X & Milad MP (2008). Preimplantation genetic screening to improve in vitro fertilisation pregnancy rates: a prospective randomized controlled trial. Fertil Steril 90, 1287-9.

Meseguer M, Herrero J, Tejera A, Hilligsøe KM, Ramsing NB, Remohí J (2011). The use of morphokinetics as a predictor of embryo implantation. Hum Reprod. 26(10):2658-71

Middlebrooks CD, N Mukhopadhyay, SW Tinker, EG Allen, LJ Bean, F Begum, R Chowdhury, V Cheung, K Doheny, M Adams, E Feingold and SL Sherman (2013). 'Evidence for dysregulation of genome-wide recombination in oocytes with nondisjoined chromosomes 21.' Human molecular genetics.

Monk M, Muggleton-Harris AL, Rawlings E and Whittingham DG (1988). Preimplantation diagnosis of HPRT-deficient male and carrier female mouse embryos by trophectoderm biopsy. Human Reproduction 3 (3) 377-381.

Montag M, Van der Ven H (1999). Laser-assisted hatching in assisted reproduction. Croat Med J 40: 398–403.

Montag M, Van der Ven K, Delacretaz G, Rink K, Van der Ven H (1998). Laser-assisted microdissection of the zona pellucida facilitates polar body biopsy. Fertil Steril 69: 539–42.

Montag M, Köster M, van der Ven K, Bohlen U, & van der Ven H (2012). The benefit of artificial oocyte activation is dependent on the fertilisation rate in a previous treatment cycle. Reproductive Biomedicine Online, 24(5), 521–6. doi:10.1016/j.rbmo.2012.02.002

Muggleton-Harris AL, Glazier AM, Pickering SJ (1993). Biopsy of the human blastocyst and polymerase chain reaction (PCR) amplification of the beta-globin gene and a dinucleotide repeat motif from 2-6 trophectoderm cells. Hum Reprod. 8(12):2197-205.

Munné S, Alikani M, Tomkin G, Grifo J & Cohen J (1995). Embryo morphology, developmental rates, and maternal age are correlated with chromosome abnormalities. Fertil.Steril. 64, 382-91.

Munné S, Bahce M, Sandalinas M, Escudero T, Marquez C, Velilla E, Colls P, Oter M, Alikani M & Cohen J (2004). Differences in chromosome susceptibility to aneuploidy and survival to first trimester. Reprod Biomed Online 8, 81-90.

Munné S, Chen S, Colls P, Garrisi J, Zheng X, Cekleniak N, Lenzi M, Hughes P, Fischer J, Garrisi M, Tomkin G, Cohen J (2007). Maternal age, morphology, development and chromosome abnormalities in over 6000 cleavage-stage embryos. Reprod. Biomed. Online 14, 628–634.

Munné S, Cohen J (1993). Unsuitability of multinucleated human blastomeres for preimplantation genetic diagnosis. Hum Reprod 8: 1120–5.

Munné S, Fragouli E, Colls P, Katz-Jaffe M, Schoolcraft W, Wells D. Improved detection of aneuploid blastocysts using a new 12-chromosome FISH test. Reprod Biomed Online [Internet] 2010;20:92–97.

Munné S, Gianaroli L, Tur-Kaspa I, Magli C, Sandalinas M, Grifo J, Cram D, Kahraman S, Verlinsky Y, Simpson JL. Substandard application of preimplantation genetic screening may interfere with its clinical success. Fertil Steril [Internet] 2007;88:781–784.

Munné S, Lee A, Rosenwaks Z, Grifo J, Cohen J (1993). Diagnosis of major chromosome aneuploidies in human preimplantation embryos. Hum Reprod;8(12):2185–2191

Munné S, Magli C, Cohen J, Morton P, Sadowy S, Gianaroli L, Tucker M, Marquez C, Sable D, Ferraretti AP, Massey JB & Scott R (1999). Positive outcome after preimplantation diagnosis of aneuploidy in human embryos. Hum Reprod 14, 2191-9.

Munné S, Sandalinas M, Escudero T, Marquez C & Cohen J (2002). Chromosome mosaicism in cleavage-stage human embryos: evidence of a maternal age effect. Reprod Biomed Online 4, 223-32.

Munné S, Wells D & Cohen J (2010). Technology requirements for preimplantation genetic diagnosis to improve assisted reproduction outcomes. Fertil Steril 94, 408-30.

Munné S (2006). Chromosome abnormalities and their relationship to morphology and development of human embryos. Reprod Biomed Online 12, 234-53.

Myers S, L Bottolo *et al.* (2005). 'A fine-scale map of recombination rates and hotspots across the human genome.' Science 310(5746): 321-324.

Nagaoka SI, TJ Hassold and PA Hunt (2012). 'Human aneuploidy: mechanisms and new insights into an age-old problem.' Nature reviews. Genetics 13(7): 493-504.

Nasr-Esfahani MH, Deemeh MR, & Tavalaee M (2010). Artificial oocyte activation and intracytoplasmic sperm injection. Fertility and Sterility, 94(2), 520–6. doi:10.1016/j.fertnstert.2009.03.061

Natesan SA, Coskun S, Qubbaj W, Prates R, Munné S, Coonen E, Van Uum CM, Dreesen JC, Stock-Meyer SE, Wilton LJ, Brown APC and Handyside AH (2014). Genome wide Karyomapping accurately identifies the inheritance of genetic defects in human preimplantation embryos in vitro. Genetics in medicine. Published online 08 May, doi:10.1038/gim.2014.45

Natesan SA, Handyside AH, Thornhill AR, Ottolini CS, Sage K, Summers MC, Gordon A, Konstantinidis M, Wells D and Griffin DK (2014). Live birth after PGD with confirmation by a comprehensive approach (Karyomapping) for simultaneous detection of monogenic and chromosomal disorders. Reproductive Biomedicine Online. Published online on 25 July 2014, DOI: 10.1016/j.rbmo.2014.07.007

Natesan SA, Bladon AJ, Coskun S, Qubbaj W, Prates R, Munné S, Coonen E, Dreesen JC, Stevens SJ, Paulussen AD, Stock-Myer SE, Wilton LJ, Jaroudi S, Wells D, Brown AP and Handyside AH (2014). Genome-wide karyomapping accurately identifies the inheritance of single-gene defects in human preimplantation embryos in vitro. Genet Med

Navidi W and Arnheim N (1991). Using PCR in preimplantation genetic disease diagnosis. Hum Reprod. 6 (6) 836-849.

Nekkebroeck J, Bonduelle M, Desmyttere S, Van den Broeck W, Ponjaert-Kristoffersen I (2008). Mental and psychomotor development of 2-year-old children born after preimplantation genetic diagnosis/screening. Hum Reprod. [Epub ahead of print].

Nijs M, Van Steirteghem A (1990). Developmental potential of biopsied mouse blastocysts. J Exp Zool 256: 232–6.

Northrop LE, Treff NR, Levy B & Scott Jr RT (2010). SNP microarray-based 24 chromosome aneuploidy screening demonstrates that cleavage-stage FISH poorly predicts aneuploidy in embryos that develop to morphologically normal blastocysts. Mol Hum Reprod 16, 590-600.

Oliver TR, E Feingold, K Yu, V Cheung, S Tinker, M Yadav-Shah, N Masse and SL Sherman (2008). 'New insights into human nondisjunction of chromosome 21 in oocytes.' PLoS genetics 4(3): e1000033.

Ottolini C.S., Griffin D.K., Thornhill A.R. (2012). The Role of Aneuploidy Screening in Human Preimplantation Embryos, Aneuploidy in Health and Disease, Dr Zuzana Storchova (Ed.), ISBN: 978-953-51-0608-1, InTech, DOI: 10.5772/36199.

Ottolini CS, LJ Newnham, A Capalbo, SA Natesan, HA Joshi, D Cimadomo, DK Griffin, K Sage, MC Summers, AR Thornhill, E Housworth, AD Herbert, L Rienzi, FM Ubaldi, AH Handyside and ER Hoffmann (2015). 'Genome-wide maps of recombination and chromosome segregation in human oocytes and embryos show selection for maternal recombination rates.' Nat Genet 47(7): 727-735.

Ottolini C, Rienzi L & Capalbo A (2014). A cautionary note against embryo aneuploidy risk assessment using time-lapse imaging. Reproductive BioMedicine Online, 28(3), pp.273–275.

Ottolini CS, Rogers S, Sage K, Summers MC, Capalbo A, Griffin DK, Sarasa J, Wells D, Handyside AH. (2015a) Karyomapping identifies second polar body DNA persisting to the blastocyst stage: implications for embryo biopsy. Reprod Biomed Online [Internet] 2015; ElsevierAvailable from: http://www.rbmojournal.com/article/S1472648315003661/fulltext.

Ozil JP (1983). Production of identical twins by bisection of blastocysts in the cow. J. Reprod. Fertil. 69: 463-468.

Palermo GD, J Cohen, M Alikani, A Adler and Z Rosenwaks (1995). 'Development and implementation of intracytoplasmic sperm injection (ICSI).' Reprod Fertil Dev 7(2): 211-217; discussion 217-218.

Palermo G, Joris H, Devroey P, & Van Steirteghem AC (1992). Pregnancies after intracytoplasmic injection of single spermatozoon into an oocyte. Lancet, 340(8810), 17–8. Retrieved from http://www.ncbi.nlm.nih.gov/pubmed/1351601

Pantos K, Athanasiou V, Stefanidis K, Stavrou D, Vaxevanoglou T & Chronopoulou M (1999). Influence of advanced age on the blastocyst development rate and pregnancy rate in assisted reproductive technology. Fertil Steril 71, 1144-6.

Papadopoulos G, Templeton AA, Fisk N & Randall J (1989). The frequency of chromosome anomalies in human preimplantation embryos after in-vitro fertilisation. Hum.Reprod. 4, 91-8.

Papanikolaou EG, Kolibianakis EM, Tournaye H, Venetis CA, Fatemi H, Tarlatzis B *et al.* (2008). Live birth rates after transfer of equal number of blastocysts or cleavage-stage embryos in IVF. A systematic review and meta-analysis. Hum Reprod. 23(1):91-9.

Pardo-Manuel de Villena F and C Sapienza (2001). 'Nonrandom segregation during meiosis: the unfairness of females.' Mammalian genome: official journal of the International Mammalian Genome Society 12(5): 331-339.

Park S, Kim EY, Yoon SH, Chung KS, Lim JH (1999). Enhanced hatching rate of bovine IVM/IVF/IVC blastocysts using a 1.48-micron diode laser beam. J Assist Reprod Genet 16: 97–101.

Parriego M, Sole M, Aurell R, Barri PN, Veiga A (2007). Birth after transfer of frozen-thawed vitrified biopsied blastocysts. J Assist Reprod Genet. 24(4):147-9.

Pellestor F (1995). The cytogenetic analysis of human zygotes and preimplantation embryos. Hum Reprod Update 1, 581-5.

Pellestor F, Andreo B, Arnal F, Humeau C & Demaille J (2002). Mechanisms of non-disjunction in human female meiosis: the co-existence of two modes of malsegregation evidenced by the karyotyping of 1397 in- vitro unfertilized oocytes. Hum Reprod 17, 2134-45.

Penketh R and McLaren A (1987). Prospects for prenatal diagnosis during preimplantation human development. Baillieres Clin Obstet Gynaecol. 1(3):747-64.

Picton HM, Elder K, Houghton FD, Hawkhead JA, Rutherford AJ, Hogg JE, Leese HJ & Harris SE (2010). Association between amino acid turnover and chromosome aneuploidy during human preimplantation embryo development in vitro. Mol Hum Reprod 16, 557-69.

Pierce KE, Michalopoulos J, Kiessling AA, Seibel MM, Zilberstein M (1997). Preimplantation development of mouse and human embryos biopsied at cleavage stages using a modified displacement technique. Hum Reprod. 12(2):351-6.

Piyamongkol W, Garcia Bermudez M, Harper JC, Wells D (2003). Detailed investigation of factors influencing amplification efficiency and allele dropout in single cell PCR: implications for preimplantation genetic diagnosis. Mol Hum Reprod 9, 411-420.

Porter RN, Tucker MJ, Graham J, Sills ES (2002). Advanced embryo development duringextended in vitro culture: observations of formation and hatching patterns innon-transferred human blastocysts. Hum. Fertil. (Camb.) 5, 215–220.

Preimplantation Genetic Diagnosis International Society (PGDIS) (2008). Guidelines for good practice in PGD: programme requirements and laboratory quality assurance. Reprod Biomed Online. 16(1):134-47.

Rabinowitz M, Beltsos A, Potter D, Bush M, Givens C & Smortrich D (2010). Effects of advanced maternal age are abrogated in 122 patients undergoing transfer of embryos with euploid microarray screening results at cleavage stage.

Rawe VY, Olmedo SB, Nodar FN, Doncel GD, Acosta AA, & Vitullo AD (2000). Cytoskeletal organisation defects and abortive activation in human oocytes after IVF and ICSI failure.

Molecular Human Reproduction, 6(6), 510–6. Retrieved from http://www.ncbi.nlm.nih.gov/pubmed/10825367

Ray P, Winston R, Handyside A (1996). Reduced allele dropout in single-cell analysis for preimplantation genetic diagnosis of cystic fibrosis. J Assist Reprod Genet. 13(2):104-6.

Rechitsky S, Kuliev A, Sharapova T, Laziuk K, Ozen S, Barsky I, Verlinsky O, Tur-Kaspa I, Verlinsky Y (2006). Preimplantation HLA typing with aneuploidy testing. Reprod Biomed Online.;12(1):89-100.

Rechitsky S, Pomerantseva E, Pakhalchuk T, Pauling D, Verlinsky O, Kuliev A (2011). First systematic experience of preimplantation genetic diagnosis for de-novo mutations. Reprod Biomed Online.;22(4):350-61.

Rechitsky S, Verlinsky O, Kuliev A (2013). PGD for cystic fibrosis patients and couples at risk of an additional genetic disorder combined with 24-chromosome aneuploidy testing. Reprod Biomed Online.;26(5):420-30.

Reiger R, A Michaelis *et al.* (1968). Glossary of genetics and cytogenetics, Springer Verlag, Berlin, Heidelberg, New York.

Renwick P, Trussler J, Lashwood A, Braude P, Ogilvie CM (2010). Preimplantation genetic haplotyping: 127 diagnostic cycles demonstrating a robust, efficient alternative to direct mutation testing on single cells. Reprod Biomed Online;20(4):470-6.

Renwick PJ, Trussler J, Ostad-Saffari E, Fassihi H, Black C, Braude P, Ogilvie CM, Abbs S (2006). Proof of principle and first cases using preimplantation genetic haplotyping – a paradigm shift for embryo diagnosis. Reprod Biomed Online. Jul;13(1):110-9.

Retrospective analysis of outcomes after IVF using an aneuploidy risk model derived from time-lapse imaging without PGS. Reprod Biomed Online. 27(2):140-6

Robbins WA, Baulch JE, Moore D, 2nd, Weier HU, Blakey D & Wyrobek AJ (1995). Three-probe fluorescence in situ hybridisation to assess chromosome X, Y, and 8 aneuploidy in sperm

of 14 men from two healthy groups: evidence for a paternal age effect on sperm aneuploidy. Reprod Fertil Dev 7, 799-809.

Rockmill B, K Voelkel-Meiman *et al.* (2006). 'Centromere-proximal crossovers are associated with precocious separation of sister chromatids during meiosis in Saccharomyces cerevisiae.' Genetics 174(4): 1745-1754.

Rossant J (1976). Postimplantation development of blastomeres isolated from 4- and 8-cell mouse eggs. J Embryol Exp Morphol 36: 283–90.

Roudebush WE, Kim JG, Minhas BS, Dodson MG (1990). Survival and cell acquisition rates after preimplantation embryo biopsy: use of two mechanical techniques and two mouse strains. Am J Obstet Gynecol. 162(4):1084-90.

Ruangvutilert P, Delhanty JD, Serhal P, Simopoulou M, Rodeck CH, Harper JC (2000). FISH analysis on day 5 post-insemination of human arrested and blastocyst stage embryos. Prenat Diagn. 20(7):552-60.

Rycke M De, Belva F, Goossens V, Moutou C, SenGupta SB, Traeger-Synodinos J, Coonen E. ESHRE PGD Consortium data collection XIII: cycles from January to December 2010 with pregnancy follow-up to October 2011. Hum Reprod [Internet] 2015; Available from: http://www.ncbi.nlm.nih.gov/pubmed/26071418.

Sabhnani TV, Elaimi A, Sultan H, Alduraihem A, Serhal P & Harper JC (2011). Increased incidence of mosaicism detected by FISH in murine blastocyst cultured in vitro. Reprod Biomed Online 22, 621-31.

Sandler L and E Novitski (1957). 'Meiotic Drive as an Evolutionary Force.' American Naturalist 91(857): 105-110.

Saunders CM, Larman MG, Parrington J, Cox LJ, Royse J, Blayney LM, Lai FA (2002). PLC zeta: a sperm-specific trigger of Ca(2+) oscillations in eggs and embryo development. Development (Cambridge, England), 129(15), 3533–44. Retrieved from http://www.ncbi.nlm.nih.gov/pubmed/12117804

Schoolcraft WB, Fragouli E, Stevens J, Munné S, Katz-Jaffe MG, Wells D (2010). Clinical application of comprehensive chromosomal screening at the blastocyst stage. Fertil Steril. 94:1700-6

Schoolcraft WB, Treff NR, Stevens JM, Ferry K, Katz-Jaffe M, Scott RT Jr (2011). Live birth outcome with trophectoderm biopsy, blastocyst vitrification, and single-nucleotide polymorphism microarray-based comprehensive chromosome screening in infertile patients. Fertil Steril. 96:638-40.

Schoolcraft WB, Katz-Jaffe MG (2013). Comprehensive chromosome screening of trophectoderm with vitrification facilitates elective single-embryo transfer for infertile women with advanced maternal age. Fertil Steril. 100(3):615-9

Scott Jr RT, Ferry K, Su J, Tao X, Scott K, Treff NR (2012). Comprehensive chromosome screening is highly predictive of the reproductive potential of human embryos: a prospective, blinded, nonselection study. Fertil. Steril. 97, 870–875.eprod. Biomed. Online 14, 628–634.

Scott Jr RT, Upham KM, Forman EJ, Hong KH, Scott KL, Taylor D, Tao X, Treff NR (2013). Blastocyst biopsy with comprehensive chromosome screening and fresh embryo transfer significantly increases in vitro fertilisation implantation and delivery rates: a randomised controlled trial. Fertil Steril 100:697-703.

Scott Jr RT, Upham KM, Forman EJ, Zhao T and Treff NR (2013). Cleavage-stage biopsy significantly impairs human embryonic implantation potential while blastocyst biopsy does not: a randomised and paired clinical trial. Fertil Steril 100, 624-30.

Selva J, Martin Pont B, Hugues JN, Rince P, Fillion C, Herve F, Tamboise A & Tamboise E (1991). Cytogenetic study of human oocytes uncleaved after in vitro fertilisation. Hum.Reprod. 6, 709-13.

Shi Q & Martin RH (2000). Aneuploidy in human sperm: a review of the frequency and distribution of aneuploidy, effects of donor age and lifestyle factors. Cytogenet Cell Genet 90, 219-26.

Shi Q & Martin RH (2001). Aneuploidy in human spermatozoa: FISH analysis in men with constitutional chromosomal abnormalities, and in infertile men. Reproduction 121, 655-66.

Shinar S, Almog B, Levin I, Shwartz T, Amit A & Hasson J (2014). Total fertilisation failure in intra-cytoplasmic sperm injection cycles – classification and management. Gynecological Endocrinology, 30(8), 593–6. doi:10.3109/09513590.2014.911275

Simpson JL (2008). What next for preimplantation genetic screening? Randomised clinical trial in assessing PGS: necessary but not sufficient. Hum Reprod 23, 2179-81.

Sousa M & Tesarik J (1994). Ultrastructural analysis of fertilisation failure after intracytoplasmic sperm injection. Human Reproduction (Oxford, England), 9(12), 2374-80. Retrieved from http://www.ncbi.nlm.nih.gov/pubmed/7714161

Stachecki JJ, Cohen J, Munné S (2005). Cryopreservation of biopsied cleavage stage human embryos. Reprod Biomed Online. 11(6):711-5.

Staessen C, Platteau P, Van Assche E, Michiels A, Tournaye H, Camus M, Devroey P, Liebaers I & Van Steirteghem A (2004). Comparison of blastocyst transfer with or without preimplantation genetic diagnosis for aneuploidy screening in couples with advanced maternal age: a prospective randomized controlled trial. Hum Reprod 19, 2849-58.

Steptoe PC & Edwards RG (1978). Birth after the reimplantation of a human embryo [letter]. Lancet 2, 366.

Strom CM, Levin R, Strom S, Masciangelo C, Kuliev A, Verlinsky Y (2000). Neonatal outcome of preimplantation genetic diagnosis by polar body removal: the first 109 infants. Pediatrics. 106(4):650-3.

Summers MC & Foland AD (2009). Quantitative decision-making in preimplantation genetic (aneuploidy) screening (PGS). J Assist Reprod Genet 26, 487-502.

Summers PM, Campbell JM and Miller MW (1988). Normal in vivo development of marmoset monkey embryos after trophectoderm biopsy. Human Reprod. 3 (3) 389-393.

Sutcliffe AG, D'Souza SW, Cadman J, Richards B, McKinlay IA, Lieberman B (1995). Outcome in children from cryopreserved embryos. Arch Dis Child. 72(4):290-3.

Tarin JJ, Conaghan J, Winston RM, Handyside AH (1992). Human embryo biopsy on the 2nd day after insemination for preimplantation diagnosis: removal of a quarter of embryo retards cleavage. Fertil Steril 58: 970–6.

Tarin JJ, Handyside AH (1993). Embryo biopsy strategies for preimplantation diagnosis. Fertil Steril 59: 943–52.

Taylor TH, Gitlin SA, Patrick JL, Crain JL, Wilson JM, Griffin DK. The origin, mechanisms, incidence and clinical consequences of chromosomal mosaicism in humans. Hum Reprod Update [Internet] 2014;20:571–581.

Tease C, GM Hartshorne and MA Hulten (2002). 'Patterns of meiotic recombination in human fetal oocytes.' American journal of human genetics 70(6): 1469-1479.

Tempest HG, Griffin DK (2004). The relationship between male infertility and increased levels of sperm disomy. Cytogenet Genome Res 2004;107:83–94.

Tempest HG, Homa ST, Dalakiouridou M, Christopikou D, Wright D, Zhai XP, Griffin DK (2004).The association between male infertility and sperm disomy: evidence for variation in disomy levels among individuals and a correlation between particular semen parameters and disomy of specific chromosome pairs. Reprod Biol Endocrinol 2004;2:82.

Templado C, Bosch M, Benet J. Frequency and distribution of chromosome abnormalities in human spermatozoa. Cytogenet Genome Res [Internet] 2005;111:199–205.

Tesarik J, Kopecny V, Plachot M & Mandelbaum J (1988). Early morphological signs of embryonic genome expression in human preimplantation development as revealed by quantitative electron microscopy. Dev.Biol. 128, 15-20.

Tesarik J, Rienzi L, Ubaldi F, Mendoza C & Greco E (2002). Use of a modified intracytoplasmic sperm injection technique to overcome sperm-borne and oocyte-borne oocyte activation

failures. Fertility and Sterility, 78(3), 619–24. Retrieved from http://www.ncbi.nlm.nih.gov/pubmed/12215343

The Human MeioMap Project (www.sussex.ac.uk/lifesci/hoffmannlab/research/meiomap)

Thornhill AR, deDie-Smulders CE, Geraedts JP, Harper JC, Harton GL, Lavery SA *et al.* (2005). ESHRE PGD Consortium 'Best practice guidelines for clinical preimplantation genetic diagnosis (PGD) and preimplantation genetic screening (PGS)'. Hum. Reprod.; 20: 35-48.

Thornhill AR, Ottolini C and Handyside AH (2012). Human embryo biopsy procedures. In Textbook of Assisted Reproductive Technologies, 4th Edition pp. 197-211. Editors: David K. Gardner, Colin M. Howles, Ariel Weissman and Zeev Shoham. Informa Healthcare, London, UK.

Thornhill A.R , Ottolini C., Harton G., Griffin G. (2014a) Invasive Techniques: Aneuploidy Testing by Array-CGH in A Practical Guide to Selecting Gametes and Embryos, Markus Montag (Ed.), ISBN: 978-1-84214-547-0, CRC Press, DOI: 10.1201/b16881-19

Thornhill A, Repping S (2008). Quality Control and Quality Assurance in Preimplantation Genetic Diagnosis. In Preimplantation Genetic Diagnosis (In Press). Editor. Harper, J., Wiley and Sons, UK.

Thornhill AR, Handyside AH (2009). The Role of Aneuploidy Screening in Human Preimplantation Embryos. Biennial Rev Infert;276-288. Springer

Thornhill AR, Handyside AH, Ottolini C, Natesan SA, Taylor J, Sage K, Harton G, Cliffe K, Affara N, Konstantinidis M, et al. Karyomapping-a comprehensive means of simultaneous monogenic and cytogenetic PGD: comparison with standard approaches in real time for Marfan syndrome. J Assist Reprod Genet [Internet] 2015;32:347–356.

Treff N, Ferry KM, Zhao T, Su J, Forman EJ, Scott RT (2011). Cleavage stage embryo biopsy significantly impairs embryonic reproductive potential while blastocyst biopsy does not: a

novel paired analysis of cotransferred biopsied and non-biopsied sibling embryos. Fertil Steril 96 (3) S2

Treff NR, Levy B, Su J, Northrop LE, Tao X & Scott Jr RT (2010a). SNP microarray-based 24 chromosome aneuploidy screening is significantly more consistent than FISH. Mol Hum Reprod 16, 583-9.

Treff NR, Northrop LE, Kasabwala K, Su J, Levy B & Scott Jr RT (2011). Single nucleotide polymorphism microarray-based concurrent screening of 24-chromosome aneuploidy and unbalanced translocations in preimplantation human embryos. Fertil Steril 95, 1606-12 e1-2.

Treff NR, Su J, Tao X, Levy B, Scott Jr RT (2010b). Accurate single cell 24 chromosome aneuploidy screening using whole genome amplification and single nucleotide polymorphism microarrays. Fertil Steril. 94(6):2017-21.

Treff NR, Tao X, Ferry KM, Su J, Taylor D, Scott Jr RT (2012). Development and validation of an accurate quantitative real-time polymerase chain reaction-based assay for human blastocyst comprehensive chromosomal aneuploidy screening. Fertil Steril. 97(4):819-24

Tsunoda Y, McLaren A (1983). Effect of various procedures on the viability of mouse embryos containing half the normal number of blastomeres. J Reprod Fertil 69: 315–22.

Twisk M, Mastenbroek S, Hoek A, Heineman MJ, van der Veen F, Bossuyt PM, Repping S & Korevaar JC (2008). No beneficial effect of preimplantation genetic screening in women of advanced maternal age with a high risk for embryonic aneuploidy. Hum Reprod.

Van Blerkom J (1989). The origin and detection of chromosomal abnormalities in meiotically mature human oocytes obtained from stimulated follicles and after failed fertilisation in vitro. Prog.Clin.Biol.Res. 296, 299-310.

Van Blerkom J, Davis P, Alexander S (2000). Differential mitochondrial distribution in human pronuclear embryos leads to disproportionate inheritance between blastomeres:

relationship to microtubular organisation, ATP content and competence. Hum Reprod15: 2621-33

Van Blerkom J, Cohen J & Johnson M (2015). A plea for caution and more research in the “experimental” use of ionophores in ICSI. Reproductive Biomedicine Online, 30(4), 323–4. doi:10.1016/j.rbmo.2015.02.002

Van de Velde H, De Vos A, Sermon K, Staessen C, De Rycke M, Van Assche E *et al.* (2000). Embryo implantation after biopsy of one or two cells from cleavage-stage embryos with a view to preimplantation genetic diagnosis. Prenat Diagn. 20 (13):1030-7.

Vanden Meerschaut F, D’Haeseleer E, Gysels H, Thienpont Y, Dewitte G, Heindryckx B, De Sutter P (2014). Neonatal and neurodevelopmental outcome of children aged 3-10 years born following assisted oocyte activation. Reproductive Biomedicine Online, 28(1), 54–63. doi:10.1016/j.rbmo.2013.07.013

Vanden Meerschaut F, Nikiforaki D, De Gheselle S, Dullaerts V, Van den Abbeel E, Gerris J, De Sutter P (2012). Assisted oocyte activation is not beneficial for all patients with a suspected oocyte-related activation deficiency. Human Reproduction (Oxford, England), 27(7), 1977–84. doi:10.1093/humrep/des097

Vanden Meerschaut F, Nikiforaki D, Heindryckx B & De Sutter P (2014). Assisted oocyte activation following ICSI fertilisation failure. Reproductive Biomedicine Online, 28(5), 560–71. doi:10.1016/j.rbmo.2014.01.008

Vanneste E, Voet T, Caignec C, Ampe M, Konings P, Melotte C, Debrock S, Amyere M, Vikkula M, Schuit F, Fryns J-P, Verbeke G, D'Hooghe T, Moreau Y, Vermeesch JR (2009). Chromosome instability is common in human cleavage-stage embryos. Nat Med;15:577-583

Varrela J, Larjava H, Jarvelainen H, Penttinen R, Eerola E & Alvesalo L (1989). Effect of sex chromosome aneuploidy on growth of human skin fibroblasts in cell culture. Ann Hum Biol 16, 9-13.

Veiga A, Sandalinas M, Benkhalifa M, Boada M, Carrera M, Santalo J *et al.* (1997). Laser blastocyst biopsy for preimplantation diagnosis in the human. Zygote. 5(4):351-4.

Verlinsky Y, Cieslak J, Ivakhnenko V *et al.* Preimplantation diagnosis of common aneuploidies by the first- and second-polar body FISH analysis. J Assist Reprod Genet 1998; 15: 285–9.

Verlinsky Y, Cohen J, Munné S, Gianaroli L, Simpson JL, Ferraretti AP *et al.* (2004). Over a decade of experience with preimplantation genetic diagnosis: a multicenter report. Fertil Steril. 82(2):292-4.

Verlinsky Y, Ginsberg N, Lifchez A, Valle J, Moise J, Strom CM (1990). Analysis of the first polar body: preconception genetic diagnosis. Hum Reprod 5: 826–9.

Verlinsky Y, Rechitsky S, Cieslak J, Ivakhnenko V, Wolf G, Lifchez A *et al.* (1997). Preimplantation diagnosis of single gene disorders by two-step oocyte genetic analysis using first and second polar body. Biochem Mol Med 62: 182–7.

Verlinsky Y, Rechitsky S, Schoolcraft W, Strom C, Kuliev A (2001). Preimplantation diagnosis for Fanconi anemia combined with HLA matching. JAMA;285:3130-3.

Verlinsky Y, Cieslak J, Freidine M, Ivakhnenko V, Wolf G, Kovalinskaya L, White M, Lifchez A, Kaplan B, Moise J, Valle J, Ginsberg N, Strom C & Kuliev A (1996). Polar body diagnosis of common aneuploidies by FISH. J Assist Reprod Genet 13, 157-62.

Viera A, J Page *et al.* (2009). 'Inverted meiosis: the true bugs as a model to study.' Genome dynamics 5: 137-156.

Voullaire L, Slater H, Williamson R & Wilton L (2000). Chromosome analysis of blastomeres from human embryos by using comparative genomic hybridisation. Hum Genet 106, 210-7.

Walsh PS, Erlich HA & Higuchi R (1992). Preferential PCR amplification of alleles: mechanisms and solutions. PCR.Methods Appl. 1, 241-50.

Wang T, H Sha *et al.* (2014). 'Polar body genome transfer for preventing the transmission of inherited mitochondrial diseases.' Cell 157(7): 1591-1604.

Wells D & Delhanty JD (2000). Comprehensive chromosomal analysis of human preimplantation embryos using whole genome amplification and single cell comparative genomic hybridisation. Mol Hum Reprod 6, 1055-62.

Wells D, Escudero T, Levy B, Hirschhorn K, Delhanty JD & Munné S (2002). First clinical application of comparative genomic hybridisation and polar body testing for preimplantation genetic diagnosis of aneuploidy. Fertil Steril 78, 543-9.

Whittingham DG (1980). Parthenogenesis in mammals. Oxford Reviews of Reproductive Biology, 2, 205–231. Retrieved from:

http://www.cabdirect.org/abstracts/19810158626.html;jsessionid=F6D09C015A95498E2282307B7EECA6F6

Wickham H (2009). "ggplot2: Elegant Graphics for Data Analysis." Ggplot2: Elegant Graphics for Data Analysis: 1-212.

Wilton L (2002). Preimplantation genetic diagnosis for aneuploidy screening in early human embryos: a review. Prenat Diagn 2002;22:512–518.

Wilton L (2012). Chromosomal mosaicism in the cleavage stage embryo revisited. Reproductive Biomedicine Online; 24(Suppl 2): PS35, S-11.

Wilton LJ, Shaw JM and Trounson AO (1989). Successful single-cell biopsy and cryopreservation of preimplantation mouse embryos. Fertil Steril 51 (3) 513-517.

Wolstenholme J and RR Angell (2000). ‘Maternal age and trisomy – a unifying mechanism of formation.’ Chromosoma 109(7): 435-438.

Wong CC, Loewke KE, Bossert NL, Behr B, De Jonge CJ, Baer TM, Reijo Pera RA (2010). Non-invasive imaging of human embryos before embryonic genome activation predicts development to the blastocyst stage. Nat Biotechnol. 28(10):1115-21.

Xu YW, Peng YT, Wang B, Zeng YH, Zhuang GL & Zhou CQ (2011). High follicle-stimulating hormone increases aneuploidy in human oocytes matured in vitro. Fertil Steril 95, 99-104.

Yang Z, Liu J, Collins GS, Salem SA, Liu X, Lyle SS, Peck AC, Sills ES, Salem RD (2012). Selection of single blastocysts for fresh transfer via standard morphology assessment alone and with arrayCGH for good prognosis IVF patients: results from a randomised pilot study. Molecular Cytogenetics 5:24.

Yang X and Foot RH (1987). Production of identical twin rabbits by micromanipulation of embryos. Biol. Reprod. 37: 1007-1014.

Yoon S-Y, Jellerette T, Salicioni AM, Lee HC, Yoo M-S, Coward K, Fissore RA (2008). Human sperm devoid of PLC, zeta 1 fail to induce Ca(2+) release and are unable to initiate the first step of embryo development. The Journal of Clinical Investigation, 118(11), 3671–81. doi:10.1172/JCI36942

Zaragoza MV, PA Jacobs, RS James, P Rogan, S Sherman and T Hassold (1994). 'Nondisjunction of human acrocentric chromosomes: studies of 432 trisomic foetuses and liveborns.' Human genetics 94(4): 411-417.

Zenzes MT & Casper RF (1992). Cytogenetics of human oocytes, zygotes, and embryos after in vitro fertilisation. Hum.Genet. 88, 367-75.

Zhang K, Martiny AC, Reppas NB, Barry KW, Malek J, Chisholm SW & Church GM (2006). Sequencing genomes from single cells by polymerase cloning. Nat Biotechnol 24, 680-6.

12. And Finally, my Acknowledgments

"On the shoulders of giants”

I am going to begin by acknowledging and thanking my mentor Dr John Yovich. Without your expertise and wisdom I would not have been here to write this thesis. For this I am eternally grateful and hope that I can continue your legacy for many years to come.

Thank you to my dear parents, Leo and Franca, for being brave and putting their faith in Dr Yovich by taking the plunge those 33-odd years ago on a new and unknown technology. You are the true pioneers of our field! Your love and support over the years enabled me to pursue my dreams and repay the science that helped create me. You made me the man I am today and I love you very very much. This thesis is for you.

I must also acknowledge the contribution of the Bridge Centre. First, Mr Paul Williams who offered me the opportunity to undertake a PhD and funded my studies from the outset. Also, thanks must go to Dr Kamal Ahuja who saw potential in me and continued my funding through times of upheaval and hardship at the clinic. I thank you both for your kindness.

Thanks to my co-supervisor Professor Alan Thornhill. Although in the later stages of my thesis we were unable to work so closely together, I thank you for your enthusiasm and support in the critical early stages of my studies that provided a stable platform for me to continue my work. Your pearls of wisdom were, and still are, always appreciated and help me to get through the hard times.

To Dr Antonio Capalbo, thank you for your massive contribution to my work over the last few years. Our countless discussions inspire and force me to keep an open mind, something that is so important. You are an inspiration to me and I aspire to achieve what you have already accomplished. Your friendship is one of the most important things to come out of my PhD experience and I look forward to many years of working alongside you.

Special thanks must go to Professor Alan Handyside. Prof, you are a true genius! Thank you for sharing some of that with me. I look forward to continuing to work with you and hope to repay you

in some way for all that you have done for me. Hopefully we have many productive years of publishing together ahead of us whilst we endeavour to innovate in the clinical realm.

Many many thanks to my supervisor Professor Darren Griffin. Professore, thank you for everything! I especially thank you for trusting me to work independently and for allowing me to go in my own direction whilst still providing me with rock-like support. Although we may not always see eye-to-eye (cricket and football being good examples), you have always been there for me and because of this our common goal has been more than successfully achieved. I sincerely hope I have done you proud. You are the best PhD supervisor one could have hoped for and I look forward to contributing, in a different capacity, to the Griffin lab in the future.

Thanks also to Dr Eva Hoffman, Dr Louise Newnham, Dr Filippo Ubaldi, Dr Laura Rienzi and all other collaborators on this thesis. Your collective expertise and help was much appreciated and integral to the finished work. I hope to continue our collaborations in the future.

Lastly, but by no means least, words cannot express the debt of gratitude I owe to my beautiful wife Carrie. The last five years have been a long journey for the both of us. Not only have you supported me through my studies but so much has happened besides. Two weddings, the births of our beautiful daughter Ilaria Rose and our hadsome little man Federico, to name but a few. You are my pillar of strength and I know that without you I would fall apart. This thesis is as much yours as it is mine. I love you and am forever yours. Thank you.